The role of Death Receptor 3 in the accumulation of immune cells in inflammatory disease

A thesis submitted in the candidature for the degree of
Doctor of Philosophy

by

William Victor Thomas Perks

Monday, 05 August 2013

Infection and Immunity,

Tenovus Building

School of Medicine

Cardiff University

Cardiff, CF14 4XN, UK

Declaration

This work has not previously been accepted in substance for any degree and is not currently submitted in candidature for any degree.

Signed……..……..(William Perks) Date……....

Statement 1

This thesis is being submitted in partial fulfilment of the requirements for the degree of PhD

Signed……..……..(William Perks) Date …….....

Statement 2

This thesis is the result of my own independent work/investigation, except where otherwise stated.

Other sources are acknowledged by explicit references

Signed……..……..(William Perks) Date …….....

Statement 3

I hereby give consent for my thesis, if accepted, to be available for photocopying and for inter-library loan, and for the title and summary to be made available to outside organisations.

Signed……..……..(William Perks) Date ……...

Statement 4: Previously approved bar on access

I hereby give consent for my thesis, if accepted, to be available for photocopying and for inter-library loans **after expiry of a bar on access previously approved by the graduate development committee.**

Signed……..……..(William Perks) Date ……...

Dedication

For My Family

Acknowledgements

Firstly, I would like to thank my supervisors Dr Eddie Wang and Prof Simon Jones for their guidance and continual support throughout my PhD. Without your never-ending enthusiasm I doubt this thesis would have ever been completed.

I would also like to thank Prof Phil Taylor and Dr Pete Tomasec, for all of their time, advice and knowledge over the past 3 years.

Special thanks also go to all the members of Team DR3 (Jason, Ravinder, Fraser and Caroline) for all of your daily optimism, help and support.

To everyone in the Tenovus building, a massive thank you for your friendship and making the last 3 years so enjoyable. I consider myself truly blessed to work with such a special group of people.

I would like to acknowledge Cardiff University and the Medical Research Council (MRC) without whose funding this project could not have been undertaken.

Finally, I would like to thank my family for their unconditional love and support. Without you I would have never made it this far.

Summary

Death Receptor 3 (DR3) is a death domain (DD) containing member of the Tumour Necrosis Factor Receptor Superfamily (TNFRSF) and has a single acknowledged TNFSF ligand called TNF-like protein 1A (TL1A). Previous research has implicated roles for DR3 in host immune defence and in various inflammatory diseases such as rheumatoid arthritis, inflammatory bowel disease (IBD), atherosclerosis and allergic lung inflammation. This thesis investigated a potential role for DR3 in co-ordinating the innate immune response, using an *in vivo Staphylococcus epidermidis* supernatant (SES) model of acute peritoneal inflammation. A further point of investigation looked at the effect of the absence of DR3 on thickening of the peritoneal membrane induced by repeated SES inflammation.

My results showed that the DR3/TL1A pathway is not essential in maintaining the number of peritoneal or blood leukocytes during naive conditions. Stromal DR3 was found to be important in co-ordinating the innate immune response after the induction of acute SES induced inflammation, with significantly lower numbers of specific myeloid and lymphoid cell subsets accumulating in the peritoneal cavity of DR3 knockout ($DR3^{-/-}$) mice. Despite this reduction in selected leukocyte numbers, the proportion of infiltrating cells exhibiting proliferation and cell death was unaffected by the absence of DR3. However reduced leukocyte numbers were associated with a significant reduction in the concentration of multiple chemoattractants in $DR3^{-/-}$ peritoneal supernatants compared to those from $DR3^{+/+}$ mice. Quantitative RT-PCR data (qPCR) were consistent with the peritoneal membrane being a source of many of these chemoattractants.

Results presented here identify for the first time a pro-inflammatory role for stromal DR3 in the innate immune response. However after repeatedly inducing inflammatory conditions DR3 promoted thickening of the peritoneal membrane, while an absence of DR3 prevented aberrant inflammation-induced tissue fibrosis.

Publications, presentations & awards

Publications

Twohig JP, Marsden M, Cuff SM, Ferdinand JR, Galimore AM, Perks WV, Al-Shamkhani A, Humphreys IR, Wang EC. (2012) The Death Receptor 3/TL1A pathway is essential for efficient development of antiviral $CD4^+$ and $CD8^+$ T cell immunity. ***FASEB J*** 26: 3575-86.

*Wang EC, *Newton Z, Hayward OA, Clark SR, Collins F, Perks WV, Singh RK, Twohig JP, Williams AS. (2012) Regulation of early cartilage destruction in inflammatory arthritis by Death Receptor 3. ***Ann Rhuem Dis*** (planned submission 2013) (* Joint first author).

William V T Perks, Zarabeth Newton, Olivia A Hayward, Fraser Collins, Ravinder K Singh, Jason P Twohig, Phil R Taylor, Anwen S Williams, Simon A Jones & Eddie C Y Wang. (2012) ECI 2012 meeting abstract. Investigating the function of the TL1A/DR3 pathway during the early stages of inflammation. ***Immunology***, Volume 137, S1 (September 2012), p133.

Presentations

William V T Perks, Ravinder K Singh, Jason P Twohig, Ceri A Fielding, Gareth W Jones, Phil R Taylor, Simon A Jones & Eddie C Y Wang. (2010) Poster presentation. The role of Death Receptor 3 in leukocyte recruitment during peritoneal inflammation. **26th Annual Post Graduate Research Day**, Cardiff University.

William V T Perks, Ravinder K Singh, Jason P Twohig, Ceri A Fielding, Gareth W Jones, Phil R Taylor, Simon A Jones & Eddie C Y Wang. (2011) Oral presentation. The role of Death Receptor 3 in leukocyte recruitment during acute inflammation. **Infection, Immunity & Biochemistry Seminar series**, Cardiff University.

William V T Perks, Ravinder K Singh, Jason P Twohig, Ceri A Fielding, Phil R Taylor, Simon A Jones & Eddie C Y Wang. (2011) Poster presentation. The role of Death Receptor 3 in leukocyte accumulation during peritoneal inflammation. **I^3-IRG Annual Conference**, New House Country Hotel, Cardiff.

William V T Perks, Ravinder K Singh, Jason P Twohig, Phil R Taylor, Simon A Jones & Eddie C Y Wang. (2011) Oral presentation. The role of Death Receptor 3 in leukocyte accumulation during peritoneal inflammation. **27th Annual Post Graduate Research Day**, Cardiff University.

William V T Perks, Ravinder K Singh, Jason P Twohig, Phil R Taylor, Simon A Jones & Eddie C Y Wang. (2012) Oral presentation. The role of Death Receptor 3 in leukocyte accumulation during acute inflammation. **Infection & Immunity Seminar series**, Cardiff University.

William V T Perks, Zarabeth Newton, Olivia A Hayward, Fraser Collins, Ravinder K Singh, Jason P Twohig, Phil R Taylor, Anwen S Williams, Simon A Jones & Eddie C Y Wang. (2012) Oral presentation. Investigating the function of the TL1A/DR3 pathway during the early stages of inflammation. **3rd European Congress of Immunology**, SECC, Glasgow. Published in ***Immunology***, Volume 137, S1 (September 2012), p133.

William V T Perks, Ravinder K Singh, Jason P Twohig, Phil R Taylor, Simon A Jones & Eddie C Y Wang. (2012) Oral presentation. The role of Death Receptor 3 in leukocyte accumulation during peritoneal inflammation. **Institute of Infection & Immunity Annual Meeting**, Royal Welsh College of Music & Drama, Cardiff.

William V T Perks, Ravinder K Singh, Jason P Twohig, Phil R Taylor, Simon A Jones & Eddie C Y Wang. (2012) Poster presentation. The role of Death Receptor 3 in leukocyte accumulation during peritoneal inflammation. **Institute of Infection & Immunity Annual Meeting**, Royal Welsh College of Music & Drama, Cardiff. **WON 1st POSTER PRIZE.**

William V T Perks, Zarabeth Newton, Olivia A Hayward, Fraser Collins, Ravinder K Singh, Jason P Twohig, Phil R Taylor, Anwen S Williams, Simon A Jones & Eddie C Y Wang. (2012) Oral presentation. Investigating the function of the TL1A/DR3 pathway during the early stages of inflammation. **MITReG Post Graduate Research Day**, Cathays campus, Cardiff University.

William V T Perks, Ravinder K Singh, Jason P Twohig, Phil R Taylor, Simon A Jones & Eddie C Y Wang. (2012) Oral presentation. The role of Death Receptor 3 in leukocyte accumulation during peritoneal inflammation. **27th Annual Post Graduate Research Day**, Cardiff University.

Awards

1st POSTER PRIZE at inaugural Institute of Infection & Immunity annual meeting, Sep 2012, "The role of Death Receptor 3 in the accumulation of immune cells in acute inflammatory disease"

The Davey Fund Travel Award: £200 to attend the 3rd European Congress of Immunology, Glasgow 2012

William Morgan Thomas Travel Fund: £200 to attend the 3rd European Congress of Immunology, Glasgow 2012

Contents List **Page**

List of Figures

Chapter 1 – General Introduction

Chapter 2 - Materials and Methods

Chapter 3 - Phenotypic characterisation of the peritoneal cavity and peripheral blood

Chapter 4 – The role of DR3 in accumulation of leukocytes into the peritoneal cavity during the early stages of an *in vivo* acute inflammatory event

Chapter 5 – The role of DR3 in accumulation of leukocytes into the peritoneal cavity during later stages of an *in vivo* acute inflammatory event

Chapter 7 – General Discussion

List of Tables

Chapter 2 - Materials and Methods

Chapter 3 - Phenotypic characterisation of resident peritoneal leukocyte and peripheral blood cellular subsets

Chapter 4 - Role of DR3 in accumulation of leukocytes into the peritoneal cavity during the early stages of an *in vivo* acute inflammatory event

Abbreviations

7AAD	7-Aminoactinomycin D
aa	Amino acid
ABC	ATP-binding cassette
AIA	Antigen induced arthritis
Alum	Aluminium hydroxide
ANOVA	Analysis of variance
APC	Antigen presenting cell
BAFFR	B cell-activating factor receptor
BAL	Bronchoalveolar lavage
BLK6	Black 6
bp	Base pairs
BSA	Bovine serum albumin
^{o}C	Celsius
CBS	Central biotechnology services
CD	Cluster of differentiation
cDNA	Complementary DNA
CIA	Collagen induced arthritis
c-IAP	Cellular inhibitor of apoptosis
cm	Centimetre
CO_2	Carbon dioxide
Cox-2	Cyclooxygenase-2
CRR	Cysteine-rich repeat
DAB	3,3-Diaminobenzidine
DC	Dendritic cell
DcR	Decoy receptor

DD	Death domain
DISC	Death inducing signalling complex
DR	Death receptor
$DR3^{-/-}$	DR3 knockout
$DR3^{+/+}$	Wildtype
$DR3^{+/-}$	Heterozygous
dH_20	Distilled water
DMEM	Dulbecco's modified eagle's medium
DNA	Deoxyribonucleic acid
dNTP	Deoxynucleotide triphosphate
DSS	Dextran sodium sulphate
DST	Diagnostic sensitivity testing
EAE	Experimental autoimmune encephalitis
ECD	Extracellular domain
ECM	Extracellular matrix
EDTA	Ethylenediaminetetra-acetic (Ethanoic) acid
ELISA	Enzyme linked immunosorbant assay
ELR	Glutamic acid-leucine-arginine
EMT	Epithelial to mesenchymal transition
EST	Expressed sequence tag
FACS	Fluorescent activated cell sorter
FADD	Fas associated death domain
FasL	Fas ligand
FC	Fragment crystallisable
FCγR	Fragment crystallisable gamma receptor
FCS	Foetal calf serum
FISH	Fluorescence *in situ* hybridisation

FSC	Forward scatter
FSC-A	Forward scatter-area
G	Gauge
GFR	Glomerular filtration rate
GM-CSF	Granulocyte-macrophage colony-stimulating factor
h	Human
H_2O_2	Hydrogen peroxide
HCl	Hydrochloric acid
HLA-DR	Human lymphocyte antigen-DR
HSS-HRP	High sensitivity streptavidin-horse radish peroxidise
IBD	Inflammatory bowel disease
IC	Immune complex
ICAM	Intercellular adhesion molecule
ICD	Intracellular domain
IFN	Interferon
Ig	Immunoglobulin
IHC	Immunohistochemistry
IκB	Inhibitor of kappa B
IKK	IκB kinase complex
IL	Interleukin
I.p.	Intra-peritoneal
IRES	Internal ribosome entry site
kDa	Kilodaltons
LDL	Low density lipoprotein
LPS	Lipopolysaccharide
LT	Lymphotoxin
LUBAC	Linear ubiquitin chains

m	Mouse
mAb	Monoclonal antibody
MAP3K	Mitogen-activated 3 kinases
mBSA	Methylated bovine serum albumin
MC	Mesothelial cell
MCMV	Mouse cytomegalovirus
MFI	Median fluorescence intensity
mg	Milligram
$MgCl_2$	Magnesium chloride
MHC	Major histocompatiability complex
ml	Millilitre
mM	Micromolar
mm	Millimetre
MMP	Matrix metalloproteinase
mRNA	Messenger ribonucleic acid
n	Number
NaCl	Sodium chloride
NBFS	Neutral buffered formalin saline
NCBI	National Center for Biotechnology Information
NETs	Neutrophil extracellular traps
NFκB	Nuclear factor kappa B
ng	Nanogram
NIK	NFκB inducing kinase
nm	Nanometre
NO	Nitric oxide
N.S.D	No significant difference
OD	Optical density

Ova	Ovalbumin
PAMPs	Pathogen-associated molecular patterns
PBMC	Peripheral blood mononuclear cell
PBS	Phosphate buffered saline
PCR	Polymerase chain reaction
PECAM	Platelet endothelial cell adhesion molecule
pg	Picogram
PG	Prostaglandin
PI3K	Phosphatidylinositol 3-kinase
pIC	Polyinosinic-polycytidylic acid
PM	Peritoneal macrophage
PMN	Polymorphonuclear neutrophil
PRR	Pattern recognition receptor
qPCR	Quantitative polymerase chain reaction
RBC	Red blood cell
RF	Relative fluorescence
RIP	Receptor interacting protein
RNA	Ribonucleic acid
ROS	Reactive oxygen species
Rpm	Revolutions per minute
RPMI-1640	1640 Media developed at the Roswell Park Memorial Institute
RQ	Relative quantity
RT-PCR	Reverse transcription polymerase chain reaction
SDS	Sodium dodecyl sulphate
S. enterica	*Salmonella enterica*
S. epidermidis	*Staphylococcus epidermidis*
SEM	Standard error of the mean

SES	*Staphylococcus epidermidis* supernatant
SSC	Side scatter
SSC-A	Side scatter-area
STAT	Signal transducer and activator of transcription
TBE	Tris/Borate/EDTA
TBS	Tris/Borate saline
TCR	T cell receptor
TEC	Tubular epithelial cell
TGFβ	Transforming growth factor β
Th	T helper cell
THD	Tumour necrosis factor superfamily homology domain
TL1A	TNF-like protein 1A
TLR	Toll like receptor
TMB	3, 3', 5, 5'-Tetramethylbenzidine
TNF	Tumour necrosis factor
TNFRSF	Tumour necrosis factor receptor superfamily
TRADD	TNF receptor associated death domain
TRAF	Tumour necrosis factor receptor associated factor
Treg	Regulatory T cells
Tris	Tris (hydroxymethyl) methylamine
TWEAKR	Tumor necrosis factor-like weak inducer of apoptosis receptor
UBAN	Ubiquitin binding domain
UV	Ultra violet
VCAM	Vascular adhesion molecule
VEC	Vascular endothelial cell
VEGI	Vascular endothelial growth inhibitor
µl	Microlitre

µg	Microgram
µM	Micromolar

Chapter 1 – General Introduction

1.1 The Tumour Necrosis Factor Superfamily

1.1.1 History

Observations based on the effects of the Tumour Necrosis Factor Superfamily (TNFSF) date back to the mid-19th century, when tumours from cancer patients were shown to regress after acute bacterial infection (Brunes et al. 1868). The name Tumour Necrosis Factor (TNF) was not used until 1975 with reference to these observations (Carswell, Old et al. 1975). By 1985 another cytotoxic protein had been discovered, known as Lymphotoxin (LT). Comparison of LT and TNF found 30 % amino acid sequence homology between them and common cell surface receptors (Aggarwal 2003), suggesting the presence of a larger gene superfamily. This was confirmed with the discovery of 2 Tumour Necrosis Factor Receptor Superfamily (TNFRSF) members in 1989, CD40 (Stamenkovic, Clark et al. 1989) and 4-1BB (Weissman 1989), and many more in subsequent years through sequencing using expressed sequence tags (ESTs).

The late 1990s saw a final surge in TNFRSF discovery initiated by the human genome project, which identified more remote relatives such as TWEAKR (Wiley, Cassiano et al. 2001) and BAFFR (Thompson, Bixler et al. 2001). Currently the TNFSF comprises 19 members which link to 29 TNFRSF members (Aggarwal 2003) forming more than 40 distinct TNFSF-TNFRSF interactions (Figure 1.1) (Idriss and Naismith 2000; Ashkenazi 2002; Ware 2008).

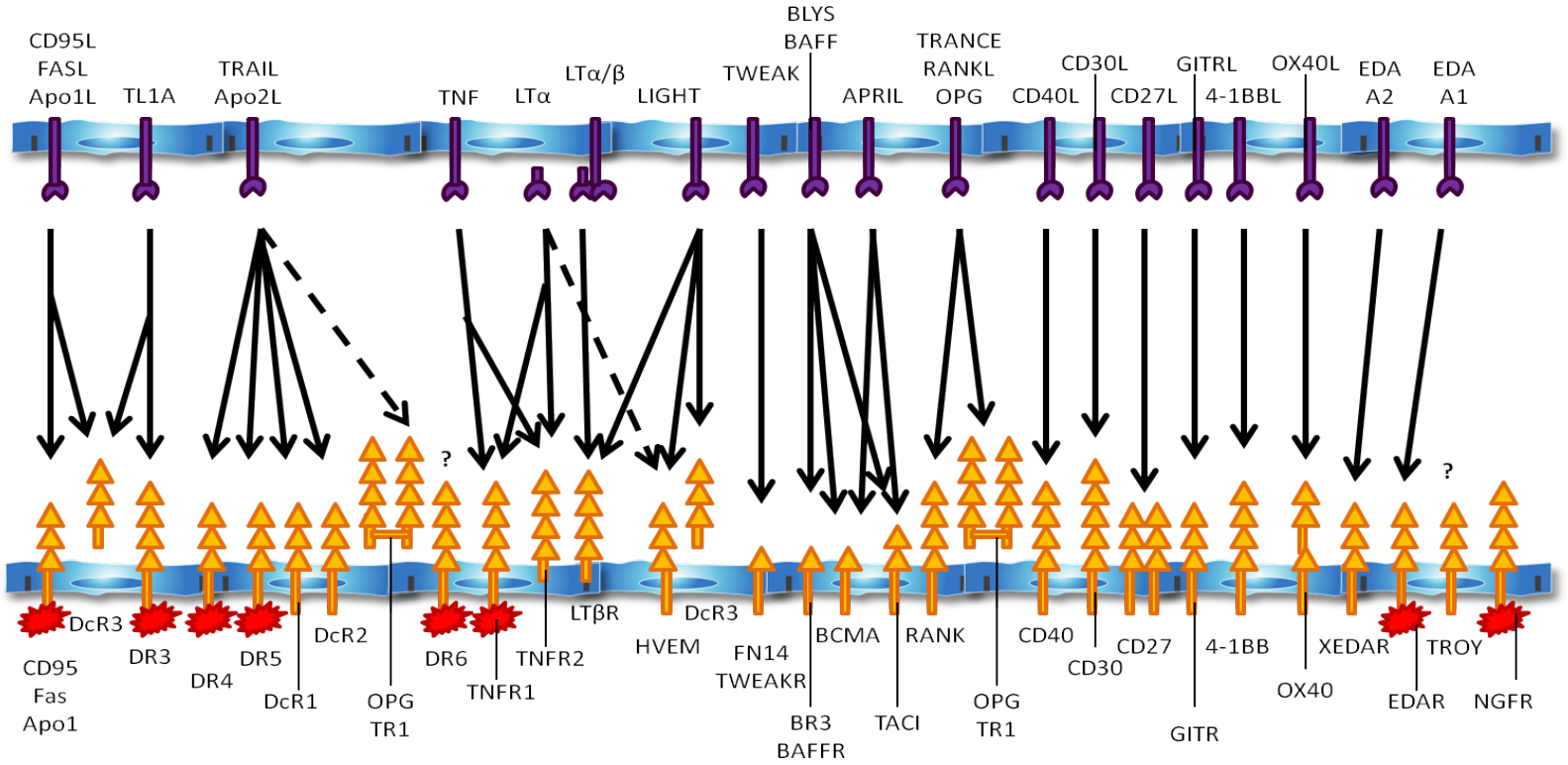

Figure 1.1 - Complete list of the known TNFSF, TNFRSF and their interactions. The TNFSF members are shown in purple and TNFRSF members in yellow; number of triangles correlates with the number of extracellular cysteine-rich repeats and intracellular death domains are indicated by a red star burst. Arrows represent TNFSF-TNFRSF interactions. Figure adapted from Ashkenazi 2002.

1.1.2 Structure and binding of TNFSF members and their receptors

The 19 TNFSF members are type 2 homotrimeric transmembrane proteins that can be embedded within the cell surface (pro form, cell to cell interaction) or cleaved from the membrane (mature form, soluble molecule) (Idriss and Naismith 2000). Within the extracellular region, the TNFSF include a homologous section of around 150 amino acids, known as the TNF homology domain (THD), however 15-35 % of the THD of each member is divergent, allowing specific binding to members of the TNFRSF (Orlinick and Chao 1998; Bodmer, Schneider et al. 2002).

The 29 TNFRSF members are mostly type 1 transmembrane proteins (with the exception of the soluble DcR3 and OPG), which are made up of 3 receptor monomers that are defined by their number (between 1 and 4) of extracellular cysteine-rich domains (MacEwan 2002; Bossen, Ingold et al. 2006). TNFRs with multiple cysteine-rich domains (between 2 and 4) have an extended configuration that combines with TNFSF members by using all 3 receptor monomers, which bind crevasses between pairs of TNFSF member monomers (Banner, Darcy et al. 1993; Hymowitz, Christinger et al. 1999; Hymowitz, Patel et al. 2005). However TNFRs with 1 cysteine-rich domain have a more condensed formation that only attaches to 1 TNFSF member monomer (Hymowitz, Patel et al. 2005).

Within the 29 members that make up the TNFRSF is a subpopulation of 8 receptors which share a homologous death domain (DD) region in the cytoplasmic tail, so called as this region recruits adaptor proteins that activate executioner caspases which can promote apoptosis (Ashkenazi 2002). These death receptors are believed to share a single common ancestor that incorporated a cytoplasmic DD, rather than

DDs evolving individually in separate evolutionary events for each receptor (Locksley, Killeen et al. 2001).

1.1.3 Intracellular receptor signalling by TNFSF members

Once a TNFSF member is bound to its TNFRSF ligand one of two intracellular signalling cascades can be initiated (Locksley, Killeen et al. 2001); which signalling pathway employed is dependent on the cytoplasmic adaptor proteins the TNFRSF member recruits (Ashkenazi and Dixit 1998). TNFRSF members associated with a DD can engage the cell's apoptotic mechanism by assembling an intracellular death inducing signalling complex (DISC) (Shen and Pervaiz 2006). The DISC can include the adaptor proteins Fas-associated death domain protein (FADD), TNFR-associated death domain protein (TRADD) (Locksley, Killeen et al. 2001) and Receptor interacting protein (RIP) (Shen and Pervaiz 2006) and the cysteine proteases Caspase 8 and 10 (Bodmer, Holler et al. 2000; Wang, Chun et al. 2001). These initiator caspases may then activate pro forms of executioner caspases (Caspase 3, 6 and 7) that are responsible for initiating apoptosis (Figure 1.2) (Ashkenazi and Dixit 1998).

The other signalling cascade is available to all TNFRSF members linked to an intracellular TNF receptor-associated factor (TRAF) binding motif (Ashkenazi and Dixit 1998). Following TNFSF/TNFRSF binding recruited TRAFs, along with cellular-Inhibitor of apoptosis 2 (cIAP2) form a complex which can initiate the canonical Nuclear factor kappa B (NFκB) pathway via ubiquitination of molecules in the signal complex, most notably RIP1 (Skaug, Jiang et al. 2009; Dynek, Goncharov et al. 2010; Verhelst, Carpentier et al. 2011). Ubiquitination is a 3

enzyme post transcriptional process by which ubiquitin (a 76 amino acid polypeptide) is joined to a target protein; 1) an ATP dependent thiolester bond is formed between the C-terminal of ubiquitin and the active site of the ubiquitin activating enzyme (E1), 2) ubiquitin is then transported to the ubiquitin conjugating enzyme (E2) before, 3) being attached via its C-terminal by an isopeptide bond to the epsilon amino group of a lysine residue (an essential amino acid) on the target protein (in this case RIP1) by a ubiquitin protein ligase (E3 e.g TRAF2, cIAP2) (Skaug, Jiang et al. 2009; Verhelst, Carpentier et al. 2011). RIP1 is then polyubiquitinated with lysine (K) ubiquitin chains, as lysine residues on ubiquitin itself allow covalent attachment of other ubiquitins, polyubiquitin chains formed by different lysine residues on ubiquitin (e.g K63, K48, K11, linear) can have differential structure and downstream effects (Skaug, Jiang et al. 2009; Verhelst, Carpentier et al. 2011).

Polyubiquitination of RIP1 then leads to the recruitment of TAK1 (a mitogen-activated 3 kinase (MAP3K) molecule) and the IκB kinase complex (IKK) via binding of TAB2 (an adaptor protein of TAK1) and IKKγ (otherwise known as NEMO, the modulator subunit of IKK that activates the p50/RelA dimer, NFκB family members) to ubiquitin chains via specialised ubiquitin binding domains (UBAN) (Haas, Emmerich et al. 2009; Rahighi, Ikeda et al. 2009; Skaug, Jiang et al. 2009; Tokunaga, Sakata et al. 2009; Gerlach, Cordier et al. 2011). This binding to polyubiquitin chains stabilises the signalling complex and either promotes IKKγ activation by direct transformation of IKKγ, TAK1 phosphorylation of IKK or close proximity of IKKγ subsections due to ubiquitination promoting trans-autophosphorylation (Skaug, Jiang et al. 2009; Ikeda, Crosetto et al. 2010; Walczak, Iwai et al. 2012). IKK can then phosphorylate Inhibitor of kappa B (IκB) leading to

its polyubiquitination (on lysine 21 and 22) triggering its degradation by the proteasome, permitting p50/RelA influence in the nucleus and triggering gene transcription (Shen and Pervaiz 2006; Verhelst, Carpentier et al. 2011) (Figure 1.2).

In addition to canonical NFκB signalling a subset of TNFRSF members including; BAFFR (Claudio, Brown et al. 2002; Kayagaki, Yan et al. 2002), LTβR (Dejardin, Droin et al. 2002; Norris and Ware 2007), CD40 (Bishop, Moore et al. 2007), TWEAKR (Brown, Richards et al. 2003; Saitoh, Nakayama et al. 2003), RANK (Novack, Yin et al. 2003; Vaira, Johnson et al. 2008), CD30 (Nishikori, Ohno et al. 2005; Nonaka, Horie et al. 2005), CD27 (Ramakrishnan, Wang et al. 2004) and TNFR2 (Munroe and Bishop 2004; Rauert, Wicovsky et al. 2010) can signal using a non-canonical NFκB pathway (Xiao, Harhaj et al. 2001).

Rather than the canonical pathway (which relies on degradation of the inhibitor IκB), non-canonical signalling depends on an inducible processing mechanism that is dependent on NFκB inducing kinase (NIK), a MAP3K molecule which is essential in processing p100 (Xiao, Harhaj et al. 2001; Claudio, Brown et al. 2002; Coope, Atkinson et al. 2002; Dejardin, Droin et al. 2002; Kayagaki, Yan et al. 2002; Novack, Yin et al. 2003; Sun 2011). p100 is the precursor of p52, which is one of the NFκB family members (along with RelB) that promotes gene transcription in this signalling pathway, but p100 also acts as an IκB-like protein preventing the translocation of RelB to the nucleus (Coope, Atkinson et al. 2002; Solan, Miyoshi et al. 2002; Derudder, Dejardin et al. 2003). Following TNFSF-TNFRSF binding TRAFs (predominantly TRAF2 and TRAF3) are recruited into the TRAF binding motif and their degradation promotes NIK activation (Sun 2010). NIK via the kinase IKKα (but not IKKβ or IKKγ) (Senftleben, Cao et al. 2001) then phosphorylates p100 at the NIK responsive domain (found at the C-terminal, near the inhibitory

ankyrin repeat domain and processing inhibitory domain regions) leading to its polyubiquitination and processing by the proteasome (Heusch, Lin et al. 1999; Xiao, Harhaj et al. 2001; Liang, Zhang et al. 2006) activating the p52/RelB, that can effect target genes (Figure 1.2).

Through these mechanisms of signalling, the TNFRSF can have dramatic effects on the cell, from typical cytokine responses, proliferation and differentiation to cell death (apoptosis).

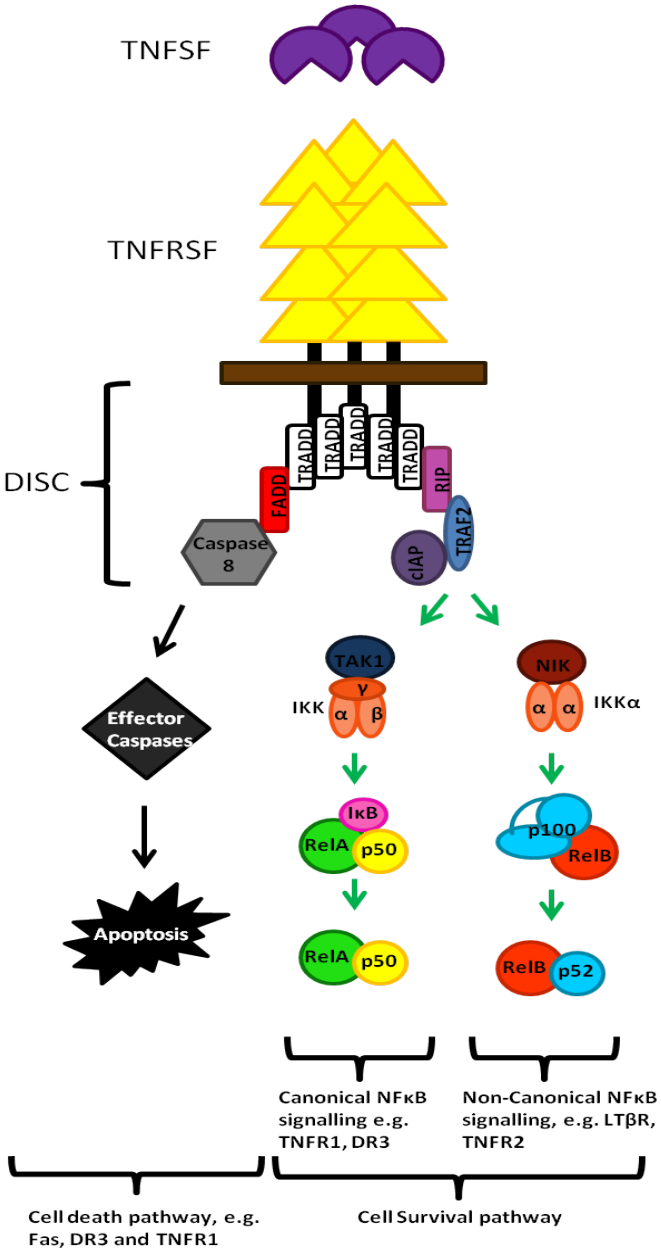

Figure 1.2 - Intracellular signalling by TNFRSF members. Signalling is dependent on adaptor proteins recruited to the intracellular portion of the TNFRSF and their differential association with downstream signalling cascades, that can exert different outcomes for the cell. TNFRSF members containing a death domain can signal for apoptosis via a DISC, which consists of adaptor proteins FADD, TRADD and RIP and initiator caspases, which activate executioner caspases that are responsible for initiating apoptosis. The canonical NFκB pathway is accessible to TNFRSF members associated with a TRAF binding motif. TRAFs along with cIAP2 initiate NFκB signalling via RIP1 and TAK1 which recruit and activate IKK, IKK then triggers degradation of IκB allowing p50/RelA access to the nucleus. In addition to canonical signalling a subset of the TNFRSF can signal via a non-canonical NFκB pathway, which depends on inducible processing of p100 by NIK. p100 is the precursor of p52, but also acts as an IκB-like protein stopping translocation of RelB to the nucleus. After activation TRAFs activate NIK that via IKKα phosphorylates p100 activating p52/RelB, which can affect gene transcription in the nucleus. Figure adapted from Baud and Karin 2001; Yeh 2002 and Sun 2011.

1.2 Death Receptor 3

TNFR1 was the first identified member of the TNFRSF and Death Receptor 3 (DR3) is its closest known relative. It was discovered due to its homology with TNFR1 and has been implicated in causing a variety of cellular responses from proliferation to initiation of apoptotic pathways.

1.2.1 Human DR3

The human DR3 (hDR3) gene was simultaneously discovered by a number of different laboratories, the majority of whom screened complementary DNA (cDNA) libraries with ESTs for sequence homology with TNFR1 and Fas; one group used a functional binding assay, namely a yeast 2-hybrid system incorporating the TNFR1 DD as a target (Kitson, Raven et al. 1996). Thus the DR3 gene (Chinnaiyan, Orourke et al. 1996) has been cited under an array of different names; these are TRAMP (Bodmer, Burns et al. 1997), LARD (Screaton, Xu et al. 1997), TR3 (Tan, Harrop et al. 1997), Wsl-1 (Kitson, Raven et al. 1996) and Apo3 (Marsters, Sheridan et al. 1996), though it is officially recorded in the National Center for Biotechnology Information (NCBI) database under TNFRSF25. The location of DR3 in the human genome was pinpointed using fluorescence *in situ* hybridisation (FISH) to the short arm of chromosome 1 between regions p36.2 (Bodmer, Burns et al. 1997) and p36.3 (Marsters, Sheridan et al. 1996), near several other TNFSF and TNFRSF members (including; TNFR2, 4-1BB, CD30, OX40) suggesting clustering in the genome (Bodmer, Burns et al. 1997).

The DR3 gene consists of 1665 base pairs in 10 exons, which encode a type 1 transmembrane protein of around 417 amino acids with 4 cysteine-rich repeats and a DD (Kitson, Raven et al. 1996; Screaton, Xu et al. 1997). DR3 and TNFR1 share 29 % of their overall cDNA sequence with 28 % homology in the extracellular domain (ECD) and 32 % in the intracellular domain (ICD), though this increases to 48 % in the DD (Marsters, Sheridan et al. 1996). After TNFR1, DR3 shares most resemblance to Fas, with which it shares 23 % of its overall sequence (Bodmer, Burns et al. 1997). At least 13 splice variants of hDR3 have been identified, 9 of which lack a transmembrane domain suggesting the presence of soluble forms that will be discussed in more detail in Section 1.2.3.1 (Screaton, Xu et al. 1997).

1.2.2 Mouse DR3

The mouse homologue of the hDR3 gene was isolated in 2001, by screening a 129Sv mouse genomic library with a full-length hDR3 cDNA. Screening identified a single cDNA clone and reverse transcription polymerase chain reaction (RT-PCR) and sequencing was used to characterise exon-intron boundaries, as reduced homology at the 5' end of the gene limited the signal from hDR3 probes in this region. The genomic location of the mouse homologue was pinpointed using FISH to chromosome 4 region E1, which is syntenic with the location of the hDR3 gene (Wang, Kitson et al. 2001).

Analysis of mouse DR3 (mDR3) cDNA indicates the coding portion of the gene spans 5kb and, similar to hDR3, contains 10 exons. The mDR3 gene shares significant similarities to its human counterpart, with a 55 % identical base pair sequence; homology rises even further at the protein level to 63 % across the whole

protein, including a highly conserved DD exhibiting 94 % homology. The ECDs of hDR3 and mDR3 share 52 % amino acid homology; both have 2 N-linked glycosylation sites and 25 of the 28 cysteine residues are conserved, though mDR3 has a 2 amino acid substitution and a 9 amino acid deletion in the second half of the 3rd cysteine-rich repeat leading to the absence of 2 cysteine residues and a switch between cysteine and phenylalanine (in humans) with threonine and cysteine (in mice). However these alterations are not predicted to affect interactions with the ligand, as the first section of the 3rd cysteine-rich repeat maintains a fundamentally similar structure and it is this region along with the 2nd cysteine-rich repeat, which is believed to bind its ligand TL1A (Section 1.2.5) (Wang, Kitson et al. 2001).

1.2.3 Expression of DR3

1.2.3.1 Human DR3 expression and Decoy receptor 3 (DcR3)

Unlike TNFR1, which is ubiquitously expressed in all tissues, DR3 is more selective. Northern blot analysis initially identified 3.4-4kb hDR3 RNA transcripts in the thymus, spleen, colon, small intestine, brain, foetal lung, prostate and peripheral blood T cells (Chinnaiyan, Orourke et al. 1996; Kitson, Raven et al. 1996; Marsters, Sheridan et al. 1996; Bodmer, Burns et al. 1997; Screaton, Xu et al. 1997). However later studies have also detected DR3 expression in the epidermis and dermis of skin (Bamias, Evangelou et al. 2011), vascular endothelial cells (VECs) and tubular epithelial cells (TECs) of rejecting or injured renal allografts (Al-Lamki, Wang et al. 2008), foam cells in atherosclerotic plaques from carotid endoarterectomy tissue (Kang, Kim et al. 2005) and on activated B cells (Cavallini, Lovato et al. 2013), monocytes (Kang, Kim et al. 2005), NK cells (Papadakis, Prehn

et al. 2004) and bone marrow differentiated osteoblasts (Borysenko, Garcia-Palacios et al. 2006).

The hDR3 gene was initially reported to produce 12 splice variants, the majority of which are truncated forms of the full-length DR3 transcript and produced by splicing out one or more exons resulting in stop codons (Screaton, Xu et al. 1997). Of these 12 splice variants 9 lack a transmembrane domain suggesting they are secreted in a soluble form (Screaton, Xu et al. 1997). However a 13th longer variant was later classified (initially named DR3β) that contained 2 insertions producing a sequence of 28 amino acids longer than the 417 amino acids reported for the original DR3 protein. Expression of this variant appears to be more restricted with its presence only on lymphoid T cell and immature B cell lines (Warzocha, Ribeiro et al. 1998).

In addition to soluble hDR3 splice variants, a soluble decoy receptor is also found in humans, known as Decoy receptor 3 (DcR3, also known as TR6 and M68). DcR3 expression has been found in several tissues, including; the spleen, stomach, colon, lung, spinal cord, lymph node and weakly in the thymus, but is overexpressed in cancerous tumours and during inflammatory diseases (Pitti, Marsters et al. 1998; Yu, Kwon et al. 1999; Bai, Connolly et al. 2000; Connolly, Cho et al. 2001; Zhang, Salcedo et al. 2001; Yang, Wang et al. 2004; Han and Wu 2009). Indeed increased DcR3 has been linked with more severe tumour and inflammatory disease progression (Roth, Isenmann et al. 2001; Chen, Yang et al. 2009), including peritonitis (Chang, Lin et al. 2012).

Structurally DcR3 contains a repeat of the TNFRSF's extracellular region but has no transmembrane region, thus it forms a soluble protein that can competitively bind DR3's ligand TL1A (Section 1.2.5) (Migone, Zhang et al. 2002). In addition to

disrupting DR3/TL1A interactions, DcR3 can also bind Fas ligand and LIGHT and so can also encroach on their signalling pathways (Pitti, Marsters et al. 1998; Yu, Kwon et al. 1999). Initially DcR3 was viewed as an anti-inflammatory molecule, which competes with DR3, Fas and HVEM to bind their respective ligands, therefore DcR3 can act to neutralise their effects and dampen down the inflammatory response (Zhang, Salcedo et al. 2001). However more recent studies in Crohn's disease have suggested DcR3 could also promote inflammation by blocking apoptosis (Macher-Goeppinger, Aulmann et al. 2008).

1.2.3.2 Mouse DR3 expression

Mouse DR3 expression was initially analysed by Northern blot and transcripts were identified in the brain, spleen, thymus, skin, heart, kidney, liver and on activated T cells (Wang, Kitson et al. 2001) (Figure 1.3). Later studies also confirmed DR3 expression in the synovial membrane and fat pad of the inflamed knee joint (Wang, Newton et al. appendix) and on differentiated $CD4^+$ T cell subsets; including T helper 17 (Th17) (Pappu, Borodovsky et al. 2008; Jones, Stumhofer et al. 2011) and regulatory T (Treg) cells (Fang, Adkins et al. 2008; Pappu, Borodovsky et al. 2008) as well as $CD8^+$ T cells (Fang, Adkins et al. 2008; Twohig, Marsden et al. 2012) and NKT cells (Fang, Adkins et al. 2008; Twohig, Marsden et al. 2012).

Significant differences were found in the number, length and expression pattern of mouse transcripts compared to hDR3, with 3 found between 1.8-7kb compared to 4 in hDR3. Further all of these 4 main hDR3 transcripts were seen in the human spleen and brain whilst only the larger 7kb transcript was found in the mouse brain, heart and kidney, with only the 2 smaller mDR3 transcripts of 1.8kb and 2.8kb observed

in the mouse spleen and thymus suggesting the function of DR3 may vary between species (Figure 1.3) (Wang, Kitson et al. 2001).

Variants of mDR3 are also produced by alternative splicing of one or more exons, but fewer are found in the mouse with 3 isoforms identified (variant 1- full-length membrane-bound, variant 2- soluble form and variant 3- truncated membrane-bound) (Wang, Kitson et al. 2001). Current investigations using DR3 mRNA suggest these mouse isoforms may be differentially regulated and may perform different immunological functions (Bamias, Mishina et al. 2006; Pappu, Borodovsky et al. 2008; Twohig, Marsden et al. 2012), which could explain some of the differing functions ascribed to DR3. However, exactly how different DR3 variants are regulated on the surface and how this relates to function is not yet known.

Nor has any mouse homologue of DcR3 been identified in the mouse, though it has been theorised that soluble DR3 (sDR3) in mice may perform a comparable role to DcR3 (Bamias, Mishina et al. 2006; Pappu, Borodovsky et al. 2008). However the function of sDR3 is yet to be determined and does not clarify the sustained existence of sDR3 isoforms, as well as DcR3 in humans (Screaton, Xu et al. 1997).

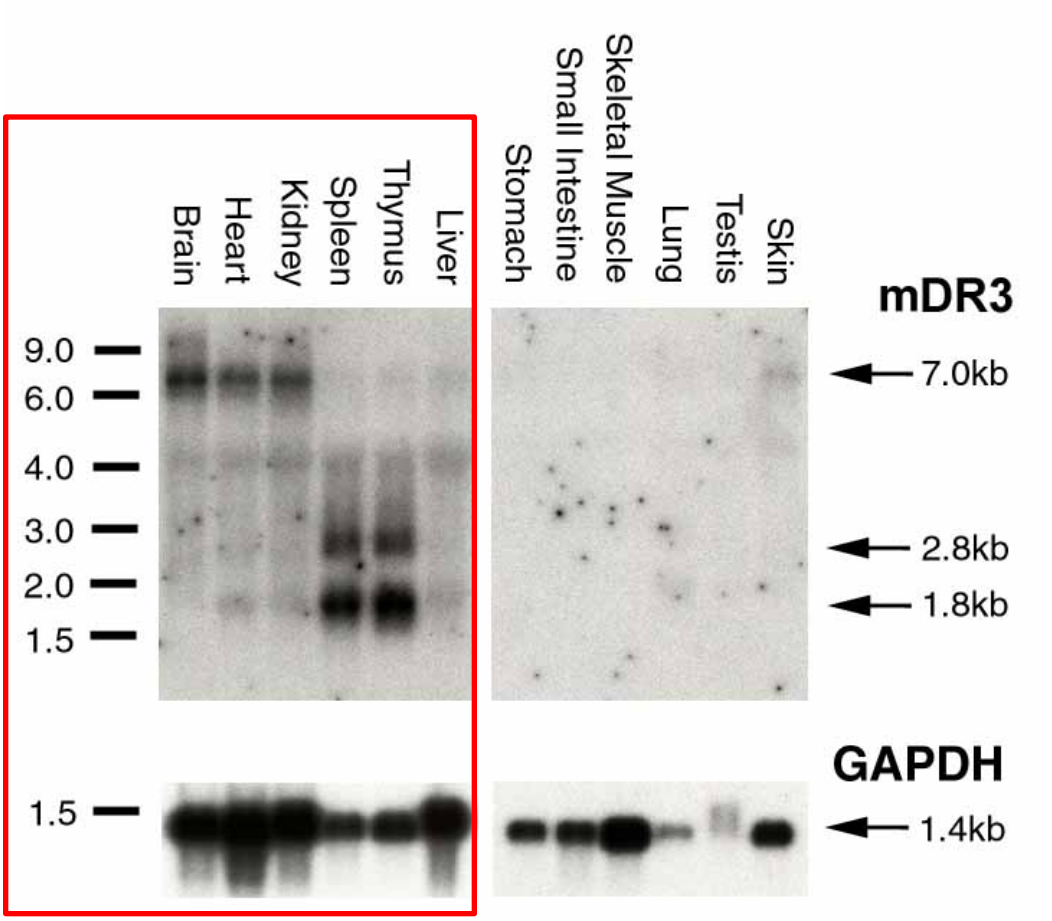

Figure 1.3 - DR3 expression in the mouse. Mouse DR3 (mDR3) was originally shown by Northern blot to be expressed in the brain, spleen, thymus, skin, heart, kidney, liver and on activated T cells. However later studies also found mDR3 on the synovial membrane and fat pad of the inflamed knee joint, differentiated $CD4^+$ T cell subsets, $CD8^+$ T cells and NKT cells. Figure taken from Wang et al. 2001.

1.2.4 Signalling through DR3

DR3 signalling occurs via a similar mechanism to other DD containing TNFRSF members (Section 1.1.3) (Figure 1.4). After TL1A binding DR3 signals for proliferation through canonical NFκB activation (Kitson, Raven et al. 1996; Bodmer, Burns et al. 1997), which was confirmed using a luciferase reporter gene that was amplified in a dose-dependent manner in the presence of DR3 (Bodmer, Burns et al. 1997). Whilst DR3 signalling can support cell survival (Chinnaiyan, Orourke et al. 1996; Kitson, Raven et al. 1996; Bodmer, Burns et al. 1997), overexpression on 293 T cells resulted in an 18 % increase in cell death (Screaton, Xu et al. 1997) (Kitson, Raven et al. 1996).

Thus to further understand the two contrasting pathways initiated by DR3, TF-1 cells (a DR3 expressing human erythroleukemic cell line) were used to investigate the formation of signalling complexes. The DISC was found to contain adaptor proteins which favour survival pathways (Wen, Zhuang et al. 2003), whilst limited apoptotic molecules were found in the signalling complex. Apoptosis was only initiated after blockade of NFκB, preventing the production of the c-IAP2 (Wen, Zhuang et al. 2003). Thus initial signalling molecules recruited after TNFSF-TNFRSF binding favour cell survival. However survival signals may be overridden if protein synthesis and proliferation signals are inhibited within the cell (Migone, Zhang et al. 2002).

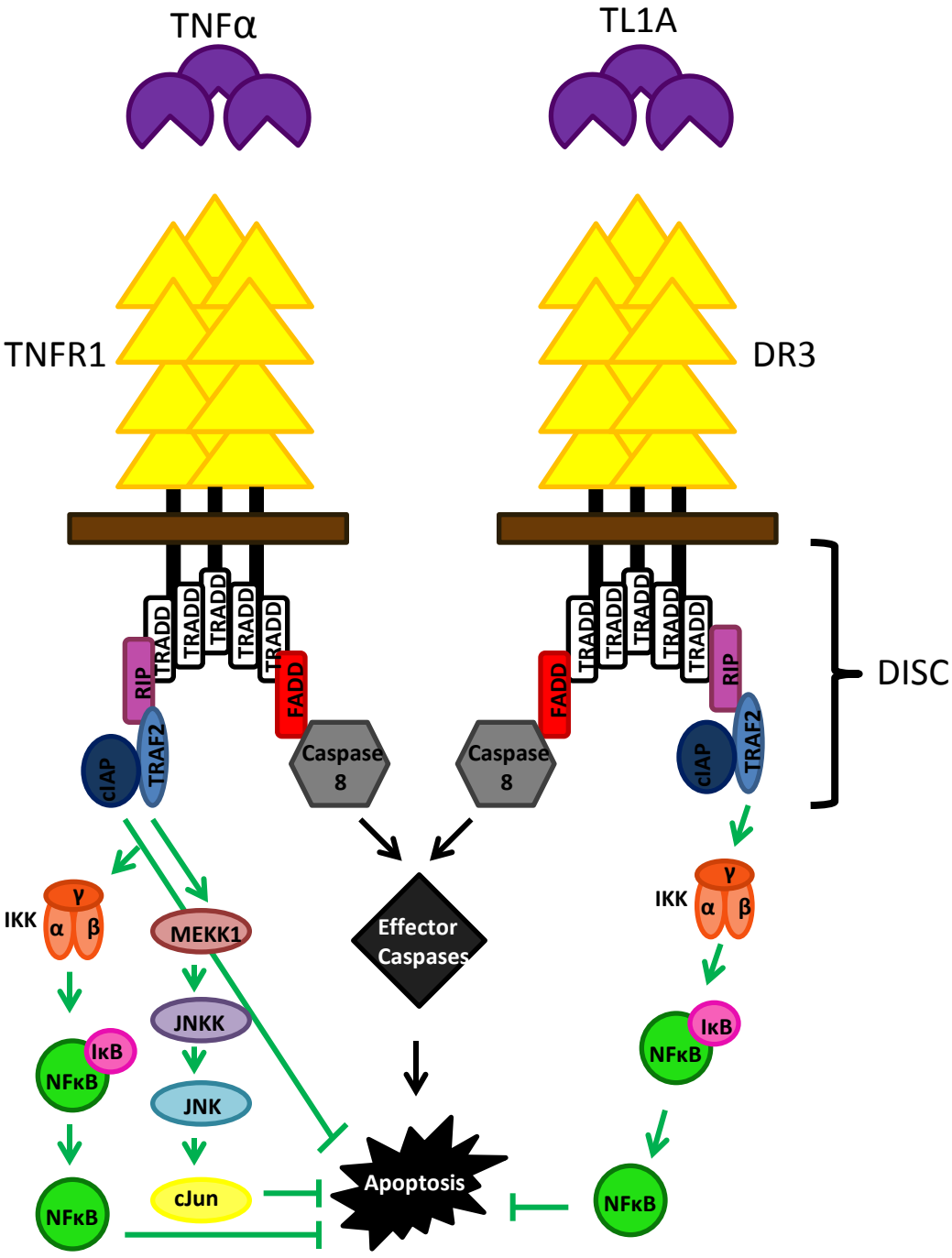

Figure 1.4 - DR3 and its intracellular signalling cascades. After TL1A binds DR3, adaptor proteins bind to the intracellular portion of DR3 forming a death inducing signalling complex (DISC). It is these effector molecules within the DISC that link DR3 into downstream signalling pathways such as the NFκB pathway, via RIP and TRAF2 and the caspase pathway by TRADD and FADD . Figure adapted from Ashkenazi 2002.

1.2.5 TNF-like protein 1A (TL1A)

Early investigations identified TWEAK (also known as Apo3L and TNFSF12) as the TNFSF member which bound DR3 (Marsters, Sheridan et al. 1998). However further research suggested this was not the case (Lynch, Wang et al. 1999) and TWEAK signalling was detected in DR3 knockout ($DR3^{-/-}$) cells (Kaptein, Jansen et al. 2000). TWEAK has since been shown to bind the TNFRSF member TWEAKR (also known as Fn14) (Wiley, Cassiano et al. 2001) and DR3 was found to bind the TNFSF member TL1A (also known as TNFSF15), which was discovered using ESTs (Migone, Zhang et al. 2002) and its specificity confirmed using $DR3^{-/-}$ mice (Bull, Williams et al. 2008; Meylan, Davidson et al. 2008; Twohig, Marsden et al. 2012).

In addition to DR3, TL1A can also be bound by DcR3 in humans (Migone, Zhang et al. 2002), though currently TL1A is the only identified TNFSF member that binds DR3 (and vice versa in mouse) (Migone, Zhang et al. 2002). It has also been suggested that DR3 on colon carcinoma cells can bind the adhesion molecule E-selectin, promoting tumour adhesion to endothelial cells and migratory and survival pathways in the tumour (Gout, Morin et al. 2006; Porquet, Poirier et al. 2011).

TL1A is a homotrimeric type 2 protein of 252 amino acids and a longer variant of vascular endothelial growth inhibitor (VEGI, also known as TL1) (Migone, Zhang et al. 2002) that has formerly been shown to be produced by the endothelium and prevent tumour development and endothelial expansion (Tan, Harrop et al. 1997; Yue, Ni et al. 1999; Zhai, Ni et al. 1999; Zhai, Yu et al. 1999). Both TL1A and VEGI were mapped to the TNFSF15 gene on the long arm of chromosome 9 in the

region q32 (Zhang, Wang et al. 2009). Compared to VEGI, TL1A was found to be the predominant full-length translation product of the TNFSF15 gene able to generate the transmembrane domain (allowing both membrane-bound and soluble TL1A) and the initial conserved β strand found in other TNFSF members. TL1A was also produced in significantly greater quantities (15 times higher) than VEGI (Migone, Zhang et al. 2002). Within the TNFSF, TL1A is most closely related to TNFR1's ligand TNFα to which it shares 24.6 % homology followed by FasL (22.9 %) (Migone, Zhang et al. 2002). Human and mouse TL1A are very similar showing 63.7 % cDNA sequence identity (Migone, Zhang et al. 2002).

Following the induction of inflammation, upregulation of TL1A expression has been detected on multiple tissues including the kidney, prostate, placenta, stomach, intestine, lung, spleen, thymus, skin, brain, renal allografts and atheromatous arteries (Migone, Zhang et al. 2002; Al-Lamki, Wang et al. 2008; Twohig, Roberts et al. 2010; Bamias, Evangelou et al. 2011; Bamias, Stamatelopoulos et al. 2013) and TL1A production has been noted by multiple cell types including endothelial cells (Migone, Zhang et al. 2002; Al-Lamki, Wang et al. 2008), chondrocytes, fibroblasts (Zhang, Wang et al. 2009), monocytes (Bamias, Martin et al. 2003; Bamias, Mishina et al. 2006; Cassatella, da Silva et al. 2007; Prehn, Thomas et al. 2007; Meylan, Davidson et al. 2008) and T cells (Bamias, Martin et al. 2003; Meylan, Davidson et al. 2008). However how TL1A is induced varies between different tissues and cell subsets.

TL1A expression (either membrane-bound or soluble form) on chondrocytes, fibroblasts and endothelial cells is upregulated after stimulation with other pro-inflammatory cytokines (TNFα and Interleukin 1β (IL1β)) (Migone, Zhang et al.

2002; Zhang, Wang et al. 2009), whereas release of TL1A (soluble form) from monocytes (including macrophages and dendritic cells) occurs after stimulation with LPS or immune complexes (IC) via Toll Like Receptors (TLRs) and Fragment crystallisable gamma receptors (FCγRs), respectively (Cassatella, da Silva et al. 2007; Prehn, Thomas et al. 2007; Meylan, Davidson et al. 2008). Upregulation of soluble TL1A production by T cells was seen after activation with anti-CD3 and/or anti-CD28, though this was dependent on DR3 expression, suggesting T cell TL1A secretion acts later than other sources of TL1A to sustain its own DR3 expression in an autocrine manner (Meylan, Davidson et al. 2008).

Different sources of TL1A and mechanisms of release suggest TL1A may fulfil several different functions. Initially TL1A was shown to act as a $CD4^+$ T cell co-stimulator promoting IL2-dependent proliferation and the release of pro-inflammatory cytokines (Interferon γ (IFNγ) and Granulocyte-macrophage colony-stimulating factor (GM-CSF)) that activate cell defences by recruiting peripheral blood leukocytes to the site of infection (Migone, Zhang et al. 2002). However, since this finding, TL1A has been found to promote other $CD4^+$ T cell responses such as, Th1 differentiation, via TL1A acting in synergy with IL12 and IL18, which promotes the release of IFNγ (Bamias, Martin et al. 2003; Bamias, Mishina et al. 2006). TL1A co-stimulation with IL12 may also enhance IFNγ release from NK cells (Papadakis, Prehn et al. 2004) and TL1A was seen to increase cytotoxity of IL12/IL18 activated NK cells (Heidemann, Chavez et al. 2010). In addition to its role in Th1 responses, TL1A was found to promote the accumulation of effector Th2 cells that provoke the release of IL13 by NKT cells (Fang, Adkins et al. 2008; Meylan, Davidson et al. 2008).

TL1A can maintain already differentiated Th17 cells but inhibit Th17 differentiation from naive T cells (Jones, Stumhofer et al. 2011) and was also shown to co-stimulate IL2-dependent Treg expansion (Schreiber, Wolf et al. 2010; Taraban, Slebioda et al. 2011). However the functional result of this may depend on the context of inflammation, as while TL1A-dependent Treg proliferation conveyed resistance in allergic lung inflammation (Schreiber, Wolf et al. 2010) their suppressive effects were overcome by TL1A-dependent Th17 effects in the ileum of TL1A-transgenic mice, causing goblet cell hyperplasia (Taraban, Slebioda et al. 2011). TL1A regulation of IL2-independent $CD8^+$ T cell expansion has been found in viral host defence (Twohig, Marsden et al. 2012) and TL1A's control of IL2-dependent $CD4^+$ T cell expansion has also been confirmed in both bacterial and viral challenge studies (Buchan, Taraban et al. 2012; Twohig, Marsden et al. 2012).

1.2.6 DR3 and health

Thus far only cellular interactions and pathways initiated by DR3 have been described, but what is known about the results of these interactions in terms of health and disease models?

1.2.6.1 Inflammatory bowel disease (IBD)

Both TL1A (on macrophages, $CD4^+$ and $CD8^+$ T cells and plasma cells) and DR3 (expressed on $CD4^+$ and $CD8^+$ T cells) are upregulated in the intestinal lamina propria of patients suffering from Crohn's disease and ulcerative colitis, while increased TL1A levels also correlated with disease severity (Bamias, Martin et al.

2003). TL1A and DR3 were also elevated in 2 mouse strains ($TNF^{\Delta ARE}$ mice; which are deficient in TNF adenosine-uracil (AU) rich elements (ARE), that are important in destabilisation and repression of TNF mRNA translation, resulting in higher and more sustained production of TNF and SAMP1/YitFc mice; that are a sub-strain of SAMP1/Yit mice, which were in turn developed from a sub-strain of AKR/J mice that unexpectedly acquired a senescence accelerated phenotype (including terminal ileitis), likely due to breeding with another unknown strain and were further selectively inbred) which spontaneously develop mouse ileitis, the mouse equivalent of IBD (Bamias, Mishina et al. 2006). In these experimental mouse disease models, increased TL1A expression on monocytes and $CD11c^+$ APC (dendritic cells) (Prehn, Thomas et al. 2007) bound upregulated full-length DR3, that was preferentially expressed on activated $CD4^+$ $CCR9^+$ memory T cells (Bamias, Mishina et al. 2006), which have been implicated as a causative cell in this disease (Papadakis, Zhu et al. 2005). TL1A interaction with mDR3 on these cells can then act in synergy with IL12 and IL18 (released from NK cells, cytotoxic and memory T cells) to co-stimulate IFNγ production (Bamias, Mishina et al. 2006), which was found to be upregulated in IBD patients promoting chronic inflammation of the intestinal mucosa (Bamias, Martin et al. 2003; Papadakis, Zhu et al. 2005). These findings suggest TL1A is important during the effector phase in Th1 inflammatory disease (Papadakis, Zhu et al. 2005).

In addition to Th1 effects, Th17 responses have also been associated with Crohn's disease progression (Fuss, Neurath et al. 1996; Matsuoka, Inoue et al. 2004). Lamina propria macrophages from Crohn's disease patients were found to produce IL23, which can act in synergy with TL1A (also released by the lamina propria) to produce IL17 as well as IFNγ (Kamada, Hisamatsu et al. 2010). TL1A released by lamina

propria macrophages have also been suggested to promote Th17 differentiation from naive T cells (Kamada, Hisamatsu et al. 2010), though this has been disputed in other studies (Jones, Stumhofer et al. 2011). Dual TL1A-dependent Th1 and Th17 responses were also noted in the mouse Dextran sodium sulphate (DSS) induced chronic colitis model and $G\alpha i2^{-/-}$ mice (that lack the $alpha_{i2}$ subunit from G proteins, which are a family of GTP binding proteins important in signal transduction), which develop spontaneous colitis. In these mouse models TL1A promoted the release of both IFNγ in synergy with IL12 (also noted by Bamias et al.) and IL17 in synergy with IL23. Furthermore, addition of an anti-TL1A neutralising antibody lowered Th1 and Th17 response and reduced markers of chronic colitis (Takedatsu, Michelsen et al. 2008).

Phenotyping of TL1A-transgenic mice (which constitutively produce DR3's only identified ligand TL1A on DCs) initially appeared normal during early development (first 2 months), with standard fertility and measurements of the colon, small intestine and spleen observed in transgenic mice. However after 6 (Taraban, Slebioda et al. 2011) and 10 months (Shih, Barrett et al. 2011), inflammation was identified in the small intestine (goblet cell hyperplasia) and greater fibrosis was seen in the intestine and colon compared to wildtype mice. Increased activation of leukocytes present in these mice also produced increased levels of IFNγ, IL13 and IL17 and an increase in gut homing chemokine receptors (CCR9 and CCR10) on T cells. Tregs also increased in these mice though pro-inflammatory signals were reported to overcome their suppressive effects (Shih, Barrett et al. 2011; Taraban, Slebioda et al. 2011).

Genetically, TNFSF15 polymorphisms have also been shown to correlate with the development of Crohn's disease in Japanese and European patients (Yamazaki, McGovern et al. 2005; Tremelling, Massey et al. 2008). This was confirmed in Swedish and American groups, which also identified the allele rs4263839 in TNFSF15 as a potential risk allele in Crohn's disease (Zucchelli, Camilleri et al. 2011). To date TNFSF15 is the only gene which has been linked to both European and Asian IBD (Shih, Kwan et al. 2009).

1.2.6.2 Atherosclerosis

TL1A is highly expressed in the foam cell region of carotid atherosclerotic plaques in humans (Kang, Kim et al. 2005; Kim, Kang et al. 2008). Foam cells are differentiated from macrophages, thus previous studies have used THP1 cells (a human peripheral blood monocyte cell line) to investigate DR3 activation (Kim, Lee et al. 2001; Kang, Kim et al. 2005; Kim, Kang et al. 2008). Addition of an anti-DR3 antibody to THP1 cells induced the matrix metalloproteinases MMP1, MMP9 and MMP13 (Kim, Lee et al. 2001), which have been reported to destabilise the atherosclerotic plaque (Kim, Lee et al. 2001). Following the addition of IFNγ with the anti-DR3 antibody, IL8, CCL2 and TNFα was also detected (Kang, Kim et al. 2005). However addition of TL1A rather than the anti-DR3 antibody only induced MMP9 and IL8 in a dose-dependent fashion (Kang, Kim et al. 2005).

It has also been suggested that TL1A binding of DR3 may drive differentiation of macrophages in this region into foam cells as seen with other TNFSF members, such as TNFα (Rus, Niculescu et al. 1991; Mei, Chen et al. 2007; Persson, Nilsson et al. 2008), by promoting cholesterol (low density lipoprotein) uptake and reducing

cholesterol efflux from the cell. DR3/TL1A interaction achieves this by (i) promoting scavenger receptors and proteins important in incorporating low density lipoprotein (LDL) into the cell, such as; SR-A, CD36, LPL and SR-PSOX and (ii) decreasing ATP-binding cassette (ABC) transporter members and proteins, such as; ABCA1, ABCG1 and apoE which are important in cholesterol transport from the cell (McLaren, Calder et al. 2010).

These findings suggest DR3/TL1A may play a complex role in the carotid atherosclerotic plaque.

1.2.6.3 Arthritis

TL1A was found to be elevated in serum of patients suffering from rheumatoid arthritis (Bamias, Siakavellas et al. 2008) and has been associated with increased bone and cartilage destruction (Cassatella, da Silva et al. 2007; Bamias, Siakavellas et al. 2008; Zhang, Wang et al. 2009). Arthritis is mediated by a Th1 immune response that includes the release of the inflammatory cytokines TNFα and IL1β, which were found to induce TL1A from fibroblast-like synoviocytes and mononuclear phagocytes (Cassatella, da Silva et al. 2007; Zhang, Wang et al. 2009).

Further investigation using 2 mouse models of arthritis (Antigen induced arthritis (AIA) and Collagen induced arthritis (CIA)) found increased TL1A and DR3 expression in wildtype ($DR3^{+/+}$) mice, but reduced neutrophil recruitment, MMP9 levels (Wang, Newton et al. appendix) and osteoclastogenesis (bone destruction/reabsorbtion) (Bull, Williams et al. 2008) in $DR3^{-/-}$ mice, which resulted in reduced cartilage damage (Wang, Newton et al. appendix; Bull, Williams et al. 2008) and bone pathology (Bull, Williams et al. 2008; Zhang, Wang et al. 2009).

Manipulation of the DR3/TL1A interaction also altered bone pathology, which was more severe in AIA following TL1A injections, but ameliorated by a neutralising anti-TL1A antibody in both AIA and CIA (Bull, Williams et al. 2008).

Additionally a DR3 gene duplication was identified in humans by FISH and sequencing and this duplication was shown to be more prominent in rheumatoid arthritis patients (Osawa, Takami et al. 2004).

Thus TL1A has been implicated as a pro-inflammatory cytokine in rheumatoid arthritis patients.

1.2.6.4 Allergic lung inflammation

Allergic lung inflammation is a defining characteristic of asthma and was provoked in mice by a local injection of ovalbumin (Ova) following systemic priming with Ova and aluminium hydroxide (Alum) (Gavett, Chen et al. 1994). TL1A interaction with DR3 was found to promote allergic lung inflammation by $CD4^+$ T cell differentiation into Th2 cells, caused by release of IL13 by NKT cells and increased eosinophil and mucus accumulation (Fang, Adkins et al. 2008; Meylan, Davidson et al. 2008). DR3/TL1A effects in allergic lung inflammation have been confirmed using (i) an antagonistic anti-TL1A antibody (Fang, Adkins et al. 2008) and (ii) $DR3^{-/-}$ mice (Meylan, Davidson et al. 2008). Both of these disruptions of the DR3/TL1A interaction resulted in amelioration of lung inflammation including, lower levels of IL13 and other Th2 cytokines (IL4 and IL5), fewer T cells, NK cells and eosinophils in the bronchoalveolar lavage (BAL) and reduced mucus volume.

These findings suggest DR3/TL1A enhances allergic lung inflammation by developing a Th2 autoimmune response.

1.2.6.5 Experimental autoimmune encephalitis (EAE)

Increased DR3 expression was found on Th17 cells during EAE, an autoimmune disease model driven by Th17 and Th1 subsets. Further study using $TL1A^{-/-}$ and particularly $DR3^{-/-}$ mice noted significantly reduced paralysis compared to $TL1A^{+/+}$ and $DR3^{+/+}$ mice. Additionally, adoptive transfer of $TL1A^{-/-}$ and $DR3^{-/-}$ T cells into $TL1A^{+/+}$ and $DR3^{+/+}$ mice respectively was also shown to attenuate paralysis (Meylan, Davidson et al. 2008; Pappu, Borodovsky et al. 2008).

The mechanism by which DR3/TL1A enhances EAE is not yet fully understood, however it appears from studies in $DR3^{-/-}$ mice that DR3 promotes increased T cell numbers in the spinal cord (Meylan, Davidson et al. 2008). DR3/TL1A may then act differentially on $CD4^{+}$ T cells based on activation status, maintaining the effector phenotype of prior differentiated Th17 cells, while not supporting Th17 development (differentiation or proliferation) from naive T cells (Pappu, Borodovsky et al. 2008; Jones, Stumhofer et al. 2011).

Thus TL1A interaction with DR3 on activated T cells is necessary for autoimmune damage in EAE.

1.2.6.6 Antimicrobial immunity

DR3/TL1A interaction has been associated with promoting host defence in both bacterial (Buchan, Taraban et al. 2012) and viral infections (Twohig, Marsden et al.

2012). Following *Salmonella enterica* infection the bacteria replicates in the spleen, where TL1A was found to be upregulated in macrophages (after 4 hours). A second peak of TL1A (day 14) also overlapped with $CD4^+$ T cell proliferation in the spleen and study of $DR3^{-/-}$ mice found reduced numbers and percentage proliferation of $CD4^+$ T cells (on day 14) compared to $DR3^{+/+}$ mice. $DR3^{-/-}$ $CD4^+$ T cells also displayed a more immature phenotype, with lower numbers of $IFN\gamma^+$ and primed T cells compared to those found in $DR3^{+/+}$ mice.

The Th1 response is central in clearing *S. enterica* infection and, unsurprisingly, elimination of this bacteria from the spleen in $DR3^{-/-}$ mice (and in follow up studies in the liver) was compromised compared to their $DR3^{+/+}$ counterparts. Further, injection of *S. enterica* into $RAG^{-/-}$ mice (that do not contain mature T and B lymphocytes, as absence of recombination activation genes prevents rearrangement of immunoglobulin and T cell receptor genes) which had received $DR3^{-/-}$ T cells displayed increased bacterial load and delayed kinetics compared to $RAG^{-/-}$ mice with $DR3^{+/+}$ T cells, confirming bacterial removal to be both DR3 and T cell dependent (Buchan, Taraban et al. 2012).

$DR3^{-/-}$ mice have also been associated with increased viral loads following mouse cytomegalovirus (MCMV) and Vaccinia infection. Similarly to *S. enterica* infection, $DR3^{-/-}$ $CD4^+$ T cells were present at lower numbers and displayed reduced proliferation, activation and IFNγ production after viral infection. However unlike *S. enterica* infection DR3 also mediated $CD8^+$ T cell immunity, in which similar defects to $CD4^+$ T cells were observed (Twohig, Marsden et al. 2012). These viral infection studies also noted differential regulation of DR3 splice variants, with upregulation of the full-length variant 1 (also noted by Bamias et al 2006 in mouse

models of IBD) and the soluble variant 2 following infection (Twohig, Marsden et al. 2012).

These studies indicate DR3 may play an important role in mediating host defence to pathogens by affecting the Th1 response and its action may be associated with careful regulation of splice variants.

1.2.7 Mouse DR3 knockout model

The $DR3^{-/-}$ mouse was made to investigate any non-redundant DR3 function *in vivo*. $DR3^{-/-}$ mice were generated by disrupting exon 1 and substituting all coding exons of the DR3 gene, eliminating the possibility of the expression of full-length DR3 or any of its splice variants. The DR3 gene was replaced with a β galactosidase *(lacZ)* gene, an internal ribosome entry site (IRES) and a neomycin resistance gene, which were bordered by *loxP* regions (Wang, Thern et al. 2001) (Figure 1.5).

$DR3^{-/-}$ mice had significantly enlarged thymuses compared to $DR3^{+/+}$ and heterozygous ($DR3^{+/-}$) mice with an increase in size of around 10 % at 2-5 weeks rising to 30 % by 29-32 weeks of age, yet this was not due to increased thymocyte proliferation and/or turnover. $DR3^{-/-}$ mice showed impaired negative selection in the thymus, though they were not found to suffer from any autoimmune diseases. Other than these observations, normal development akin to $DR3^{+/+}$ and $DR3^{+/-}$ littermates was seen in the $DR3^{-/-}$ spleen, brain heart, kidney, thymus lymph node and Peyer's patches.

Figure removed by author for copyright reasons

1.3 The Peritoneum

1.3.1 Anatomy

The peritoneum is made up of an uninterrupted serous membrane that assembles into a closed sack covering the abdominal wall, internal viscera and base of the diaphragm. The membrane can be split into 3 separate sections: (i) the partial peritoneum, which covers the anterior, lateral and posterior abdominal walls, the bottom of the diaphragm and the pelvis; (ii) The visceral peritoneum that encloses the intra-peritoneal organs and the abdominal viscera, containing a hanging fold called the mesentery; (iii) The omentum fold of the peritoneum which is suspended from the greater curvature of the stomach and originates from the dorsal mesentery (Figure 1.6) (Hjelle, Millerhjelle et al. 1995; Nagy and Jackman 1998).

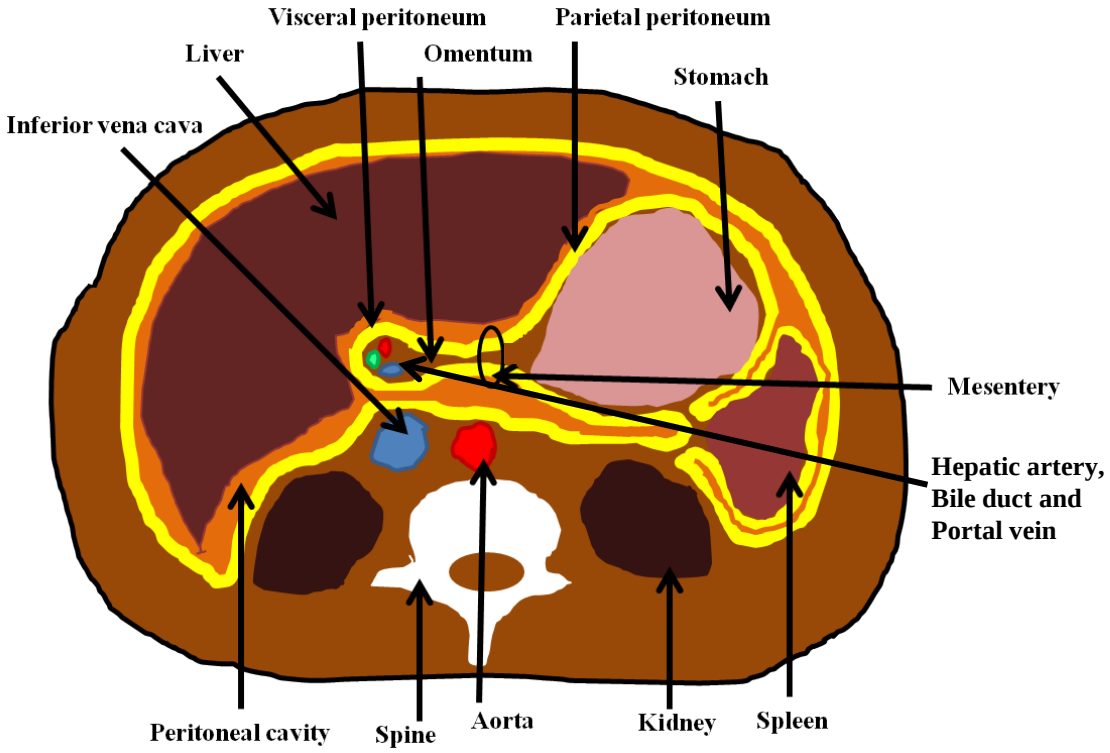

Figure 1.6 - The peritoneum. The peritoneal membrane forms a closed sack which can be divided into 3 different areas; (i) the partial peritoneum, that envelops the anterior, lateral and posterior abdominal walls, the bottom of the diaphragm and the pelvis, (ii) the visceral peritoneum, which contains the mesentery and surrounds the intra-peritoneal organs and the abdominal viscera and (iii) the omentum fold that hangs from the greater curvature of the stomach and originates from the dorsal mesentery. Figure adapted from Bowen 2006 and Agur, Drake 2004.

1.3.2 The peritoneal membrane

The peritoneal membrane is composed of 2 cell layers: (i) the mesothelium, that is an epithelial-like monolayer which is split by a discontinuous cell layer from; (ii) the interstitium (or compact zone), that forms a basal layer of connective tissue that supports the mesothelium (Digenis 1984; Krediet, Lindholm et al. 2000). Blood vessels are also present in the peritoneum and alongside the lymphatic system, can play an important role in movement of peripheral blood leukocytes into and out of the peritoneal cavity during an inflammatory response (Figure 1.7) (Nagy and Jackman 1998; Williams, Craig et al. 2002).

1.3.2.1 Mesothelial layer

The mesothelium is responsible for preserving homeostasis in the peritoneal cavity by coordinating the movement of leukocytes and solutes into the cavity (Mutsaers 2004; Yung and Chan 2009) and plays an essential role in organising the initial immune response after peritoneal infection (i.e. chemokine release) (Lanfrancone, Boraschi et al. 1992; Topley, Brown et al. 1993; Hurst, Wilkinson et al. 2001; McLoughlin, Witowski et al. 2003; McLoughlin, Hurst et al. 2004; Jones 2005).

The mesothelial monolayer is entirely made up of mesothelial cells that group collectively to form a continuous layer of compressed cells. These mesothelial cells are the most numerous cells found within the peritoneal cavity and contain projecting nuclei, rough endoplasmic reticulum, microvilli and pinocytic vesicles (Digenis 1984; Dipaolo, Sacchi et al. 1986; Rubin, Clawson et al. 1988; Dobbie and Anderson 1996). Mesothelial cells join together and to the interstitium by anchoring

junctions (made up of desmosomes and adherence junctions), whereas gap junctions in the membrane manage messages sent by cells in this layer (Simionescu and Simionescu 1977).

The mesothelium is held in place by a base layer found underneath the mesothelial monolayer made of glycoproteins, proteoglycans and type collagen 4 and may be maintained by the mesothelial layer itself (Rennard, Jaurand et al. 1984; Nagy and Jackman 1998).

1.3.2.2 Interstitium

The interstitium layer contains slack connective tissue formed by extracellular matrix (ECM) which includes elastin, fibronectin, type collagen 1 and type collagen 3, that together produce a structured formation that gives flexibility and strength (Flessner 1997; Witz, Montoya-Rodriguez et al. 2001). The interstitium can be important in regulating the passage of macromolecules and cells through the peritoneal membrane via glycosaminoglycans, which can produce a gel-like structure of differing aperture dimensions and charge density (Flessner 1997). The movement of nutrients, electrolytes, hormones, water molecules and gases from capillaries to resident cells in the cavity is governed by the aqueous environment within the interstitium (Nagy and Jackman 1998).

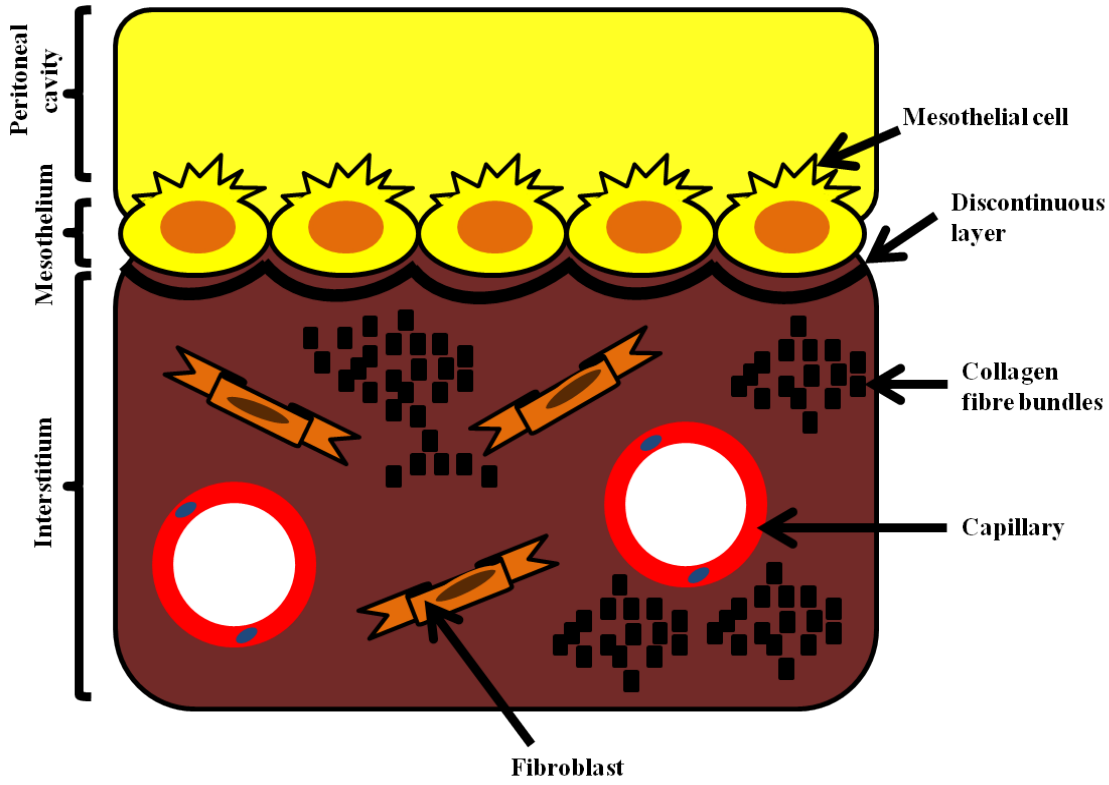

Figure 1.7 - Peritoneal membrane structure. Section of the peritoneal membrane showing the mesothelial layer and interstitium, which are separated by a discontinuous base layer. Figure also displays cells and proteins found in these layers.

1.4 The peritoneal inflammatory response

1.4.1 Immune cells present in the peritoneal cavity and their response to a bacterial infection

Different cell subsets present in the peritoneal cavity can act to produce an immunological response due to injury or infection. The main cell types present in a naive mouse cavity are mesothelial cells, resident macrophages and resident B1 cells. Other cell subsets such as NK cells, NKT cells, T cells, eosinophils and mast cells are also present but at lower numbers in the cavity (Turchyn, Baginski et al. 2007; Kolaczkowska 2010; Kolaczkowska, Koziol et al. 2010).

During a bacterial challenge acute peritoneal inflammation is provoked when foreign material is detected by TLRs which promotes the release of pro-inflammatory cytokines (i.e. TNFα and IL1) by resident leukocytes such as resident macrophages (Turchyn, Baginski et al. 2007). These pro-inflammatory cytokines can act to release inflammatory mediators including neutrophil chemoattractants, which have a N-terminal tripeptide sequence of glutamic acid, leucine and arginine (ELR^+ motif) (Hartmann, Tschettier et al. 1997; Zabel, Zuniga et al. 2006). ELR^+ chemoattractants lead to an initial influx of neutrophils from the peripheral blood into the cavity (Figure 1.8) (Hurst, Wilkinson et al. 2001; McLoughlin, Witowski et al. 2003; McLoughlin, Hurst et al. 2004; Jones 2005). Other inflammatory mediators may also help direct the immune response such as adhesion molecules, which allow strong association between leukocytes in the blood and mesothelial cells encouraging migration into the cavity (Figure 1.9) (Springer 1990; Jonjic, Peri et al. 1992; Suassuna, Dasneves et al. 1994; Liberek, Topley et al. 1996; Hams, Colmont et al. 2008).

Later in the inflammatory response, neutrophils upregulate apoptotic markers on their cell surface allowing phagocytosis by resident macrophages and clearance from the cavity (Sanui, Yoshida et al. 1982; Savill, Wyllie et al. 1989; Akgul, Moulding et al. 2001). Other chemoattractants then cause a shift in the leukocyte subsets recruited into the cavity; promoting the influx of monocytes from the peripheral blood and a later accumulation of lymphocytes (Figure 1.8) (Topley, Liberek et al. 1996; Jones 2005). Acute inflammation is then resolved by apoptosis or drainage of monocytes into the lymphatic system and the removal of lymphocytes, though the mechanism by which they are removed is yet to be established (Bellingan, Caldwell et al. 1996; Messmer and Pfeilschifter 2000).

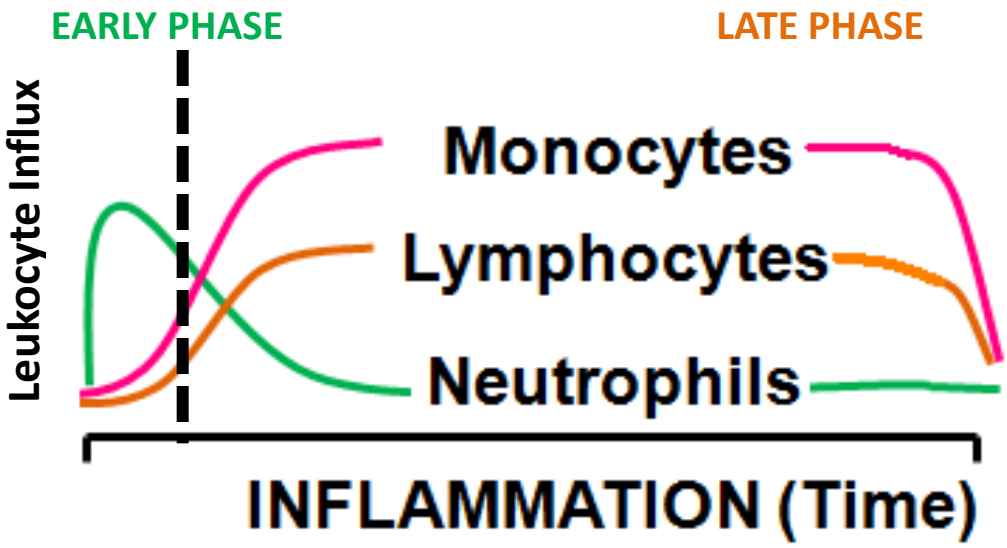

Figure 1.8 - S*taphylococcus epidermidis* supernatant (SES) induced acute inflammation cellular recruitment profile. Induction of acute SES inflammation promotes an early phase of inflammation, that is primarily made up of an initial influx of neutrophils. This is followed by a later more sustained phase of other myeloid and lymphoid cell subset accumulation into the cavity. Figure adapted from Jones 2005.

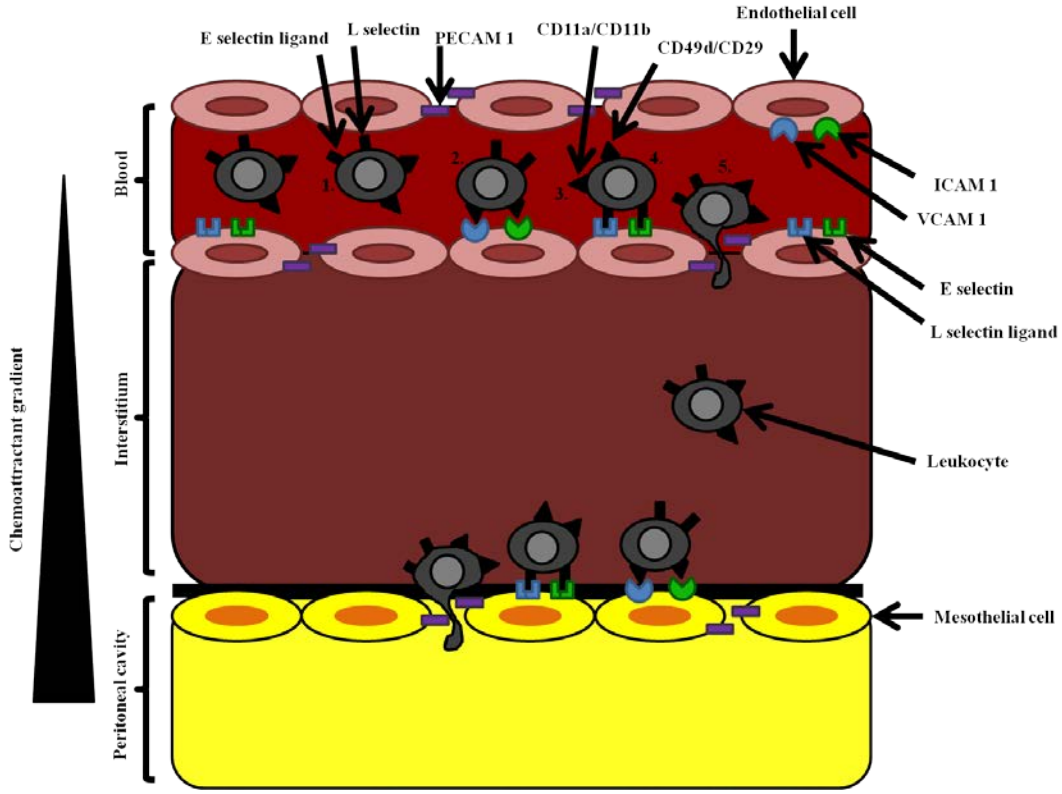

Figure 1.9 - Leukocyte recruitment from the peripheral blood and into the peritoneal cavity during inflammation. Following detection of a foreign stimulus constitutive expression of adhesion molecules is enhanced on the activated endothelium and inducible chemoattractants are released from the cavity. These molecules then promote leukocytes to move across the endothelium and out of the blood stream by 1) margination, 2) capture, 3) rolling, 4) adhesion and 5) transmigration. Leukocytes then pass though the interstitium towards the cavity via glycosaminoglycans and the chemotactic gradient. Leukocytes then cross the mesothelial layer and enter the cavity by a similar mechanism used to leave the blood stream.

Repeated episodes of peritoneal inflammation can result in a recurrent inflammatory state where activated T cells are maintained in the cavity (Fielding et al. appendix). Pro-inflammatory cytokines may act on these T cells encouraging the release of IFNγ (Buchan, Taraban et al. 2012; Fielding et al. appendix). This IFNγ can promote Signal Transducer and Activator of Transcription 1 (STAT1) signalling by the peritoneal membrane increasing chemoattractant production and so stronger accumulation of leukocytes (Boehm, Klamp et al. 1997; Gabay 2006; Fielding et al. appendix) (Figure 1.10).

Recruited leukocytes can maintain the inflammatory phenotype by producing more pro-inflammatory cytokines, chemokines and degrading factors (Fielding et al. appendix). These degrading factors such as MMPs and reactive oxygen species (Nitric oxide (NO), Hydrogen peroxide (H_2O_2)) can lead to tissue damage (Duffield, Erwig et al. 2000; Duffield, Ware et al. 2001; Kipari and Hughes 2002; Serbina, Salazar-Mather et al. 2003; Gueders, Foidart et al. 2006; Stary, Bangert et al. 2007) and Transforming growth factor beta (TGFβ) release to repair the tissue. However TGFβ may disrupt the homeostatic turnover of the extracellular matrix promoting epithelial to mesenchymal transition (EMT) of mesothelial cells, resulting in changes to the structure (fibrosis) of the peritoneal membrane (Bissell, Wang et al. 1995; Williams, Craig et al. 2002; Selgas, Bajo et al. 2006; Wynn 2007) (Figure 1.11).

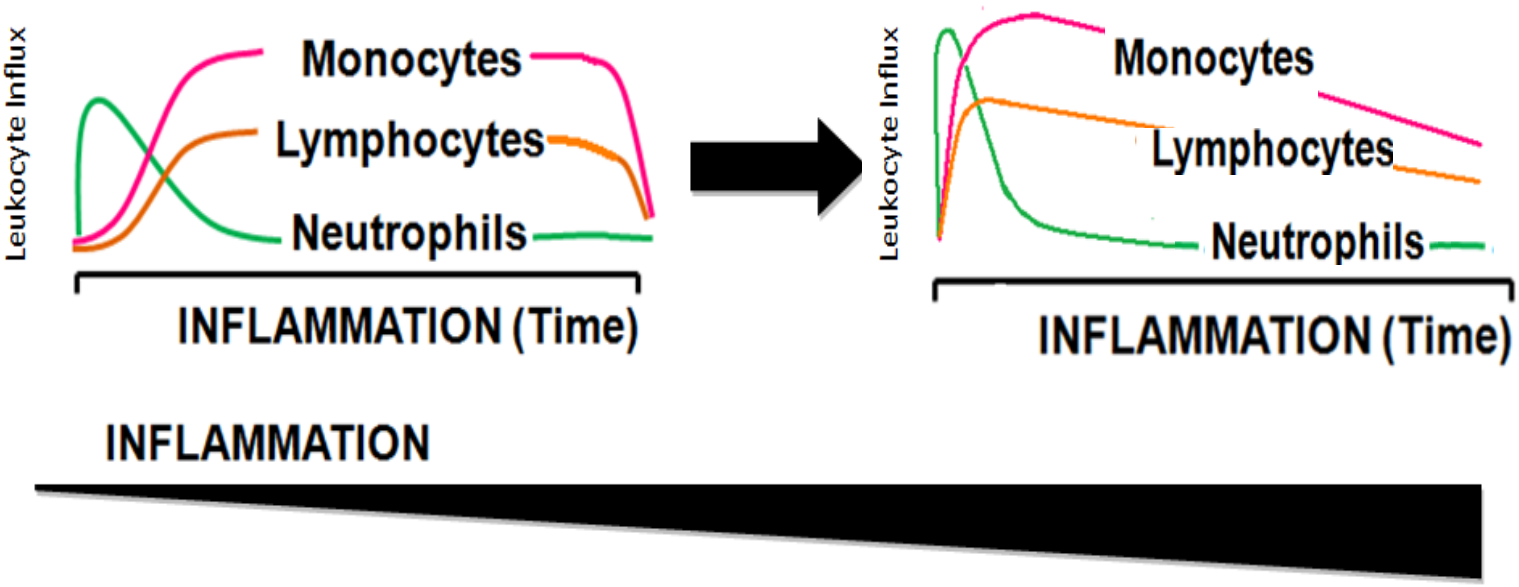

Figure 1.10 - S*taphylococcus epidermidis* supernatant (SES) induced acute peritoneal inflammation recruitment profile and how this profile alters after repeated inflammatory events. Induction of acute SES inflammation leads to an early phase of inflammation which is predominantly composed of neutrophils, followed by a later phase of inflammation made up of other myeloid and lymphoid subsets. However after multiple inflammatory episodes there is stronger influx of neutrophils into the cavity followed rapidly by the other myeloid and lymphoid subsets. Figure adapted from Jones 2005.

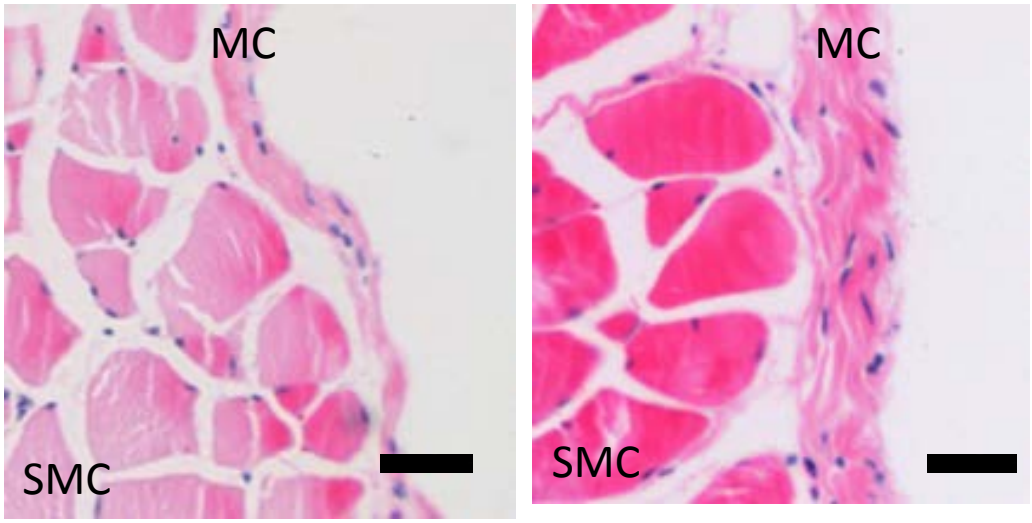

Figure 1.11 - Deterioration of the peritoneal membrane after repeated episodes of peritoneal inflammation. The left panel depicts a healthy mouse peritoneal membrane prior to any peritoneal inflammation. Whereas the right panel demonstrates the transformation of the membrane after multiple inflammatory events, characterised by a marked increase in fibrosis (thickening) of the mesothelial cell layer. Membrane stained using haematoxylin and eosin, bar corresponds to 25μm (MC- mesothelial cell layer, SMC- sub mesothelial compact zone).

1.4.2 Resident macrophages

Resident peritoneal macrophages originate in the bone marrow as $CD34^+$ myeloid progenitor cells and differentiate into monocytes expressing a CX_3CR1^{Lo} $CCR2^+$ $GR1^+$ phenotype before being released into the blood stream (Geissmann, Jung et al. 2003; Gordon and Taylor 2005). Under unchallenged conditions, monocytes can switch their phenotypic and functional properties (via an intermediate cellular subset) and express a CX_3CR1^{Hi} $CCR2^-$ $GR1^-$ resident phenotype (Sunderkotter, Nikolic et al. 2004). These resident monocytes are then recruited into the peritoneal cavity by CX_3CL1, where they differentiate into resident macrophages restocking the residential population (Sunderkotter, Nikolic et al. 2004; Gordon and Taylor 2005). Maintenance of this local population can also occur by local proliferation of these cells in the cavity (Gordon and Taylor 2005; Davies, Rosas et al. 2011). Resident macrophages are important in maintaining homeostasis within the cavity by removing senescent cells and controlling the process of tissue repair and modification (Taylor, Martinez-Pomares et al. 2005).

When a foreign substance is detected in the cavity, resident macrophages are the first cell type to respond and play a key role in directing the innate immune response, through the release of pro-inflammatory cytokines (such as TNFα and IL1β) which can promote the upregulation of inflammatory mediators including adhesion molecules and chemoattractant release by other cell types (Desouza and Ferreira 1985; Dunn, Barke et al. 1985; Fieren 1996). Peritoneal macrophages are also able to directly remove invading organisms from the cavity by phagocytosis. Using pattern recognition receptors (PRRs) on their surface e.g. mannose receptors, peritoneal macrophages detect conserved molecular patterns known as pathogen associated molecular patterns (PAMPs) (Taylor, Martinez-Pomares et al. 2005).

Depending on the microorganism peritoneal macrophages are not able to take up invading organisms immediately, as some pathogens must first be opsonised (enhances binding) by immunoglobulin, C3b and fibronectin. Once this process has been completed phagocytosis of the pathogen can occur (Griffin 1981; Holmes 1994). The exceptions to this rule are the Gram negative bacterium *Escherichia coli* and the Gram positive *Staphylococcus aureus* as peritoneal macrophages have the ability to bind (via immunoglobulin to cell wall protein A of these bacterium) and phagocytose these cells directly (Holmes 1994).

After uptake into the peritoneal macrophage the pathogen is surrounded by a vacuole, which is bound by lysosomes in the cytoplasm of the cell. These lysosomes contain digestive enzymes that synthesise reactive oxygen (H_2O_2) and reactive nitrogen (NO) species killing the pathogen. Peritoneal macrophages are also able to release these proteolytic products into the cavity to increase the removal rate of infection or process the products of the now destroyed pathogen to its surface and act as an APC. These processed products along with Major histocompatiability complex (MHC) class II can then promote the adaptive immune response by interacting with T cells inducing their activation, differentiation and proliferation (Nathan and Root 1977; Nathan, Silverstein et al. 1979; Sasada and Johnston 1980; Nathan and Hibbs 1991; Holmes 1994).

Peritoneal macrophages are also important in the clearance of recruited leukocytes, such as neutrophils once the pathogen has been removed, preventing exacerbated inflammation and promoting a return to homeostatic conditions in the cavity (Fadok, McDonald et al. 1998). This dampening of inflammatory capabilities is also important in reducing the likelihood of an autoimmune response (Pickering, Botto et al. 2000).

1.4.3 Mesothelial cells

Mesothelial cells are central to regulating the peritoneal environment and are essential in engaging and directing the inflammatory response (Topley, Petersen et al. 1994). Following the release of pro-inflammatory cytokines by resident peritoneal leukocytes mesothelial cells can release chemokines (such as KC, CCL2 and CCL5) which produce a gradient promoting the recruitment of leukocytes from the circulation into the cavity (Betjes, Tuk et al. 1993; Kinnaert, DeWilde et al. 1996; Liberek, Topley et al. 1996; Li, Davenport et al. 1998; Visser, Tekstra et al. 1998; Robson, McLoughlin et al. 2001).

Pro-inflammatory cytokines also upregulate the expression of InterCellular Adhesion Molecule-1 (ICAM-1) (which binds CD11a or CD11b found on all leukocytes) and VasCular Adhesion Molecule-1 (VCAM-1) (which binds CD49d/CD29 usually found on monocytes) on mesothelial cells, which enhance binding of leukocytes to the peritoneal membrane (Jonjic, Peri et al. 1992; Cannistra, Ottensmeier et al. 1994; Suassuna, Dasneves et al. 1994; Liberek, Topley et al. 1996). Variation of these adhesion molecules may also allow mesothelial cells to selectively regulate the type of cells recruited into the cavity, e.g. decreasing neutrophil attachment and increasing monocyte/macrophage binding, through increasing the proportion of VCAM-1 receptors compared to ICAM-1 receptors present on the peritoneal membrane cell surface (Springer 1990; Liberek, Topley et al. 1996).

Cell migration across the peritoneal membrane is further increased by prostaglandins (PGI_2 and PGE_2), which mesothelial cells enhance by amplifying the levels of transcription and translation of Cyclooxygenase-2 (Cox-2) mRNA. These

prostaglandins augment the permeability of the peritoneal membrane itself allowing easier passage of leukocytes into the cavity (Coene, Vanhove et al. 1982; Steinhauer and Schollmeyer 1986; Topley, Petersen et al. 1994).

Mesothelial cells also assist the acquired immune response by the presentation of foreign antigens on their surface and activating leukocytes in the cavity. When a pathogen invades the peritoneal cavity, IFNγ release acts on mesothelial cells to upregulate the number of MHC class II molecules and human lymphocyte antigen-DR (HLA-DR) on their cell surface and in conjunction with IL15 encourages the activation and proliferation of B, T and NK cells (Valle, Deglinnocenti et al. 1995; Gjersten, Saeterdal et al. 1996; Hausmann, Rogachev et al. 2000).

1.4.4 Neutrophils

Neutrophils develop from myeloid progenitors in the bone marrow and move into the circulatory system, where they are present at high concentrations. Neutrophils are incapable of proliferating, have a limited life span (~3 days) and are programmed to apoptose when recruited into tissues (Akgul, Moulding et al. 2001). Whilst neutrophils are not found in the naive cavity, they are the first cell subset to be recruited into the cavity from the peripheral blood during the innate immune response after the invasion of a pathogen (Hurst, Wilkinson et al. 2001; McLoughlin, Witowski et al. 2003; McLoughlin, Hurst et al. 2004; Jones 2005). Neutrophils accumulate due to the rapid release of the chemoattractant CXCL8 by mesothelial cells and the upregulation of adhesion molecules on the mesothelial cell

surface, which promote margination and transmigration into the cavity (Borregaard and Cowland 1997).

Once in the cavity neutrophils remove invading organisms by phagocytosis and destroy them intracellularly using digestive enzymes. Additionally granules (containing more antimicrobial proteins e.g. β defensins) present within the neutrophil release their contents into the cavity, killing more of the pathogen (Borregaard and Cowland 1997; Faurschou and Borregaard 2003; Dale, Boxer et al. 2008). TLR4 activated platelets can also promote the release of neutrophil extracellular traps (NETs) from neutrophils into the cavity. NETs are made of chromatin and serine protease, which produce a dense region of antimicrobial products that can attach to and destroy pathogens and possibly provide a physical barrier reducing the dissemination of microbes (Brinkmann, Reichard et al. 2004; Clark, Ma et al. 2007).

Aside from pathogen removal, neutrophils can also promote the accumulation of myeloid and lymphocytic leukocytes involved in the inflammatory response by secreting cytokines (such as TNFα, IL1β) and chemoattractants (such as CCL3, CCL4 and CXCL10) whilst in the cavity (Kasama, Strieter et al. 1993; Kasama, Strieter et al. 1994; Cassatella, Gasperini et al. 1997; Cassatella, Gasperini et al. 1997; Scapini, Lapinet-Vera et al. 2000; Molesworth-Kenyon, Popham et al. 2012).

1.4.5 Inflammatory macrophages

Inflammatory macrophages are produced in the bone marrow from the same $CD34^+$ myeloid progenitor cells as resident macrophages (Geissmann, Jung et al. 2003).

However when these cells are released into the circulation they maintain their inflammatory CX_3CR1^{Lo} $CCR2^+$ $GR1^+$ phenotype, so are not chemotactically recruited into the peritoneal cavity during naive conditions (Geissmann, Jung et al. 2003; Gordon and Taylor 2005).

During inflammatory conditions these monocytes are recruited via the release of chemoattractants by mesothelial cells and other leukocytes in the cavity, such as neutrophils and extravasation is promoted by the upregulation of adhesion molecules (Springer 1990; Geissmann, Jung et al. 2003; Jones 2005; Auffray, Fogg et al. 2007). Once in the cavity inflammatory monocytes undergo maturation into inflammatory macrophages and eliminate the pathogen by equivalent processes to resident macrophages (Section 1.4.2) (Gordon and Taylor 2005; Gordon 2007). However inflammatory macrophages have a much greater destructive action than their resident counterparts (Taylor and Gordon 2003; Gordon and Taylor 2005). Once the infection is cleared, inflammatory macrophages are believed to be removed from the cavity by either apoptosis or drainage into the lymphatic system (Bellingan, Caldwell et al. 1996; Messmer and Pfeilschifter 2000).

1.4.6 Peritoneal lymphocytes

B cells are the most common lymphocytic cells found in the naive cavity and these can be further split into the abundant resident B1 cells and more scarce infiltrating B2 cells. In addition to B cells a small population of other resident lymphocytes are also found in the naive cavity; including $CD4^+$ T, $CD8^+$ T, γδ T, NK and NKT cell subsets (Hastings, Tumang et al. 2006; Turchyn, Baginski et al. 2007; Kolaczkowska, Koziol et al. 2009).

It has been suggested that some of these resident lymphocytes may be produced independently of the thymus in lymphoid structures known as milky spots, present in the omentum of the peritoneal membrane (Borisov 1964). These cells may also undergo differentiation within the peritoneal cavity i.e. producing T cells which present the homodimer surface marker $CD8\alpha^{+}\beta^{-}$ (Hartmann, Maassen et al. 1995). However the bulk of resident lymphocytes present within the cavity undergo development in the bone marrow and thymus. Recruitment into the cavity then occurs by the release of chemokines, and migration aided by adhesion molecules (ICAM-1 and VCAM-1) on mesothelial cells (Springer 1990; Cannistra, Ottensmeier et al. 1994; Visser, Tekstra et al. 1998; McLoughlin, Jenkins et al. 2005). Further accumulation of these lymphocytes can occur during an inflammatory response, which if maintained can result in the development of a recurrent inflammatory state that may promote T cell differentiation into mature Th1 cells and IFNγ release (Jones 2005; Fielding et al. appendix).

1.5 Chemokines

Chemokines are a specific group of related cytokines which vary from 8-14 kDa in size and are responsible for regulating inflammatory leukocyte subset activation and migration (Strieter, Standiford et al. 1996; Baggiolini and Loetscher 2000), by interacting with 7 transmembrane G protein coupled receptors and are vital for host defence (Wu, Larosa et al. 1993; Kuang, Wu et al. 1996). Chemokines also fulfil an important function in maintenance of a steady state environment, expansion and cancer metastasis (Baggiolini and Loetscher 2000; Zlotnik and Yoshie 2000).

Chemokines can be separated into 4 subsets, based on the location of their N-terminal cysteines, which are highly conserved and important in tertiary structure formation. Cysteines are either found next to each other (CC chemokines), separated by a single amino acid (CXC chemokines), 3 amino acids (CX_3C chemokine), or have only one N-terminal cysteine (XC chemokines) (Houck and Chang 1977; Adams and Lloyd 1997; Baggiolini, Dewald et al. 1997; Bazan, Bacon et al. 1997; Baggiolini 1998; Segerer, Nelson et al. 2000; Zlotnik and Yoshie 2000) (Figure 1.12).

All chemokines can be viewed as either constitutive or inducible, though there is crossover in function of most. Constitutive chemokines (CCL12, CCL17, CCL25 and CXCL12) are important in maintaining homeostasis by controlling leukocyte movement into secondary tissues. Inducible chemokines, however, are secreted in reaction to an infectious or immune response and are charged with regulating leukocyte chemotaxis to the site of inflammation.

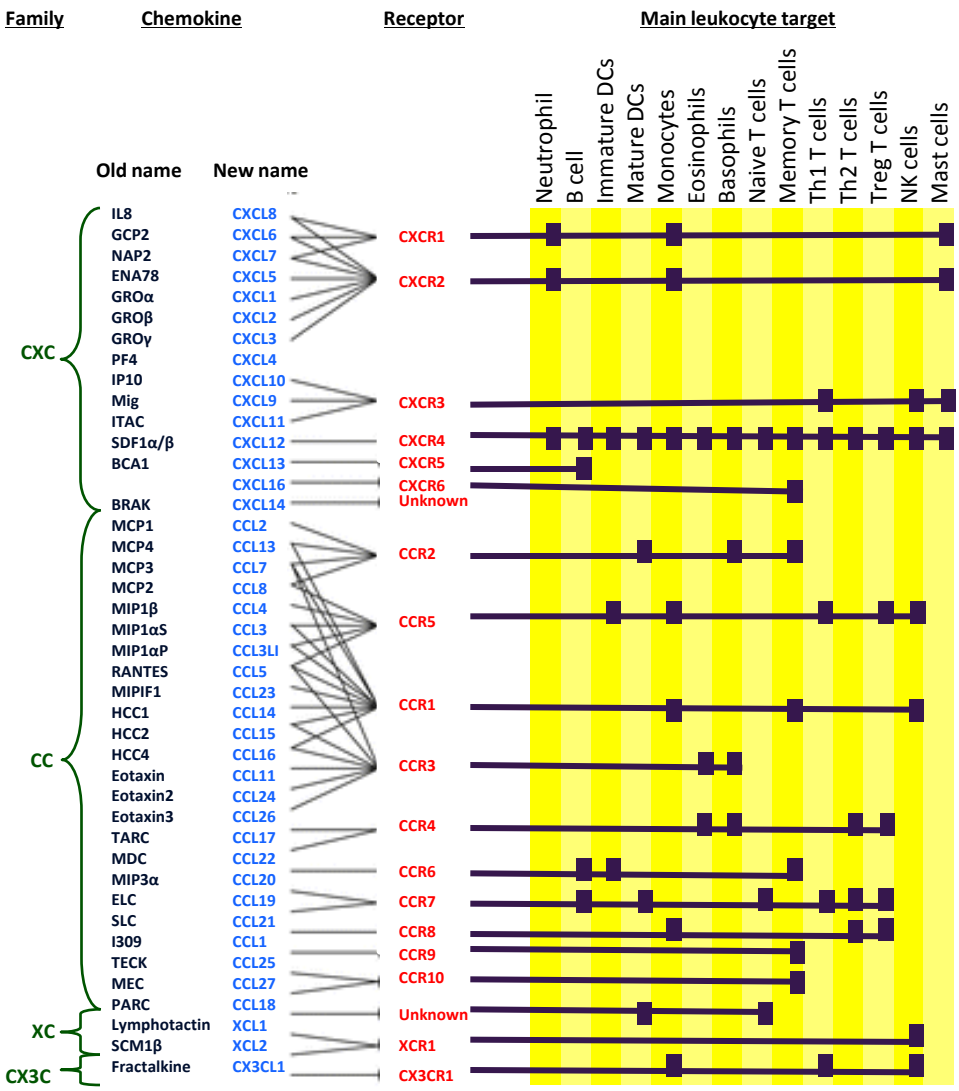

Figure 1.12 - Chemokines and the chemokine receptors which they bind. Chemokines (new classification- light blue text, old classification- dark blue text) and their receptors (red text) can be subdivided into 3 separate families CXC, CC, XC and CX_3C (green text). Many of these chemokines, especially in the CC family are able to bind many different chemokine receptors allowing them to recruit different leukocyte subsets depending on the context of inflammation. Figure adapted from Viola & Luster 2007.

1.5.1 CXC chemokines

The CXC chemokine subset can be further subdivided into 2 groups by the presence (or lack) of an ELR motif located at the N terminus prior to the first cysteine. CXC chemokines that are ELR^+ (CXCL1-8) are important very early during an inflammatory event and bind the chemokine receptors CXCR1 and CXCR2, that are found on neutrophils promoting their movement into the tissue (Strieter, Burdick et al. 2005). Once neutrophils reach the site of inflammation, ELR^+ CXC chemokines can further aid the immune response by encouraging neutrophil degranulation, the release of proteolytic enzymes and activation of the respiratory burst through NADPH oxidase (Jones, Wolf et al. 1996; Jones, Dewald et al. 1997).

ELR^- CXC chemoattractants are predominantly inducible chemokines important in recruiting lymphocyte subsets during an inflammatory event, by binding the chemokine receptors CXCR3 (bound by CXCL9-11) and CXCR5 (bound by CXCL13). However the ELR^- CXC chemokine CXCL12 differs from other ELR^- CXC chemokines in that it is constitutive. CXCL12 binds CXCR4, which is found on a variety of cell types and concerns itself with homeostatic control such as lymphocyte maturation and directly progenitor cells into the correct areas of the bone marrow (Baggiolini 1998; Lapidot, Dar et al. 2005).

1.5.2 CC chemokines

CC chemokines are the largest subset of chemokines and even more promiscuous than any of the other chemokine families. This allows them to act on a greater variety of cell types including monocytes, basophils, eosinophils, T cells, NK and

NKT cells. Release of inducible CC chemokines (CCL2, CCL8, CCL11 and CCL5) after an inflammatory stimulus promotes the movement of these cell subsets to the site of infection. Constitutive CC chemokines (CCL12, CCL17 and CCL25) are released in the lymph node, thymus and other lymphoid tissues and are required to direct T cell movement to secondary lymph nodes (Baggiolini 1998; Kim, Pelus et al. 1998).

1.5.3 CX_3C and XC chemokines

Both of these 2 subsets of chemokines only have one member. CX_3CL1 is the member of the CX_3C subset and in addition to having 3 amino acids separating its 2 N-terminal cysteines, it is also the only identified membrane-bound chemokine (attached by a mucin stalk) and functions as both a chemokine and an adhesion molecule.

XCL1 is in turn the only member of the XC chemokine subset (though it does share homology with the CC subset of chemokines) and has lost 2 of the 4 cysteines present in all other chemokines, 1 of which is one of the 2 N-terminal cysteines which are used to characterise chemokine subsets.

1.5.4 Chemokine receptor/ligand interaction and subsequent downstream signalling

There are 7 transmembrane domain G protein coupled receptors that bind all known chemokines (Wu, Larosa et al. 1993; Kuang, Wu et al. 1996; Murdoch and Finn 2000). Many receptors can bind multiple chemokines, thus individual chemokines

are capable of the recruitment of more than one cell subset so regulation of receptor expression on cells is vital to ensure specificity of chemokine action (Kuang, Wu et al. 1996; Segerer, Nelson et al. 2000; Moser, Wolf et al. 2004). In addition to these classical receptors there are a small number of atypical chemokine receptors (such as Duffy antigen receptor for chemokines (DARC), D6, CXCR7 and CCXCKR) which are defined by an apparent absence in signalling after chemokine binding. This lack of signalling in atypical chemokine receptors is predominantly due to a missing or modified DRYLAIV motif (located in the second intracellular loop of the receptor) which is important in connecting the receptor to the G protein. However these atypical chemokine receptors can impact chemokine/receptor interactions by acting as internalising receptors that either; 1) take up and degrade chemokines (such as D6) or 2) transfer internalised chemoattractants through biological barriers (DARC) (Mantovani, Locati et al. 2001; Graham 2009; Ulvmar, Hub et al. 2011).

When a chemokine binds its ligand the extracellular section of the receptor changes shape, permitting the intracellular section to stimulate the G protein. The G protein is made up of 3 subunits (α,β and γ) and after chemokine binding the exchange of GDP for GTP leads to the separation of the α subunit from the βγ complex. This split can activate other intracellular pathways including increased intracellular calcium, activation of the MAP3K pathway, Phosphatidylinositol 3-kinase (PI3K) and NFκβ pathway (Murdoch and Finn 2000; Rossi and Zlotnik 2000).

1.6 Aims

There were 3 primary aims of this thesis that can be summarised as follows:

- **Examine TL1A and DR3 expression patterns in the peritoneal cavity.** The expression profile of DR3 was determined on leukocytes and on the stroma in the naive cavity and whether this expression changed after the induction of an acute *Staphylococcus epidermidis* supernatant (SES) induced inflammatory event was investigated. The peritoneal membrane and resident macrophages were also investigated as potential sources of TL1A following the induction of acute inflammation.

- **Investigate the role of DR3 in the peritoneal cavity during; (i) homeostasis, (ii) innate inflammation and (iii) repeated inflammation using an *in vivo* experimental mouse model of SES induced inflammation.** Resident peritoneal and peripheral blood leukocytes were characterised in $DR3^{-/-}$ mice and compared to $DR3^{+/+}$ mice, to determine if DR3 played a role in maintaining homeostasis. The potential role of DR3 in the accumulation of leukocytes during the early and late phase of innate inflammation were then examined by challenging with SES. Any DR3-dependent affects on fibrosis of the mesothelial layer were then studied following repeated induction of inflammation.

- **Establish the mechanism DR3 may utilise to affect the numbers of specific leukocyte subsets during acute inflammation.** Cell subset proliferation and chemokine levels from supernatants were determined in $DR3^{-/-}$ mice and compared to $DR3^{+/+}$ mice following SES challenge. The peritoneal membrane was also investigated as a potential source of chemoattractants in $DR3^{+/+}$ mice and how this may vary in $DR3^{-/-}$ mice during acute inflammation.

Chapter 2 - Materials and Methods

2.1 Reagents

2.1.1 Chemicals

All chemicals were purchased from Sigma-Aldrich Co. Ltd (Poole, Dorset) unless otherwise stated

2.1.2 Solutions

Orange G (DNA loading buffer)

2.5 mg/ml Orange G loading dye in 2x Tris/Borate/EDTA (TBE) containing 30 % (w/v) glycerol

Eosin solution

10 mg/ml Eosin dissolved in distilled H_2O

FACS buffer

PBS containing 1 % (v/v) Foetal calf serum (FCS) and 2 mM EDTA

Freezing Medium

90 % (v/v) FCS and 10 % (v/v) Dimethyl sulfoxide (DMSO)

Lysis buffer

0.5 ml 50 mM TRIS-HCl (pH 8), 1ml 10 % (w/v) SDS, 2 ml 0.5M EDTA, 1 ml 1 M NaCl, 100 µl 10mg/ml proteinase K (Roche), 5 ml distilled H_2O

10 % Neutral Buffered Formal Saline (NBFS)

3.7 % (w/v) Formaldehyde, 46 mM Sodium phosphate dibasic (Na_2HPO_4)

Phosphate Buffered Saline (PBS)

0.8 % (w/v) sodium chloride, 0.2 % (w/v) potassium chloride, 0.12 % (v/v) anhydrous sodium hydrogen phosphate at pH 7.4

Wash Buffer (PBS-Tween20)

PBS containing 0.05 % (v/v) Tween20

RAW 264 Culture medium

Dulbecco's Modified Eagle's Medium-10 (DMEM-10) (Invitrogen Ltd**,** Paisley, UK) with 10 % (v/v) FCS, 2 mM L-Glutamine, 100 U/ml Penicillin, 100 U/ml Streptomycin, 5 mg/ml Insulin/Transferrin and 0.4 mg/ml Hydrocotisone.

TBE (10X)

54 g TRIS, 27.5 Boric acid dissolved in distilled H_2O to final volume of 990 ml and 10 ml 1M EDTA pH 8 added.

TBE agarose gel

1x TBE containing 1.6 % (w/v) agarose

Tris Buffered Saline (TBS)

0.05 M Tris, 0.15 M NaCl pH 7.6

2.2 Animals and *in vivo* experiments

2.2.1 Housing conditions and Home Office approval

All animals were housed in the Joint Biological Services Unit (at Heath Park, Cardiff University) at a room temperature range of 18-23 ˚C and a relative humidity of 55 ± 10 % on a 12 hour light/dark cycle. Animals were kept in filter top containers until they were transferred to conventional housing for intra-peritoneal (i.p.) administration of SES. Food and water was available to the animal's ad libitum, as well as environmental enrichment in the form of cardboard tubes. $DR3^{+/+}$ and $DR3^{-/-}$ animals were bred in house on a C57/BLK6J background. All experimental procedures complied with the Home Office approved licence 30/2401.

2.2.2 Genotyping

2.2.2.1 DNA extraction

Ear punches were lysed at 56 ˚C overnight in lysis buffer, DNA was extracted by the addition of 310 µl 5M sodium chloride (NaCl), which was vortexed and left at room temperature for 1 hour. This was centrifuged at 13000 rpm for 25 minutes, and 800 µl of the aqueous phase was removed and added to 500 µl of chilled (-20 ˚C) isopropanol. This was vortexed and centrifuged at 13000 rpm for 10 minutes. The supernatant was removed and the pellet resuspended in 500 µl of 70 % ethanol for 30 minutes at room temperature. This was centrifuged at 13000 rpm for 10 minutes and supernatant removed. Any remaining ethanol was removed by air-drying for 1 hour at 37 ˚C. The remaining pellet was resuspended in 50 µl distilled H_2O (for longer storage resuspended in 10 mM Tris) and incubated at 37 ˚C for 3 hours.

2.2.2.2 Genotyping PCR

Using thin walled PCR tubes, 8 µl of the DNA extracted (Section 2.2.2.1) was added to 20 µl of distilled H_2O. A master mix was made up consisting of 5 µl Deoxynucleotide triphosphates (dNTPs), 4 µl 10x PCR buffer, 1.2 µl of Magnesium chloride ($MgCl_2$) , 0.2 µl 100 µM Av1 primer, 0.4 µl 100 µM 4F primer, 0.8 µl 100 µM 2R primer and 0.5 µl *Taq* DNA polymerase per sample. This master mix (12.1 µl) was aliquoted into the PCR tubes and the samples were run on a thermocycler (Hangzhou Long Gene Scientific Instruments Co, Zhejiang, China) using the following program.

Primers:

Av1- 5’ CAT CGC CTT CTA TCG CCT TC 3’

2R- 5’ GAA AGG ATG AAA CTT GCC TGT TGG 3’

4F- 5’ AGA AGG AGA AAG TCA GTA GGA CCG 3’

Thermocycling program:

Denaturation:	94 ˚C for 5 minutes	
Annealing:	62.5 ˚C for 30 seconds	1 cycle
Extension:	72 ˚C for 40 seconds	

Denaturation:	94 ˚C for 30 seconds	
Annealing:	62.5 ˚C for 30 seconds	33 cycle
Extension:	72 ˚C for 40 seconds	

Denaturation:	95 ˚C for 30 seconds	
Annealing:	62.5 ˚C for 30 seconds	1 cycle
Extension:	72 ˚C for 5 minutes	

After completion of the PCR protocol, DNA from the samples was separated by size using gel electrophoresis. Samples were mixed with 4 µl of Orange G loading buffer and 20 µl of each sample was loaded onto a 1.6 % gel (v/v), which included 7.5 µl of ethidium bromide, this gel was submerged under 1x TBE buffer in a gel tank. The samples (including a positive and negative control) along with a 100 base pair (bp) DNA ladder were run for 90 minutes at 100 volts and visualised under UV light (Ultra-Violet Products Ltd**,** Trinity Hall Farm Estate, Cambridge, UK) (Figure 2.1).

2.2.3 Harvesting of peripheral blood and intra-peritoneal cell populations

2.2.3.1 Intra-peritoneal lavage

Mice were sacrificed using a rising concentration of carbon dioxide (CO_2), followed by cervical dislocation (schedule 1). The peritoneal membrane was exposed by removing the skin over the abdomen. A ventflon 2 intra-venous cannula (18 gauge (G), 45 mm) (Becton Dickinson Ltd, Cowley, Oxford, UK) was inserted through the abdominal wall and into the cavity, the intra-venous cannula was removed leaving the ventflon in the cavity. The peritoneal cavity was lavaged using a 2.5 ml syringe (Becton Dickinson Ltd, Cowley, Oxford, UK) containing 2 ml of PBS, which was attached to the plastic injection port of the ventflon and plunger depressed. Fluid was allowed to reside in the cavity for 30-60 seconds and then as much as possible (1.7 ml-2.0 ml) was recovered into the 2.5 ml syringe via the ventflon and stored on ice in a 2 ml eppendorf tube (Greiner Bio One Ltd, Stonehouse, UK).

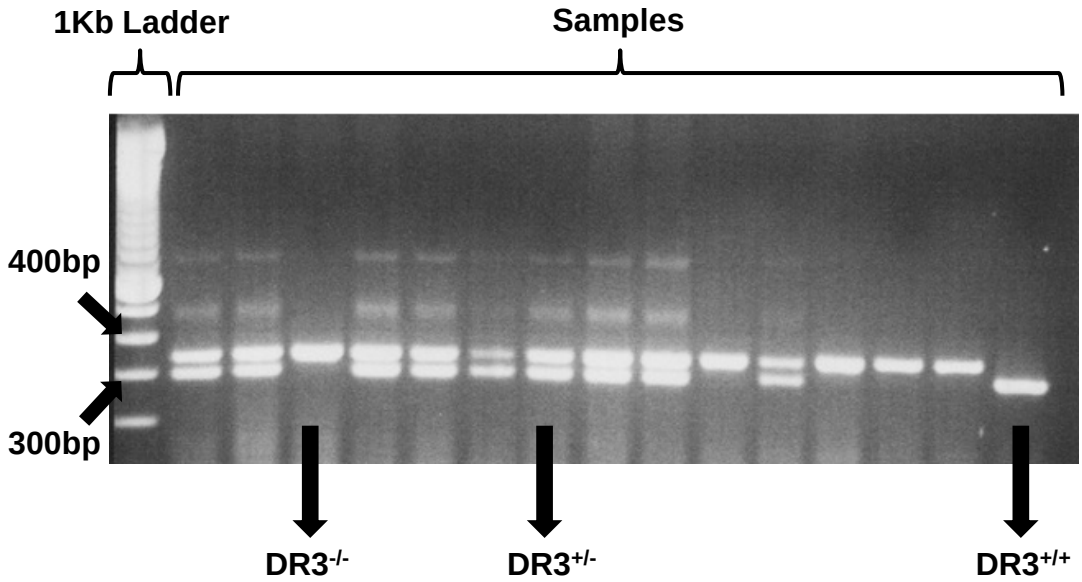

Figure 2.1 – DR3 genotyping PCR gel. Sample DNA was separated by size using gel electrophoresis (1.6% TBE agarose gel (v/v) and 7.5µl of ethidium bromide, submerged in 1x TBE buffer) and visualised under UV light. $DR3^{+/+}$ mice were identified by one band at a molecular weight of 280bp, which equates to the DR3 gene coding region. $DR3^{-/-}$ mice were identified by one band at a larger molecular weight of 320bp, that equates to the inserted construct which replaced the DR3 gene. $DR3^{+/-}$ mice were identified by two bands, which are made up of both the $DR3^{+/+}$ band (280bp) and $DR3^{-/-}$ band (320bp) as $DR3^{+/-}$ mice contain both $DR3^{+/+}$ and $DR3^{-/-}$ alleles.

2.2.3.2 Cardiac puncture

Mice were sacrificed using a rising concentration of CO_2 followed by cervical dislocation (schedule 1). The heart was exposed by pinning back the rib cage and a 25 G, 16 mm needle (Becton Dickinson Ltd, Cowley, Oxford, UK) containing 1 µl of heparin, attached to a 2.5 ml syringe (Becton Dickinson Ltd, Cowley, Oxford, UK) was inserted into the heart ventricle. Blood was collected in the syringe by maintaining a constant pressure by slowly pulling back the syringe plunger, to avoid collapsing the heart. As much blood as possible was extracted into the syringe and stored on ice in a 2 ml eppendorf tube.

2.2.4 Determination of peritoneal leukocyte numbers

Total number of peritoneal leukocytes present in each peritoneal lavage sample was counted using a Coulter counter Z2 (Beckman Coulter UK Ltd., Oakley Court, High Wycombe, UK). Well-mixed lavage (20 µl) was diluted in 20 ml of isoton 2 balanced electrolyte solution (Beckman Coulter UK Ltd., Oakley Court, High Wycombe, UK) in a Coulter vial and inserted into the machine. From this, 2 counts were taken and averaged to give the number of cells per ml.

2.2.5 *S. epidermidis* supernatant (SES)

2.2.5.1 Preparation of *S. epidermidis* supernatant

A stored *S. epidermidis* stock (from the peritoneal effluent of a peritonitis patient), on Dorset egg medium slopes (Oxoid, Basingstoke, UK) was used to inoculate a

Diagnostic Sensitivity testing (DST) agar plate (Oxoid, Basingstoke, UK) and incubated at 37 ˚C (Heraeus Instruments, Buckinghamshire, UK) for 48 hours. A single colony of *S. epidermidis* (white circular colony) was inoculated into 500 ml of Nutrient broth 2 (Oxoid, Basingstoke, UK) and incubated overnight at 37 ˚C with shaking (170 rpm). The bacterial culture was centrifuged at 4000 g for 20 minutes at 20 ˚C (Sorvall Laboratory Centrifuges, Buckinghamshire, UK). The supernatant was removed and bacteria (pellet) resuspended in Tyrodes salt solution (Sigma-Aldrich Co. Ltd, Poole, Dorset, UK) until an optical density (using a Beckman DU-64 spectrophotometer, Beckman Coulter UK Ltd., Oakley Court, High Wycombe, UK) of 0.5 at 560 nm was achieved (which is equivalent $5x10^8$ colony forming units/ per ml) and incubated for 24 hours at 37 ˚C.

The bacterial culture was centrifuged at 4000 g for 30 minutes at 20 ˚C and the supernatant removed and filter sterilised (0.22 µl Stericup filter bottle, Millipore, Livingston, UK) to eliminate any remaining live bacteria. Once filtered, excess salts in the solution were removed by transferring 60 ml aliquots of the solution into dialysis membrane tubing (Medicell International Ltd, London, UK), which was fastened at either end and placed in water (at a ratio of 2 tubes/5 litres). The water was changed 4 times every 12 hours, to maintain the osmotic gradient. This final solution was pooled and dispensed into 10 ml aliquots which were freeze dried and kept at -70 ˚C until use.

2.2.5.2 *S. epidermidis* supernatant activity bioassay

To replicate levels of SES activity between *in vivo* experiments SES activity was standardised. To assess this, SES induced IL6 release from the mouse macrophage

cell line RAW 264 (European Collection of Cell Cultures, Sailsbury, Wiltshire) was measured using a commercially available ELISA (Figure 2.2).

2.2.5.3 RAW 264 mouse macrophage culture

RAW 264 cells were cultured in 75 cm^2 cell culture flasks (Corning B.V. Life Sciences, Amsterdam, The Netherlands) containing supplemented DMEM-10 (Invitrogen Ltd**,** Paisley, UK). These cells were kept in a humidified incubator in an atmosphere of 5 % CO_2. Cells were passaged every 3-4 days, using 5 ml 0.05 % Trypsin-EDTA (Invitrogen Ltd**,** Paisley, UK) to detach cells from the surface of the flask. Once detached the Trypsin-EDTA was inactivated by the addition of 10 ml of fresh supplemented DMEM-10.

Once a density of $7.5x10^4$ cells/ml was reached, RAW 264 cells were seeded into 24 well plates in 1 ml volumes of DMEM-10 and were allowed to adhere for 3 hours. A freeze dried aliquot of SES was reconstituted with DMEM-10 and serial dilutions prepared (Dilutions- Neat, 1/2, 1/10, 1/50, 1/100). These SES dilutions were added to the RAW 264 cells and along with an unstimulated negative control incubated for 24 hours. Supernatants were then collected in eppendorfs and stored at -70 ˚C until quantitation for IL6 by ELISA (Figure 2.2).

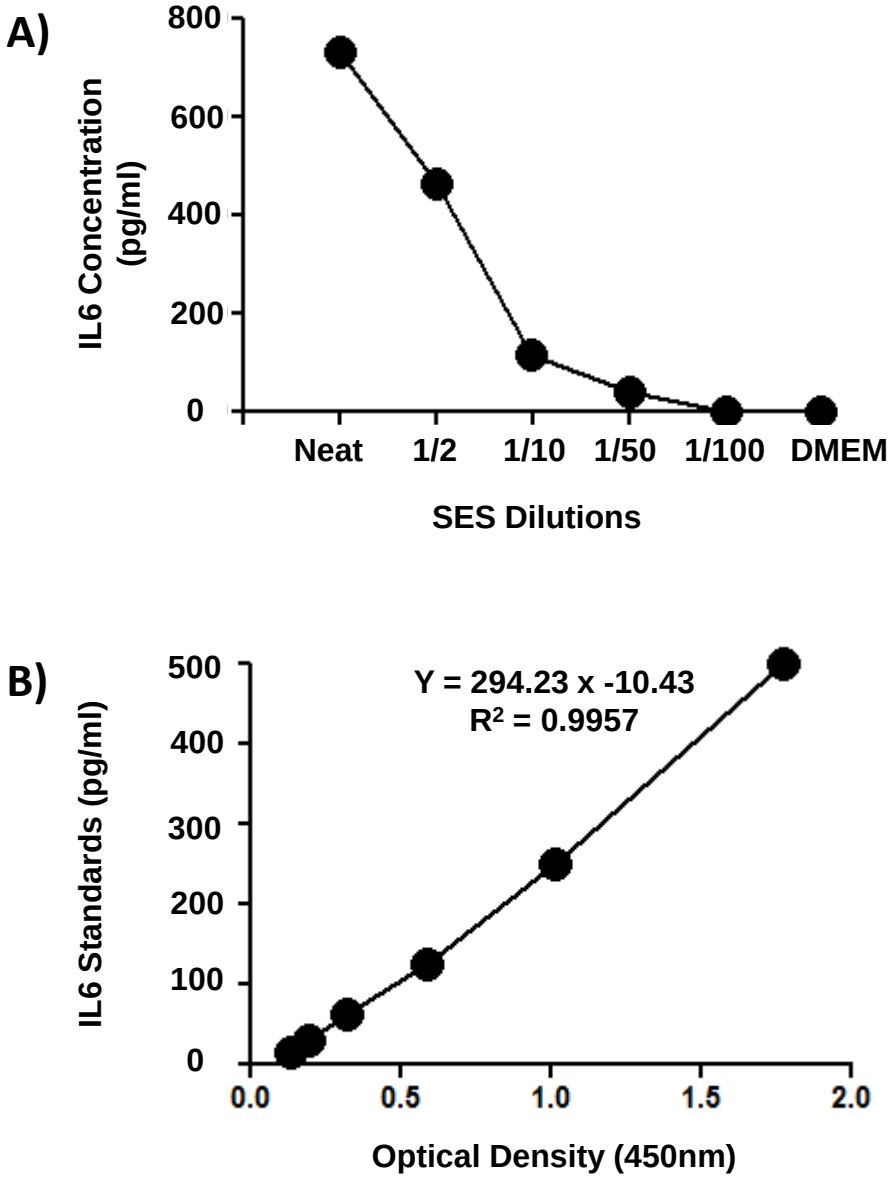

Figure 2.2 – *In vitro* bioactivity assay of *S. epidermidis* supernatant (SES) on RAW 264 cells. A) RAW 264 cells (a mouse leukaemic monocyte-macrophage cell line) were used to test each batch of SES before its use *in vivo*, this was accomplished by stimulating RAW 264 cells at a density of $7.5x10^4$ cells/ml with several dilutions of SES (Neat, 1/2, 1/10, 1/50, 1/100 and a negative DMEM control). After a 24 hour incubation, supernatants were removed and SES quantified by measuring IL6 levels by ELISA (each symbol represents IL6 production per $7.5x10^4$ RAW 264 cells/ml). B) Optical density (OD) was measured at 450 nm using a FLUOstar microplate reader (Omega BMG Labtech), IL6 levels were then calculated from the OD using IL6 standards to plot a standard curve, producing a linear equation (Y= 294.23 x -10.43, R2 = 0.9957). This equation was used to calculate IL6 concentration from the optical density.

2.2.5.4 Cryopreservation of cells

Cells were put into suspension using Trypsin-EDTA and centrifuged at 400 g for 4 minutes. The supernatant was poured away and cells resuspended in freezing media and aliquoted into cryovials at $1x10^6$ cells per ml. All cryovials were placed in a Nalgene 5100 Cryo 1 ˚C freezing container containing isopropanol at room temperature and left in a -70˚C freezer overnight. Cryovials were then moved into liquid nitrogen storage.

2.2.6 Intra-peritoneal administration of *S. epidermidis* supernatant

Before all injections, all animals were gently scruffed to expose the abdominal area. SES (500 µl) (which was prepared under sterile conditions in a MicroFlow Biological class 2 safety cabinet) was injected i.p. using a 1 ml syringe (Becton Dickinson Ltd, Cowley, Oxford, UK) attached to a 25 G, 16 mm needle (Becton Dickinson Ltd, Cowley, Oxford, UK). I.p. injections were made into the lower abdomen, (avoiding the bladder) using the line of the hip as a guide to run parallel with the abdominal skin surface. Post injection, animals were placed in a separate cage where their recovery was observed.

2.2.6.1 Acute model of SES induced peritoneal inflammation

Each mouse received a single i.p. injection of 500 µl of SES as outlined above. Mice were sacrificed by schedule 1 at 8 defined time points over a 96 hour time course and the contents of the peritoneal cavity collected by peritoneal lavage (Section 2.2.3.1) and membrane collected by snap freezing in liquid nitrogen.

2.2.6.2 Recurrent model of SES induced peritoneal inflammation

Repeated inflammation was induced in mice by 4x 500 µl i.p. injections of SES (administered as outlined in Section 2.2.6) over the time course. Each mouse received one i.p. injection per week for 4 weeks (injections administered on day 0, 7, 14 and 21) and aged to the endpoint (day 49) of the time course. Mice were sacrificed by schedule 1 and the contents of the peritoneal cavity collected by lavage (Section 2.2.3.1) and membrane collected and fixed using 10 % neutral buffered formal saline (NBFS) (Section 2.6.1).

2.3 Phenotypic analysis of peritoneal leukocytes using flow cytometry

2.3.1 Preparation of peritoneal leukocytes for flow cytometry

Peritoneal leukocytes were harvested from the cavity of mice as previously described in Section 2.2.3.1. These leukocytes were isolated by centrifugation at 1600 g for 2 minutes in 15 ml centrifuge tubes (Corning B.V. Life Sciences, Amsterdam, Netherlands). The supernatant was removed without disturbing the cell pellet and frozen down at -70 ˚C for chemokine testing. The cell pellet was resuspended in 1 ml of FACS buffer and 200 µl of cells were added to the assigned well of a U bottomed 96 well plate (NUNC A/S Roskilde, Denmark).

2.3.2 Staining of peritoneal leukocytes with fluorochrome conjugated antibodies

Once peritoneal leukocytes had been transferred to the U bottomed 96 well plate they were centrifuged at 1600 g for 2 minutes and supernatant removed without disturbing the pellet. Cells were reuspended by gently tapping the plate, followed by

the addition of 50 µl of Fc Block (CD16/CD32) diluted (1/200) in FACS buffer to all wells and incubated at 4 ˚C for 30 minutes. Cells on the plate were centrifuged at 1600 g for 2 minutes and supernatant discarded. All primary conjugated antibody cocktails were diluted to their optimum concentration (verified by titration) in FACS buffer (Table 2.1) and 50 µl was added to the appropriate wells and incubated at 4 ˚C for 30 minutes. Identical antibody preparation of isotype control and single colour controls were carried out, and only FACS buffer was added to 1 well of cells to provide an unstained control sample. The best antibody dilutions were determined by antibody dose response titration measurements. After incubation, cells were centrifuged at 1600 g for 2 minutes and supernatant removed. Cells were washed 3 times with 200 µl of FACS buffer and centrifuged at 1600 g for 2 minutes between each wash. Where required (DR3 staining) cells were incubated at 4 ˚C for 30 minutes with a suitable fluorochrome conjugated streptavidin secondary to bind a biotinylated primary antibody. Cells were washed 3 times with 200 µl of FACS buffer and centrifuged at 1600 g for 2 minutes between each wash. The contents of each well were resuspended in 200 µl of FACS buffer and transferred into microtubes for analysis via flow cytometry.

2.3.3 Preparation of peripheral blood leukocytes for flow cytometry

Prior to staining peripheral blood leukocytes, as outlined above in Section 2.3.1 contaminating red blood cells (RBC) were lysed from the sample. Cells were pelleted by centrifuging at 1600 g for 2 minutes, the supernatant was removed and cells resuspended in 5 ml of 1x RBC lysis buffer (Biolegend) (diluted 1/10 from a 10x concentrated stock using deionised water) for 5 minutes on ice. The reaction was stopped by adding 20 ml of PBS to the sample; cells were centrifuged at 1600 g for

2 minutes and supernatant removed. Peripheral blood leukocytes were resuspended in FACS buffer and counted as outlined in Section 2.2.4, 200 µl of cells were added to the assigned well of a U bottomed 96 well plate and antibody staining carried out as show in Section 2.3.1.

2.3.4 Intracellular staining of peritoneal leukocytes

Peritoneal leukocytes were fixed in 4 % paraformaldehyde and spun at 1600 g for 2 minutes, the supernatant was removed and cells permeabilised using 100 µl of saponin buffer (500 ml 1x PBS, 2.5 ml 10 % sodium azide, 2.5 g saponin) for 20 minutes at 4 ˚C. Following permeabilisation cells were centrifuged at 1600 g for 2 minutes and supernatant removed, cells were reuspended by gently tapping the plate. The intracellular antibody was diluted to its optimum concentration (Table 2.1) in saponin buffer and 50 µl was added per well and incubated at 4 ˚C for 30 minutes. Cells were washed twice with saponin buffer and centrifuged at 1600 g for 2 minutes between each wash, a final wash with FACS buffer and spin at 1600 g for 2 minutes was carried out and cells resuspended in 200 µl of FACS buffer and transferred into microtubes for analysis via flow cytometry.

2.3.5 DR3 staining for analysis of peritoneal leukocytes by flow cytometry

DR3 staining was achieved following the steps outlined in Section 2.3.1, up to the addition of 50 µl of Fc Block (CD16/CD32) in diluted FACS buffer. Following this step, cells were resuspended in 200 µl FACS buffer containing 1 % (v/v) normal goat serum and incubated for 30 minutes at 4 ˚C. Cells were centrifuged at 1600 g

for 2 minutes and supernatant discarded. The biotinylated DR3 antibody (or biotinylated Goat IgG isotype control) along with any other primary antibodies were added at their optimum concentration (Table 2.1) in FACS buffer containing 0.5 % normal goat serum and incubated for 30 minutes at 4 ˚C. The remainder of the steps described in Section 2.3.1, including the addition of fluorochrome conjugated secondary reagents, were then followed.

Table 2.1 - Mouse antibodies used for flow cytometry

	Antibody	Fluorochrome	Supplier	Clone	Catalogue Number	Dilution	Isotype
Target Antibody	CD19	FITC	BD Pharmingen	ID3	557398	1/200	Rat IgG_{2a}
	MHC 2 (I-A/I-E)	FITC	BD Pharmingen	2G9	553623	1/200	Rat IgG_{2a}
	CD8a	FITC	BD Pharmingen	53-6.7	553030	1/100	Rat IgG_{2a}
	KI67	FITC	BD Pharmingen	MOPC-21	556026	1/5	Mouse IgG_1
	NK1.1	PE	BD Pharmingen	PK136	553165	1/200	Mouse IgG_{2a}
	B220 (CD45R)	PE	Invitrogen	RA3-6B2	RM2604	1/200	Rat IgG_{2a}
	Ly-6B.2	PE	AbD Serotec	7/4	MCA771PE	1/200	Rat IgG_{2a}
	Gr-1	PerCP-cy5.5	BD Pharmingen	RB6-8C5	552093	1/500	Rat IgG_{2b}
	CD4	PerCP-cy5.5	BD Pharmingen	RM 4-5	550954	1/200	Rat IgG_{2a}
	CD11c	PE-Cy7	BD Pharmingen	CX1	558078	1/100	Rat IgG_{2b}
	Ly-6G	V450	BD Horizon	1A8	560603	1/200	Rat IgG_{2a}
	CD44	V450	BD Horizon	IM7	560452	1/200	Rat IgG_{2b}
	F4/80	APC	Invitrogen	BM8	MF48005	1/400	Rat IgG_{2a}
	TCR αβ	APC	Caltag Laboratories	H57-597	HM3605	1/100	Hamster IgG
	CD11b	APC-Cy7	BD Pharmingen	M1/70	557657	1/500	Rat IgG_{2b}
	CD3	APC-Cy7	BD Pharmingen	17A2	560590	1/400	Rat IgG_{2b}
	DR3	Biotin	RnD Systems	*	BAF2437	1/100	Goat IgG
Isotype Controls	Rat IgG_{2a}	FITC	BD Pharmingen	R35-95	554688	1/100	-
	Rat IgG_{2b}	PE	BD Pharmingen	A95-1	553989	1/100	-
	Mouse IgG_{2a}	APC	RnD Systems	20102	IC003A	1/200	-
	Hamster IgG	APC-Cy7	BioLegend	HTK888	400927	1/100	-
	Goat IgG	Biotin	RnD Systems	*	BAF108	1/100	-
Other	CD16/CD32 (Fc Block)	Purified	BD Pharmingen	2.4G2	553142	1/200	Rat IgG_{2b}
	Streptavidin	APC	Invitrogen	-	S-32362	1/500	-
	7AAD	-	BD Pharmingen				

*Polyclonal antibody

2.3.6 Flow cytometry acquisition

Data on peritoneal leukocytes stained with fluorochrome conjugated antibodies were collected by running cells (including the unstained, isotype and single colour controls) through a Beckman Coulter CyAn™ ADP Analyzer Flow Cytometer (Beckman Coulter Ltd, High Wycombe, UK). All analysis and compensation was carried out offline in Summit software v4.2 (Beckman Coulter Ltd**,** High Wycombe, UK).

2.3.7 Beckman Coulter CyAn™ ADP Analyzer Flow Cytometer operation procedure and cell acquisition

Operation of the Beckman Coulter CyAn was achieved using the Summit computer program. Following the manufacturer's guidelines a protocol was designed, including either histograms or dot plots of the required parameters. Data were acquired by placing the sample tube on the probe. Events were collected automatically, following an initial boost at the start of acquisition. Once sufficient events were acquired, the F2 and F3 keys stopped and saved the sample data collected, this was repeated for all samples (all compensation was carried out offline and will be addressed later). Once all sample data were collected the flow cytometer was shut down.

2.3.8 Multi-parameter flow cytometry compensation

The Beckman Coulter CyAn™ ADP Analyzer Flow Cytometer allows 9 cellular markers to be analysed at once providing the emission peaks of different fluorochromes are sufficiently separated to be detected by different detectors (Table 2.2), though the emission tails of neighbouring channels fluorochromes overlap (spectral overlap). This was overcome by using the compensation function in the Summit software, as outlined by the manufacturer's instructions.

Table 2.2 - Flow cytometry fluorochromes and related detectors

Detector	Fluorochrome	Abbreviation	Emission peak	Laser	Voltage
FL1	Fluorescein isothiocyanate	FITC	521 nm	Argon 488	550
FL2	Phycoerythrin	PE	578 nm	Argon 488	650
FL3	Phycoerythrin Texas Red	PE Texas Red	615 nm	Argon 488	700
FL4	Peridinin-chlorophyll protein-cyanine5.5	PerCP-cy5.5	695 nm	Argon 488	750
FL5	Phycoerythrin Cyanine 7	PE cy7	767 nm	Argon 488	752
FL6	Violet 450	V450	448 nm	He-Ne 633	600
FL8	Allophycocyanin	APC	660 nm	Violet 405	850
FL9	Allophycocyanin Cyanine 7	APC cy7	767 nm	Violet 405	900

2.3.9 Calculation of peritoneal leukocyte populations

The previously designed protocol (Section 2.3.7) contained dot plots which divided the total leukocyte population into various subsets (Figure 2.3-2.5) using previous defined cellular phenotypic markers (Table 2.3), (which are linked to an appropriate fluorochrome) on the XY axis. Gates were drawn around the identified subpopulation providing the percentage of that subpopulation in the sample. This percentage was used to find the total number of that subpopulation in the sample by multiplying the subpopulation percentage against the total leukocyte cell count (determined in Section 2.2.4).

2.3.10 Cell sorting of resident macrophages

Cells were harvested from the cavity as described in Section 2.2.3.1 and stained with the fluorochrome conjugated antibodies CD11b and F4/80 outlined in Section 2.3.2. Leukocytes were then outsourced to Central Biotechnology Services (CBS) for cell sorting; this involved passing all leukocytes though a BD Aria flow cytometer which separated resident macrophages ($CD11b^{+}$, $F4/80^{+}$) from other cell subsets, producing a pure population.

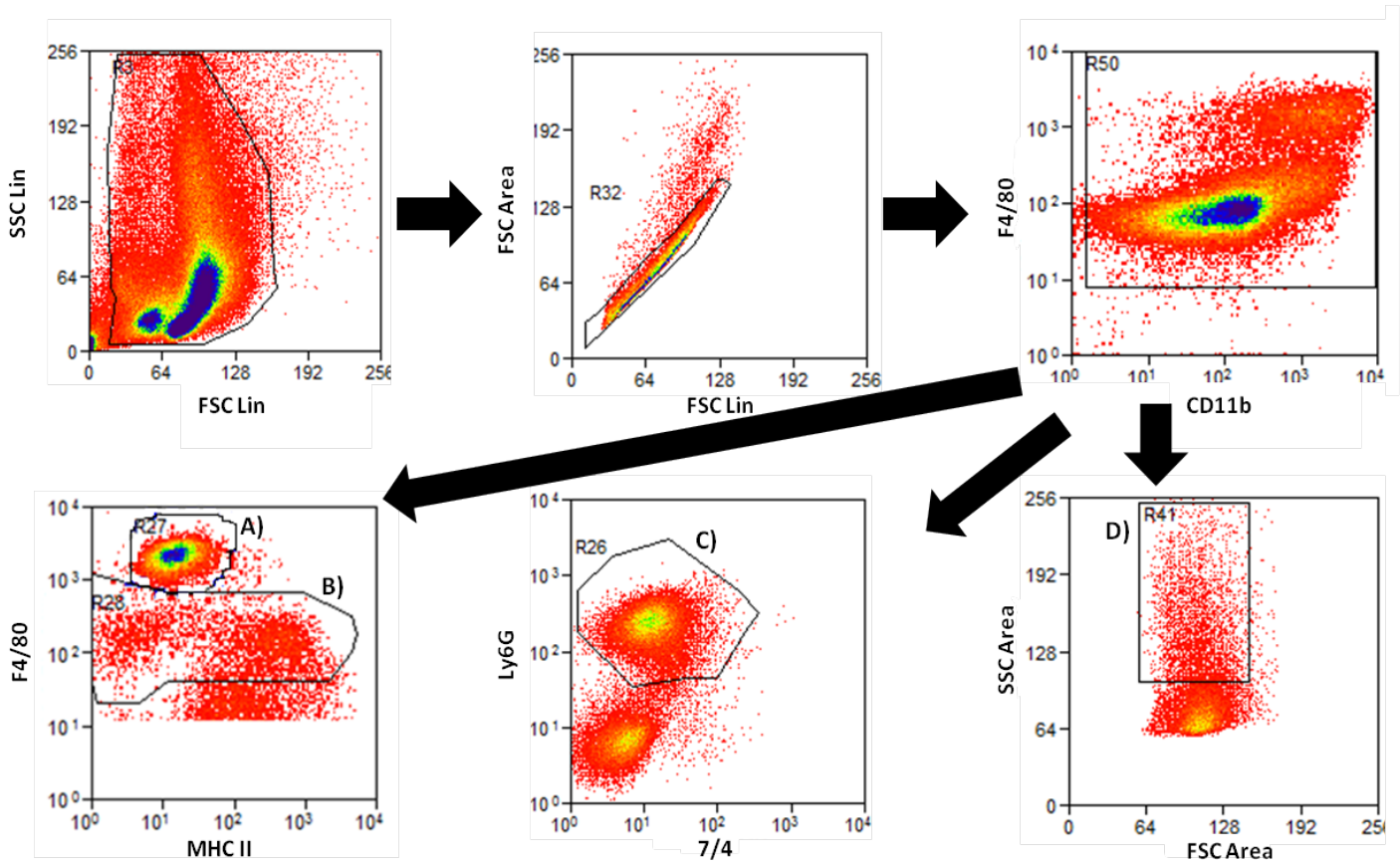

Figure 2.3 – Identification of specific myeloid subsets by flow cytometry. Myeloid subsets were identified by staining cells with specific monoclonal antibodies linked to fluorochromes. Leukocytes were passed through a flow cytometer and myeloid subsets identified by their known cellular markers. A) Resident Macrophages ($F4/80^{+}$, $CD11b^{+}$) B) Inflammatory Macrophages ($F4/80^{int}$, $CD11b^{int}$) C) Neutrophils ($7/4^{+}$, $LY6\text{-}G^{+}$) D) Eosinophils ($F4/80^{int}$, $CD11b^{int}$, FSC-A+ SSC-A)

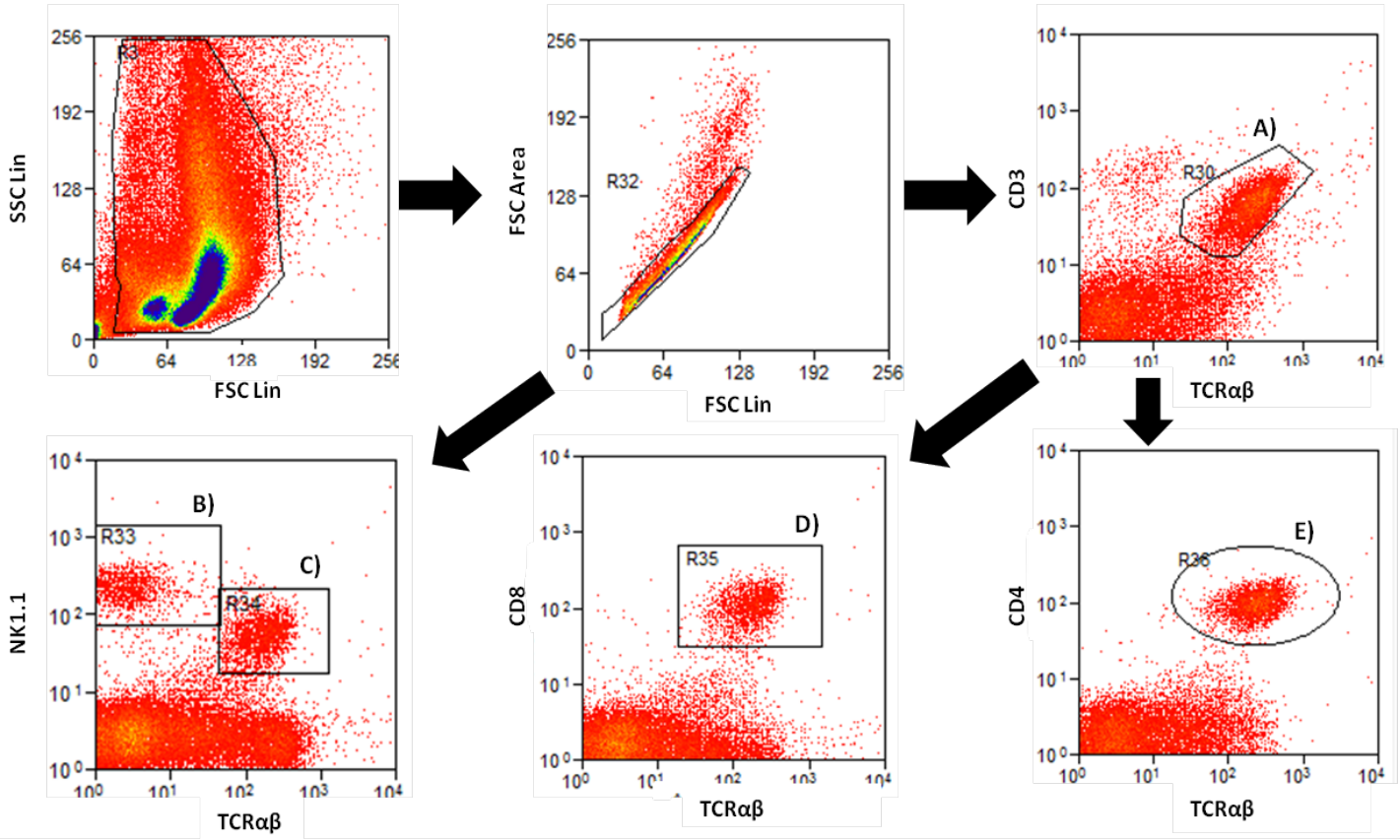

Figure 2.4 - Identification of specific T & NK lymphocyte subsets by flow cytometry. T & NK cell subsets were identified by staining cells with specific monoclonal antibodies linked to fluorochromes. Leukocytes were passed through a flow cytometer and lymphocyte subsets identified by their known cellular markers. A) T cells ($CD3^+$, TCR^+) B) NK Cells ($NK1.1^+$, TCR^-) C) NKT Cells ($NK1.1^+$, TCR^+) D) Cytotoxic T cells ($CD8^+$, $CD3^+$, TCR^+) E) Helper T Cells ($CD4^+$, $CD3^+$, TCR^+)

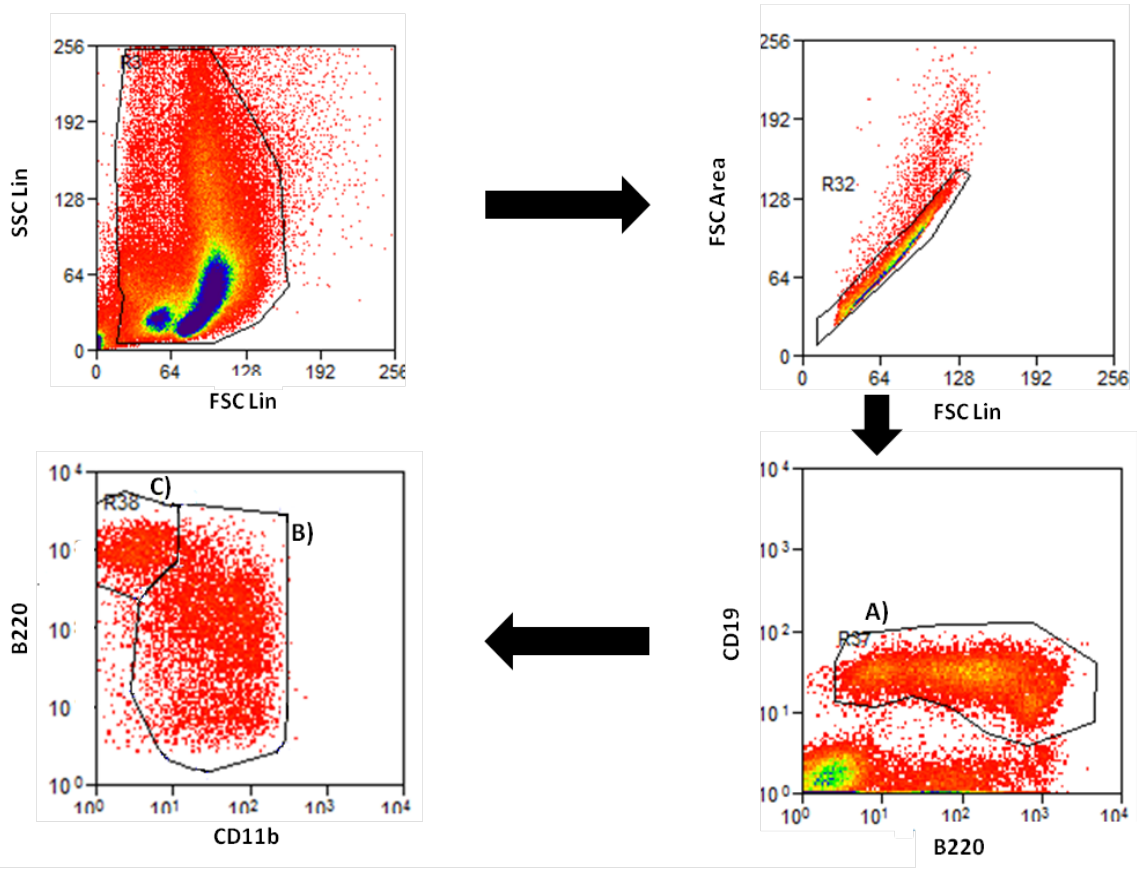

Figure 2.5 - Identification of B lymphocyte subsets by flow cytometry. B lymphocytes were identified by staining cells with specific monoclonal antibodies linked to fluorochromes. Leukocytes were then passed through a flow cytometer and B cell subsets were identified by their known cellular markers. A) B cells ($CD19^{+}$ / $B220^{+}$) B) B1 cells ($CD19^{+}$ / $B220^{int}$ / $CD11B^{int}$) C) B2 cells ($CD19^{+}$ / $B220^{+}$ / $CD11B^{-}$)

Table 2.3 - Cell markers used to identify phenotype of different cell lineages and subsets

Leukocyte subpopulation	Cell markers to split cell subpopulations by flow cytometry
T cells	$CD3^+$ / TCR^+
T helper cells	$CD4^+$ / $CD3^+$ / TCR^+
T cytotoxic cells	$CD8^+$ / $CD3^+$ / TCR^+
NK cells	$NK1.1^+$ / TCR^-
NKT cells	$NK1.1^+$ / TCR^+
B cells	$CD19^+$ / $B220^+$
Resident B1 cells	$CD19^+$ / $B220^{int}$ / $CD11B^{int}$
Infiltrating B2 cells	$CD19^+$ / $B220^+$ / $CD11B^-$
Resident macrophages	$F4/80^+$ / $CD11b^+$
Inflammatory macrophages	$F4/80^{int}$ / $CD11b^{int}$
Dendritic cells	$F4/80^{int}$ / $CD11b^+$ / $CD11c^+$
Neutrophils	$7/4^+$ / LY6-G^+
Eosinophils	$F4/80^{int}$ / $CD11b^{int}$/FSC-A + SSC-A

2.4 Enzyme linked immunosorbent assay (ELISA)

All ELISA's were purchased from R&D systems unless otherwise stated and were carried out in accordance with manufacturer's instructions (see Table 2.4 for individual ELISA information).

Table 2.4 - Mouse ELISA assays used

Target	1^{o} capture antibody conc.	2^{o} detection antibody conc.	Top standard	Supplier	Product Code
IL-6	1 in 250	1 in 250	1000 pg/mL	BD OptEIA	555240
KC	2.0 µg/mL	200 ng/mL	1000 pg/mL	RnD Systems	DY453
MIP-2	2.0 µg/mL	75 ng/mL	1000 pg/mL	RnD Systems	DY452
CXCL5 (LIX)	2.0 µg/mL	400 ng/mL	2000 pg/mL	RnD Systems	DY443
CXCL10 (IP-10)	2.0 µg/mL	600 ng/mL	4000 pg/mL	RnD Systems	DY446
CXCL13 (BCA-1)	1.0 µg/mL	200 ng/mL	1000 pg/mL	RnD Systems	DY470
CCL2 (MCP-1)	0.2 µg/mL	50 ng/mL	250 pg/mL	RnD Systems	DY479
CCL3 (MIP-1α)	0.4 µg/mL	100 ng/mL	500 pg/mL	RnD Systems	DY450
CCL4 (MIP-1β)	4.0 µg/mL	800 ng/mL	1000 pg/mL	RnD Systems	DY451
CCL5 (RANTES)	2.0 µg/mL	400 ng/mL	2000 pg/mL	RnD Systems	DY478
CCL7 (MCP-3)	1.0 µg/mL	250 ng/mL	1000 pg/mL	Antigenix America	RMF328ckc

2.4.1 ELISA protocol

Briefly, flat bottomed 96 well plates were coated with 100 µl of the appropriately diluted monoclonal capture antibody in PBS and incubated overnight at 4 ˚C. The plate was washed 5 times with wash buffer and knocked on blue roll to remove any remaining buffer from the wells. Plates were blocked using 200 µl of 1 % Bovine serum albumin (BSA) in PBS for 1 hour at room temperature. Plates were then washed 5 times with wash buffer.

Samples and standards were diluted in 1 % bovine serum albumin (BSA) in PBS and 100 µl was added to the appropriate wells and incubated at room temperature for 2 hours. Plates were washed 5 times with 200 µl of wash buffer before adding 100 µl of the biotinylated detection antibody diluted in 1 % BSA in PBS for 2 hours at room temperature. Wells were washed a further 5 times with wash buffer and 100 µl of streptavidin-horse radish peroxidise (HRP) diluted 1/200 in 1 % BSA in PBS was added for 20 minutes at room temperature. Plates were washed a final 5 times with wash buffer before the addition of 100 µl of 3, 3', 5, 5'-Tetramethylbenzidine (TMB) substrate solution. Plates were incubated in the dark, after sufficient blue colour development (around 10 minutes) all reactions were stopped by adding 50 µl of 2 M sulphuric acid.

The optical density was measured at 450 nm using a FLUOstar microplate reader (Omega BMG Labtech). To calculate chemokine levels from the optical density, standards were used to plot a standard curve, which was used to produce a linear equation. This equation was used to calculate the concentration of the chemokine in each sample from its optical density.

2.5 Quantitative polymerase chain reaction (qPCR)

2.5.1 SES stimulation of resident macrophages

A pure population of resident macrophages (Section 2.3.10) were seeded into a 48 well plate in 500 µl of 1640 Media developed at the Roswell Park Memorial Institute (RPMI-1640) at a density of $1x10^6$ cells/ml and allowed to adhere for 3 hours. A freeze dried aliquot of SES was reconstituted with RPMI-1640 and a 1/2 dilution was added to the macrophages and along with an unstimulated negative control incubated for 1 hour, RNA from resident macrophages was then extracted.

2.5.2 RNA extraction

Total RNA was extracted using a RNAeasy mini kit (Qiagen, Crawley, West Sussex, UK). Firstly, either (i) a resident macrophage monolayer (Section 2.5.1) was lysed using RLT buffer and homogenised by passing though a QiaShredder, or (ii) a piece of liquid nitrogen snap frozen peritoneal membrane (Section 2.2.6.1) was broken down into a fine powder using a homogeniser (Omni International, Georgia, USA). This powder was resuspended in 1 ml of Trizol solution for 5 minutes on ice. To this 200 µl of chloroform was added per sample and mixed vigorously for 15 seconds and left at room temperature for 3 minutes. After this period the solution was spun at 12000 g for 15 minutes at 4 ˚C and supernatant transferred into a fresh eppendorf.

An equal volume of 70 % ethanol was added to the supernatant and gently mixed. This solution was transferred to an RNAeasy spin column within a 2 ml collection tube and spun for 15 seconds at 8000 g and flow through in the collection tube discarded. RW1 buffer (700 µl) was added to the same RNAeasy spin column within

a 2 ml collection tube and spun for 15 seconds at 8000 g and flow through discarded. RPE buffer (500 µl) was added to the same RNAeasy spin column and spun as above discarding the flow through and repeated. The RNAeasy spin column was moved into a fresh 2 ml collection tube and spun as above for 1 minute. The RNAeasy spin column was moved into an eppendorf and 50 µl of RNAse free water added onto the membrane within the spin column and spun for 1 minute at 8000 g. The flow through was re-pipetted onto the membrane and the spin repeated. The eluted RNA in solution was stored at -80 ˚C until required and volume of RNA extracted measured using a nanodrop spectrometer.

2.5.3 Reverse transcription

RNA was diluted to 100 ng/ml and added to a 0.2 ml PCR tube along with 0.5 µl of Oligo-dT and 0.5 µl of Random hexamer primers and made up to a final volume of 10 µl with RNAse free water (Primer Design, Mill Yard, Southampton, UK). The primers were annealed to the RNA by heating the PCR tubes on a heat block to 65 ˚C for 5 minutes and immediately moved onto ice; 10 µl of the extension mix (2 µl of nanoscript 10X buffer, 1 µl of 10 mM dNTPs, 2 µl of Dithiothreitol (DTT), 4 µl RNAse free water and 1 µl nanoscript enzyme) (Primer Design, Mill Yard, Southampton, UK) was added to the samples on ice and mixed. These samples were left at room temperature for 5 minutes, heated to 55 ˚C for 20 minutes and reaction stopped by increasing the temperature to 75 ˚C for 15 minutes. Finally the cDNA generated was diluted to a working concentration by adding 180 µl of RNAse free water and kept at -20 ˚C until required.

2.5.4 Primer design

The cDNA sequence and the intron-exon boundaries of the test gene were obtained from the ensemble website (www.ensemble.org). This cDNA sequence along with a sequence of several base pairs from either side of a 3' intron-exon boundary were inputted into the Primer3 program, which generated several possible primers producing a product of 80-150 bp. These primers were assessed for their potential to form secondary structures (www.sigmagenosys.com/calc/DNACalc.asp) and bind other similar sequences from other gene transcripts (www.ncbi.nlm.nih.gov/tools/primer-blast). Those least likely to form secondary structures or bind to other transcripts were selected to identify the relative quantity of test gene mRNA levels in the peritoneal membrane using qPCR.

2.5.5 qPCR

The cDNA generated in Section 2.5.2 was diluted to 25 ng/ml and 5 µl added per reaction along with a mastermix (containing 10 µl 2X qPCR mastermix with SYBR green included, 1 µl primer and 4 µl RNAse free water, per reaction) (Primer Design, Mill Yard, Southampton, UK) to the test wells of a qPCR plate. The qPCR plate wells containing the test primer and mastermix were run alongside a housekeeping control gene (β actin) and mastermix as well as –RNA and –RT wells in a Biorad iCycler qPCR machine (Biorad, Hemel Hempstead, Hertfordshire, UK) according to the following protocol:

	Step	Time	Temperature
	Enzyme activation	10 minutes	95 ˚C
Cycling x50	De-naturation	15 seconds	95 ˚C
	Data collection	60 seconds	60 ˚C
	Melt curve	-	-

SYBR green in the 2X qPCR mastermix is a non-specific DNA dye which was used to detect the amplification of the desired cDNA product, by measuring the increase in fluorescence as SYBR green binds amplifying DNA. However SYBR green has the ability to bind any double stranded DNA, such as contaminating DNA and self complementary primers, not only the desired cDNA product. Thus to ensure only the single desired product was amplified the melt curve of each reaction was scrutinized (Figure 2.6).

To calculate the relative quantity (RQ) of mRNA of the gene of interest from the qPCR readout, the amplification data of the gene of interest (known as the Ct value) were normalised by subtracting the amplification data from the housekeeping gene, (known as dCt) and subtracting the amplification data from the negative control (known as the ddCt). These normalised mRNA data were transformed (2^) to give relative quantity from which statistics were used to investigate how this gene transcription may have changed between experimental groups.

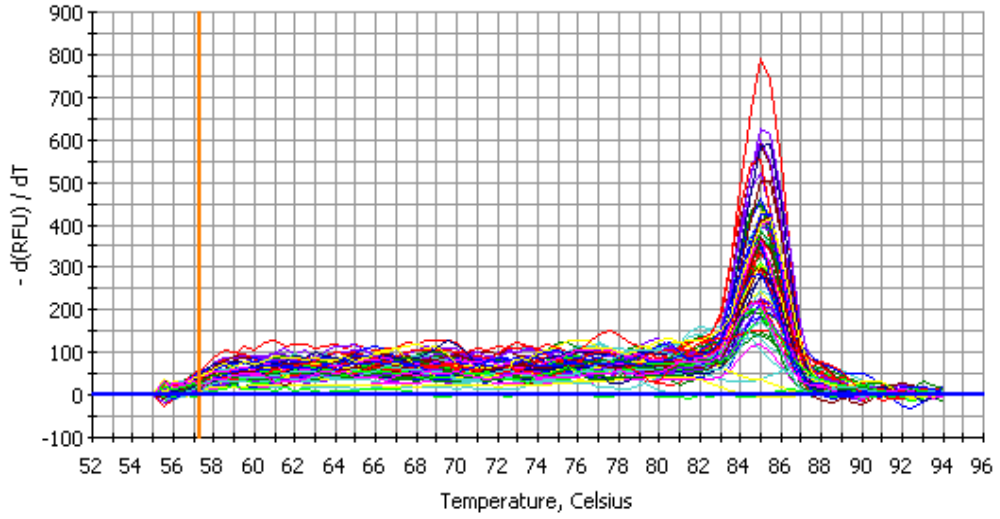

Figure 2.6 – Representative derivative melt curve following qPCR. SYBR green is a non-specific DNA dye which can bind any double stranded DNA (i.e. contaminating DNA and self complementary primers), therefore it is necessary to inspect the melt curve to confirm only the single desired product is amplified. This figure shows a representative plot of negative fluorescence vs temperature, the single peak at an inflection point of 85 ℃ (melting temperature of the desired product) is typical of the amplification of a single product. Self complementary primers or contaminating DNA would appear as separate peaks on the plot in addition to the desired product.

2.6 Histology

2.6.1 Peritoneal membrane harvest

A ~1.5 cm by ~1.5 cm square of mouse peritoneal membrane was harvested and pinned (without stretching) into a gel based Petri dish containing PBS. The PBS was removed and the membrane was fixed in 10 % NBFS for 15 minutes. Peritoneal membranes were unpinned and transferred into labelled tissue biopsy cassettes. These cassettes were stored in NBFS for 48 hours at 4 ˚C to ensure fixation.

2.6.2 Tissue preparation

After fixation, membranes were outsourced to CBS for preparation prior to staining. This entailed permeating the membrane with paraffin wax in a tissue processor (see Table 2.5). Membranes were then sliced in half and embedded vertically in wax blocks. Sections (5 µm) were cut using a microtome, which were then transferred onto a waterbath filled with distilled H_2O heated to 50 ˚C. Each section was placed onto an adhesive microscope slide and incubated overnight at 60 ˚C. These peritoneal membrane section slides were then stored at room temperature.

Table 2.5 - Peritoneal membrane processing programme

Stage	Time	Temperature
70 % Alcohol empty tank	30 minutes	Room temperature
90 % Alcohol empty tank	60 minutes	Room temperature
100 % Alcohol empty tank	60 minutes	Room temperature
100 % Alcohol empty tank	60 minutes	Room temperature
100 % Alcohol empty tank	60 minutes	Room temperature
100 % Alcohol empty tank	60 minutes	Room temperature
100 % Alcohol empty tank	60 minutes	Room temperature
Xylene empty tank	60 minutes	37 ˚C
Xylene empty tank	60 minutes	37 ˚C
Xylene empty tank	60 minutes	45 ˚C
Wax empty tank	120 minutes	60 ˚C
Wax empty tank	90 minutes	60 ˚C
Wax empty tank	90 minutes	60 ˚C
Wax empty tank	90 minutes	60 ˚C

2.6.3 Haematoxylin and eosin staining

Peritoneal membrane sections on slides were deparaffinised with 3 x 5 minutes changes of xylene and rehydrated for 3 minutes in each of 4 descending concentrations of ethanol (100 %, 100 %, 90 %, and 70 %). Slides were placed into running tap water for 5 minutes and dipped in distilled H_2O. Slides were submerged in Harris's haematoxylin solution for 90 seconds and running tap water for 5 minutes. Slides were moved into Scott's tap water for 30 seconds and running tap water again for 5 minutes. Slides were placed in eosin solution for 60 seconds and running tap water to prevent over staining of the membranes. Finally sections were dehydrated for 3 minutes in 3 ascending concentrations of ethanol (90 %, 100 %, and 100 %) and submerged in 3 x 5 minutes changes of xylene. A cover slip with Depax mounting media was added onto the slide and incubated at 65 ˚C overnight to fix.

2.6.4 Mesothelial layer thickness analysis

After haematoxylin and eosin staining, the peritoneal membrane sections were blinded and pictures were taken at x20 magnification using a Leica DFC490 camera attached to a Leica microscope. These pictures were measured using Leica QwinV3 software. The mesothelial layer of each peritoneal membrane section was measured at 6 different points of the membrane in 6 different fields of view; these were averaged to give a mean thickness (μm) for that sample. All other samples from all time points were measured the same way, ensuring similar sections of the membrane were measured to ensure consistent results.

2.6.5 DR3 immunohistochemistry (IHC)

Sections were deparaffinised and rehydrated as shown in Section 2.6.3 and washed in running tap water for 5 minutes. Excess water was removed from the slides and the peritoneal membrane sections were enclosed in a hydrophobic barrier using a pap pen. Each section was covered with peroxidase blocking reagent (from an R&D anti-goat HRP-DAB cell and tissue staining kit) for 5 minutes in an incubation chamber. Sections were rinsed in TBS buffer and washed in 2 changes of TBS buffer for 5 minutes each. Serum blocking reagent D (from the above R&D kit) was added for 15 minutes in an incubation chamber, excess serum block was blotted off and sections were incubated for a further 15 minutes with avidin blocking reagent (from the above R&D kit). Slides were rinsed in TBS buffer and excess buffer blotted off.

Sections were incubated with the biotinylated polyclonal mDR3 antibody (RnD systems) and an identical section incubated with the biotinylated goat IgG isotype control at 20 µg/ml for 2 hours in an incubation chamber. Sections were rinsed in TBS buffer and washed in 3 changes of TBS buffer for 15 minutes each. Excess buffer was removed from the slides and sections incubated with High sensitivity streptavidin (HSS)-HRP (from the above R&D kit) for 30 minutes. Sections were rinsed in TBS buffer and washed in 3 changes of TBS buffer for 2 minutes each. Excess buffer was removed and sections incubated with a mixture of 3,3-Diaminobenzidine (DAB) chromogen and DAB buffer (from the above R&D kit, 1 drop concentrated DAB chromogen in 1 ml DAB buffer) for 3 minutes, slides were rinsed in distilled H_2O and washed in fresh distilled H_2O for 2 minutes.

Sections were counterstained with Harris's haematoxylin, dipped in Scott's tap water, dehydrated in 3 ascending concentrations of ethanol, submerged in 3 changes

of xylene and mounted with Depax mounting media as shown in Section 2.6.3. Pictures of sections were taken under x20 magnification using an Olympus N457 camera and loaded onto Adobe Photoshop CS4. In Adobe Photoshop CS4 the picture was pixelated and brown pixels calculated as a percentage of total pixels.

2.7 Statistical analysis

All results were expressed as the mean $\pm$ standard error of the mean (SEM) and analysed using Graphpad prism 5, p values below 0.05 were considered significant. The statistical tests used in this study were the parametric, unpaired 2 tailed t-test (when comparing the means of 2 groups) and 2 way Analysis of variance (ANOVA) (when comparing more than 2 variables) where data were normally distributed and the non-parametric, Mann-Whitney test where data were not normally distributed (i.e. percentages).

Chapter 3 - Phenotypic characterisation of the peritoneal cavity and peripheral blood

3.1 Introduction

Previous work in inflammatory and infection models has shown that DR3 regulates effector T cell expansion at sites of pathology (Migone, Zhang et al. 2002; Meylan, Davidson et al. 2008; Pappu, Borodovsky et al. 2008; Buchan, Taraban et al. 2012; Twohig, Marsden et al. 2012), but to date, no studies have investigated the influence of DR3 expression on leukocyte populations within the peritoneal cavity. The naive mouse peritoneal cavity is predominantly composed of resident macrophages and B1 cells though other cellular subsets are found in lower numbers (e.g. T cells, Dendritic cells, Eosinophils and NK cells) (Turchyn, Baginski et al. 2007; Kolaczkowska, Koziol et al. 2009). The aim of this chapter was to determine the composition and number of peritoneal leukocytes in the naive cavity of $DR3^{-/-}$ mice and compare them to their $DR3^{+/+}$ counterparts to investigate if DR3 significantly influenced leukocyte homeostasis prior to the induction of inflammation. As leukocytes are recruited into the cavity from the peripheral blood following an inflammatory stimulus, detailed baseline measurements of leukocyte subsets in the peripheral blood of $DR3^{-/-}$ mice were also undertaken. DR3 expression patterns on these leukocyte subsets and within the peritoneal membrane were also examined to identify cell types that were potentially responsive to TL1A.

3.2 Results

3.2.1.1 Total mouse leukocyte numbers in unchallenged DR3$^{+/+}$ and DR3$^{-/-}$ peritoneal cavities

To examine if DR3 affected the number of resident peritoneal leukocytes in the naive cavity, cells were isolated by lavage (Section 2.2.3.1) and cells numbers determined using a Coulter counter (Section 2.2.4). DR3$^{-/-}$ mice (2.9 ± 0.2 x10^{6} total cells) showed no significant difference in the total number of leukocytes present in the naive cavity compared to DR3$^{+/+}$ mice (2.8 ± 0.2 x10^{6} total cells) (Figure 3.1) (Table 3.1).

3.2.1.2 Myeloid cell subset numbers in unchallenged DR3$^{+/+}$ and DR3$^{-/-}$ peritoneal cavities

Though a deficiency in DR3 did not affect the total number of cells residing in the naive cavity, numbers of different leukocyte subsets were calculated to determine if loss of DR3 altered the composition of these resident cells. Myeloid cell subsets were identified from the lavage by flow cytometry (Section 2.3.2), through use of well-characterised extracellular markers (F4/80, CD11b and CD11c) (Table 2.3) and variations in their forward and side scatter (FSC/SSC) properties (Figure 2.3). DR3$^{-/-}$ and DR3$^{+/+}$ mice were found to have comparable numbers of resident macrophages (DR3$^{+/+}$ mice 7.2 ± 1.8 x10^{5}, DR3$^{-/-}$ mice 6.4 ± 1.6 x10^{5} total resident macrophages) (Figure 3.2A), dendritic cells (DR3$^{+/+}$ mice 5.1 ± 1.6 x10^{3}, DR3$^{-/-}$ mice 3.3 ± 0.3 x10^{3} total dendritic cells) (Figure 3.2B) and eosinophils (DR3$^{+/+}$ mice 1.9 ± 0.7 x10^{5}, DR3$^{-/-}$ mice 7.6 ± 0.6 x10^{4} total eosinophils) (Figure 3.2C) in the naive cavity.

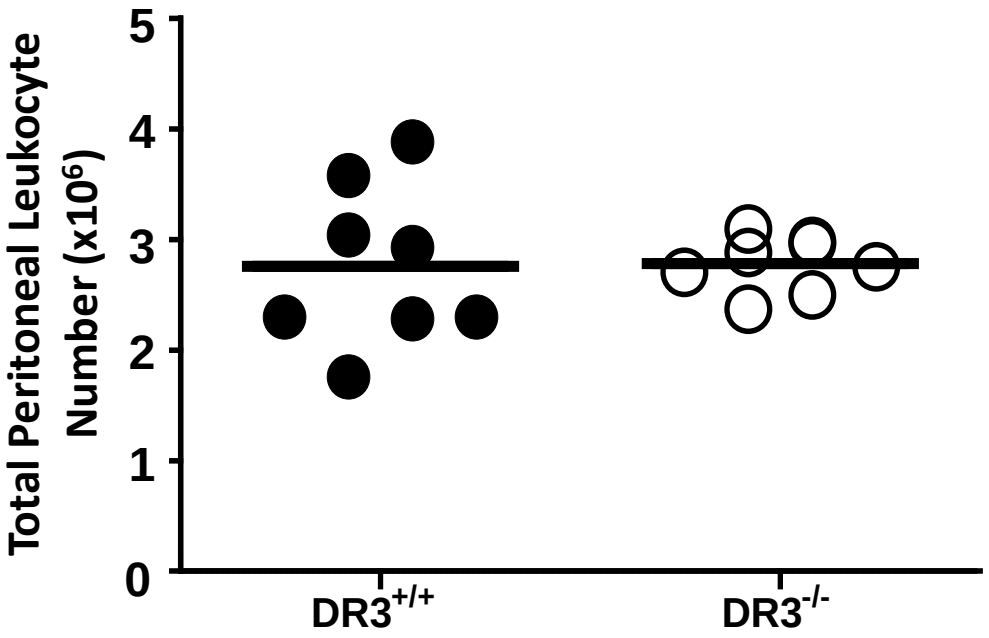

Figure 3.1 - No significant differences were seen in total peritoneal leukocyte numbers in the naive cavity of DR3$^{+/+}$ and DR3$^{-/-}$ mice. Peritoneal leukocytes were isolated from the cavities of mice by peritoneal lavage, total cell number was calculated using a Beckman Coulter counter Z2 (each symbol represents a single mouse, bar corresponds to mean from n=7 or 8, N.S.D by t-test).

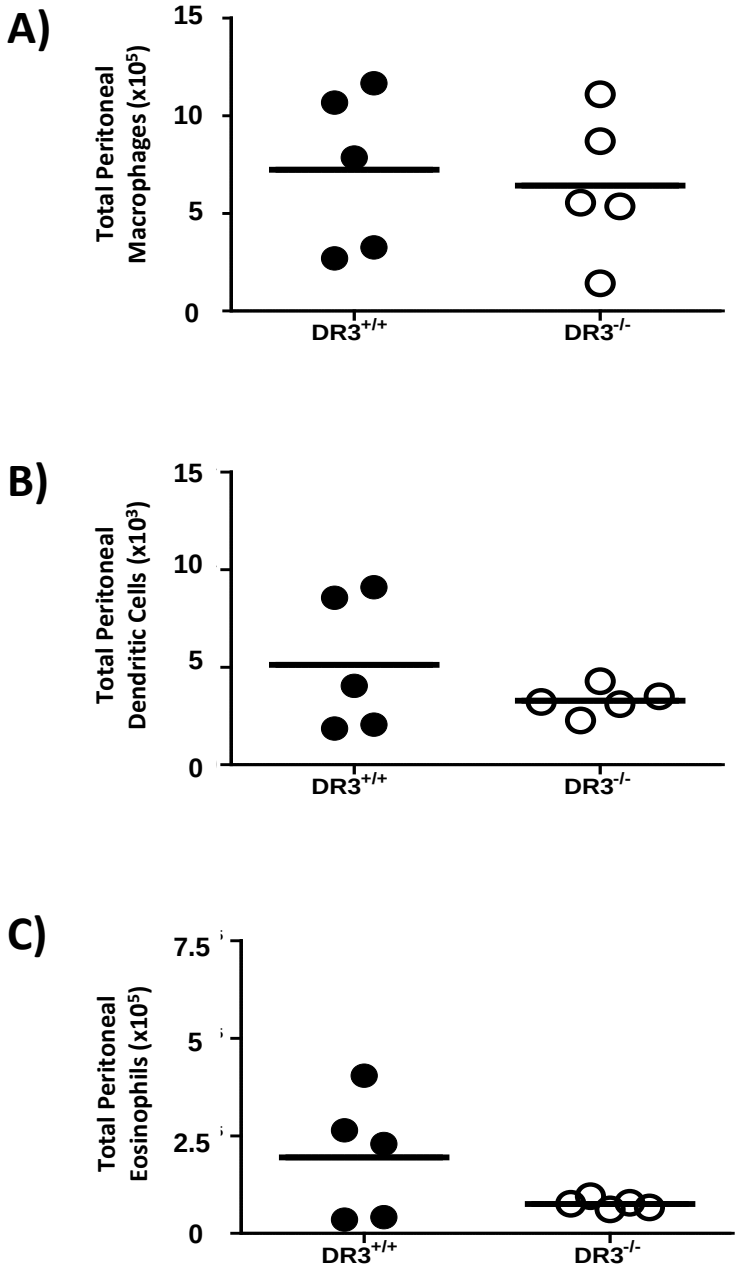

Figure 3.2 - No significant differences were seen in numbers of resident myeloid cell subsets in the unchallenged peritoneal cavity of DR3$^{+/+}$ and DR3$^{-/-}$ mice. Peritoneal leukocytes were isolated by lavage and A) Resident Macrophages were identified by a CD11b^{+} F4/80^{+} phenotype, B) Dendritic cells were identified by a F4/80^{int} CD11b^{int} CD11c^{+} phenotype and C) Eosinophils, identified by a F4/80^{int} CD11b^{int} phenotype and their forward and side scatter properties. Subset numbers calculated by percentage proportion of total leukocytes, determined using a Beckman Coulter counter Z2 (each symbol represents a single mouse, bar corresponds to mean from n=5, N.S.D by t-test).

3.2.1.3 Lymphocyte cell subset numbers in unchallenged $DR3^{+/+}$ and $DR3^{-/-}$ peritoneal cavities

Lymphocyte cell subsets in the naive cavity of $DR3^{-/-}$ mice were examined by flow cytometry. Antibodies targeted against markers found on the surface of these cells (Table 2.3) identified specific lymphocytic cell subsets from the heterogeneous leukocyte population (Figure 2.4-2.5). $DR3^{-/-}$ mice ($4.6 \pm 1.1 \times 10^5$ total T cells) showed no significant difference in the total number of peritoneal T cells in the naive cavity compared to $DR3^{+/+}$ mice ($4.5 \pm 0.5 \times 10^5$ total T cells) (Figure 3.3A) and both $DR3^{-/-}$ and $DR3^{+/+}$ shared equivalent numbers of both $CD4^+$ ($DR3^{+/+}$ mice $2.9 \pm 0.7 \times 10^5$, $DR3^{-/-}$ mice $3.0 \pm 0.4 \times 10^5$ total $CD4^+$ T cells) (Figure 3.3B) and $CD8^+$ ($DR3^{+/+}$ mice $6.1 \pm 1.4 \times 10^4$, $DR3^{-/-}$ mice $6.9 \pm 0.6 \times 10^4$ total $CD8^+$ T cells) (Figure 3.3C) T cell subsets. The number of B cells in the naive cavity of $DR3^{-/-}$ mice ($9.3 \pm 2.9 \times 10^5$ total B cells) was also not significantly different compared to $DR3^{+/+}$ mice ($8.6 \pm 1.0 \times 10^5$ total B cells) (Figure 3.4A) with both genotypes sharing similar numbers of B1 ($DR3^{+/+}$ mice $6.6 \pm 1.8 \times 10^5$, $DR3^{-/-}$ mice $5.4 \pm 0.7 \times 10^5$ total B1 cells) (Figure 3.4B) and B2 ($DR3^{+/+}$ mice $1.5 \pm 0.5 \times 10^5$, $DR3^{-/-}$ mice $1.8 \pm 0.3 \times 10^5$ total B2 cells) (Figure 3.4C) B cell subsets. The naive peritoneal cavities of $DR3^{-/-}$ and $DR3^{+/+}$ mice also shared comparable numbers of NK ($DR3^{+/+}$ mice $6.8 \pm 1.7 \times 10^4$, $DR3^{-/-}$ mice $4.7 \pm 0.8 \times 10^4$ total NK cells) (Figure 3.5A) and NKT cells ($DR3^{+/+}$ mice $7.2 \pm 1.8 \times 10^4$, $DR3^{-/-}$ mice $6.9 \pm 0.6 \times 10^4$ total NKT cells) (Figure 3.5B).

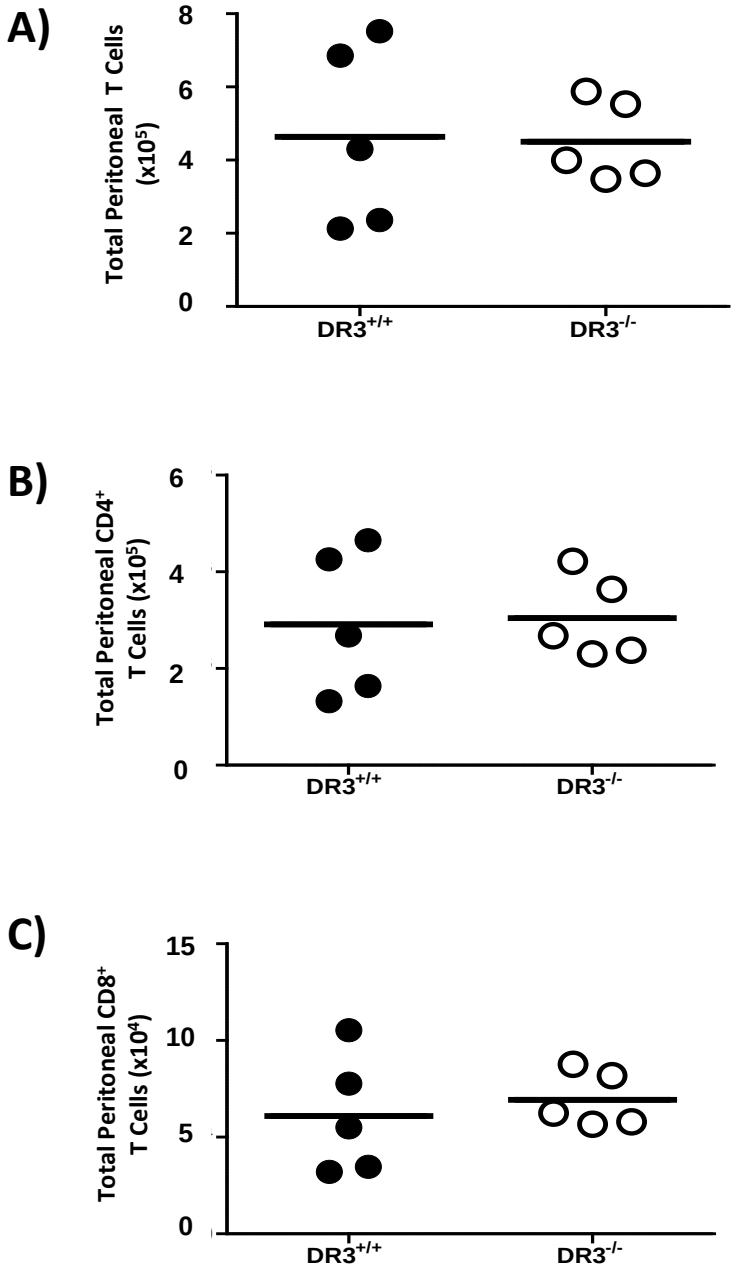

Figure 3.3 - No significant differences were seen in numbers of resident T cell subsets in the unchallenged peritoneal cavity of DR3$^{+/+}$ and DR3$^{-/-}$ mice. Peritoneal leukocytes were isolated by lavage and A) T cells were identified by a CD3$^+$, TCRαβ$^+$ phenotype, B) T helper cells were identified by a CD3$^+$ CD4$^+$, TCRαβ$^+$ phenotype and C) T cytotoxic cells identified by a CD3$^+$ CD8$^+$, TCRαβ$^+$ phenotype. Subset numbers calculated by percentage proportion of total leukocytes, determined using a Beckman Coulter counter Z2 (each symbol represents a single mouse, bar corresponds to mean from n=5, N.S.D by t-test).

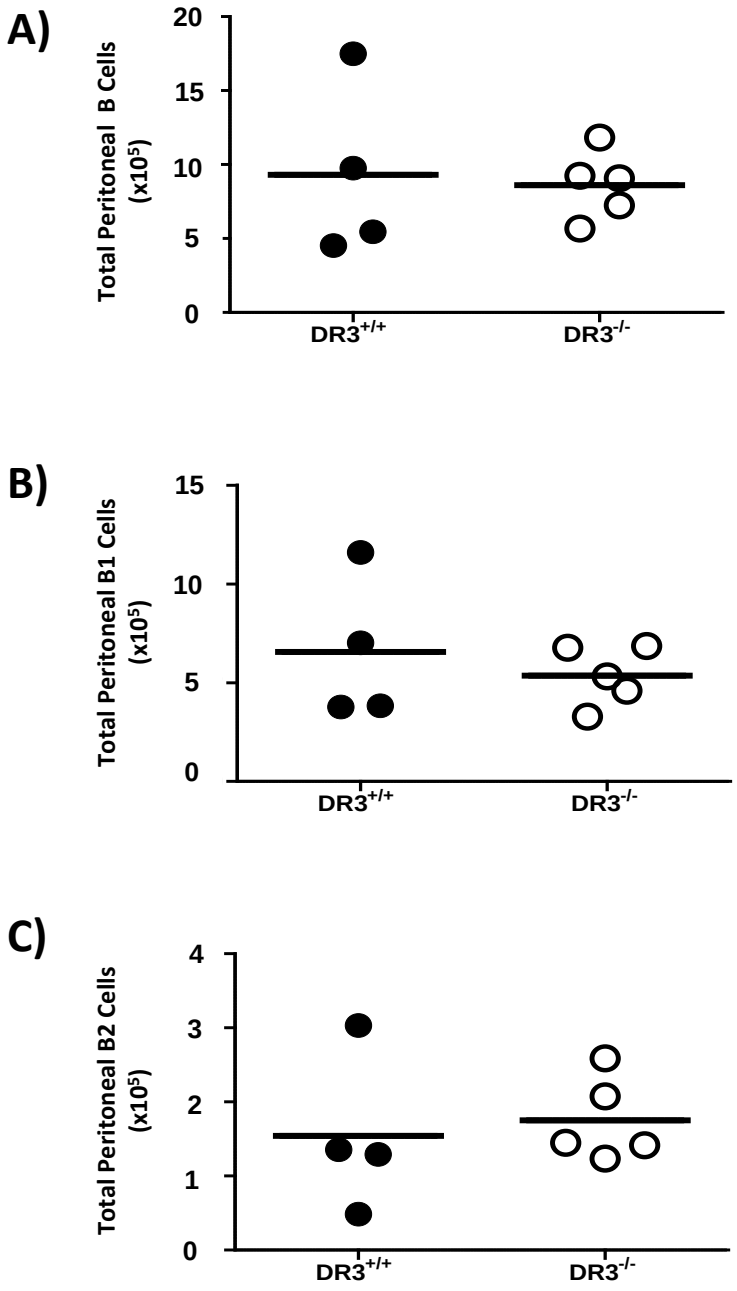

Figure 3.4 - No significant differences were seen in numbers of resident B cell subsets in the unchallenged peritoneal cavity of DR3$^{+/+}$ and DR3$^{-/-}$ mice. Peritoneal leukocytes were isolated by lavage and A) B cells were identified by a CD19^{+}, B220^{+} phenotype, B) B1 cells were identified by a CD19^{+} B220^{int}, CD11b^{int} phenotype and C) B2 cells identified by a CD19^{+} B220^{+}, CD11b^{-} phenotype. Subset numbers calculated by percentage proportion of total leukocytes, determined using a Beckman Coulter counter Z2 (each symbol represents a single mouse, bar corresponds to mean from n=4 or 5, N.S.D by t-test).

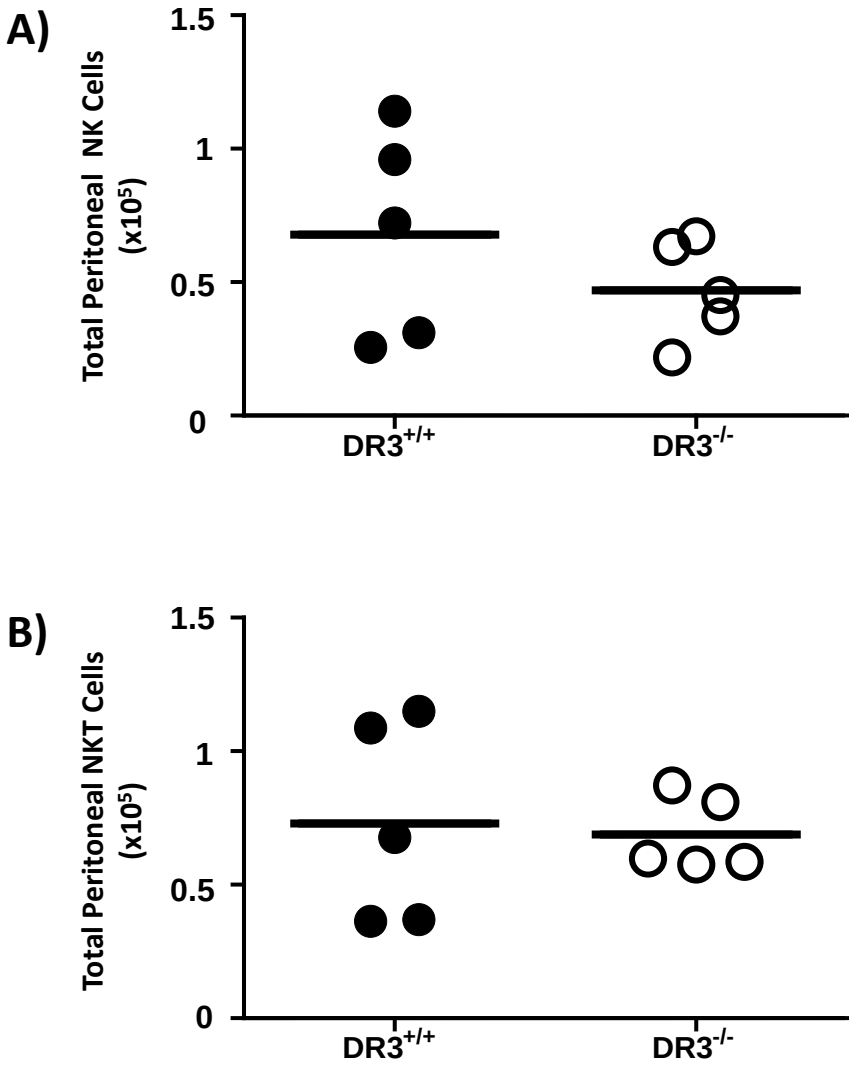

Figure 3.5 - No significant differences were seen in numbers of resident NK or NKT cell subsets in the unchallenged peritoneal cavity of DR3$^{+/+}$ and DR3$^{-/-}$ mice. Peritoneal leukocytes were isolated by lavage and A) NK cells were identified by a NK1.1^{+}, TCRαβ^{-} phenotype and B) NKT cells were identified by a NK1.1^{+}, TCRαβ^{+} phenotype. Subset numbers calculated by percentage proportion of total leukocytes, determined using a Beckman Coulter counter Z2 (each symbol represents a single mouse, bar corresponds to mean from n=5, N.S.D by t-test).

3.2.2.1 Leukocyte proliferation in unchallenged $DR3^{+/+}$ and $DR3^{-/-}$ peritoneal cavities

Earlier work has implicated DR3 in playing a role in both cell expansion (Taraban, Slebioda et al. 2011; Twohig, Marsden et al. 2012) and apoptosis *in vivo* (Wang, Kitson et al. 2001). Alterations in baseline proliferation and apoptosis in the absence of DR3 could still explain the similar cell numbers observed in the naive cavity of $DR3^{-/-}$ and $DR3^{+/+}$ mice. Percentages of proliferating resident cells in the naive cavity was therefore studied using intracellular staining for Ki67 (Figure 3.6, Gate R85), a nuclear protein widely associated with proliferating but not resting cells (G0 phase). Ki67 is first detected early during the G1 phase of proliferation and continuously expressed during the S phase and most of G_2/M phase of proliferation, but was not found in binucleate cells (Duchrow, Gerdes et al. 1994). Comparable levels of $Ki67^{+}$ cells (Gate R85) were observed in resident myeloid and lymphocyte cell subsets in $DR3^{+/+}$ mice (resident macrophages 10.7 ± 2.0 %, T cells 37.7 ± 5.5 %, B cells 13.0 ± 0.5 %, NK cells 21.6 ± 2.6 %, NKT cells 21.7 ± 2.6 %) and $DR3^{-/-}$ (resident macrophages 7.1 ± 1.1 %, T cells 35.1 ± 3.2 %, B cells 12.2 ± 1.1 %, NK cells 20.9 ± 2.1 %, NKT cells 20.9 ± 2.1 %) mice in the peritoneal cavity (Figure 3.7-3.10) (Table 3.2).

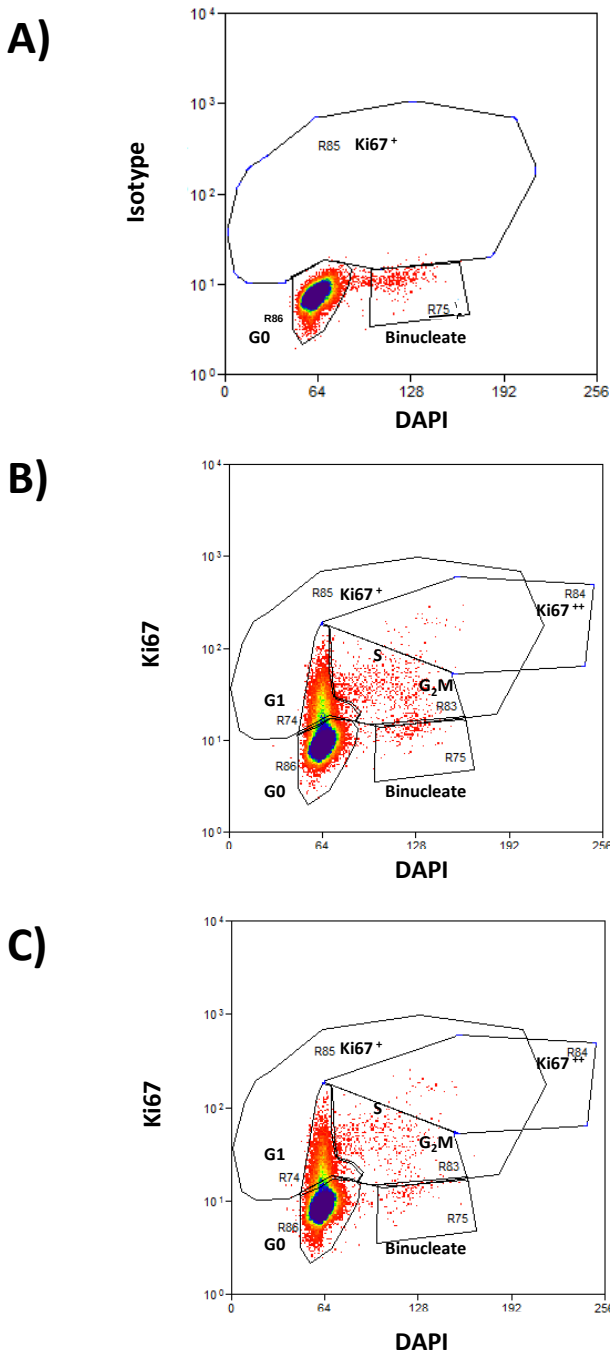

Figure 3.6 - Flow cytometry plots representing proliferation in the unchallenged peritoneal cavity. Peritoneal leukocytes were isolated from the cavity by lavage, permeabilised and proliferation measured using the intracellular marker Ki67 (Gate R85). A) isotype control, B) $DR3^{+/+}$ and C) $DR3^{-/-}$mice. Separation of mitotic phases can be achieved with the DNA marker DAPI in conjunction with Ki67. Early proliferative (G1) cells express Ki67 but are yet to replicate DNA ($Ki67^{+}$ $DAPI^{lo}$). DNA replication does occur during S and G_2M phase of proliferation ($Ki67^{+}$ $DAPI^{int/hi}$). Binucleate cells are non-proliferating but are yet to divide into two cells ($Ki67^{-}$ $DAPI^{hi}$). Once divided, cells enter resting (G0) phase ($Ki67^{-}$ $DAPI^{lo}$). $Ki67^{++}$ represent cells whose nuclear envelope has broken down during mitosis promoting more efficient antibody staining.

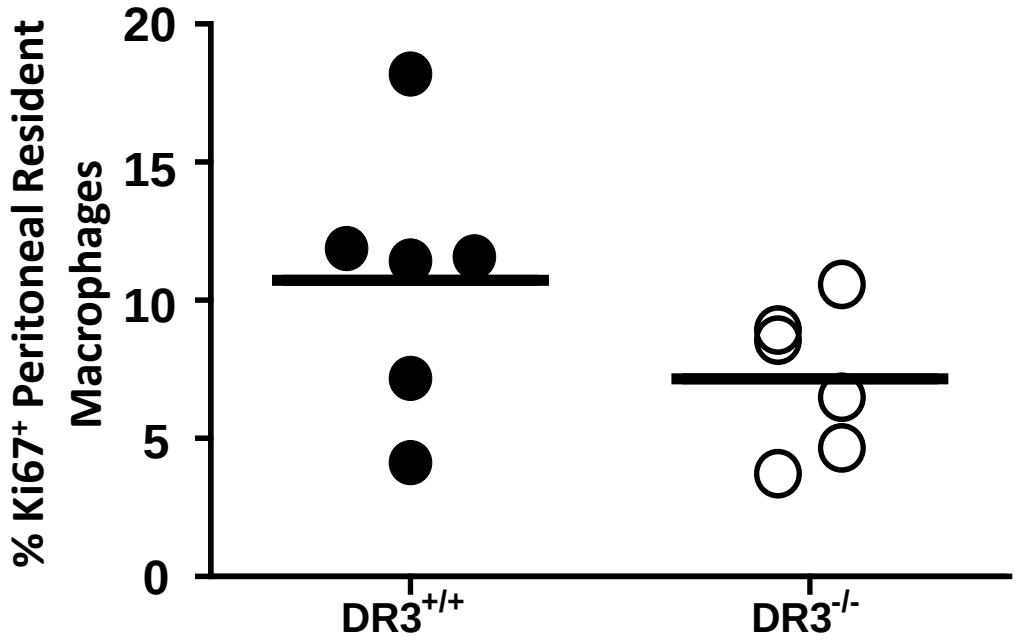

Figure 3.7 - No significant differences were seen in the percentages of proliferating resident macrophages in the unchallenged peritoneal cavity of DR3$^{+/+}$ and DR3$^{-/-}$ mice. Peritoneal leukocytes were isolated from the cavity by lavage and Resident Macrophages identified by a CD11b^{+} F4/80^{+} phenotype. Percentages of proliferating resident macrophages were calculated by the percentage of the subset positive for the marker Ki67 (each symbol represents a single mouse, bar corresponds to mean from n=6, N.S.D by Mann-Whitney test).

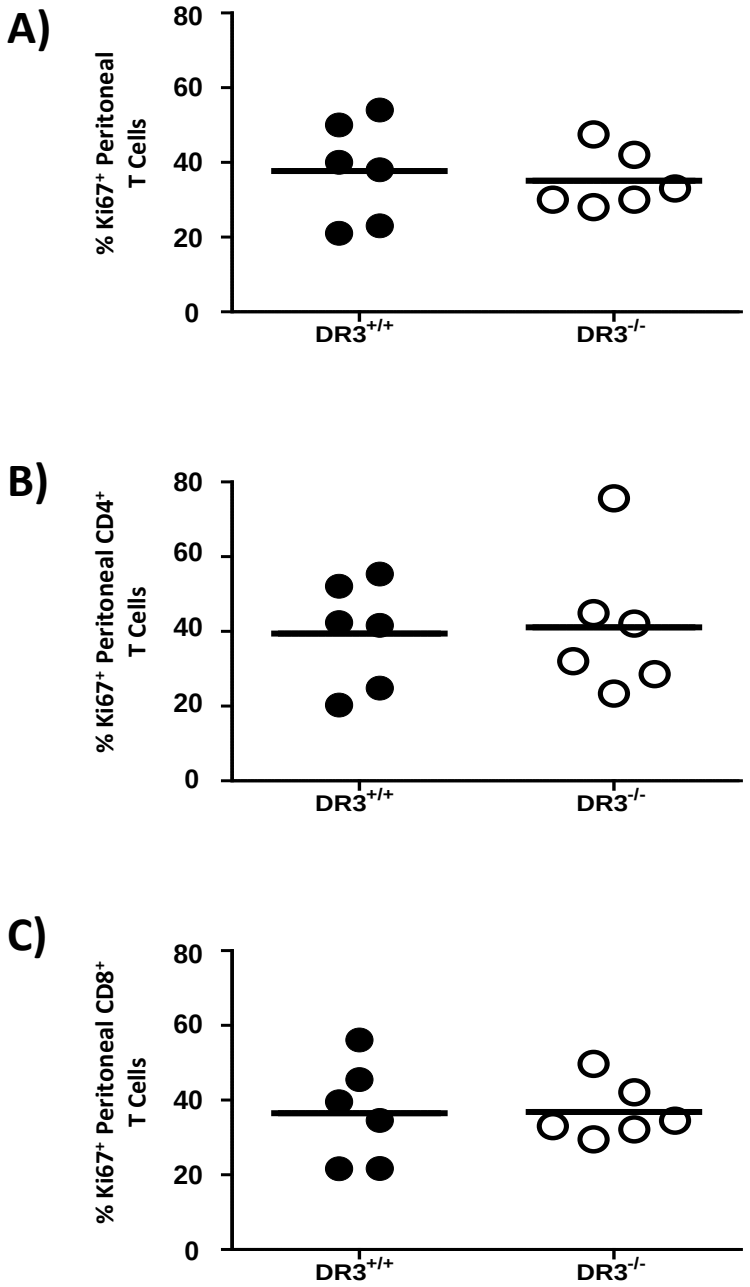

Figure 3.8 - No significant differences were seen in the percentages of proliferating T cell subsets in the unchallenged peritoneal cavity of DR3$^{+/+}$ and DR3$^{-/-}$ mice. Peritoneal leukocytes were isolated from the cavity by lavage. A) T cells were identified by a CD3^{+}, TCRαβ^{+} phenotype B) T helper cells were identified by a CD3^{+} CD4^{+}, TCRαβ^{+} phenotype and C) T cytotoxic cells identified by a CD3^{+} CD8^{+}, TCRαβ^{+} phenotype. Percentages of proliferating T cell subsets were calculated by the percentage of the subset positive for the marker Ki67 (each symbol represents a single mouse, bar corresponds to mean from n=6, N.S.D by Mann-Whitney test).

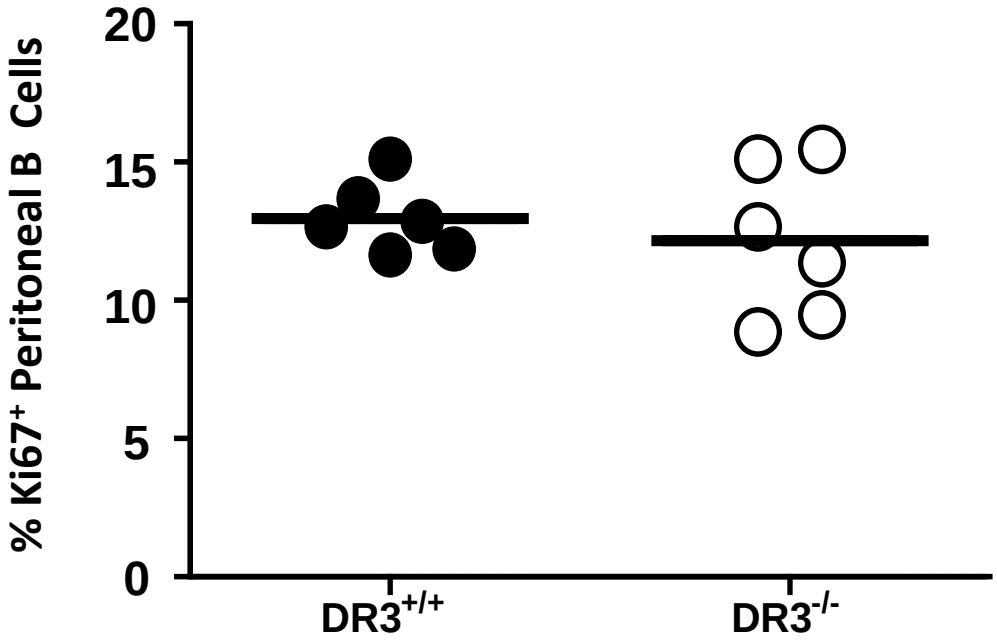

Figure 3.9 - No significant differences were seen in the percentages of proliferating B cells in the unchallenged peritoneal cavity of DR3$^{+/+}$ and DR3$^{-/-}$ mice. Peritoneal leukocytes were isolated from the cavity by lavage. Resident B cells were identified by a CD19^{+}, B220^{+} phenotype. Percentages of proliferating B cells were calculated by the percentage of the subset positive for the marker Ki67 (each symbol represents a single mouse, bar corresponds to mean from n=6, N.S.D by Mann-Whitney test).

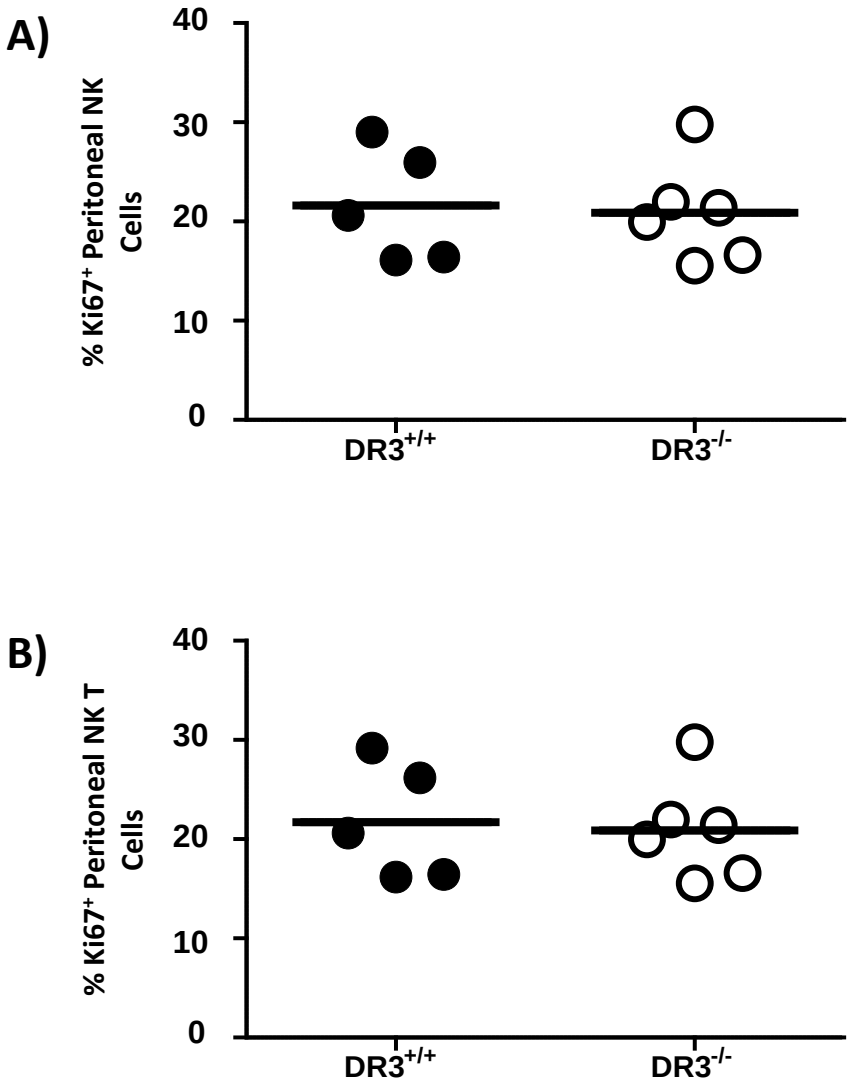

Figure 3.10 - No significant differences were seen in the percentages of proliferating NK or NKT cells in the unchallenged peritoneal cavity of DR3$^{+/+}$ and DR3$^{-/-}$ mice. Peritoneal leukocytes were isolated from the cavity by lavage. A) NK cells were identified by a NK1.1^{+}, TCRαβ^{-} phenotype and B) NKT cells were identified by a NK1.1^{+}, TCRαβ^{+} phenotype. Percentages of proliferating NK cell subsets were calculated by the percentage of the subset positive for the marker Ki67 (each symbol represents a single mouse, bar corresponds to mean from n=5 or 6, N.S.D by Mann-Whitney test).

3.2.2.2 Apoptosis and cell death in unchallenged $DR3^{+/+}$ and $DR3^{-/-}$ peritoneal cavities

Apoptosis and cell death of separate leukocyte subsets in the cavities of $DR3^{+/+}$ and $DR3^{-/-}$ mice was measured by the percentage of each subset positive for Annexin V in combination with the fluorescent DNA binding dye 7-Aminoactinomycin D (7AAD) (Figure 3.11, Gate R74 and R75). Annexin V binds phosphatidylserine in a calcium-dependent manner. Normally phosphatidylserine is held on the intracellular surface of lipid membranes, however during early apoptosis it translocates to the extracellular surface of the cell allowing detection by Annexin V in the absence of membrane permeabilisation (Vanoers, Reutelingsperger et al. 1994), while separation from dead cells can be achieved as live and early apoptotic cells maintain cell membrane integrity and exclude 7AAD (Figure 3.11, Gate R74). However after cell death (Figure 3.11, Gate R75), cell membrane integrity is lost and 7AAD and Annexin V can pass though the membrane, allowing 7AAD to bind guanine and cytosine bases within the nucleus (Philpott, Turner et al. 1996). No significant difference in Annexin V positive, 7AAD positive or double positive cells, of any leukocyte subset in the naive peritoneal cavity was seen between $DR3^{+/+}$ (Annexin V^+ and $7AAD^+$; resident macrophages 40.7 ± 5.6 %, eosinophils 14.7 ± 1.0 %, T cells 17.7 ± 0.5 %, B cells 68.3 ± 1.2 %, NK cells 33.7 ± 5.6 %, NKT cells 17.7 ± 1.8 %) and $DR3^{-/-}$ mice (Annexin V^+ and $7AAD^+$; resident macrophages 42.5 ± 1.8 %, eosinophils 15.7 ± 1.1 %, T cells 19 ± 0.9 %, B cells 72.2 ± 3.9 %, NK cells 27.8 ± 3.2 %, NKT cells 20.4 ± 2.0 %) (Figure 3.12-3.15) (Table 3.2).

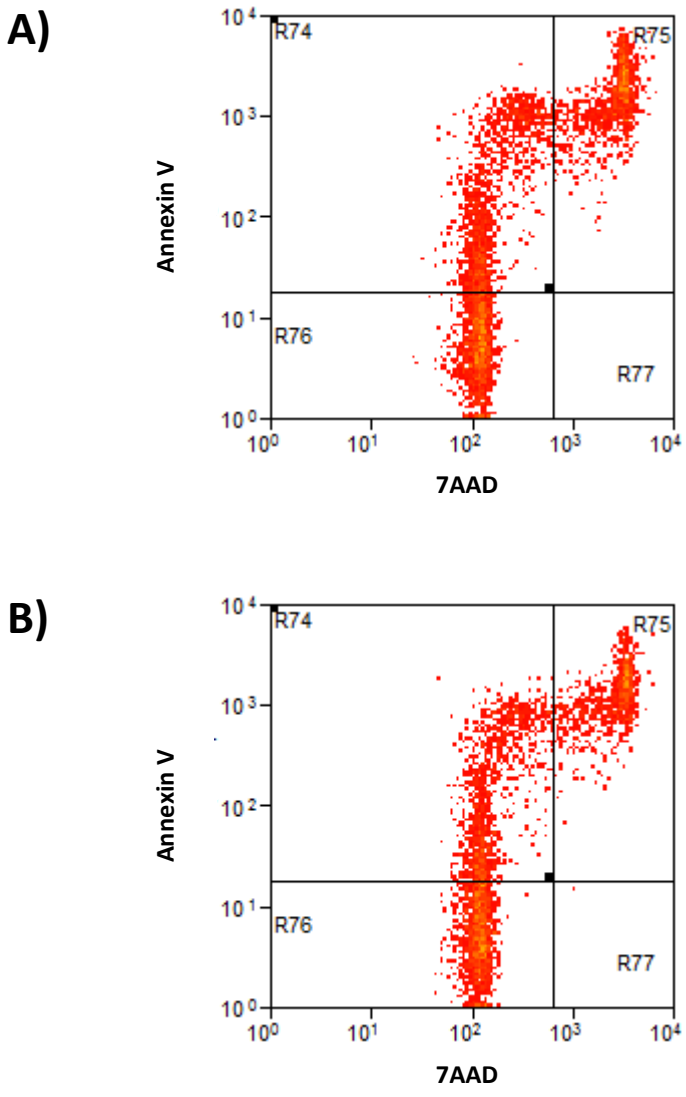

Figure 3.11 - Flow cytometry plots representing the level of apoptosis and cell death in the unchallenged peritoneal cavity. Peritoneal leukocytes were isolated from the cavity by lavage. Apoptosis (R74) and death (R75) was measured using Annexin V (Y Axis) and 7AAD (X Axis) in A) $DR3^{+/+}$ mice and B) $DR3^{-/-}$ mice.

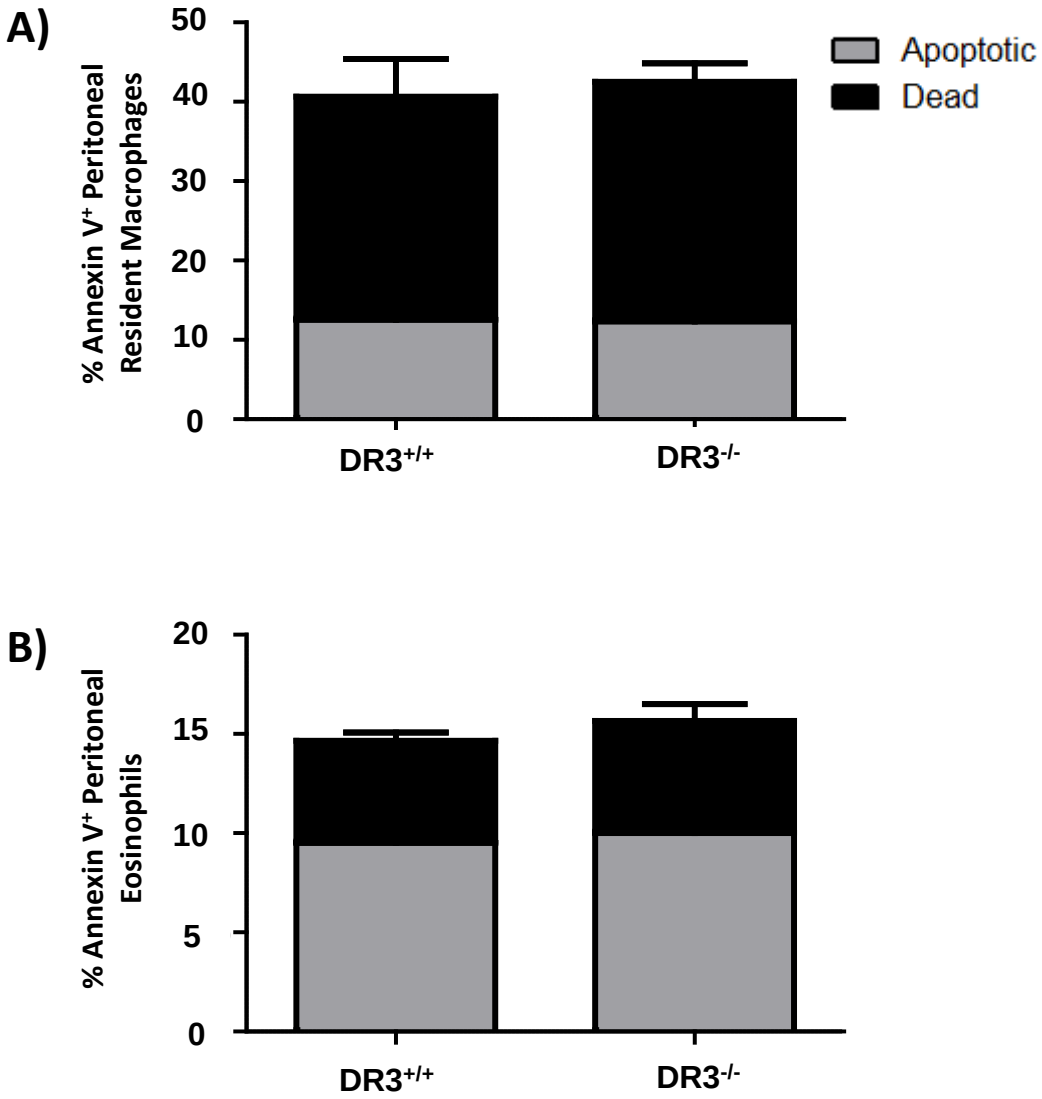

Figure 3.12 - No significant differences were seen in percentage Annexin V^+ myeloid cells in the unchallenged peritoneal cavity of $DR3^{+/+}$ and $DR3^{-/-}$ mice. Peritoneal leukocytes were isolated by lavage and A) Resident Macrophages identified by a $CD11b^+$ $F4/80^+$ phenotype and B) Eosinophils, identified by a $F4/80^{int}$ $CD11b^{int}$ phenotype and their forward and side scatter properties. Percentage apoptotic and dead cells were calculated by the percentage of the subset Annexin V^+ and $7AAD^+$ (each bar represents mean of n=6 mice, grey fill represents apoptosis and black fill represents cell death, error bars correspond to mean ± SEM, N.S.D by Mann-Whitney test).

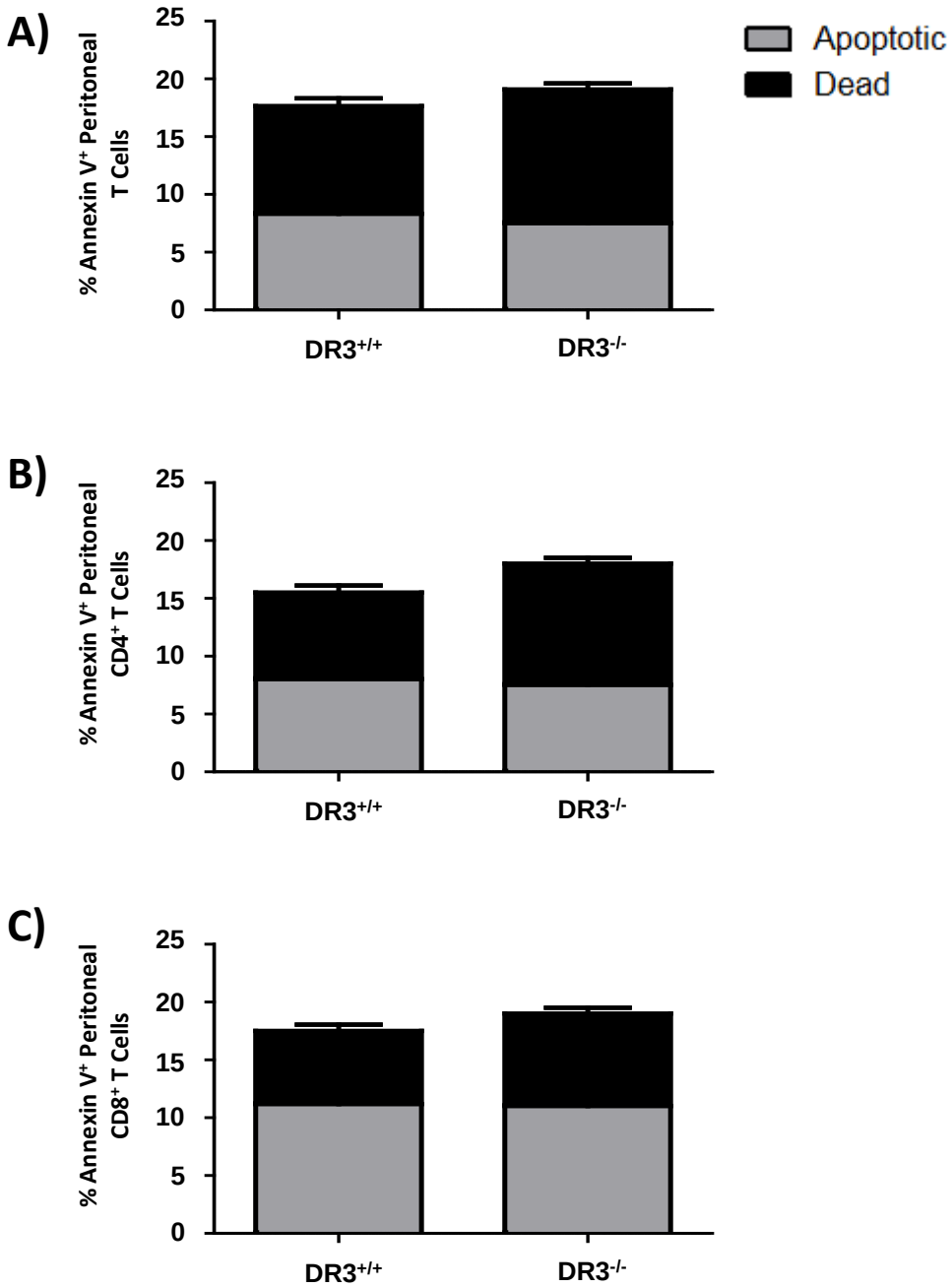

Figure 3.13 - No significant differences were seen in percentage Annexin V^+ T cells in the unchallenged peritoneal cavity of $DR3^{+/+}$ and $DR3^{-/-}$ mice. Peritoneal leukocytes were isolated by lavage and A) T cells were identified by a $CD3^+$, $TCR\alpha\beta^+$ phenotype B) T helper cells were identified by a $CD3^+$ $CD4^+$, $TCR\alpha\beta^+$ phenotype and C) T cytotoxic cells identified by a $CD3^+$ $CD8^+$, $TCR\alpha\beta^+$ phenotype. Percentage apoptotic and dead cells were calculated by the percentage of the subset Annexin V^+ and $7AAD^+$ (each bar represents mean of n=6 mice, grey fill represents apoptosis and black fill represents cell death, error bars correspond to mean ± SEM, N.S.D by Mann-Whitney test).

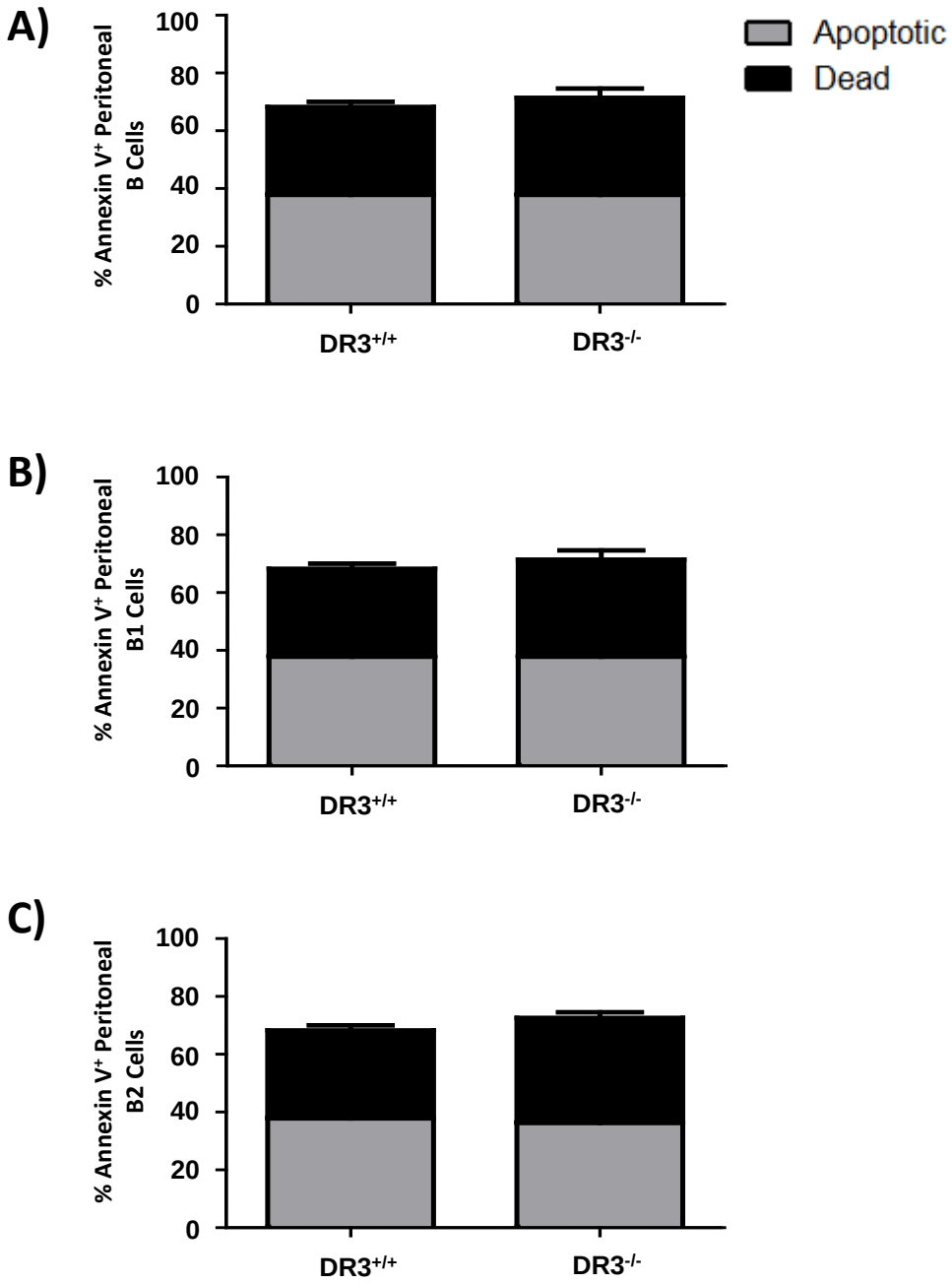

Figure 3.14 - No significant differences were seen in percentage Annexin V^+ B cells in the unchallenged peritoneal cavity of $DR3^{+/+}$ and $DR3^{-/-}$ mice. Peritoneal leukocytes were isolated by lavage and A) B cells were identified by a $CD19^+$, $B220^+$ phenotype B) B1 cells were identified by a $CD19^+$ $B220^{int}$, $CD11b^{int}$ phenotype and C) B2 cells identified by a $CD19^+$ $B220^+$, $CD11b^-$ phenotype. Percentage apoptotic and dead cells were calculated by the percentage of the subset Annexin V^+ and $7AAD^+$ (each bar represents mean of n=6 mice, grey fill represents apoptosis and black fill represents cell death, error bars correspond to mean ± SEM, N.S.D by Mann-Whitney test).

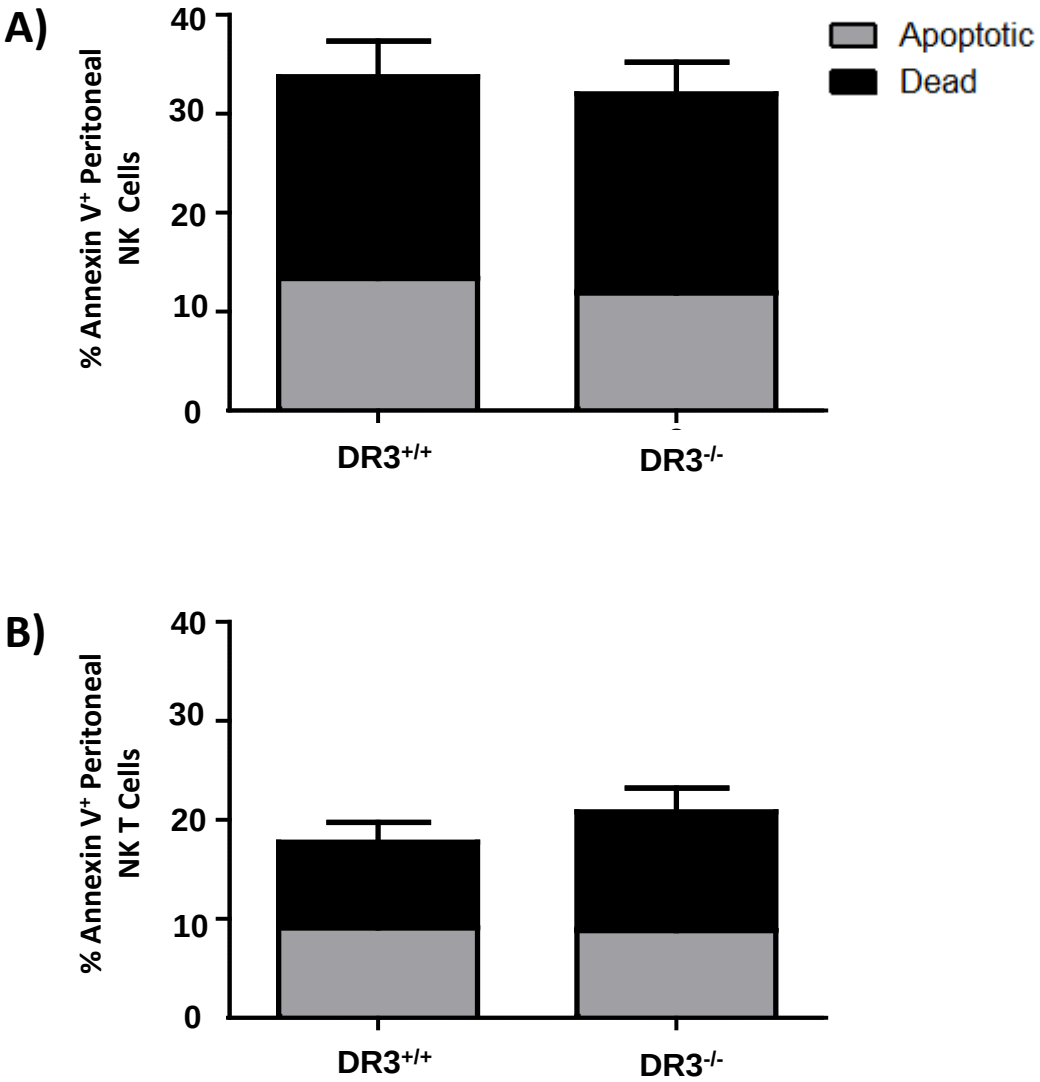

Figure 3.15 - No significant differences were seen in percentage Annexin V^+ NK and NKT cells in the unchallenged peritoneal cavity of $DR3^{+/+}$ and $DR3^{-/-}$ mice. Peritoneal leukocytes were isolated from the cavity by lavage. A) NK cells were identified by a $NK1.1^+$, $TCR\alpha\beta^-$ phenotype and B) NKT cells, identified by a $NK1.1^+$, $TCR\alpha\beta^+$ phenotype. Percentage apoptotic and dead cells were calculated by the percentage of the subset Annexin V^+ and $7AAD^+$ (each bar represents mean of n=6 mice, grey fill represents apoptosis and black fill represents cell death, error bars correspond to mean ± SEM, N.S.D by Mann-Whitney test).

3.2.3.1 DR3 expression on the mesothelial layer of the unchallenged peritoneal membrane of $DR3^{+/+}$ and $DR3^{-/-}$ mice

No previous studies have investigated DR3's expression profile in the peritoneal cavity. Stromal DR3 expression was visualised using a polyclonal antibody by immunohistochemistry (Section 2.6.5). Multiple pictures were taken along sections of the mesothelial layer from $DR3^{+/+}$ and $DR3^{-/-}$ mice following staining by the polyclonal DR3 antibody or an isotype antibody (Figure 3.16A). Percentage positive DR3 (brown) pixels within mesothelial layer of the membrane were calculated using Adobe Photoshop CS4. A positive signal for DR3 was recorded on the mesothelial layer of the unchallenged membrane of $DR3^{+/+}$ mice (6.5 ± 0.3 %), with low background staining on the $DR3^{-/-}$ (0.3 ± 0.1 %) (Figure 3.16B) ($p<0.01$) (Table 3.3) and isotype controls (0.1 ± <0.1 %).

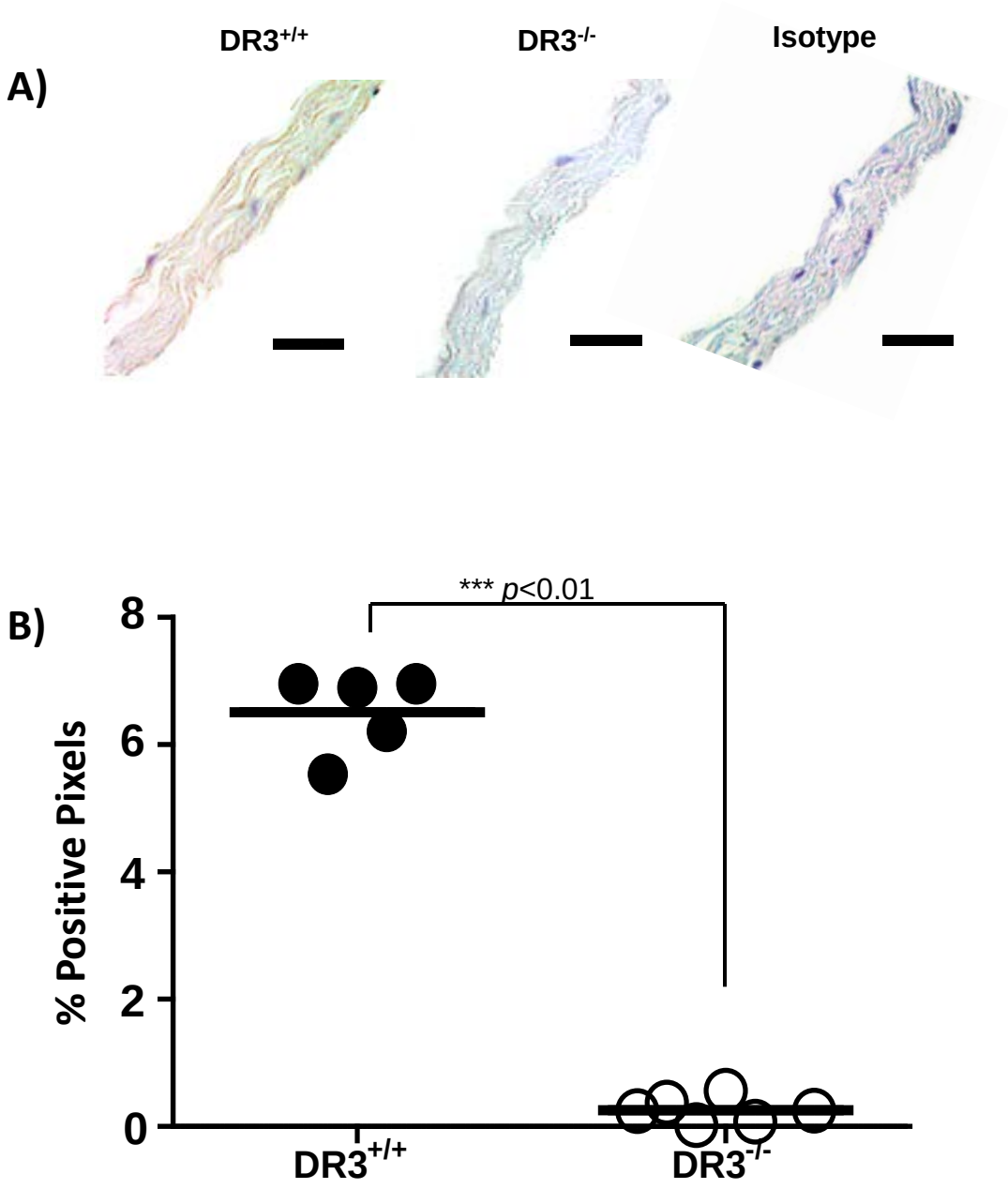

Figure 3.16 - Significant levels of DR3 expression were found on the mesothelial layer of the unchallenged peritoneal membrane of DR3$^{+/+}$ mice. A) Representative pictures of DR3 staining in the mesothelial layer of the peritoneal membrane (Bar corresponds to 25μm.) B) DR3 expression on the membrane was analysed by taking multiple pictures along the section and measuring the % of positive (brown) pixels within the mesothelial layer of the membrane using Adobe Photoshop CS4 (each symbol represents a single mouse, bar corresponds to mean from n=5 or 6, ***p<0.01 by Mann-Whitney test).

3.2.3.2 DR3 expression on resident lymphocyte cell subsets in the unchallenged peritoneal cavity of $DR3^{+/+}$ and $DR3^{-/-}$ mice

Leukocyte expression of DR3 was visualised by a polyclonal anti-DR3 antibody and flow cytometry. Relative levels of DR3 signal on T cells were estimated using median fluorescence intensity (MFI) rather than percentages (which are more easily distorted by outliers), as total population shifts were observed. A significantly greater fluorescence signal shift above the isotype (4.4 ± 0.3 MFI) was observed in both $DR3^{+/+}$ (24.0 ± 0.8 MFI) (p<0.01) and $DR3^{-/-}$ mice (9.1 ± <0.1 MFI) (p<0.01) for the T cell population, suggesting detection of some non-DR3 signal by the polyclonal DR3 antibody. However, the fluorescence signal shift was greater in $DR3^{+/+}$, compared to $DR3^{-/-}$ mice (Figure 3.17) (p<0.01). To allow a standardised comparison between the two genotypes, relative fluorescence (RF) signal increase over isotype control was calculated by dividing the test MFI by the MFI from the isotype. RF on $DR3^{+/+}$ naive peritoneal T cells (5.5 ± 0.2 RF) (Figure 3.17 and Figure 3.18A) was found to be significantly greater than on $DR3^{-/-}$ peritoneal T cells (2.1± <0.1 RF) (p<0.01), including both $CD4^+$ ($DR3^{+/+}$ mice 5.9 ± 0.2, $DR3^{-/-}$ mice 2.1± <0.1 RF) (p<0.01) (Figure 3.18B) and $CD8^+$ ($DR3^{+/+}$ mice 5.2 ± 1.8, $DR3^{-/-}$ mice 1.2 ± 0.2 RF) (p<0.01) (Figure 3.18C) subsets.

MFI ratio however was not used to analyse NK and NKT cell subsets due to a separate non-DR3 signal positive population found in $DR3^{-/-}$ NKT cells and both the $DR3^{-/-}$ and isotype control of NK cells (Figure 3.19). Instead percent positive and MFI of the positive population was used to calculate potential DR3 expression. No significant differences were seen in the percentage positive population of NK cells in $DR3^{+/+}$ mice (7 ± 1 %) compared to $DR3^{-/-}$ mice (5.5 ± 0.7 %) or isotype control (6 ± <0.1 %); equivalent MFI was also found in the positive population between $DR3^{+/+}$

(63 ± 13 MFI) and $DR3^{-/-}$ mice (63 ± 3 MFI). The positive signal in NKT cells was however significantly higher in both $DR3^{+/+}$ (69 ± 9 %) and $DR3^{-/-}$ mice (37 ± 4 %) compared to the isotype (9 ± 2 %) ($p<0.01$). The proportion of percentage positive NKT cells was significantly higher in $DR3^{+/+}$ mice compared to $DR3^{-/-}$ mice ($p<0.05$); the MFI in the NKT positive population of $DR3^{+/+}$ mice (12 ± 6 MFI) was not significantly different to those found in $DR3^{-/-}$ mice (31 ± 9 MFI). No significant differences in DR3 signals were observed on macrophages or B cells between genotypes or in the isotype control (Figure 3.20). Potential reasons for these differences in signals for DR3 in different cell subsets will be discussed in detail in Chapter 7.

3.2.4.1 Peripheral blood leukocytes in unchallenged $DR3^{+/+}$ and $DR3^{-/-}$ mice

Many cell subsets present in the naive peritoneal cavity are recruited into the cavity from the peripheral blood (Topley, Liberek et al. 1996; Jones 2005). To examine if DR3 had any effect on the number of leukocytes present in the peripheral blood, blood was obtained by cardiac puncture (Section 2.2.3.2), red blood cells lysed and remaining leukocytes were counted using a haemocytometer. $DR3^{-/-}$ mice (3.3 ± 0.6 $x10^6$ cells/ml) showed no significant difference in the number of peripheral blood leukocytes compared to $DR3^{+/+}$ mice (2.8 ± 0.3 x 10^6 cells/ml) (Figure 3.21) (Table 3.1).

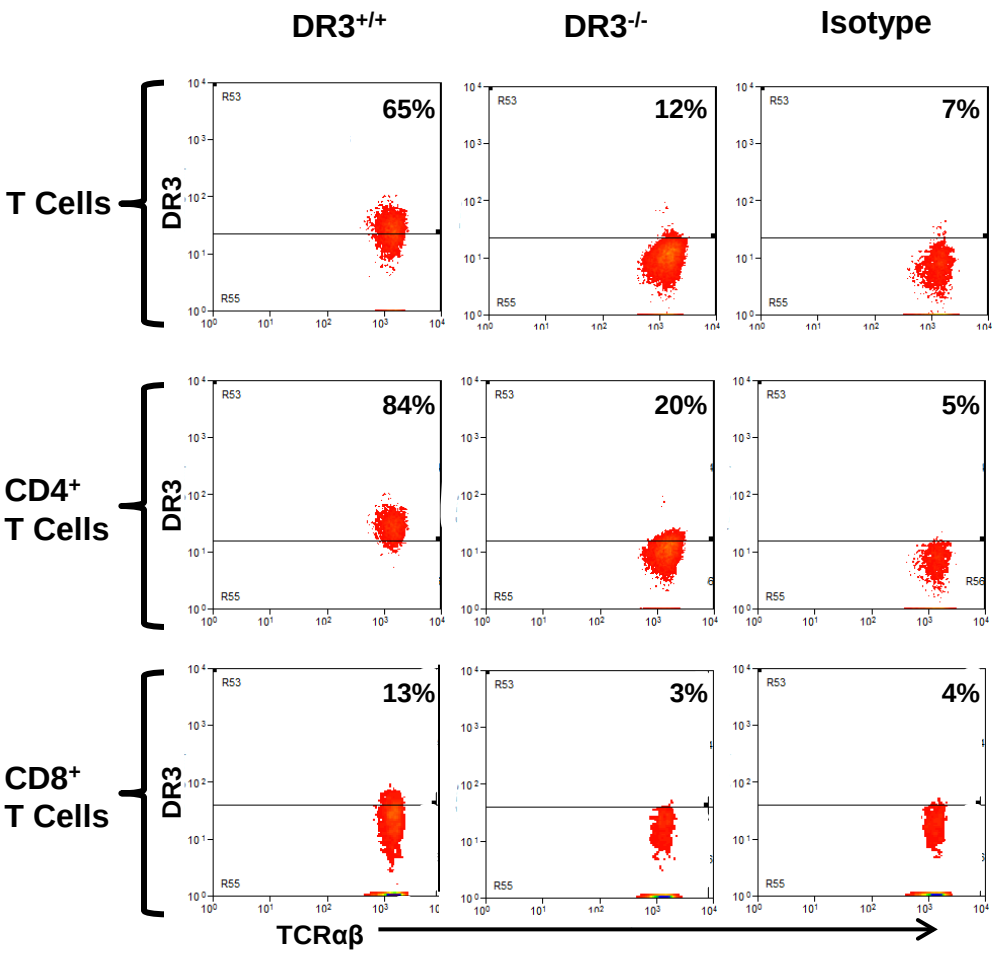

Figure 3.17 - Flow cytometry plots representing level of DR3 expression on resident T cell subsets in the unchallenged peritoneal cavity of DR3$^{+/+}$ mice. Peritoneal leukocytes were isolated from the cavity by lavage. A) T cells were identified by a CD3^{+}, TCRαβ^{+} phenotype B) T helper cells were identified by a CD3^{+} CD4^{+}, TCRαβ^{+} phenotype and C) T cytotoxic cells identified by a CD3^{+} CD8^{+}, TCRαβ^{+} phenotype.

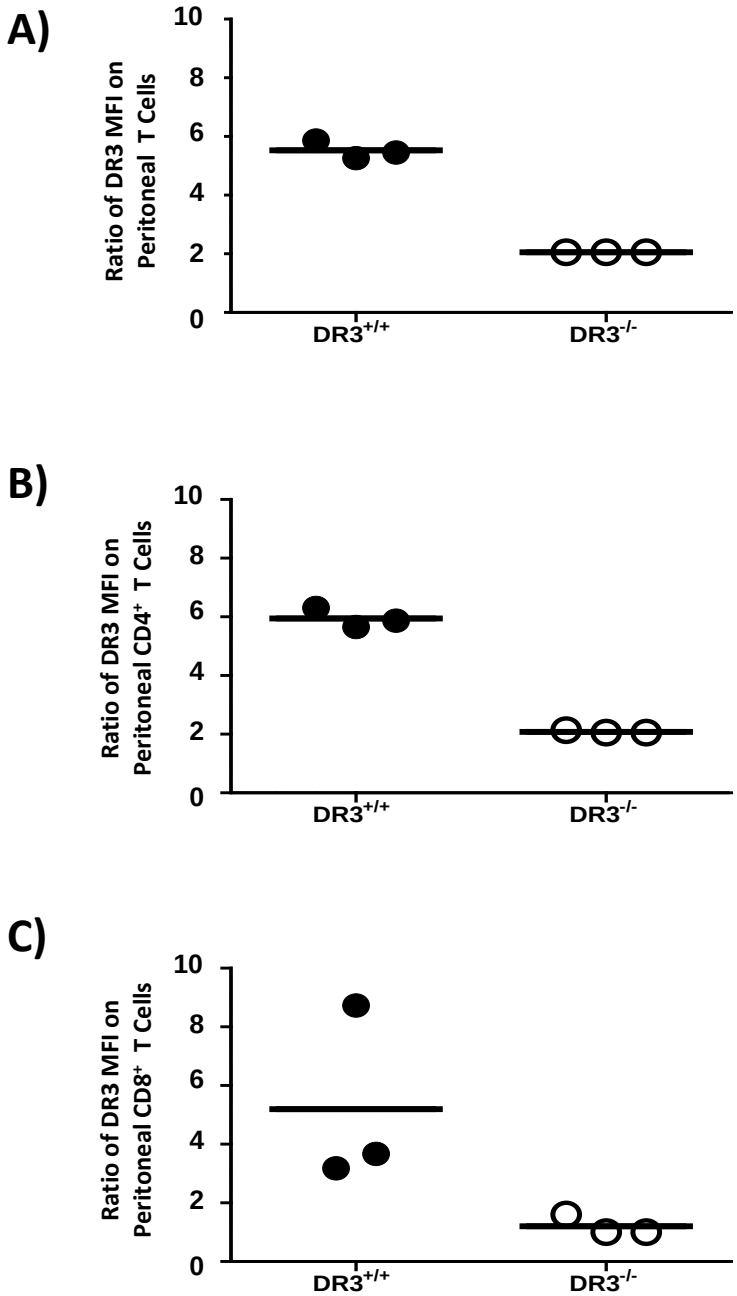

Figure 3.18 - Significant levels of DR3 expression were found on resident T cell subsets in the unchallenged peritoneal cavity of DR3$^{+/+}$ mice. Peritoneal leukocytes were isolated from the cavity by lavage. A) T cells were identified by a CD3^{+}, TCRαβ^{+} phenotype (p<0.01) B) T helper cells were identified by a CD3^{+} CD4^{+}, TCRαβ^{+} phenotype (p<0.01) C) and T cytotoxic cells identified by a CD3^{+} CD8^{+}, TCRαβ^{+} phenotype (p<0.01). Ratio of DR3 expression on subsets was calculated by the MFI fold increase compared to the isotype (each symbol represents a single mouse, bar corresponds to mean from n=3, analysed by Mann-Whitney test).

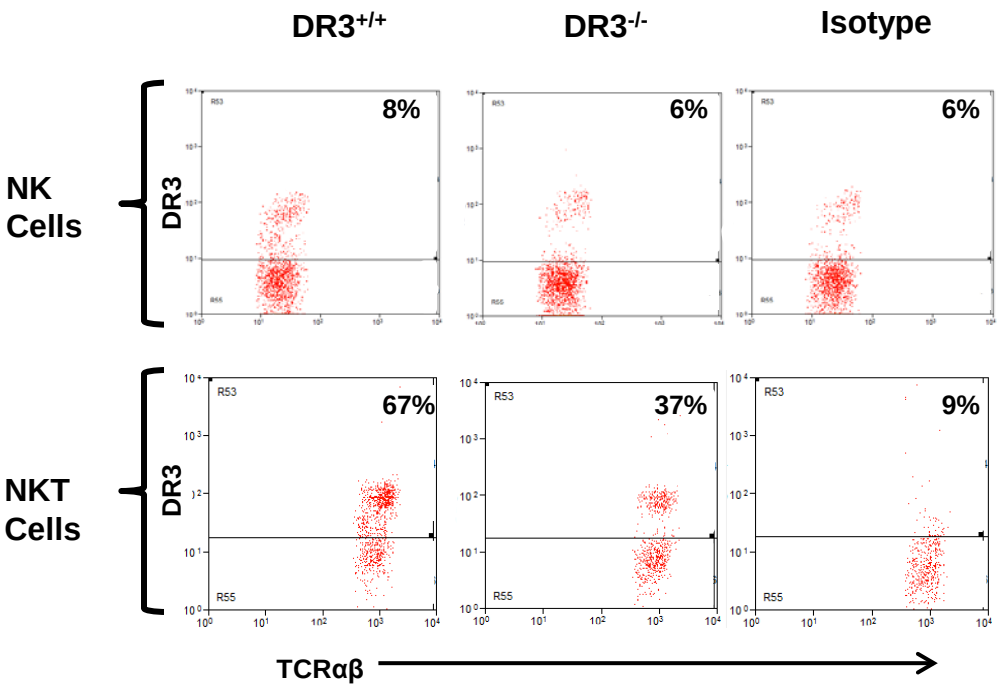

Figure 3.19 - Flow cytometry plots representing DR3 staining on resident NK and NKT cells in the unchallenged peritoneal cavity of DR3$^{+/+}$ mice. Peritoneal leukocytes were isolated from the cavity by lavage. A) NK cells were identified by a NK1.1^{+}, TCRαβ^{-} phenotype and B) NKT cells were identified by a NK1.1^{+}, TCRαβ^{+} phenotype.

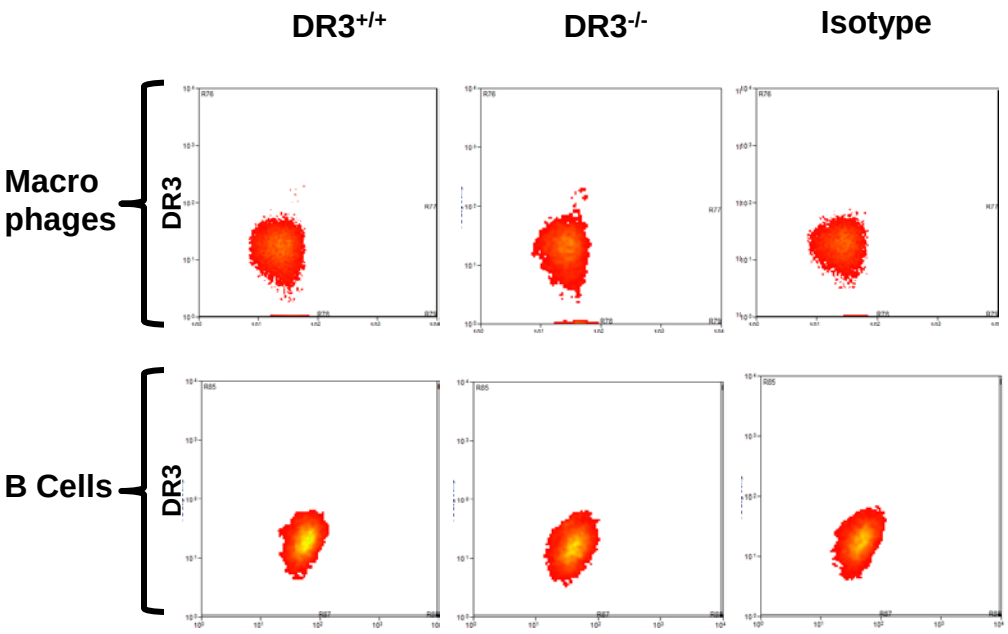

Figure 3.20 - Flow cytometry plots representing DR3 staining on macrophages and B cells in the unchallenged peritoneal cavity. Peritoneal leukocytes were isolated from the cavity by lavage. A) Resident Macrophages were identified by a $CD11b^+$ $F4/80^+$ phenotype and B) B cells were identified by a $CD19^+$, $B220^+$ phenotype.

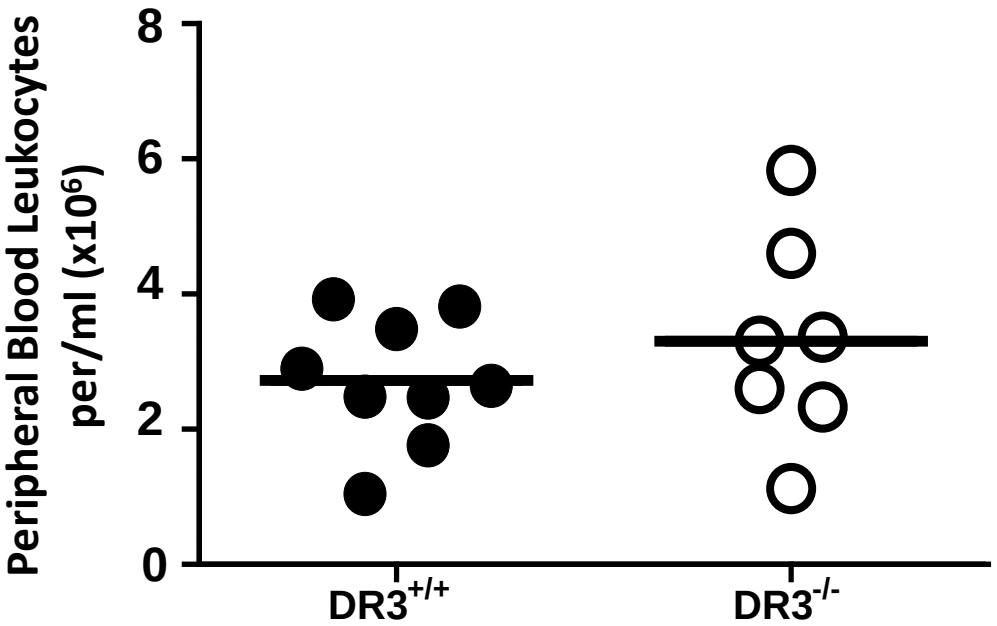

Figure 3.21 - No significant differences were seen in peripheral blood leukocyte numbers between unchallenged DR3$^{+/+}$ and DR3$^{-/-}$ mice. Peripheral blood leukocytes were collected by cardiac puncture of the heart. Leukocyte numbers were calculated, after red blood cell lysis using a haemocytometer (each symbol represents a single mouse, bar corresponds to mean from n=7 or 9, N.S.D by t-test).

3.2.4.2 Myeloid cell subset numbers in the peripheral blood of unchallenged DR3$^{+/+}$ and DR3$^{-/-}$ mice

To scrutinise if the absence of DR3 changed the composition of the leukocyte subsets in the peripheral blood, myeloid subsets were separated from the total leukocyte population. Similar numbers of all peripheral blood myeloid subsets tested (Monocytes: DR3$^{+/+}$ mice 4.2 ± 1.0 x10^5, DR3$^{-/-}$ mice 4.7 ± 1.6 x10^5 cells/ml - Figure 3.22A, Neutrophils: DR3$^{+/+}$ mice 2.3 ± 0.6 x10^5, DR3$^{-/-}$ mice 4.1 ± 2.2 x10^5 cells/ml - Figure 3.22B, and Eosinophils: DR3$^{+/+}$ mice 5.2 ± 1.3 x10^4, DR3$^{-/-}$ mice 3.5 ± 0.8 x10^4 cells/ml - Figure 3.22C) were found in both genotypes.

3.2.4.3 Lymphoid cell subset numbers in the peripheral blood of unchallenged DR3$^{+/+}$ and DR3$^{-/-}$ mice

The absence of DR3 had no effect on the number of T cells found in the peripheral blood (DR3$^{+/+}$ mice 4.0 ± 0.5 x10^5, DR3$^{-/-}$ mice 4.5 ± 0.6 x10^5 cells/ml) (Figure 3.23A) with no significant difference found in either CD4$^+$ (DR3$^{+/+}$ mice 2.3 ± 0.3 x10^5, DR3$^{-/-}$ mice 2.7 ± 0.4 x10^5 cells/ml) (Figure 3.23B) or CD8$^+$ (DR3$^{+/+}$ mice 1.6 ± 0.2 x10^5, DR3$^{-/-}$ mice 1.8 ± 0.2 x10^5 cells/ml) (Figure 3.23C) T cell subsets compared to naive DR3$^{+/+}$ peripheral blood. Other peripheral blood lymphocytes investigated such as B cells (DR3$^{+/+}$ mice 9.6 ± 1.8 x10^5, DR3$^{-/-}$ mice 1.0 ± 0.2 x10^6 cells/ml) (Figure 3.24), NK cells (DR3$^{+/+}$ mice 8.3 ± 1.4 x10^4, DR3$^{-/-}$ mice 7.2 ± 1.0 x10^4 cells/ml) (Figure 3.25A) and NKT cells (DR3$^{+/+}$ mice 1.3 ± 0.2 x10^4, DR3$^{-/-}$ mice 1.3 ± 0.2 x10^4 cells/ml) (Figure 3.25B) had analogous numbers between the 2 genotypes.

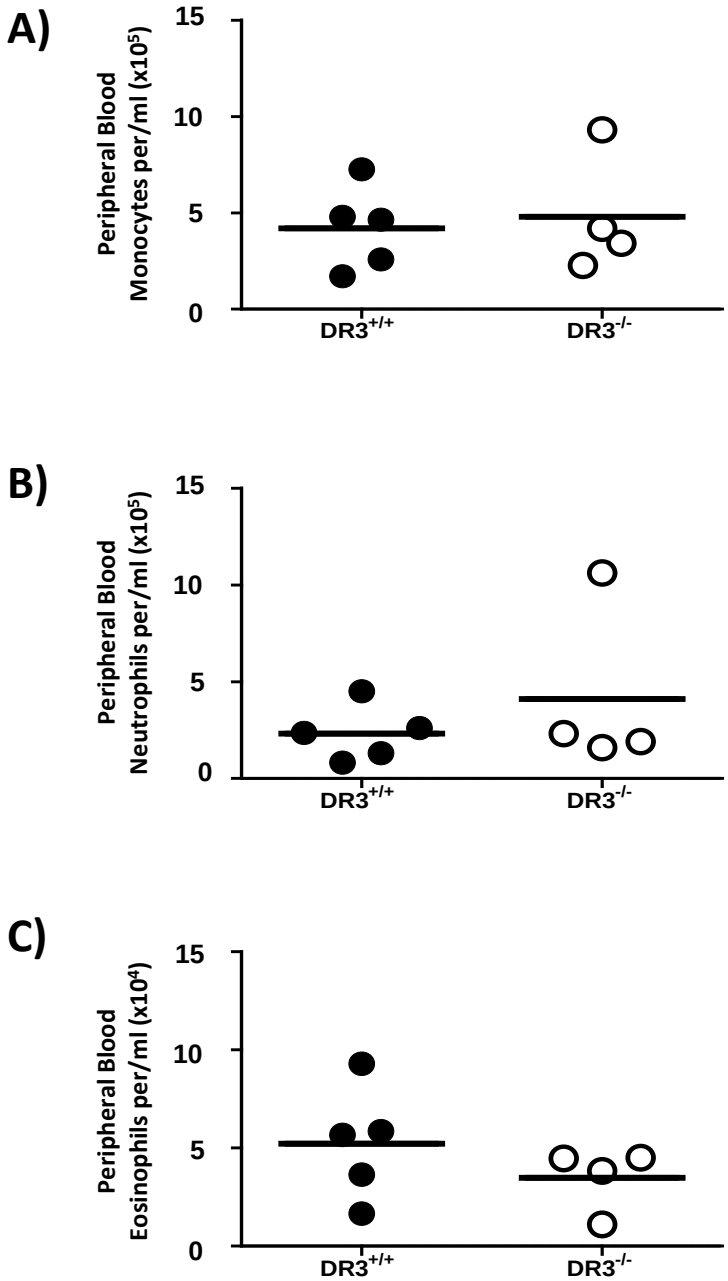

Figure 3.22 - No significant differences were seen in the numbers of peripheral blood myeloid cell subsets between unchallenged DR3$^{+/+}$ and DR3$^{-/-}$ mice. Peripheral blood leukocytes were collected by cardiac puncture of the heart. A) Monocytes were identified by a CD11b^{int} F4/80^{int} phenotype B) Neutrophils were identified by a 7/4^{+} Ly6G^{+} phenotype and C) Eosinophils, identified by a F4/80^{int} CD11b^{int} phenotype and their forward and side scatter properties. Subset numbers calculated by percentage proportion of total leukocytes/per ml (each symbol represents a single mouse, bar corresponds to mean from n=4 or 5, N.S.D by t-test).

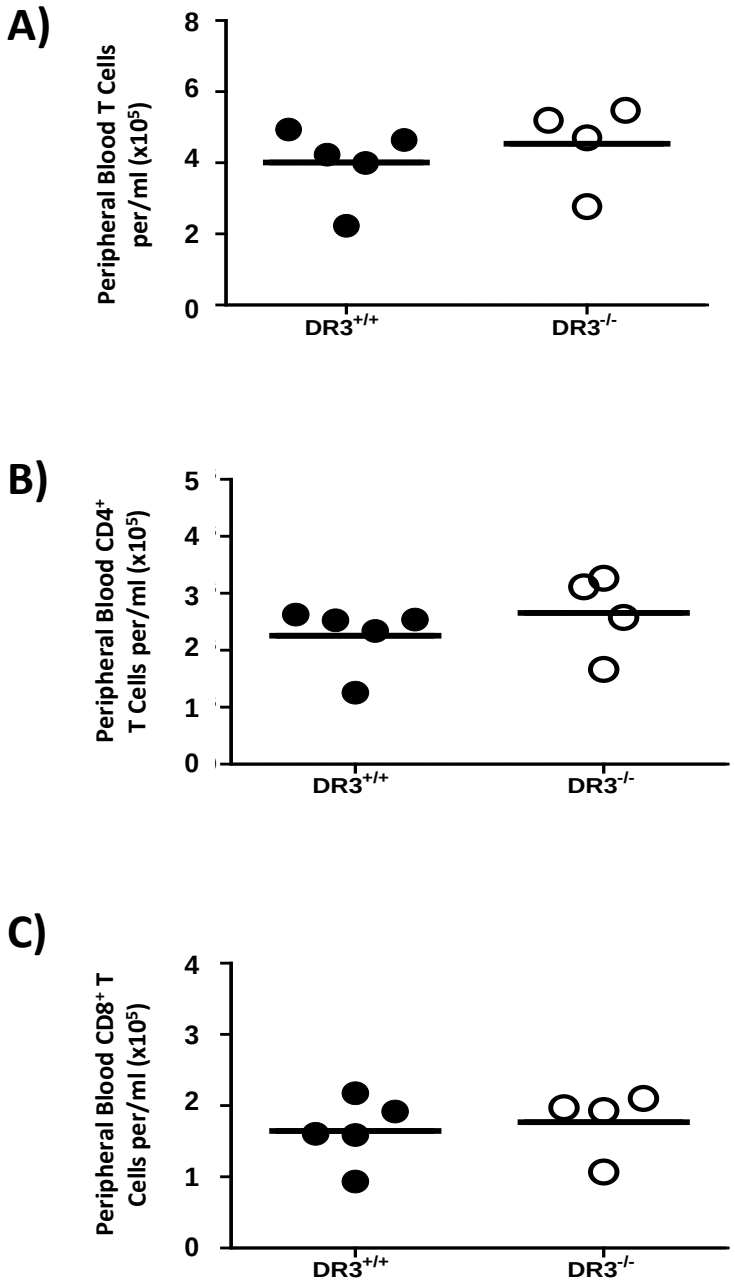

Figure 3.23 - No significant differences were seen in the numbers of peripheral blood T cell subsets between unchallenged DR3$^{+/+}$ and DR3$^{-/-}$ mice. Peripheral blood leukocytes were collected by cardiac puncture of the heart. A) T cells were identified by a CD3^{+}, TCRαβ^{+} phenotype, B) T helper cells were identified by a CD3^{+} CD4^{+}, TCRαβ^{+} phenotype and C) T cytotoxic cells identified by a CD3^{+} CD8^{+}, TCRαβ^{+} phenotype. Subset numbers calculated by percentage proportion of total leukocytes/per ml (each symbol represents a single mouse, bar corresponds to mean from n=4 or 5, N.S.D by t-test).

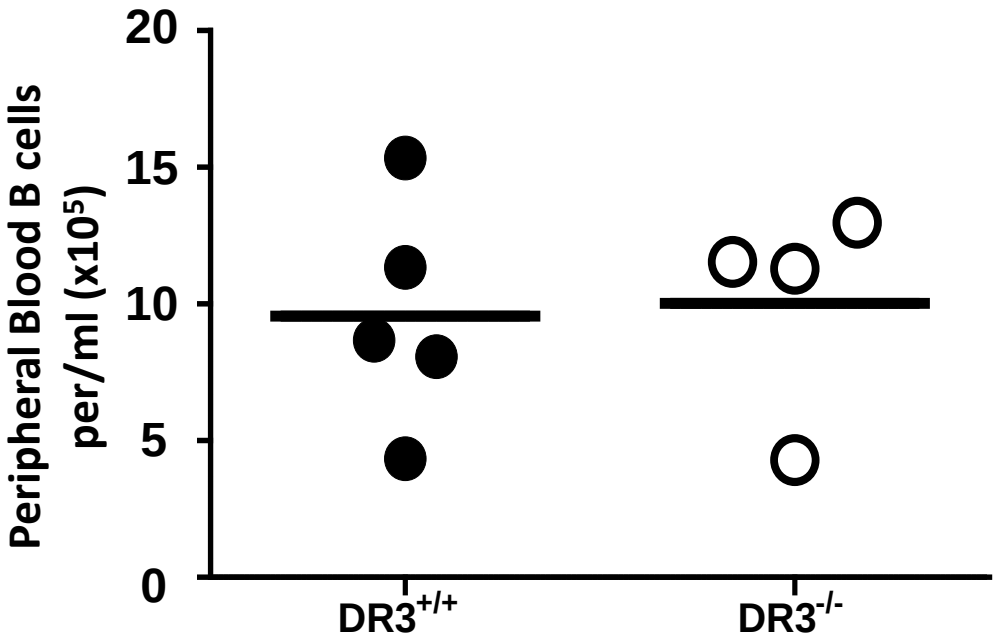

Figure 3.24 - No significant differences were seen in the numbers of peripheral blood B cells between unchallenged DR3$^{+/+}$ and DR3$^{-/-}$ mice. Peripheral blood leukocytes were collected by cardiac puncture of the heart. B cells were identified by a CD19$^+$, B220$^+$ phenotype and numbers calculated by percentage proportion of total leukocytes/per ml (each symbol represents a single mouse, bar corresponds to mean from n=4 or 5, N.S.D by t-test).

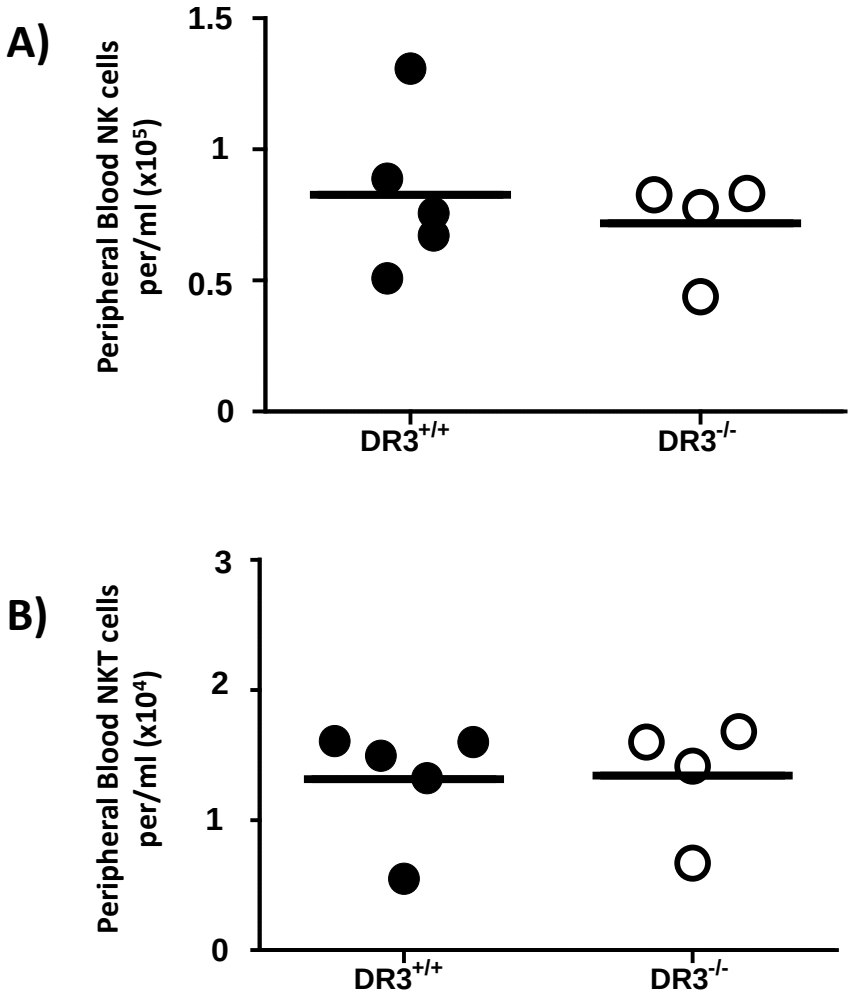

Figure 3.25 - No significant differences were seen in the numbers of peripheral blood NK or NKT cell subsets between unchallenged DR3$^{+/+}$ and DR3$^{-/-}$ mice. Peripheral blood leukocytes were collected by cardiac puncture of the heart. A) NK cells were identified by a NK1.1^{+}, TCRαβ^{-} phenotype and B) NKT cells were identified by a NK1.1^{+}, TCRαβ^{+} phenotype. Subset numbers calculated by percentage proportion of total leukocytes/per ml (each symbol represents a single mouse, bar corresponds to mean from n=4 or 5, N.S.D by t-test).

3.3 Summary

- DR3 was not essential for maintaining the total residential leukocyte number in the naive peritoneal cavity.
- Equivalent numbers of all leukocyte subsets were identified in the naive cavity of $DR3^{-/-}$ mice compared to $DR3^{+/+}$ mice.
- DR3 had no effect on proliferation or apoptotic mechanisms in the naive cavity.
- DR3 was expressed on the mesothelial layer of the peritoneal membrane and on T cell subsets in the naive cavity.
- Similar numbers of peripheral blood cell subsets were found in $DR3^{-/-}$ compared to $DR3^{+/+}$ mice.
- These data imply DR3 is not essential for homeostatic maintenance of leukocyte numbers in the peritoneal cavity or peripheral blood.

Table 3.1- Summary of cell numbers

	Peritoneal cavity^			Peripheral blood*		
Cell subset	**DR3$^{+/+}$**	**DR3$^{-/-}$**	**Significance$^{\$}$**	**DR3$^{+/+}$**	**DR3$^{-/-}$**	**Significance$^{\$}$**
Leukocytes	$2.8 \pm 0.2 \times 10^6$	$2.9 \pm 0.2 \times 10^6$	N.S.D	$2.8 \pm 0.3 \times 10^6$	$3.3 \pm 0.6 \times 10^6$	N.S.D
Macrophages/Monocytes	$7.2 \pm 1.8 \times 10^5$	$6.4 \pm 1.6 \times 10^5$	N.S.D	$4.2 \pm 1.0 \times 10^5$	$4.7 \pm 1.6 \times 10^5$	N.S.D
DC's	$5.1 \pm 1.6 \times 10^3$	$3.3 \pm 0.3 \times 10^3$	N.S.D	N/A†	N/A†	N/A†
Neutrophils	N/A†	N/A†	N/A†	$2.3 \pm 0.6 \times 10^5$	$4.1 \pm 2.2 \times 10^5$	N.S.D
Eosinophils	$1.9 \pm 0.7 \times 10^5$	$7.6 \pm 0.6 \times 10^4$	N.S.D	$5.2 \pm 1.3 \times 10^4$	$3.5 \pm 0.8 \times 10^4$	N.S.D
T Cells	$4.5 \pm 0.5 \times 10^5$	$4.6 \pm 1.1 \times 10^5$	N.S.D	$4.0 \pm 0.5 \times 10^5$	$4.5 \pm 0.6 \times 10^5$	N.S.D
CD4$^+$ T Cells	$2.9 \pm 0.7 \times 10^5$	$3.0 \pm 0.4 \times 10^5$	N.S.D	$2.3 \pm 0.3 \times 10^5$	$2.7 \pm 0.4 \times 10^5$	N.S.D
CD8$^+$ T Cells	$6.1 \pm 1.4 \times 10^4$	$6.9 \pm 0.6 \times 10^4$	N.S.D	$1.6 \pm 0.2 \times 10^5$	$1.8 \pm 0.2 \times 10^5$	N.S.D
B Cells	$8.6 \pm 1.0 \times 10^5$	$9.3 \pm 2.9 \times 10^5$	N.S.D	$9.6 \pm 1.8 \times 10^5$	$1.0 \pm 0.2 \times 10^6$	N.S.D
Peritoneal B1 Cells	$6.6 \pm 1.8 \times 10^5$	$5.4 \pm 0.7 \times 10^5$	N.S.D	N/A†	N/A†	N/A†
Peritoneal B2 Cells	$1.5 \pm 0.5 \times 10^5$	$1.8 \pm 0.3 \times 10^5$	N.S.D	N/A†	N/A†	N/A†
NK Cells	$6.8 \pm 1.7 \times 10^4$	$4.7 \pm 0.8 \times 10^4$	N.S.D	$8.3 \pm 1.4 \times 10^4$	$7.2 \pm 1.0 \times 10^4$	N.S.D
NK T Cells	$7.2 \pm 1.8 \times 10^4$	$6.9 \pm 0.6 \times 10^4$	N.S.D	$1.3 \pm 0.2 \times 10^4$	$1.3 \pm 0.2 \times 10^4$	N.S.D

^ Values correspond to number of peritoneal leukocytes ± SEM (n=5),
* Values correspond to number of peripheral blood leukocytes (per/ml) ± SEM (n= 4 or 5),
† N/A corresponds to subsets either not present at the time or not tested,
$^{\$}$ Significance between the two genotypes using t-test, N.S.D = no significant difference

Table 3.2- Summary of cell proliferation and apoptosis

	Ki67^{+} Proliferation ^			Annexin V^{+} Apoptosis and 7AAD^{+} death*		
Cell subset	**DR3$^{+/+}$**	**DR3$^{-/-}$**	**Significance$^{\$}$**	**DR3$^{+/+}$**	**DR3$^{-/-}$**	**Significance$^{\$}$**
Macrophages	10.7 ± 2.0	7.1 ± 1.1	N.S.D	40.7 ± 5.6	42.5 ± 1.8	N.S.D
Eosinophils	N/A	N/A	N/A	14.7 ± 1.0	15.7 ± 1.1	N.S.D
T Cells	37.7 ± 5.5	35.1 ± 3.2	N.S.D	17.7 ± 0.5	19 ± 0.9	N.S.D
B Cells	13.0 ± 0.5	12.2 ± 1.1	N.S.D	68.3 ± 1.2	72.2 ± 3.9	N.S.D
NK Cells	21.6 ± 2.6	20.9 ± 2.1	N.S.D	33.7 ± 5.6	27.8 ± 3.2	N.S.D
NK T Cells	21.7 ± 2.6	20.9 ± 2.1	N.S.D	17.7 ± 1.8	20.4± 2.0	N.S.D

^ Values correspond to % of proliferating cells of each subset in the peritoneal cavity ± SEM (n=6),
* Values correspond to % apoptotic and dead of each subset in the peritoneal cavity ± SEM (n=6),
$ Significance between the two genotypes using Mann Whitney test, N.S.D = no significant difference.

Table 3.3 - Summary of DR3 expression

Cell subset	DR3 Expression		
	DR3$^{+/+}$	**DR3$^{-/-}$**	**Significance$^{\$}$**
% DR3 on peritoneal membrane^	6.5 ± 0.3	0.3 ± 0.1	p<0.01
DR3 MFI ratio* on T Cells	5.5 ± 0.2	2.1± <0.1	p<0.01
DR3 MFI† on T Cells	19.7 ± 0.3	4.6 ± <0.1	p<0.01
DR3 MFI ratio* on CD4^{+} T Cells	5.9 ± 0.2	2.1± <0.1	p<0.01
DR3 MFI† on CD4^{+} T Cells	23.1 ± 0.5	5.1 ± <0.1	p<0.01
DR3 MFI ratio* on CD8^{+} T Cells	3.4 ± 0.2	1.2 ± 0.2	p<0.01
DR3 MFI† on CD8^{+} T Cells	7.8 ± 0.1	0.9 ± 0.9	p<0.01
% DR3 positive NK Cells	7 ± 1	5.5 ± 0.7	N.S.D
DR3 MFI of NK Cell positive population$^{\#}$	63 ± 13	63 ± 3	N.S.D
% DR3 positive NKT Cells	69 ± 9	37 ± 4	p<0.05
DR3 MFI of NKT Cell positive population	12 ± 6	31 ± 9	N.S.D

^ % DR3 expression on the mesothelial layer of the peritoneal membrane,
* Median fluorescence intensity (MFI) ratio calculated by gating on specified subset and dividing its median from the DR3 test stain by the median of the isotype ± SEM (n = 3),
† MFI calculated by subtracting median from the DR3 test stain by the median of the isotype ± SEM (n = 3),
$^{\#}$ MFI of positive population calculated by subtracting median of positive cells from the DR3 test stain in DR3$^{+/+}$ and DR3$^{-/-}$ mice by the median of the isotype ± SEM (n = 3),
$^{\$}$ Significance between two genotypes using Mann Whitney test, N.S.D = no significant difference.

Chapter 4 - The role of DR3 in accumulation of leukocytes into the peritoneal cavity during the early stages of an *in vivo* acute inflammatory event

4.1 Introduction

Other studies have shown that DR3/TL1A interaction can influence effector T cell proliferation and cytokine production, identifying it as a potential therapeutic target (Bamias, Mishina et al. 2006; Fang, Adkins et al. 2008; Meylan, Davidson et al. 2008; Buchan, Taraban et al. 2012; Twohig, Marsden et al. 2012). To date, the affect of DR3 expression on the innate immune response in the peritoneal cavity has not been studied. Prior to the induction of inflammation, the absence of DR3 was found to have no significant impact on maintaining the leukocyte profile in the naive cavity and peripheral blood (Chapter 3).

Peritoneal inflammation was induced by an i.p. injection of SES, which promotes a biphasic innate immune response (Jones 2005). The early phase (defined in this thesis as within the first 24 hours) is composed of an initial leukocyte influx predominately of neutrophils (peak 6-12 hours) from the peripheral blood, which are then cleared and replaced by other infiltrating cell subsets (Topley, Liberek et al. 1996; Jones 2005). The late phase (post 24 hours) (Chapter 5) entails a further increase in the number of leukocytes present in the peritoneal cavity, with the influx of other (particularly lymphocytic) cell subsets before inflammation begins to be resolved (Jones 2005; McLoughlin, Jenkins et al. 2005).

The aim of this chapter was to dissect the impact of the absence of DR3 on this early response to a bacterial inflammatory hit, including investigation of cell types that were a potential source of TL1A and alterations in DR3 expression following SES challenge.

4.2 Results

4.2.1.1 Relative quantity (RQ) of TL1A mRNA in DR3$^{+/+}$ and DR3$^{-/-}$ peritoneal membranes after SES induced inflammation

Thus far no previous studies have investigated TL1A's expression profile in the peritoneal cavity, though earlier work has shown an increase in TL1A levels after induction of inflammation (Bamias, Martin et al. 2003; Meylan, Davidson et al. 2008; Saruta, Michelsen et al. 2009). The RQ (outlined in Section 2.5) of TL1A mRNA in the peritoneal membrane was investigated by qPCR. TL1A mRNA did not increase in the membrane following SES challenge (Figure 4.1) and equivalent RQ of TL1A mRNA was found in the membrane of DR3$^{+/+}$ and DR3$^{-/-}$ mice.

4.2.1.2 RQ of TL1A mRNA in DR3$^{+/+}$ and DR3$^{-/-}$ resident macrophages after SES stimulation

Elevated RQ of TL1A mRNA in macrophages has previously been shown following LPS stimulation (Meylan, Davidson et al. 2008). RQ of TL1A mRNA was investigated in cell sorted peritoneal resident macrophages (Section 2.3.10) by qPCR (Section 2.5). Increased RQ of TL1A mRNA was found in DR3$^{+/+}$ (28.4 ± 9 RQ) (p=0.03) and DR3$^{-/-}$ (18.2 ± 7 RQ) (p=0.02) resident macrophages 1 hour after *ex vivo* challenge with SES compared to unstimulated resident macrophages (Figure 4.2). Consequently resident macrophages in the naive cavity and not the peritoneal membrane appear to be a source of TL1A after stimulating with SES.

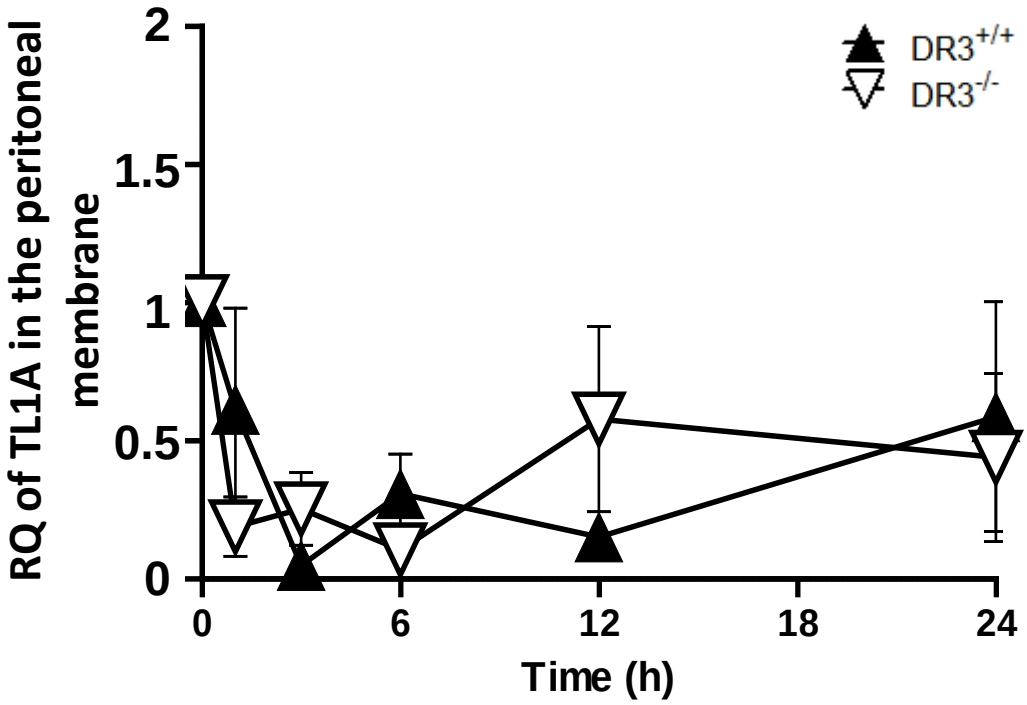

Figure 4.1 - No significant differences were seen in the relative quantity of TL1A mRNA in the peritoneal membrane of DR3$^{+/+}$ mice and DR3$^{-/-}$ mice after induction of SES inflammation. Inflammation in the cavity was induced via an i.p. injection of SES and peritoneal membranes analysed for RQ of TL1A mRNA by qPCR (each symbol represents mean of n=5 DR3$^{+/+}$ mice (▲) and DR3$^{-/-}$ mice (▽) per time point, error bars correspond to mean ± SEM, N.S.D by ANOVA).

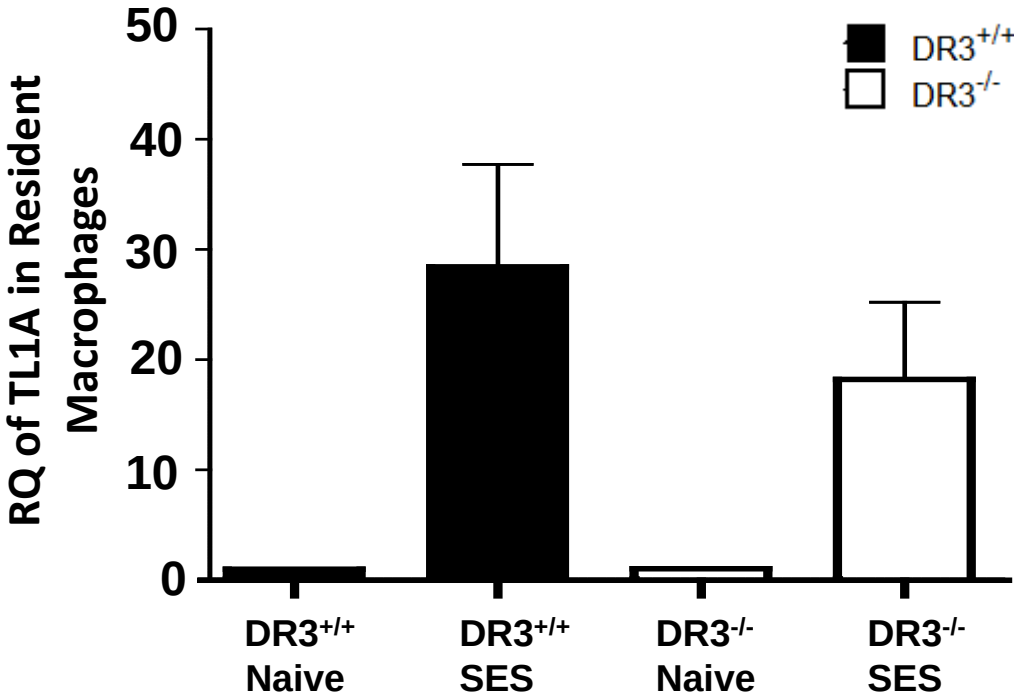

Figure 4.2 - Increased relative quantity of TL1A mRNA was found in DR3$^{+/+}$ and DR3$^{-/-}$ resident macrophages 1 hour after stimulation using SES. Resident macrophages were sorted from other leukocytes found in the peritoneal cavity and seeded into a 48 well plate. Macrophages were challenged with SES and analysed for RQ of TL1A mRNA by qPCR (each bar represents mean of 17 pooled DR3$^{+/+}$ mice (■) and DR3$^{-/-}$ mice (□) from 4 replicate experiments, error bars correspond to mean ± SEM).

4.2.1.3 DR3 expression on the mesothelial layer of the peritoneal membrane of $DR3^{+/+}$ and $DR3^{-/-}$ mice after SES induced inflammation

DR3 was detected on the mesothelial layer of the unchallenged peritoneal membrane (Section 3.2.3.1) (Figure 3.16), so DR3 expression was followed after the induction of inflammation. Multiple pictures were taken along sections of the mesothelial layer over an inflammatory time course from $DR3^{+/+}$ and $DR3^{-/-}$ mice (Figure 4.3). DR3 expression could no longer be detected 6 hours after SES challenge in $DR3^{+/+}$ mice (0.4 ± 0.4 % positive pixels). However DR3 expression returned 12 hours after inflammation was induced (7.6 ± 1.6 %) before disappearing again by 24 hours (0.1 ± 0.1 %) and for the remainder of the time course (Figure 4.4). Low background staining was detected on the $DR3^{-/-}$ (0.1 ± <0.1 %) (Figure 4.4) (p<0.01) and isotype control (0.1 ± <0.1 %).

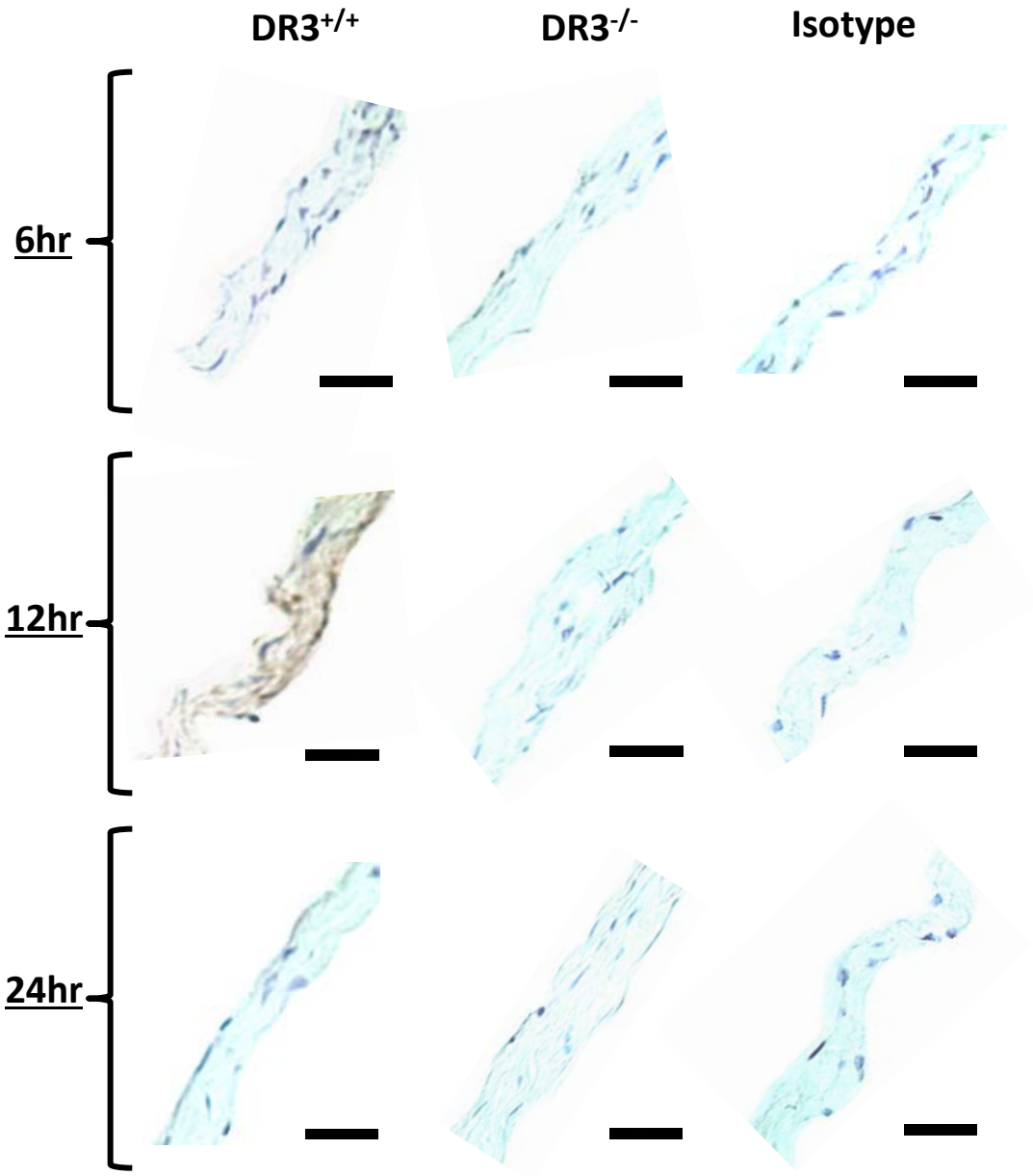

Figure 4.3 - Significant levels of DR3 expression were found on the mesothelial layer of the peritoneal membrane of DR3$^{+/+}$ mice after 12 hours of SES inflammation. Inflammation in the cavity was induced via an i.p. injection of SES. Peritoneal membranes were harvested, fixed, sectioned and stained for DR3 expression. Representative pictures show no DR3 staining in the mesothelial layer of DR3$^{+/+}$ mice after 6 hours of inflammation, though DR3 is present after 12 hours yet this expression is lost again 24 hours after SES challenge (Bar corresponds to 25μm.)

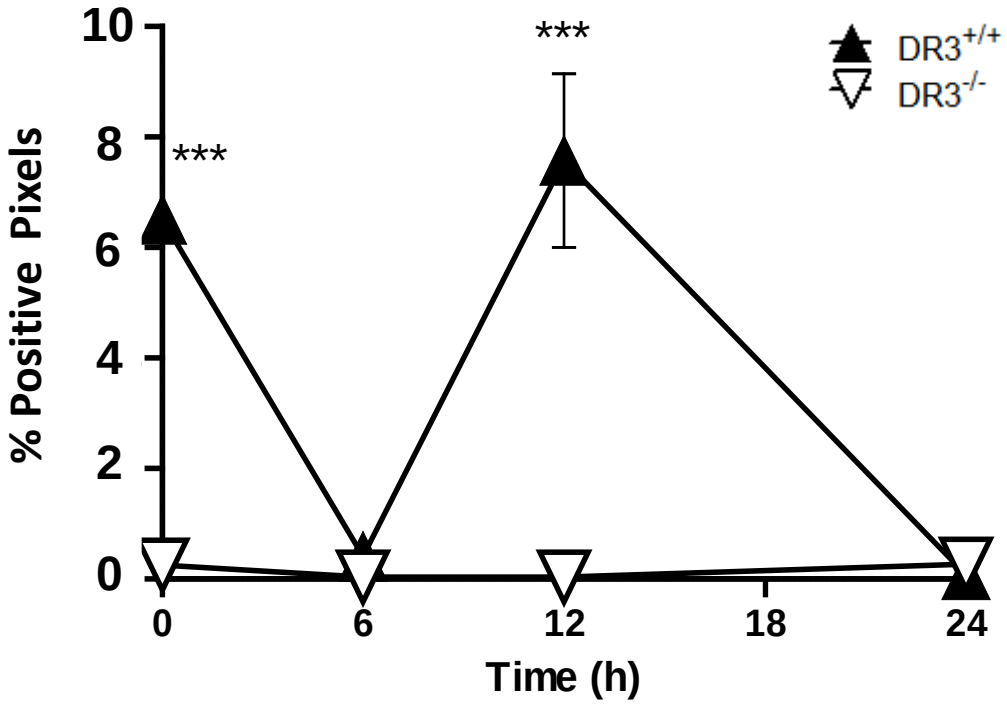

Figure 4.4 - Significant levels of DR3 expression were found on the peritoneal membrane of DR3$^{+/+}$ mice after 12 hours of SES inflammation. Inflammation in the cavity was induced via an i.p. injection of SES. Peritoneal membranes were harvested, fixed, sectioned and stained for DR3 expression. DR3 expression on the membrane was analysed by taking multiple pictures along the section and measuring the % of positive (brown) pixels within the mesothelial layer of the membrane using Adobe Photoshop CS4 (each symbol represents mean of n=3 DR3$^{+/+}$ mice (▲) and DR3$^{-/-}$ mice (▽) per time point, error bars correspond to mean ± SEM, p<0.01 by Kruskal-Wallis test, ***p<0.001 by Mann Whitney test).

4.2.1.4 DR3 expression on lymphocyte cell subsets in the peritoneal cavity of $DR3^{+/+}$ and $DR3^{-/-}$ mice after SES induced inflammation.

Alteration in DR3 expression on T and NK lymphocyte subsets after SES challenge was determined by a polyclonal DR3 antibody and flow cytometry. For T cells, MFI rather than percentages were used to estimate relative level of DR3 signal as discussed in Chapter 3. Significantly greater fluorescence signal shift above the isotype (7.2 ± 0.5 MFI after 12 hours) was once again observed in both $DR3^{+/+}$ (22.2 ± 3.1 MFI after 12 hours) ($p<0.01$) and $DR3^{-/-}$ mice (9.8 ± 0.2 MFI after 12 hours) ($p<0.05$) in the T cell population, implying recognition of some non-DR3 signal by the polyclonal DR3 antibody. However, the fluorescence signal shift was consistently greater in $DR3^{+/+}$, compared to $DR3^{-/-}$ mice ($p<0.05$ after 12 hours). Relative DR3 expression was therefore estimated using a standardised RF signal relative to the isotype control and was calculated by dividing the test MFI by the MFI from the isotype. Following induction of inflammation RF on $DR3^{+/+}$ T cells (3.0 ± 0.4 RF after 12 hours) was found to be significantly greater than on $DR3^{-/-}$ peritoneal T cells (1.5 ± <0.1 RF after 12 hours) ($p<0.01$), however RF on $DR3^{+/+}$ T cells after SES challenge was significantly reduced compared to naive $DR3^{+/+}$ T cells (5.5 ± 0.2 RF) (Figure 4.5A). Investigation of T cell subsets showed different DR3 RF expression profiles in $DR3^{+/+}$ mice; $CD8^+$ T cells lost all DR3 expression during inflammation (1.0 ± <0.1 RF after 12 hours) (Figure 4.5C) compared to naive $CD8^+$ T cells (5.2 ± 1.8 RF), whereas RF on $DR3^{+/+}$ $CD4^+$ T cells was seen to fluctuate over the time course (4.1 ± 0.6 RF after 12 hours) (Figure 4.5B).

MFI ratio was not used to analyse NK and NKT cell subsets due to a separate non-DR3 signal positive population found in $DR3^{-/-}$ NKT cells and both the $DR3^{-/-}$ and isotype control of NK cells (Figure 3.19). Instead percent positive and MFI of

the positive population was used to calculate potential DR3 expression. No significant differences were seen in the percentage positive population of NK cells at any point throughout the time course in $DR3^{+/+}$ mice (3.4 ± 1 % after 12 hours) compared to $DR3^{-/-}$ mice (2.4 ± 0.2 % after 12 hours) or isotype control (1.6 ± 0.2 % after 12 hours) (Figure 4.6A), equivalent MFI was also found in the positive population between $DR3^{+/+}$ (26.7 ± 1.4 MFI after 12 hours) and $DR3^{-/-}$ mice over the time course (27 ± 1 MFI after 12 hours). Percent positive NKT cells however was significantly higher in naive $DR3^{+/+}$ mice (69 ± 9 %) compared to $DR3^{-/-}$ mice (37 ± 4 %) ($p<0.05$) and the isotype (9 ± 2 %) ($p<0.01$), though the percentage positive in $DR3^{+/+}$ mice fell over the time course (53 ± 1.9 % after 24 hours) (Figure 4.6B); the MFI in the NKT positive population of $DR3^{+/+}$ mice (27 ± 1 MFI after 24 hours) was not significantly different to those found in $DR3^{-/-}$ mice (27 ± 1 MFI after 24 hours).

In summary, DR3 expression was found on tissue and multiple cell subsets in the peritoneal cavity and fluctuated following SES challenge. On the peritoneal membrane, it was initially expressed but showed a biphasic pattern being absent at 6 and 24 hours. On $CD8^+$ T cells, cell surface DR3 was found initially but lost within 6 hours. In contrast, DR3 expression on $CD4^+$ T cells and NKT cells was found throughout the first 24 hours after SES challenge. These tissues and cell types are potential targets for the action of TL1A.

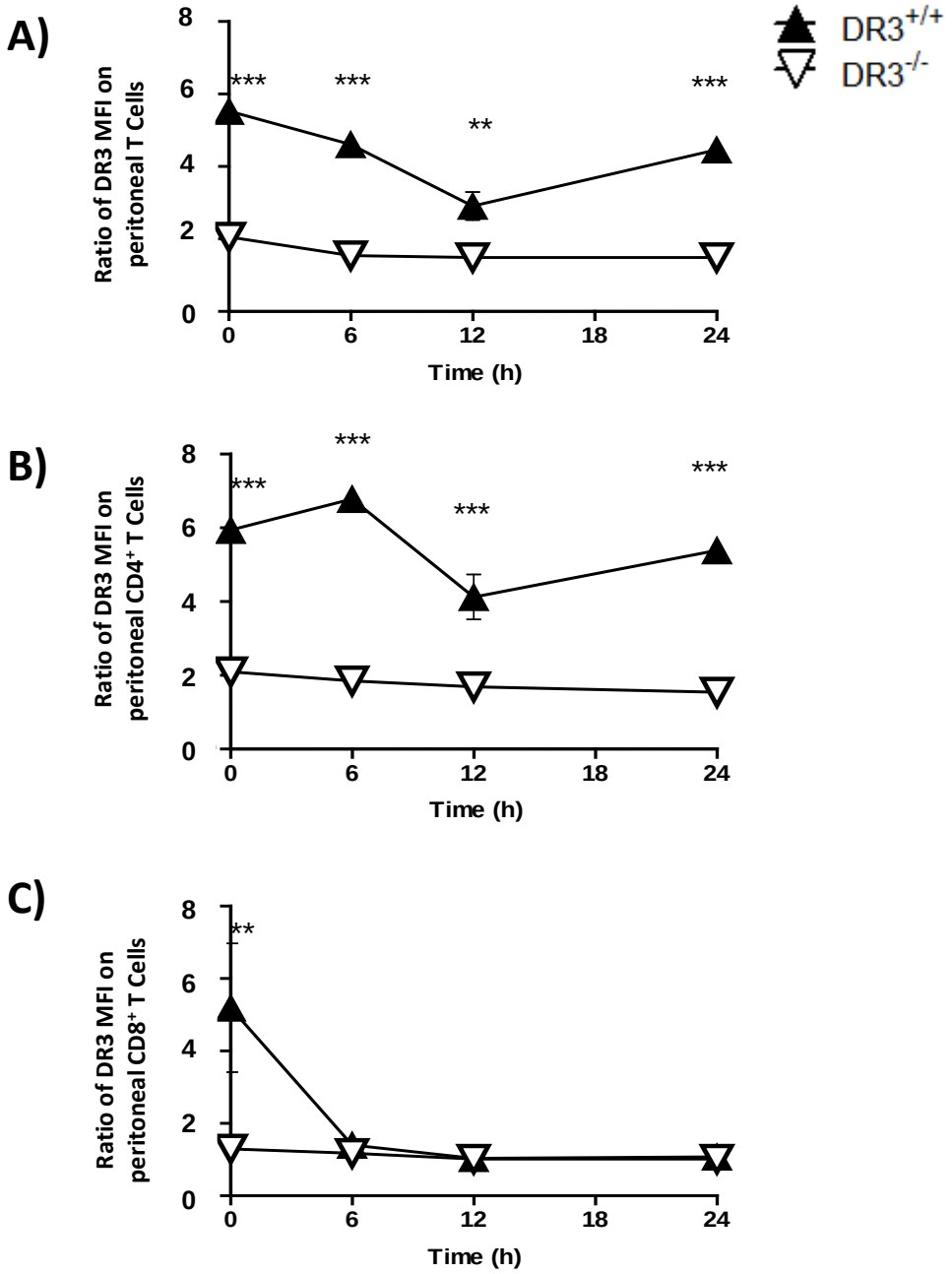

Figure 4.5 - Significant levels of DR3 expression were found on CD4$^+$, but not CD8$^+$, T cells in the peritoneal cavity of DR3$^{+/+}$ mice after induction of SES inflammation. Inflammation in the cavity was induced via an i.p. injection of SES and leukocytes isolated from the cavity by lavage. A) T cells were identified by a CD3$^+$, TCRαβ$^+$ phenotype (p<0.01 by ANOVA, Bonferroni post hoc test **p<0.01 after 12h and ***p<0.001 after 0, 6 and 24h) B) T helper cells were identified by a CD3$^+$ CD4$^+$, TCRαβ$^+$ phenotype (p<0.01 by ANOVA, Bonferroni post hoc test ***p<0.001 after all time points) and C) T cytotoxic cells identified by a CD3$^+$ CD8$^+$, TCRαβ$^+$ phenotype (Bonferroni post hoc test **p<0.01 after 0h). Ratio of DR3 expression on subsets was calculated by the MFI fold increase compared to the isotype (each symbol represents mean of n=3 DR3$^{+/+}$ mice (▲) and DR3$^{-/-}$ mice (▽) per time point, error bars correspond to mean ± SEM, analysed by ANOVA and Bonferroni post hoc test).

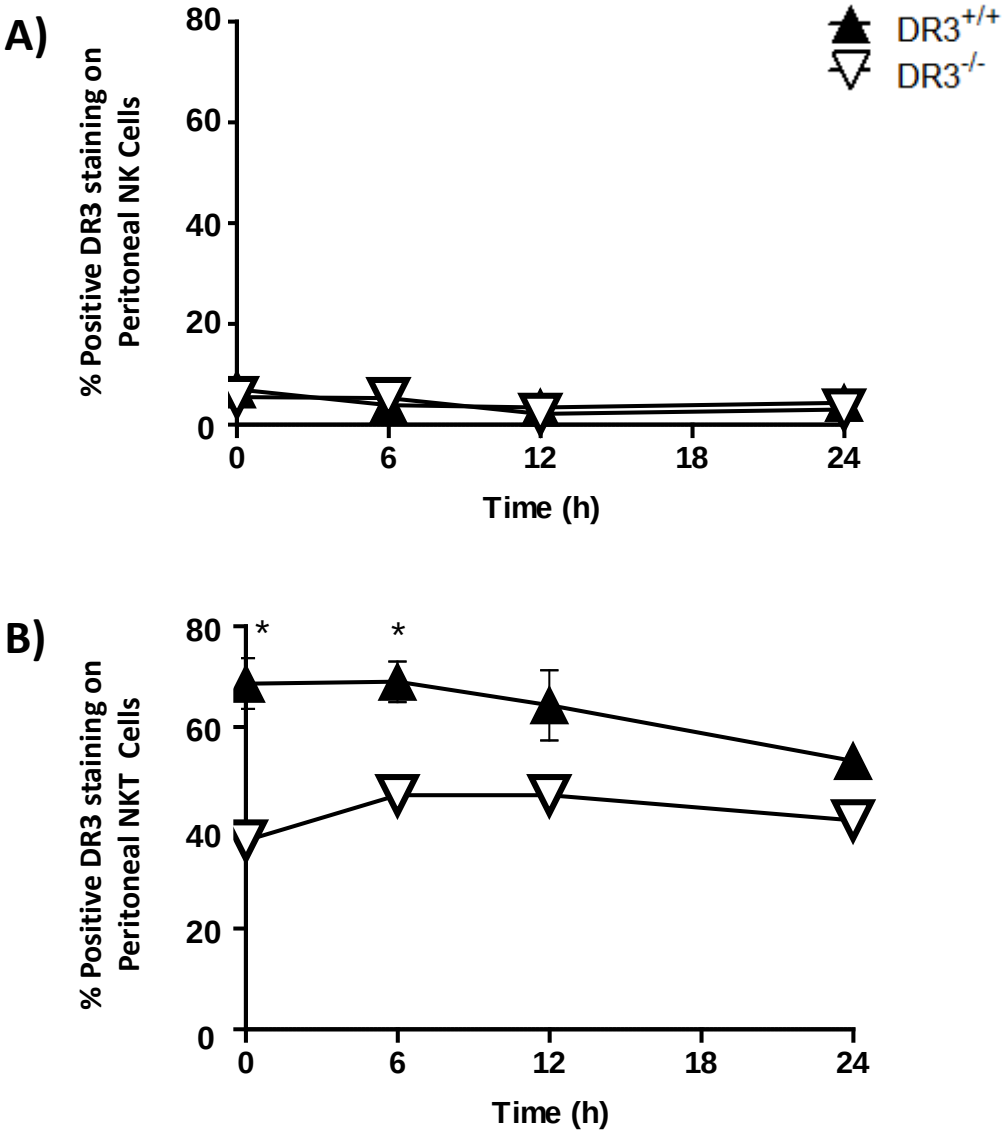

Figure 4.6 - Significant levels of DR3 expression were found on NKT cells but not NK cells in the peritoneal cavity of DR3$^{+/+}$ mice compared to DR3$^{-/-}$ mice after induction of SES inflammation. Inflammation in the cavity was induced via an i.p. injection of SES. Peritoneal leukocytes were isolated from the cavity by lavage. A) NK cells were identified by a NK1.1^{+}, TCRαβ^{-} phenotype and B) NKT helper cells were identified by a NK1.1^{+}, TCRαβ^{+} phenotype (p<0.01 by Kruskal-Wallis test, Mann Whitney test *p<0.05 after 0 and 6h). Percentage positive population was used to calculate potential DR3 expression (each symbol represents mean of n=3 DR3$^{+/+}$ mice (▲) and DR3$^{-/-}$ mice (▽) per time point, error bars correspond to mean ± SEM, analysed by Kruskal-Wallis test, and Mann Whitney test)

4.2.2.1 Accumulation of mouse leukocytes in the $DR3^{+/+}$ and $DR3^{-/-}$ peritoneal cavity during early stages of SES induced inflammation

Total leukocytes in the cavity during the early stage of inflammation were isolated by lavage at defined time points after SES challenge (Section 2.2.3.1) and counted by a Coulter counter (Section 2.2.4). There was a substantial increase in number of leukocytes in the cavity of both genotypes 1 hour after SES challenge, and total number of leukocytes continued to increase throughout the first 24 hours (Figure 1.9). $DR3^{-/-}$ mice displayed a similar profile of leukocyte accumulation as $DR3^{+/+}$ mice, though a trend towards lower cell numbers was observed in the $DR3^{-/-}$ cavity after both 6 hours ($DR3^{+/+}$ mice $7.1 \pm 1.6 \times 10^6$, $DR3^{-/-}$ mice $5.6 \pm 0.4 \times 10^6$ total cells) (p=0.35) and 24 hours ($DR3^{+/+}$ mice $8.2 \pm 1.4 \times 10^6$, $DR3^{-/-}$ mice $5.5 \pm 1.0 \times 10^6$ total cells) (p=0.19). The latter time point may be considered a transition point between early and late stages of acute inflammation in this model (Figure 4.7).

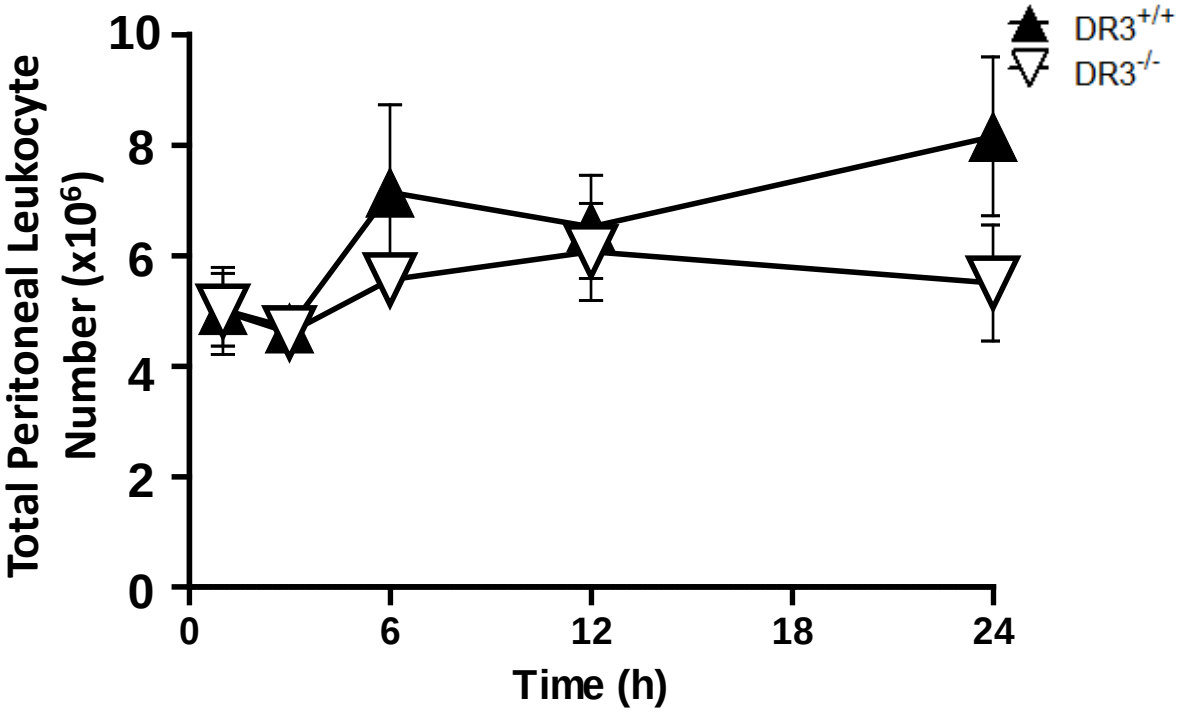

Figure 4.7 - No significant differences were seen in total peritoneal leukocyte numbers in the cavity of DR3$^{+/+}$ compared to DR3$^{-/-}$ mice following SES induced inflammation. Inflammation was induced via an i.p. injection of 500µl of SES. Peritoneal leukocytes were isolated from the cavity by lavage, total cell number over the time course was calculated using a Beckman Coulter counter Z2 (each symbol represents mean of n=6 DR3$^{+/+}$ mice (▲) and DR3$^{-/-}$ mice (▽) per time point, error bars correspond to mean ± SEM, N.S.D by ANOVA).

4.2.2.2 Neutrophil numbers in $DR3^{+/+}$ and $DR3^{-/-}$ peritoneal cavities during early stages of SES induced inflammation

Although the numbers of total infiltrating leukocytes were not significantly different between $DR3^{+/+}$ and $DR3^{-/-}$ mice, the trend towards lower numbers in $DR3^{-/-}$ animals warranted a closer analysis of individual leukocyte subsets. Neutrophils rapidly entered the $DR3^{-/-}$ and $DR3^{+/+}$ cavity (within 1 hour of inflammation being induced) and peaked in the $DR3^{+/+}$ cavity 6 hours after challenge (Figure 4.8A). $DR3^{-/-}$ mice were found to have significantly lower numbers of neutrophils in their peritoneal cavity during the early stage of inflammation ($p<0.01$) (Figure 4.8B). Peak variation in neutrophil number between the 2 genotypes was observed 6 hours after the induction of SES inflammation ($DR3^{+/+}$ mice $2.6 \pm 0.8 \times 10^6$, $DR3^{-/-}$ mice $9.0 \pm 2.6 \times 10^5$ total neutrophils) ($p<0.01$, Bonferonni's post hoc test), matching the first time point when a trend towards lower total leukocyte numbers in the $DR3^{-/-}$ cavity was observed (Figure 4.7).

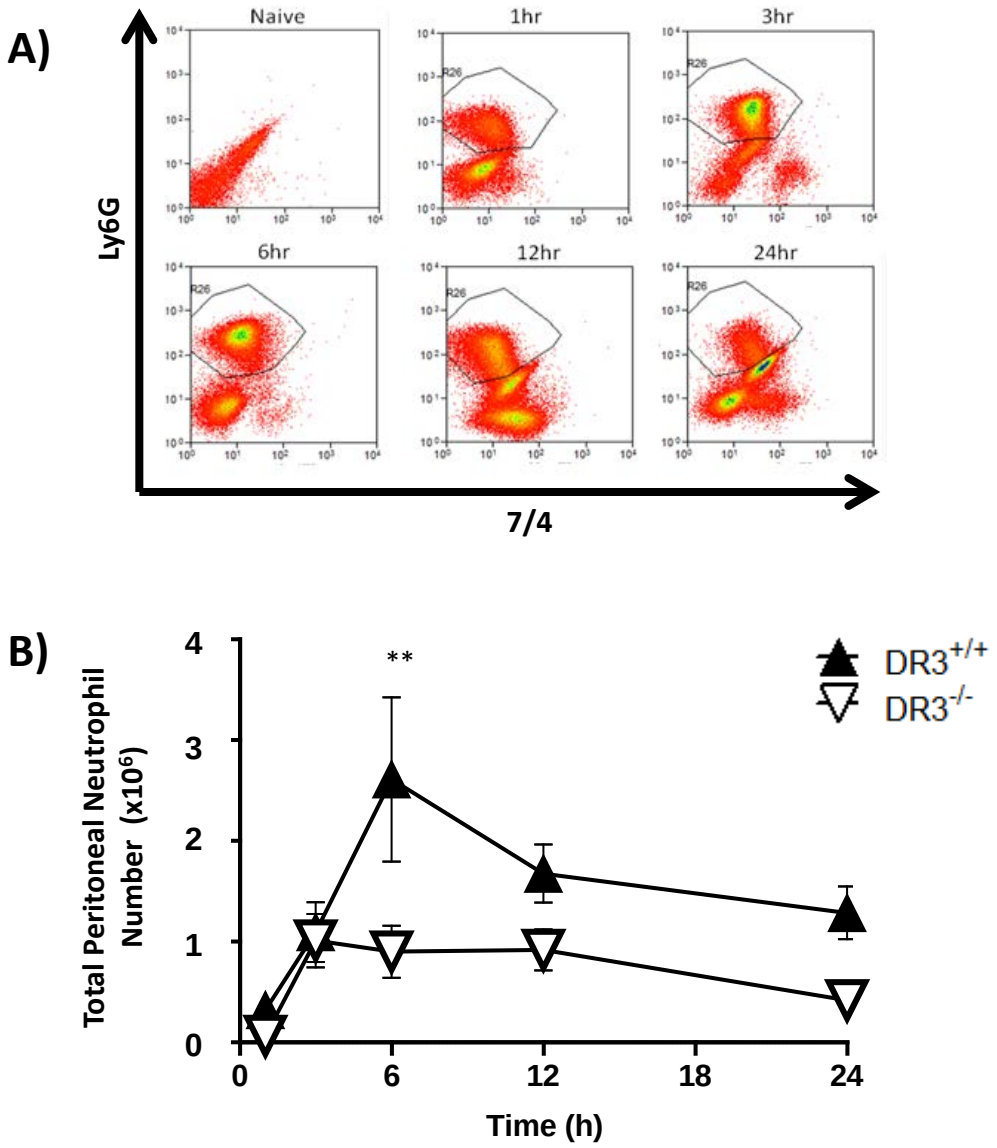

Figure 4.8 - Significantly higher numbers of neutrophils accumulated in the peritoneal cavity of DR3$^{+/+}$ mice compared to DR3$^{-/-}$ mice after induction of SES inflammation. Inflammation was induced via an i.p. injection of SES. Peritoneal leukocytes were isolated from the cavity by lavage. A) Neutrophils were identified by a 7/4^{+} Ly6G^{+} CD11b^{int} F4/80^{int} phenotype. (Gate R26) B) Neutrophil numbers at each time point were calculated by percentage proportion of total leukocytes, determined using a Beckman Coulter counter Z2 (each symbol represents mean of n=6 DR3$^{+/+}$ mice (▲) and DR3$^{-/-}$ mice (▽) per time point, error bars correspond to mean ± SEM, $p<0.01$ by ANOVA with peak impairment 6hr after inflammation, $^{**}p<0.01$ by Bonferroni post hoc test).

4.2.2.3 Accumulation of other myeloid cell subsets in the DR3$^{+/+}$ and DR3$^{-/-}$ peritoneal cavity during early stages of SES induced inflammation

Other myeloid cell subsets including resident macrophages, inflammatory macrophages and eosinophils (Figure 2.3) were also investigated. Resident macrophages composed the majority of all myeloid cells in the naive cavity (Figure 3.2) but after challenging with SES there was a significant increase in the number of eosinophils and particularly inflammatory macrophages (Figure 4.9). Over the first 24 hours, DR3$^{-/-}$ mice (2.8 ± 0.5 x10^5 total resident macrophages after 24 hours) were found to have comparable numbers of resident macrophages in their cavity as DR3$^{+/+}$ mice (3.2 ± 1.0 x10^5 total resident macrophages after 24 hours) (Figure 4.9B). However there was a substantial reduction in the accumulation of both inflammatory macrophages (Figure 4.9A) (p<0.01) and eosinophils (Figure 4.9C) (p<0.01) in DR3$^{-/-}$ mice, with differences between the 2 genotypes at their greatest after 24 hours of inflammation (total inflammatory macrophages: DR3$^{+/+}$ mice 3.0 ± 0.5 x10^6, DR3$^{-/-}$ mice 1.6 ± 0.5 x10^6, p<0.01 and total eosinophils: DR3$^{+/+}$ mice 8.8 ± 1.6 x10^5, DR3$^{-/-}$ mice 2.8 ± 1.1 x10^5, p<0.01, Bonferonni's post hoc test), matching the second timepoint at which a trend towards lower total leukocyte numbers in the DR3$^{-/-}$ cavity were observed (Figure 4.7).

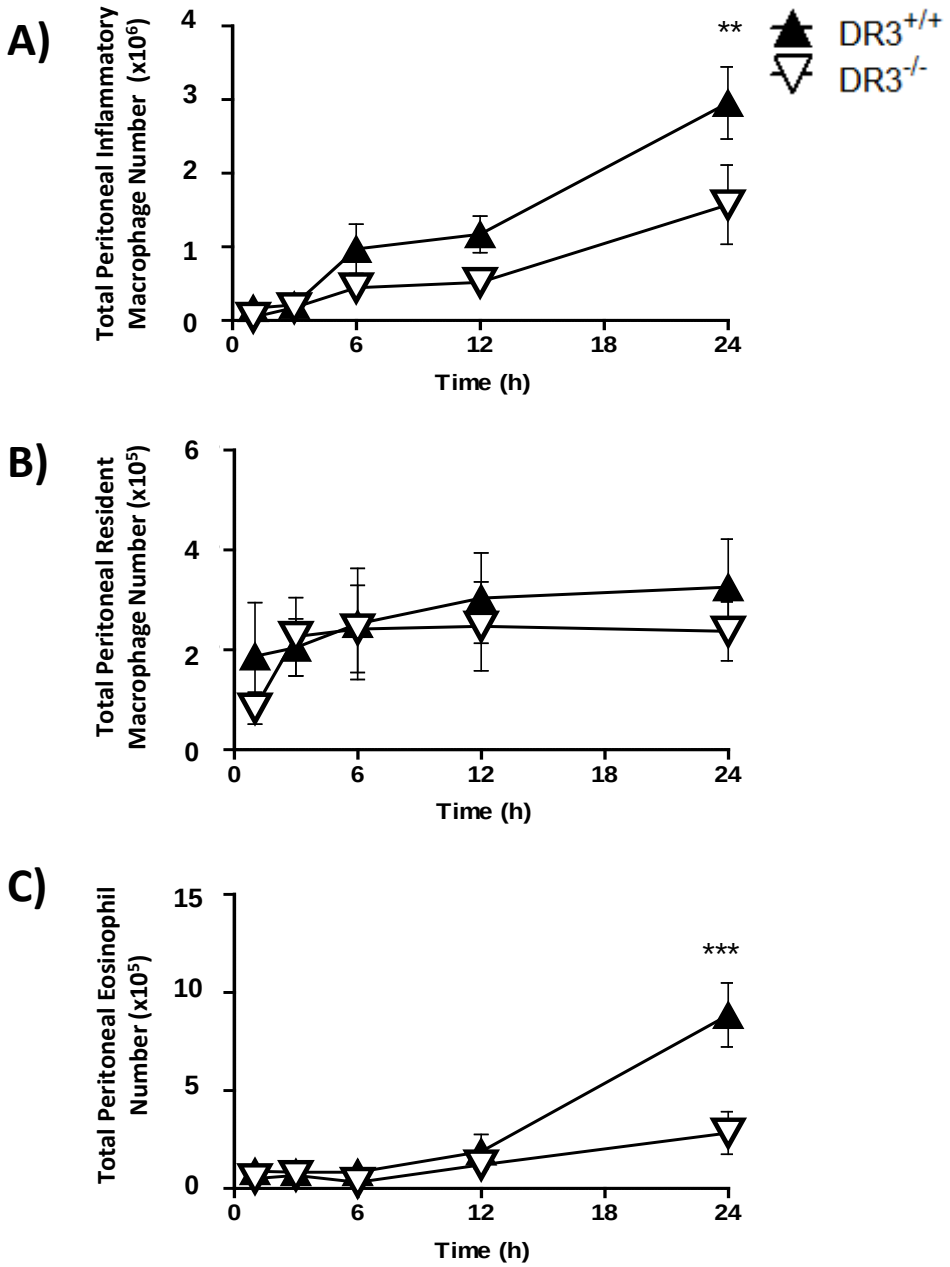

Figure 4.9 - Significantly higher numbers of inflammatory macrophages and eosinophils but not resident macrophages accumulated in the peritoneal cavity of DR3$^{+/+}$ mice compared to DR3$^{-/-}$ mice after induction of SES inflammation. Inflammation in the cavity was induced via an i.p. injection of SES. Peritoneal leukocytes were isolated by lavage. A) Inflammatory Macrophages, were identified by a CD11b^{int} F4/80^{int} phenotype (p<0.01 by ANOVA, Bonferroni post hoc test **p<0.01 after 24h). B) Resident Macrophages were identified by a CD11b^{+} F4/80^{+} phenotype and C) Eosinophils, identified by a F4/80^{int} CD11b^{int} phenotype and their forward and side scatter properties (p<0.01 by ANOVA, Bonferroni post hoc test ***p<0.001 after 24h). Subset numbers calculated by percentage proportion of total leukocytes, determined using a Beckman Coulter counter Z2 (each symbol represents mean of n=6 DR3$^{+/+}$ mice (▲) and DR3$^{-/-}$ mice (▽) per time point, error bars correspond to mean ± SEM, analysed by ANOVA and Bonferroni post hoc test).

4.2.2.4 Accumulation of lymphocyte cell subsets in $DR3^{+/+}$ and $DR3^{-/-}$ peritoneal cavities during early stages of SES induced inflammation

Lymphocyte cell subsets in the naive peritoneal cavity are composed primarily of B1 cells (Figure 3.4), but after challenging with SES there was an initial fall in the number of B and T lymphocytes over the first 6 hours. Numbers of lymphocytic cell subsets then returned to naive levels 6 hours after SES challenge and some lymphocyte subsets began to exceed the numbers present during naive conditions (NK cells, NKT cells and $CD8^+$ T cells). During the early stage of inflammation $DR3^{+/+}$ and $DR3^{-/-}$ mice had analogous numbers of T cells ($DR3^{+/+}$ mice 7.5 ± 1.8 $x10^5$, $DR3^{-/-}$ mice 4.7 ± 1.1 $x10^5$ total T cells after 24 hours), $CD4^+$ ($DR3^{+/+}$ mice 2.9 ± 1.0 $x10^5$, $DR3^{-/-}$ mice 1.8 ± 0.5 $x10^5$ total $CD4^+$ T cells after 24 hours) and $CD8^+$ ($DR3^{+/+}$ mice 1.8 ± 0.5 $x10^5$, $DR3^{-/-}$ mice 7.6 ± 2.2 $x10^4$ total $CD8^+$ T cells after 24 hours) (Figure 4.10); B cells ($DR3^{+/+}$ mice 7.0 ± 1.9 $x10^5$, $DR3^{-/-}$ mice 6.9 ± 2.1 $x10^5$ after 6 hours total B cells), B1 ($DR3^{+/+}$ mice 4.0 ± 1.0 $x10^5$, $DR3^{-/-}$ mice 3.5 ± 1.3 $x10^5$ total B1 cells after 6 hours) and B2 ($DR3^{+/+}$ mice 8.8 ± 3.8 $x10^4$, $DR3^{-/-}$ mice 1.2 ± 0.6 $x10^5$ total B2 cells after 6 hours) (Figure 4.11) and NK cells ($DR3^{+/+}$ mice 2.4 ± 0.5 $x10^5$, $DR3^{-/-}$ mice 2.3 ± 0.5 $x10^5$ total NK cells after 24 hours) (Figure 4.12A) in the peritoneal cavities. Only NKT cell number was found to be significantly reduced in the $DR3^{-/-}$ cavity compared to $DR3^{+/+}$ mice (Figure 4.12B) ($p<0.05$), with significant differences between the 2 genotypes only observed 24 hours after challenge ($DR3^{+/+}$ mice 2.0 ± 0.6 $x10^5$, $DR3^{-/-}$ mice 8.8 ± 2.3 $x10^4$ total NKT cells) ($p<0.05$, Bonferonni's post hoc test).

Thus $DR3^{-/-}$ mice are associated with reduced numbers of selected leukocyte subsets within the cavity after SES challenge. At early time points, these consist of

neutrophils but at 24 hours, inflammatory macrophages, eosinophils and NKT cells also show impaired numbers in DR3$^{-/-}$ mice.

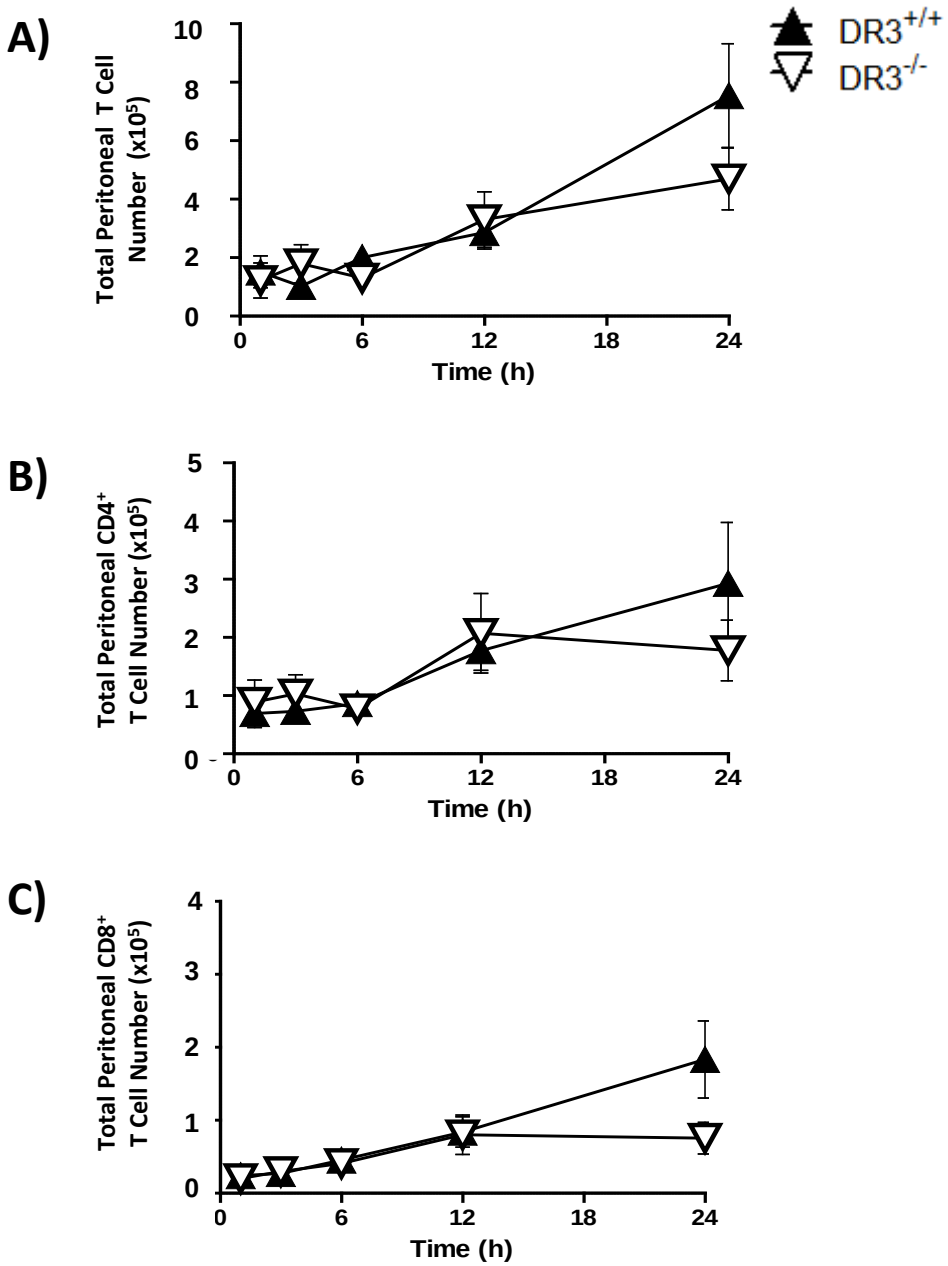

Figure 4.10 - No significant differences were seen in the numbers of T cell subsets in the peritoneal cavity of DR3$^{+/+}$ mice compared to DR3$^{-/-}$ mice following SES induced inflammation. Inflammation in the cavity was induced via an i.p. injection of SES. Peritoneal leukocytes were isolated by lavage A) T cells were identified by a CD3^{+}, TCRαβ^{+} phenotype, B) T helper cells were identified by a CD3^{+} CD4^{+}, TCRαβ^{+} phenotype and C) T cytotoxic cells identified by a CD3^{+} CD8^{+}, TCRαβ^{+} phenotype. Subset numbers calculated by percentage proportion of total leukocytes, determined using a Beckman Coulter counter Z2 (each symbol represents mean of n=6 DR3$^{+/+}$ mice (▲) and DR3$^{-/-}$ mice (▽) per time point, error bars correspond to mean ± SEM, N.S.D by ANOVA).

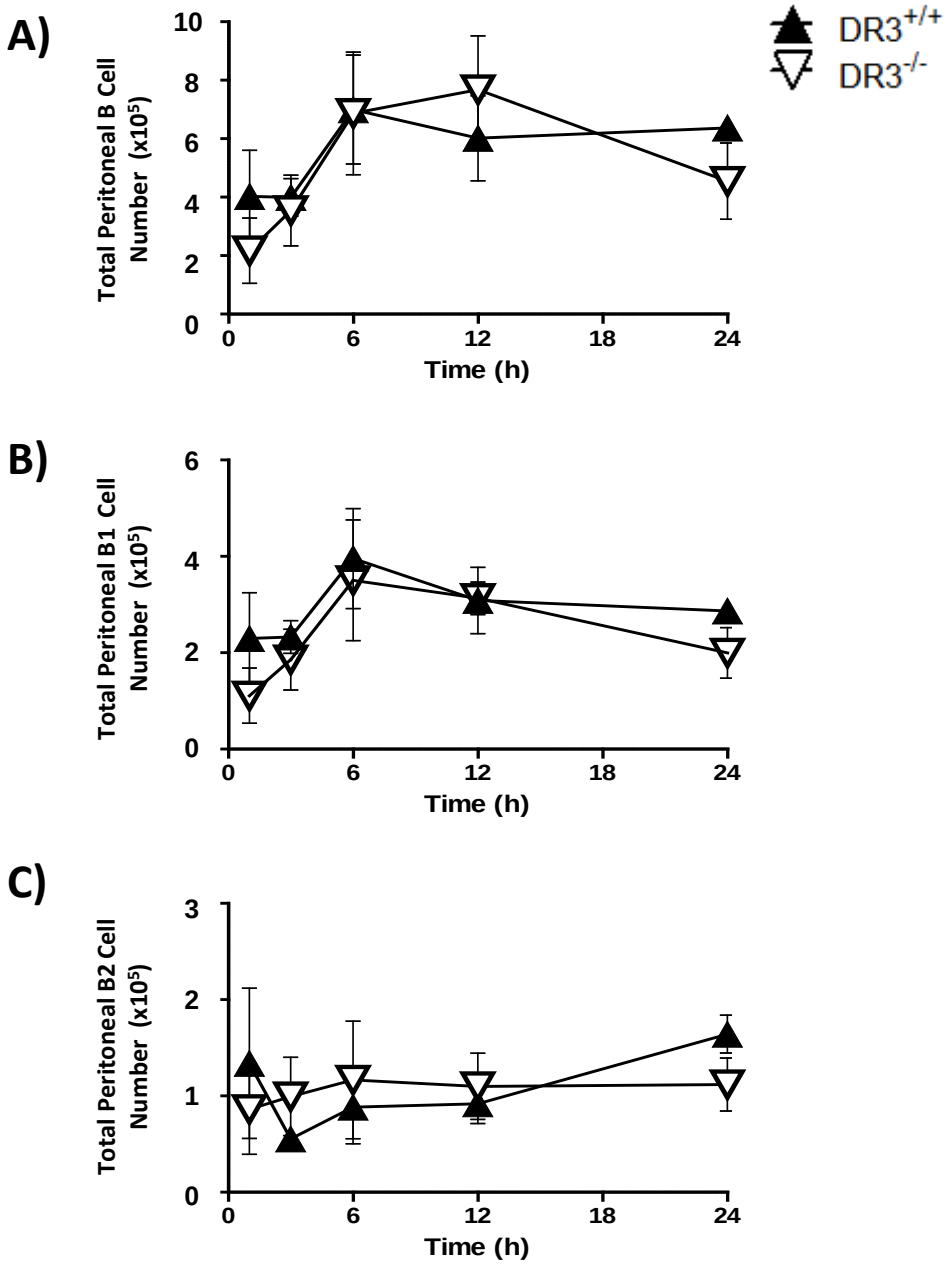

Figure 4.11 - No significant differences were seen in the numbers of B cell subsets in the peritoneal cavity of DR3$^{+/+}$ mice compared to DR3$^{-/-}$ mice following SES induced inflammation. Inflammation in the cavity was induced via an i.p. injection of SES. Peritoneal leukocytes were isolated by lavage A) B cells were identified by a CD19^{+}, B220^{+} phenotype, B) B1 cells were identified by a CD19^{+} B220^{int}, CD11b^{int} phenotype and C) B2 cells identified by a CD19^{+} B220^{+}, CD11b^{-} phenotype. Subset numbers calculated by percentage proportion of total leukocytes, determined using a Beckman Coulter counter Z2 (each symbol represents mean of n=6 DR3$^{+/+}$ mice (▲) and DR3$^{-/-}$ mice (▽) per time point, error bars correspond to mean ± SEM, N.S.D by ANOVA).

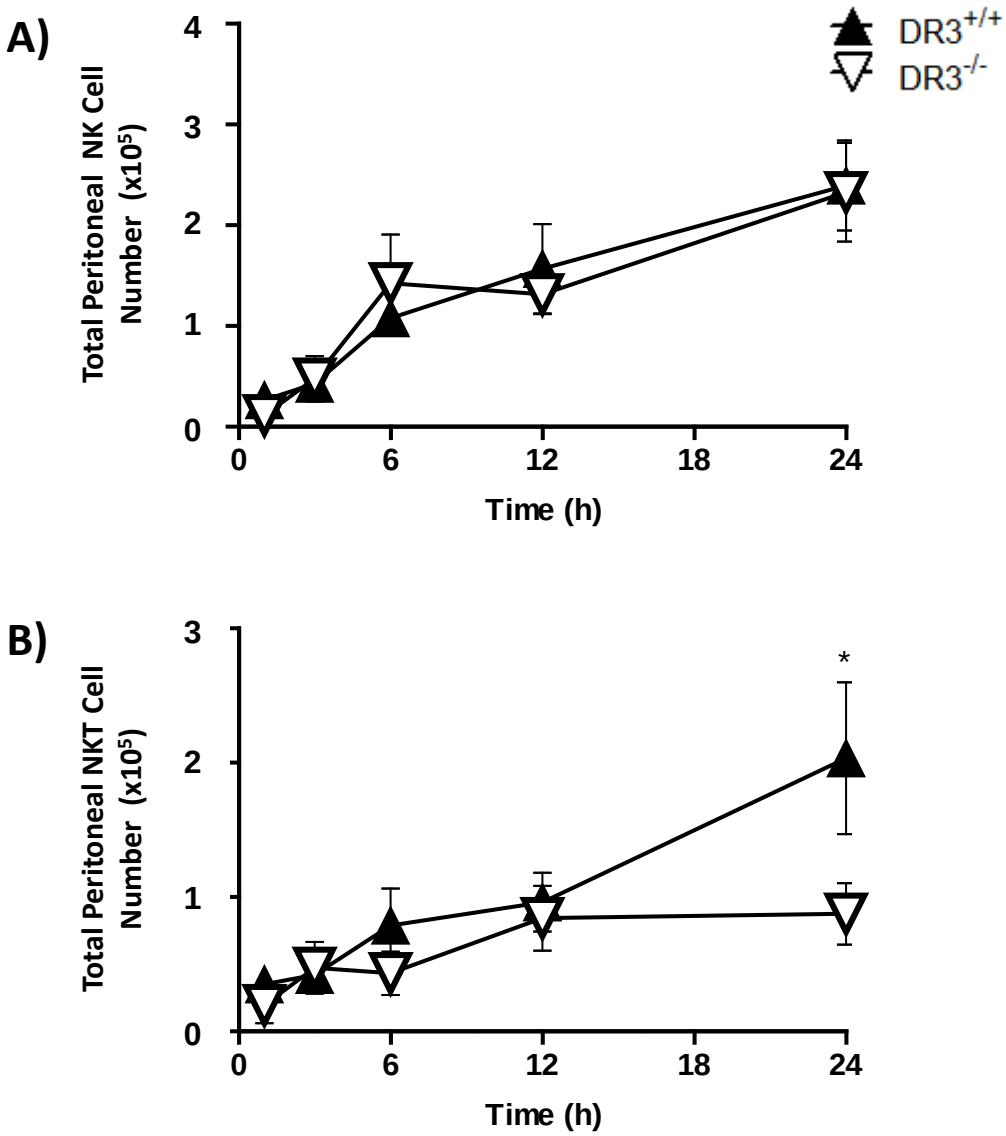

Figure 4.12 - Significantly higher numbers of NKT cells but not NK cells accumulated in the peritoneal cavity of DR3$^{+/+}$ mice compared to DR3$^{-/-}$ mice after induction of SES inflammation. Inflammation in the cavity was induced via an i.p. injection of SES. Peritoneal leukocytes were isolated from the cavity by lavage. A) NK cells were identified by a NK1.1^{+}, TCRαβ^{-} phenotype and B) NKT cells were identified by a NK1.1^{+}, TCRαβ^{+} phenotype (p<0.05 by ANOVA, Bonferroni post hoc test *p<0.05 after 24h). Subset numbers calculated by percentage proportion of total leukocytes, determined using a Beckman Coulter counter Z2 (each symbol represents mean of n=6 DR3$^{+/+}$ mice (▲) and DR3$^{-/-}$ mice (▽) per time point, error bars correspond to mean ± SEM, analysed by ANOVA and Bonferroni post hoc test).

4.2.3.1 Chemokine levels in unchallenged $DR3^{+/+}$ and $DR3^{-/-}$ peritoneal cavities

Because neutrophils are unable to proliferate and are generally not found in the naive cavity (Topley, Liberek et al. 1996; Kolaczkowska 2010), I tested the hypothesis that DR3/TL1A signalling controlled the level of chemoattractants as a potential explanation for the observed impairment in leukocyte accumulation within the $DR3^{-/-}$ cavity. Chemokines have previously been shown to be released following SES challenge, as part of the innate inflammatory response and play an important role in the movement of leukocytes from the peripheral blood to local areas of inflammation (McLoughlin, Hurst et al. 2004; McLoughlin, Jenkins et al. 2005). However before investigating chemoattractants during inflammation, chemokine levels present in the naive cavity were first determined to examine if they were significantly influenced by the absence of DR3 prior to SES challenge. No significant difference was observed in the level of any chemoattractant studied between naive $DR3^{+/+}$ and $DR3^{-/-}$ mice. Indeed only low concentrations of chemokines were measured in the unchallenged cavity of either $DR3^{+/+}$ or $DR3^{-/-}$ mice, with only CXCL13 ($DR3^{+/+}$ mice 135 ± 3 pg/ml, $DR3^{-/-}$ mice 140 ± 2 pg/ml), CCL4 ($DR3^{+/+}$ mice 51 ± 2 pg/ml, $DR3^{-/-}$ mice 52 ± 2 pg/ml), CXCL5 ($DR3^{+/+}$ mice 8 ± 1 pg/ml, $DR3^{-/-}$ mice 9 ± 2 pg/ml), CXCL10 ($DR3^{+/+}$ mice 13 ± 3 pg/ml, $DR3^{-/-}$ mice 12 ± 2 pg/ml) and CCL3 ($DR3^{+/+}$ mice 12 ± 2 pg/ml, $DR3^{-/-}$ mice 11 ± 3 pg/ml) above the level of detection. All other chemoattractants measured were below the detection level of the ELISA kits in both the $DR3^{+/+}$ and $DR3^{-/-}$ mice (Figure 4.13).

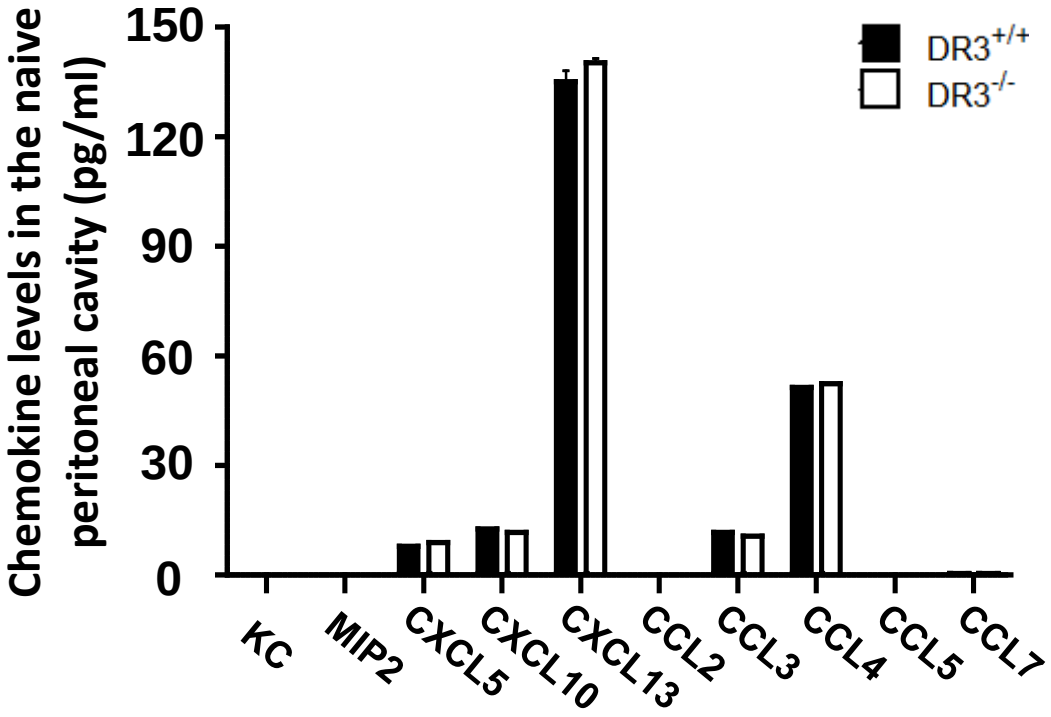

Figure 4.13 - No significant differences were seen in the level of selected chemokines in the unchallenged peritoneal cavity of DR3$^{+/+}$ and DR3$^{-/-}$ mice. Cell free supernatants from the peritoneal lavage were used to obtain chemokine concentrations in the cavity using ELISA (each bar represents mean of n=3 DR3$^{+/+}$ mice (■) and DR3$^{-/-}$ mice (□), error bars correspond to mean ± SEM, N.S.D by t-test).

4.2.3.2 Levels of ELR^+ chemoattractants in $DR3^{+/+}$ and $DR3^{-/-}$ peritoneal cavities after SES induced inflammation

As DR3 had no effect on chemokine levels in the naive cavity, the level of neutrophilic chemokines, which contain an N-terminal tripeptide sequence of glutamic acid, leucine and arginine (or ELR^+ motif) was determined during inflammation by testing peritoneal supernatants from the challenged cavity of $DR3^{+/+}$ and $DR3^{-/-}$ mice. ELR^+ chemoattractants (KC, MIP2 and CXCL5) are rapidly released and cleared after the induction of SES inflammation (Rollins 1997). No significant disparity was found in the level of MIP2 ($DR3^{+/+}$ mice 1340 ± 119 pg/ml, $DR3^{-/-}$ mice 972 ± 140 pg/ml after 1 hour) (Figure 4.14B) and CXCL5 ($DR3^{+/+}$ mice 24 ± 15 pg/ml, $DR3^{-/-}$ mice 19 ± 17 pg/ml after 6 hours) (Figure 4.14C) in the peritoneal cavity of $DR3^{+/+}$ and $DR3^{-/-}$ mice during the early phase of inflammation. However there were significantly reduced peak levels of the chemoattractant KC in the challenged cavity of $DR3^{-/-}$ mice (2319 ± 626 pg/ml after 1 hour) compared to $DR3^{+/+}$ mice (5251 ± 945 pg/ml after 1 hour) (Figure 4.14A) (p=0.03). Therefore SES inflammation leads to the release of KC and MIP2 in both $DR3^{+/+}$ and $DR3^{-/-}$ mice, with significantly lower levels of KC found in $DR3^{-/-}$ mice.

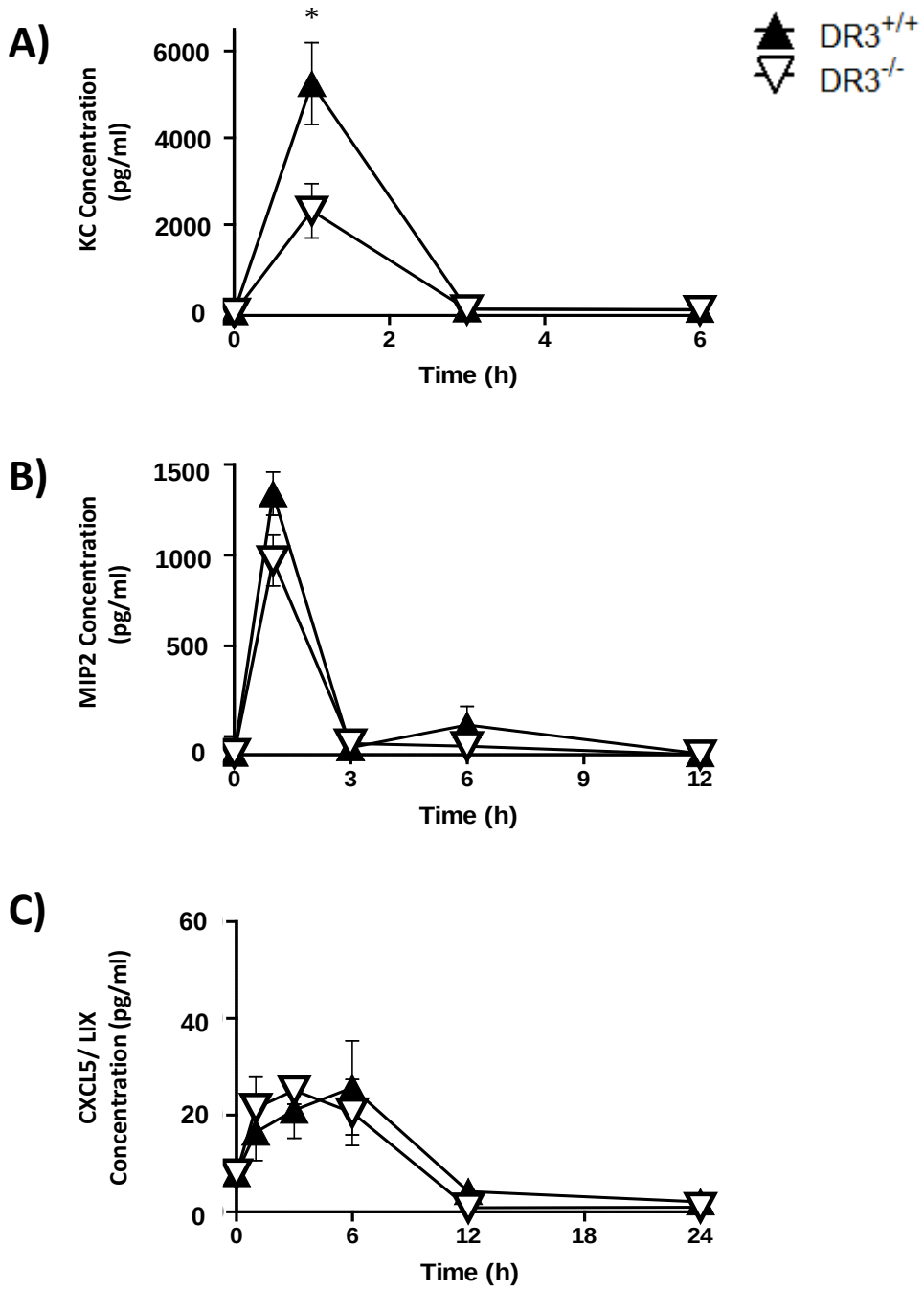

Figure 4.14 - Significantly higher levels of KC but not MIP2 and CXCL5 were found in the peritoneal cavity of DR3$^{+/+}$ mice compared to DR3$^{-/-}$ mice after induction of SES inflammation. Inflammation in the cavity was induced via an i.p. injection of SES and cell free supernatants obtained analysed for levels of A) KC (*p<0.05) B) MIP2 and C) CXCL5 by ELISA (each symbol represents mean of n=5 DR3$^{+/+}$ mice (▲) and DR3$^{-/-}$ mice (▽) per time point, error bars correspond to mean ± SEM, analysed by ANOVA and p values calculated using Bonferonni's post hoc test).

4.2.3.3 RQ of ELR^{+} chemoattractant mRNA in DR3$^{+/+}$ and DR3$^{-/-}$ peritoneal membranes after SES induced inflammation

Mesothelial cells present within the peritoneal membrane have previously been shown to be a source of chemoattractants (Li, Davenport et al. 1998; Hurst, Wilkinson et al. 2001; McLoughlin, Hurst et al. 2004); consequently the RQ of ELR^{+} chemokines in the membrane after SES challenge was investigated by qPCR (Section 2.5). KC and MIP2 mRNA rapidly increased (1 hour) after the induction of inflammation (Figure 4.15A and 4.15B) though little increase was seen in the RQ of CXCL5 mRNA (Figure 4.15C). Comparable RQ of MIP2 (DR3$^{+/+}$ mice 237 ± 89, DR3$^{-/-}$ mice 97 ± 39 RQ after 1 hour) (Figure 4.15B) and CXCL5 (DR3$^{+/+}$ mice 24 ± 15, DR3$^{-/-}$ mice 18 ± 17 RQ after 6 hours) (Figure 4.15C) mRNA was found in the peritoneal membrane of DR3$^{+/+}$ and DR3$^{-/-}$ mice. Yet there were significantly reduced quantities of KC mRNA in the membrane of DR3$^{-/-}$ mice (33 ± 4 RQ after 1 hour) compared to DR3$^{+/+}$ mice (216 ± 92 RQ after 1 hour) 1 hour after SES challenge (Figure 4.15A) (p=0.02), and correlated with reduced levels of KC in the DR3$^{-/-}$ cavity tested by ELISA (Figure 4.14A).

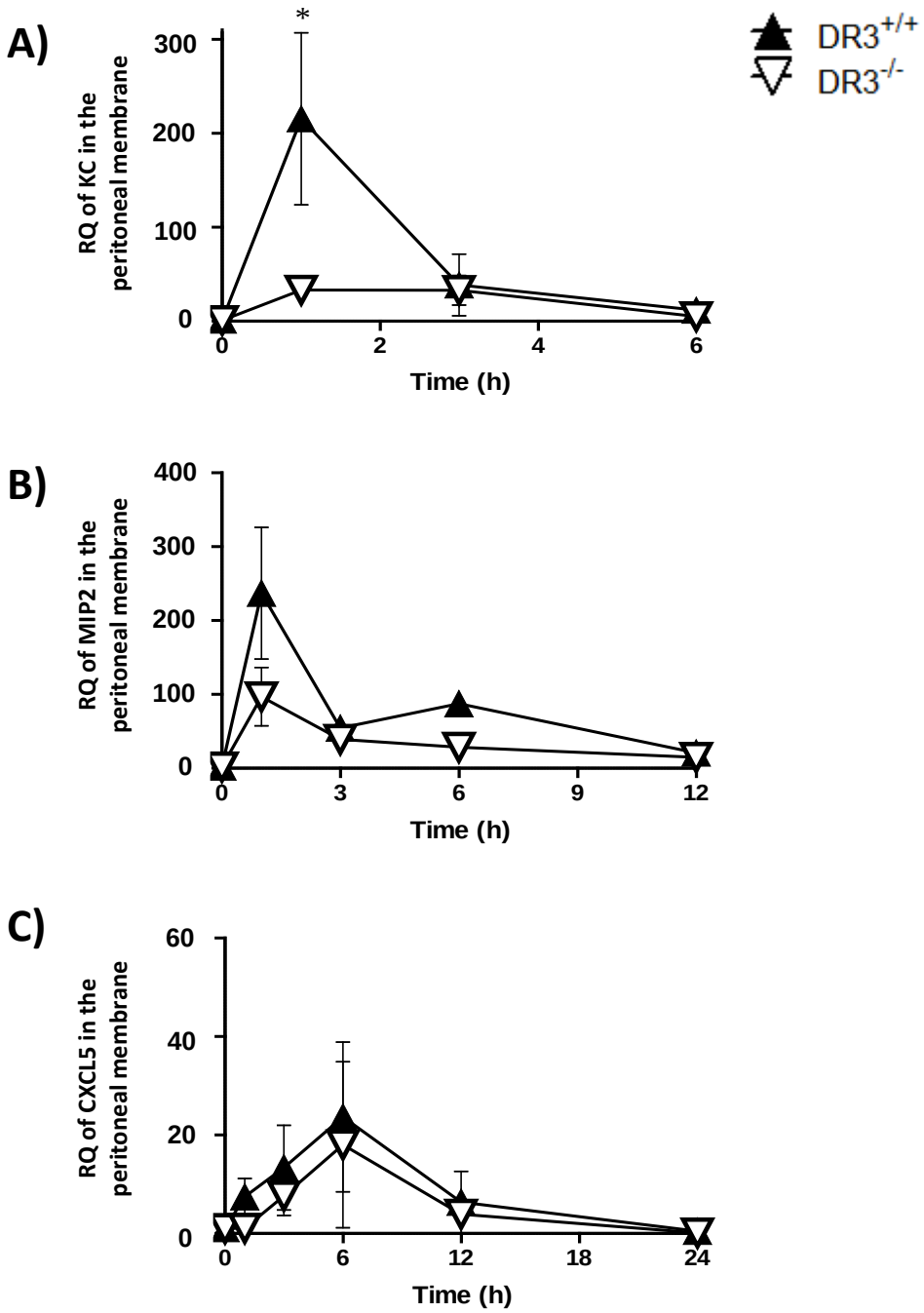

Figure 4.15 - Significantly higher relative quantity of KC mRNA but not MIP2 and CXCL5 mRNA was found in the peritoneal membrane of DR3$^{+/+}$ mice compared to DR3$^{-/-}$ mice after induction of SES inflammation. Inflammation in the cavity was induced via an i.p. injection of SES and peritoneal membranes obtained analysed for RQ of A) KC mRNA (*p<0.05) B) MIP2 mRNA and C) CXCL5 mRNA by qPCR (each symbol represents mean of n=5 DR3$^{+/+}$ mice (▲) and DR3$^{-/-}$ mice (▽) per time point, error bars correspond to mean ± SEM, analysed by ANOVA and p values calculated using Bonferonni's post hoc test).

4.2.3.4 Correlation between peak level of neutrophilic chemoattractants and peak neutrophil accumulation after the induction of SES inflammation.

To determine if higher ELR^+ chemoattractant levels correlated with an increased influx of neutrophils into the peritoneal cavity, maximum neutrophil number observed after 6 hours of SES inflammation (Figure 4.8A) was plotted against peak levels of ELR^+ neutrophilic chemoattractants observed 1 hour after challenge (Figure 4.14). No significant correlation was found between the maximum number of neutrophils in the cavity and the peak levels of the neutrophilic chemoattractants MIP2 (Figure 4.16B) and CXCL5 (Figure 4.16C) in challenged supernatants. However correlation was found between the maximum number of neutrophils in the cavity and the levels of the neutrophilic chemoattractant KC in the challenged supernatants (Figure 4.16A, R=0.96, p=0.02), with increasing levels of KC positively associated with increased neutrophil accumulation.

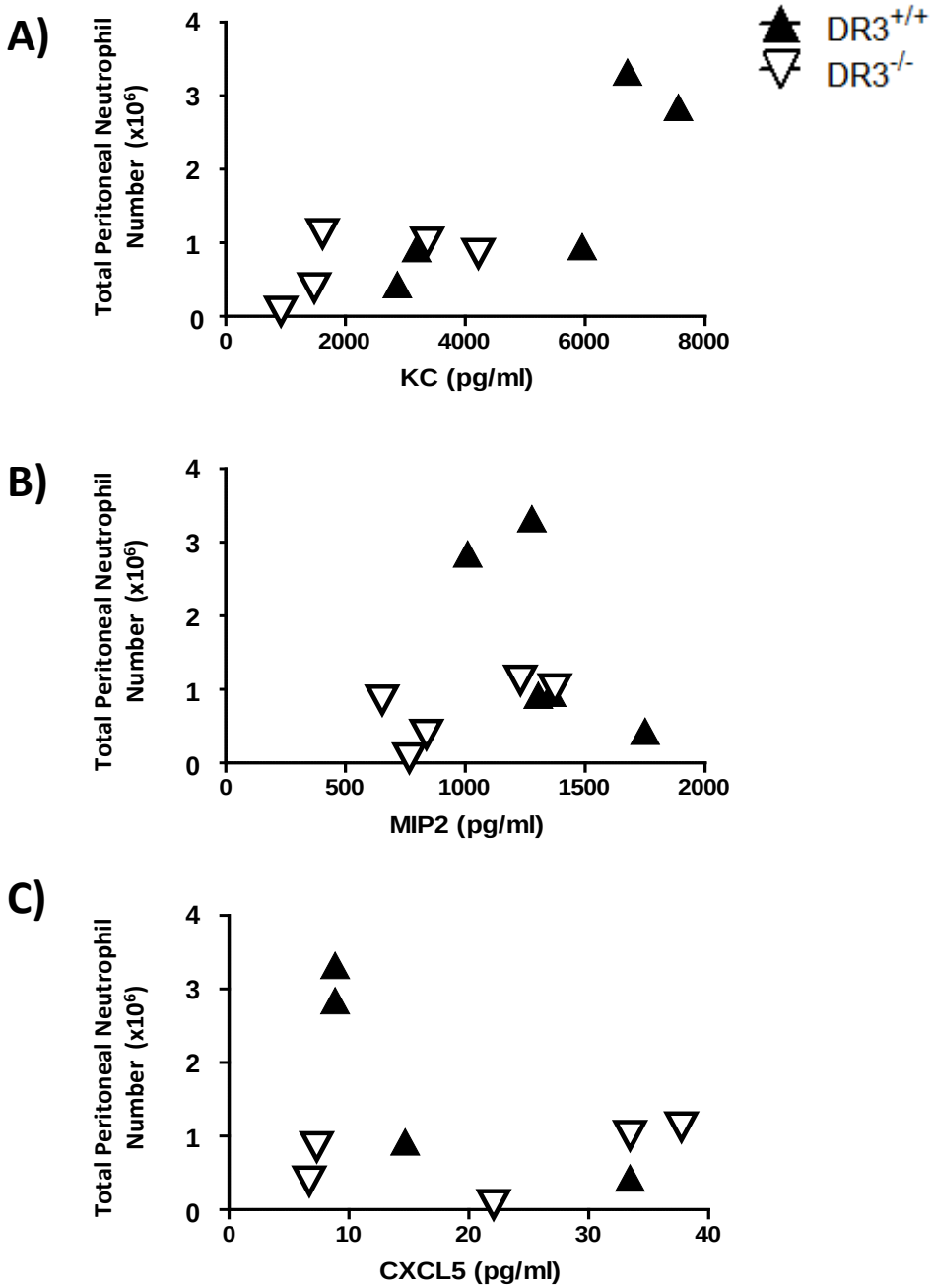

Figure 4.16 - Significant correlation was found between peak number of neutrophils in the cavity and the level of KC but not MIP2 and CXCL5 in DR3$^{+/+}$ mice and DR3$^{-/-}$ mice after induction of SES inflammation. Inflammation in the cavity was induced via an i.p. injection of SES and cell free supernatants analysed for chemokine levels by ELISA. Neutrophils in the cavity were identified by a 7/4^{+} Ly6G^{+} CD11b^{int} F4/80^{int} phenotype. Correlation between the peak level of A) KC (R=0.82, p<0.01) B) MIP2 and C) CXCL5 in the supernatants was plotted against peak number of neutrophils which accumulated in the cavity (each symbol represents a single DR3$^{+/+}$ (▲) or DR3$^{-/-}$ mouse (▽), analysed by Pearson R correlation test).

4.3 Summary

- The RQ of TL1A mRNA increased in resident macrophages after stimulation with SES, in contrast to the peritoneal membrane where there was no increase in RQ of TL1A mRNA after SES challenge.
- DR3 is expressed in the peritoneal cavity both on the mesothelial layer of the membrane and selected T cell subsets, though the level of expression varies after the induction of inflammation.
- DR3 is important in regulation of neutrophil accumulation into the peritoneal cavity following SES challenge.
- $DR3^{-/-}$ mice also have a significant reduction in the accumulation of inflammatory macrophages, eosinophils and NKT cells into their cavity compared to $DR3^{+/+}$ mice after the induction of inflammation.
- $DR3^{-/-}$ peritoneal supernatants have reduced levels of the ELR^{+} neutrophilic chemoattractant KC and levels of KC correlate with neutrophil accumulation into the cavity following SES challenge.
- The peritoneal membrane is a likely source of KC, with rapid increase in KC mRNA production in the $DR3^{+/+}$ membrane. KC mRNA production was substantially reduced in the $DR3^{-/-}$ membrane compared to those from $DR3^{+/+}$ mice.

Table 4.1 - Summary of TL1A and DR3 expression over the first 24 hours of SES challenge

Cell Subset	TL1A and DR3 expression			
	Time (h)[$]	DR3$^{+/+}$	DR3$^{-/-}$	Significance[~]
RQ of TL1A^ in the peritoneal membrane	1	0.6 ± 0.4	0.2 ± 0.1	N.S.D
RQ of TL1A^ in resident macrophages	1	28.4 ± 9	18.2 ± 7	N.S.D
% DR3 on the membrane[¥]	12	7.6 ± 1.6	0.1 ± <0.1	p<0.01
DR3 MFI ratio* on T Cells	12	3.0 ± 0.4	1.5 ± <0.1	p<0.01
DR3 MFI[†] on T Cells	12	15.2 ± 3.6	2.8 ± 0.3	p<0.05
DR3 MFI ratio* on CD4^{+} T Cells	12	4.1 ± 0.6	1.7 ± <0.1	p<0.01
DR3 MFI[†] on CD4^{+} T Cells	12	11.7 ± 2.1	2.5 ± 0.1	p<0.05
DR3 MFI ratio* on CD8^{+} T Cells	12	1.0 ± <0.1	1.0 ± <0.1	N.S.D
DR3 MFI[†] on CD8^{+} T Cells	12	2.7 ± 1.6	1.6 ± 1.6	N.S.D
% DR3 positive NK Cells	12	3.4 ± 1	2.4 ± 0.2	N.S.D
DR3 MFI of NK Cell positive population[#]	12	27 ± 1.4	27 ± 1	N.S.D
% DR3 positive NKT Cells	24	53 ± 2	42 ± 1	p<0.05
DR3 MFI of NKT Cell positive population[#]	24	27 ± 1	27 ± 1	N.S.D

^ Relative quantity of TL1A mRNA,
[¥] % DR3 expression on the mesothelial layer of peritoneal membrane,
* Median fluorescence intensity (MFI) ratio calculated by dividing median of DR3 test stain by median of isotype ± SEM (n=3),
[†] MFI calculated by subtracting median of DR3 test stain by median of isotype ± SEM (n=3),
[#] MFI of positive population calculated by subtracting median of positive from DR3 test stain by median of isotype ± SEM (n=3),
[$] Peak/ noteworthy time point,
[~] Significance between two genotypes using ANOVA or Kruskal-Wallis test, N.S.D = no significant difference.

Table 4.2- Summary of peritoneal cell numbers within the first 24 hours of SES challenge

Cell subset	Peritoneal cell numbers*			
	Time point (h)^	DR3$^{+/+}$	DR3$^{-/-}$	Significance$
Leukocytes	24	$8.2 \pm 1.4 \times 10^6$	$5.5 \pm 1.0 \times 10^6$	N.S.D
Neutrophils	6	$2.6 \pm 0.8 \times 10^6$	$9.0 \pm 2.6 \times 10^5$	$p<0.01$
Inflammatory Macrophages	24	$3.0 \pm 0.5 \times 10^6$	$1.6 \pm 0.5 \times 10^6$	$p<0.01$
Resident Macrophages	24	$3.2 \pm 1.0 \times 10^5$	$2.8 \pm 0.5 \times 10^5$	N.S.D
Eosinophils	24	$8.8 \pm 1.6 \times 10^5$	$2.8 \pm 1.1 \times 10^5$	$p<0.01$
T Cells	24	$7.5 \pm 1.8 \times 10^5$	$4.7 \pm 1.1 \times 10^5$	N.S.D
CD4$^+$ T Cells	24	$2.9 \pm 1.0 \times 10^5$	$1.8 \pm 0.5 \times 10^5$	N.S.D
CD8$^+$ T Cells	24	$1.8 \pm 0.5 \times 10^5$	$7.6 \pm 2.2 \times 10^4$	N.S.D
B Cells	6	$7.0 \pm 1.9 \times 10^5$	$6.9 \pm 2.1 \times 10^5$	N.S.D
Peritoneal B1 Cells	6	$4.0 \pm 1.0 \times 10^5$	$3.5 \pm 1.3 \times 10^5$	N.S.D
Peritoneal B2 Cells	6	$8.8 \pm 3.5 \times 10^4$	$1.2 \pm 0.6 \times 10^5$	N.S.D
NK Cells	24	$2.4 \pm 0.5 \times 10^5$	$2.3 \pm 0.5 \times 10^5$	N.S.D
NKT Cells	24	$2.0 \pm 0.6 \times 10^5$	$8.8 \pm 2.3 \times 10^4$	$p<0.05$

^ Peak time point in the peritoneal cavity during the early inflammation,
* Values correspond to number of peritoneal leukocytes ± SEM (n=6),
$ Significance between two genotypes using ANOVA and Bonferonni's post hoc test, N.S.D = no significant difference.

Table 4.3- Summary of chemokine levels and mRNA

		Chemokine levels ^			RQ of Chemokine mRNA*		
Chemokine	**Time point (h)$**	**DR3$^{+/+}$**	**DR3$^{-/-}$**	**Significance#**	**DR3$^{+/+}$**	**DR3$^{-/-}$**	**Significance#**
KC	1	5251 ± 945	2319 ± 626	p=0.03	216 ± 92	33 ± 4	p=0.03
MIP2	1	1340 ± 119	972 ± 140	N.S.D	237 ± 89	97 ± 39	N.S.D
CXCL5	6	24 ± 15	19 ± 17	N.S.D	24 ± 15	18 ± 17	N.S.D

^ Values correspond to pg/ml of chemoattractants in the inflamed peritoneal cavity ± SEM (n=5),
* Values correspond to relative quantity of chemokine mRNA in the peritoneal membrane ± SEM (n=5),
$ Peak chemokine time point,
# Significance between two genotypes using ANOVA and Bonferonni's post hoc test, N.S.D = no significant difference.

Chapter 5 – The role of DR3 in accumulation of leukocytes into the peritoneal cavity during later stages of an *in vivo* acute inflammatory event

5.1 Introduction

A two-staged innate immune response is provoked in the peritoneal cavity by i.p. injection of SES (Jones 2005). During the early phase of SES inflammation DR3 was found to be important in regulating the recruitment of selected myeloid cell subsets and NKT cells into the peritoneal cavity, which was associated with a significant reduction in the neutrophilic chemoattractant KC in $DR3^{-/-}$ mice, thus identifying a novel pro-inflammatory role for DR3 in the innate inflammatory response (Chapter 4). The late phase (post 24 hours) is characterised by further increases in the number of leukocytes in the peritoneal cavity, with the influx of other (particularly lymphocytic) cell subsets before inflammation begins to be resolved and the typical homeostatic resident leukocyte population restored (Jones 2005).

The aim of this chapter was to analyse the effect of DR3 deficiency on this late response to a bacterial-derived agonist, including correlative studies of: (i) DR3 expression in the mesothelial layer of the peritoneal membrane; (ii) proliferation of leukocytes entering the cavity during this phase, and; (iii) chemoattractant levels during this period.

5.2 Results

5.2.1 DR3 expression on $DR3^{+/+}$ and $DR3^{-/-}$ peritoneal membranes after SES induced inflammation

DR3 expression fluctuated on the mesothelial layer in the peritoneal membrane during the early phase of inflammation (Section 4.2.1.3) (Figure 4.4), consequently DR3 expression was tracked into the late phase of inflammation. Multiple pictures were taken along sections of the mesothelial layer of $DR3^{+/+}$ and $DR3^{-/-}$ mice (Figure 5.1A). DR3 expression could no longer be detected on the mesothelial layer in the membrane of $DR3^{+/+}$ mice during the late phase following SES challenge (0.31 ± 0.21 % after 48 hours). Low background staining was detected on the $DR3^{-/-}$ control (0.32 ± 0.18 % after 48 hours) (Figure 5.1B) and isotype control (0.1 ± <0.1 %). Thus DR3 is no longer expressed on the membrane after 12 hours of SES induced inflammation and does not return even after 72 hours.

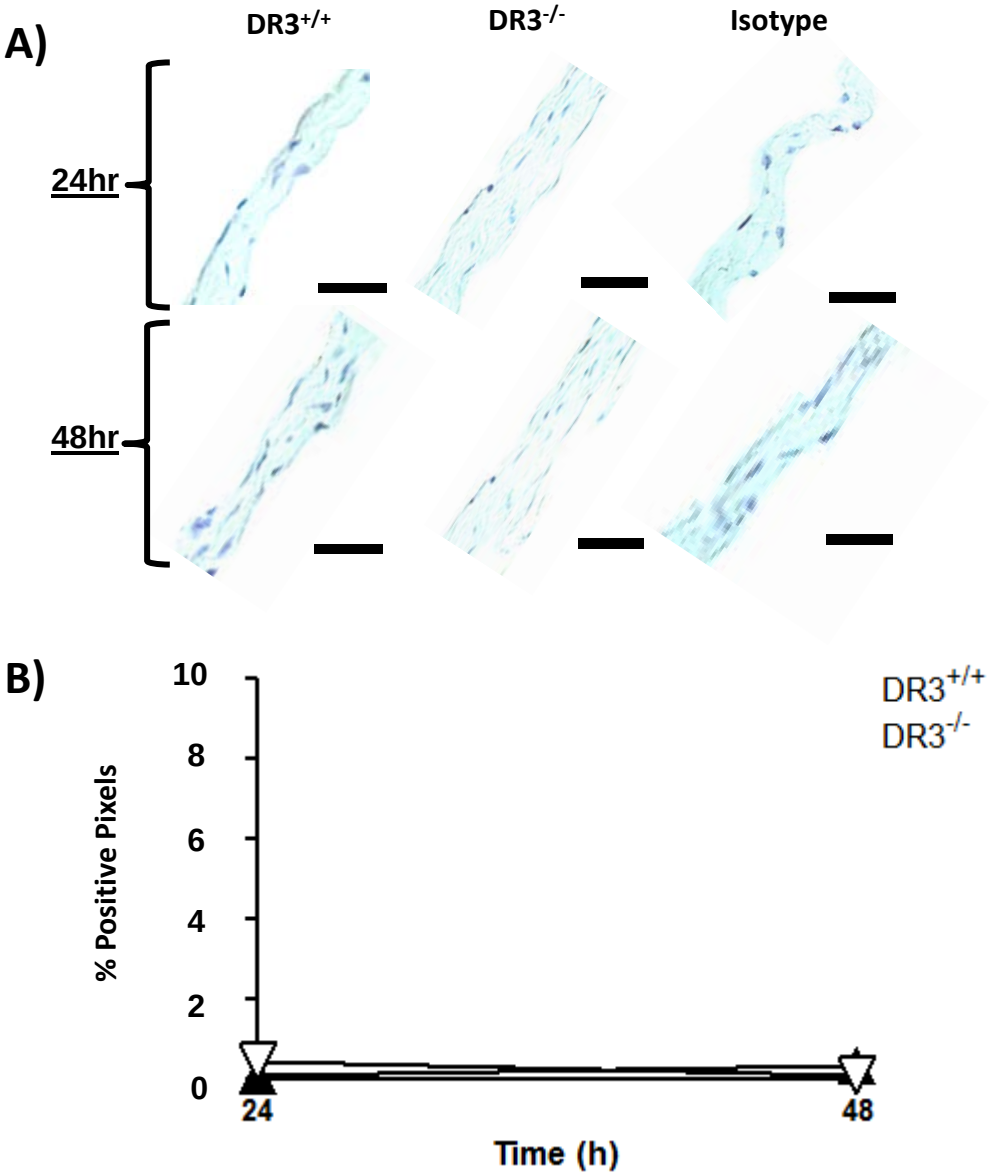

Figure 5.1 - No significant differences were seen in the level of DR3 expression on the peritoneal membrane of DR3$^{+/+}$ mice compared to DR3$^{-/-}$ mice 24 and 48 hours after SES induced inflammation. A) Representative pictures of DR3 staining in the mesothelial layer of the peritoneal membrane (Bar corresponds to 25μm.) B) DR3 expression on the membrane was analysed by taking multiple pictures along the section and measuring the % of positive (brown) pixels within the mesothelial layer of the membrane using Adobe Photoshop CS4 (each symbol represents mean of n=3 DR3$^{+/+}$ mice (▲) and DR3$^{-/-}$ mice (▽) per time point, error bars correspond to mean ± SEM, N.S.D by Mann-Whitney test).

5.2.2.1 Accumulation of mouse leukocytes in the $DR3^{+/+}$ and $DR3^{-/-}$ peritoneal cavity during later stages of acute SES induced inflammation

Peritoneal leukocyte numbers were reduced at selected time points (6 and 24 hours) during the early phase of SES induced inflammation (Chapter 4), though this was not significant (Figure 4.7). During the late phase substantially more leukocytes accumulated in the cavity of $DR3^{+/+}$ mice. $DR3^{-/-}$ mice, however, demonstrated significantly fewer leukocytes compared to $DR3^{+/+}$ mice (Figure 5.2A) ($p<0.01$). Peritoneal leukocyte number within the $DR3^{+/+}$ cavity peaked around 48 hours after SES challenge ($9.1 \pm 0.9 \times 10^6$ total cells), whereas total leukocyte number in the $DR3^{-/-}$ cavity barely changed throughout the late phase ($4.5 \pm 0.5 \times 10^6$ total cells after 48 hours) (Figure 5.2B) ($p<0.01$).

5.2.2.2 Clearance of neutrophils in $DR3^{+/+}$ and $DR3^{-/-}$ peritoneal cavities during later stages of acute SES induced inflammation

As significantly fewer leukocytes were observed in the peritoneal cavity of $DR3^{-/-}$ mice compared to $DR3^{+/+}$ mice, leukocyte subsets were investigated to determine which were altered in the $DR3^{-/-}$ mice. Neutrophils are cleared from the cavity during the late phase and their numbers decline throughout this period (Figure 5.3A). Comparable kinetics of neutrophil clearance was observed between the 2 genotypes, however $DR3^{-/-}$ mice ($3.7 \pm 0.9 \times 10^4$ total neutrophils after 48 hours) were still found to have significantly reduced numbers of neutrophils after the first 24 hours of SES challenge compared to $DR3^{+/+}$ mice ($8.9 \pm 2.8 \times 10^4$ total neutrophils after 48 hours) ($p<0.01$) (Figure 5.3B).

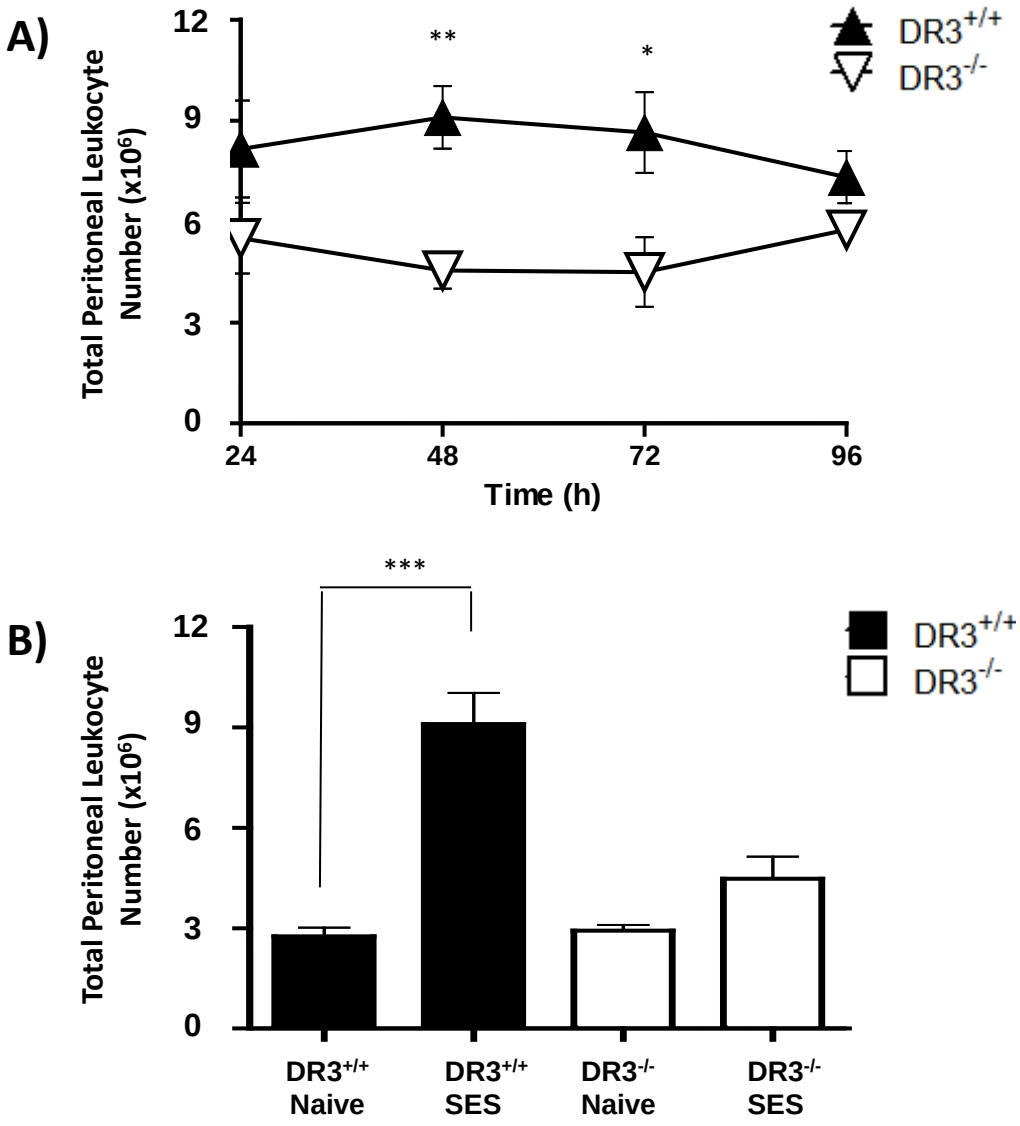

Figure 5.2 - Significantly higher numbers of leukocytes accumulated in the peritoneal cavity of DR3$^{+/+}$ mice compared to DR3$^{-/-}$ mice after SES induced inflammation. Inflammation in the cavity was induced via an i.p. injection of SES. Peritoneal leukocytes were isolated from the cavity by lavage, total cell number over the time course was calculated using a Beckman Coulter counter Z2. A) Following SES challenge significantly reduced numbers of leukocytes were found in the cavity of DR3$^{-/-}$ mice compared to DR3$^{+/+}$ (each symbol represents mean of n=6 DR3$^{+/+}$ mice (▲) and DR3$^{-/-}$ mice (▽) per time point, error bars correspond to mean ± SEM, p<0.01 by ANOVA, Bonferroni post hoc test **p<0.01 after 48h and *p<0.05 after 72h). B) At the peak of the inflammatory response (48 hours) DR3$^{-/-}$ mice present no significant increase in total leukocyte number compared to the DR3$^{-/-}$ naive control, in contrast to the significant rise in leukocytes in the DR3$^{+/+}$ (***p<0.001) (each bar represents mean of n=6 DR3$^{+/+}$ mice (■) and DR3$^{-/-}$ mice (□) per treatment, error bars correspond to mean ± SEM, analysed by t-test).

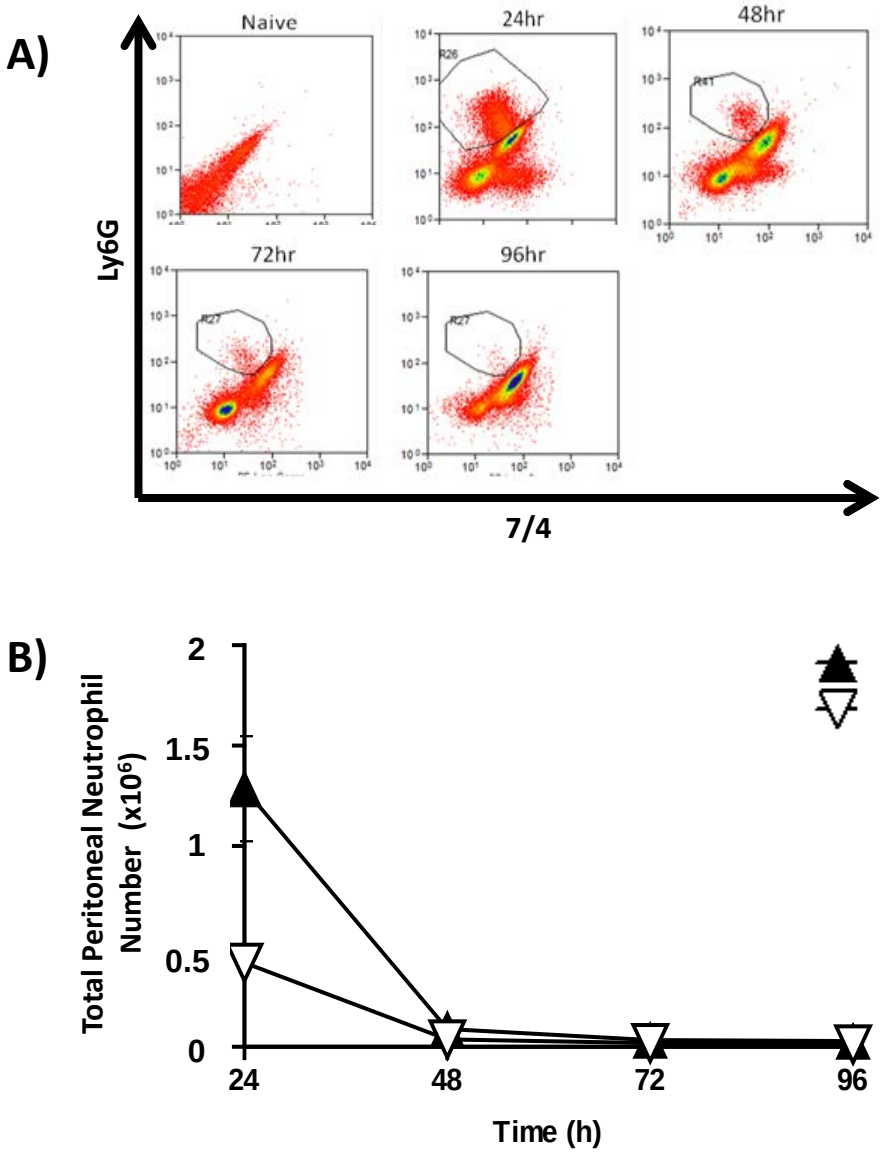

Figure 5.3 – Clearance of neutrophils from the peritoneal cavity of DR3$^{+/+}$ mice compared to DR3$^{-/-}$ mice after SES induced inflammation. Inflammation in the cavity was induced via an i.p. injection of SES. Peritoneal leukocytes were isolated from the cavity by lavage. A) Neutrophils were identified by a 7/4^{+} Ly6G^{+} CD11b^{int} F4/80^{int} phenotype. B) Neutrophil numbers at each time point were calculated by percentage proportion of total leukocytes, determined using a Beckman Coulter counter Z2 (each symbol represents mean of n=6 DR3$^{+/+}$ mice (▲) and DR3$^{-/-}$ mice (▽) per time point, error bars correspond to mean ± SEM, p<0.01 by ANOVA).

5.2.2.3 Accumulation of myeloid cell subsets in the DR3$^{+/+}$ and DR3$^{-/-}$ peritoneal cavity during later stages of acute SES induced inflammation

Other inflammatory myeloid subsets (inflammatory macrophages and eosinophils) which peak after 24 hours are steadily removed from the cavity during the late phase and replaced by resident macrophages, which constitute the majority of myeloid subsets in the naive cavity (Figure 5.4). Post 24 hours of SES challenge analogous numbers of resident macrophages were found in the peritoneal cavity of DR3$^{+/+}$ mice (7.2 ± 1.6 x10^5 total resident macrophages after 48 hours) and DR3$^{-/-}$ mice (6.1 ± 1.2 x10^5 total resident macrophages after 48 hours). However, there was a substantial decrease in the number of both eosinophils (DR3$^{+/+}$ mice 8.7 ± 3.2 x10^5, DR3$^{-/-}$ mice 2.4 ± 0.6 x10^5 total eosinophils after 48 hours) (Figure 5.4C) (p<0.01) and inflammatory macrophages (DR3$^{+/+}$ mice 2.5 ± 0.5 x10^6, DR3$^{-/-}$ mice 8.3 ± 0.9 x10^5 total inflammatory macrophages after 48 hours) (Figure 5.4A) (p<0.01) in DR3$^{-/-}$ mice.

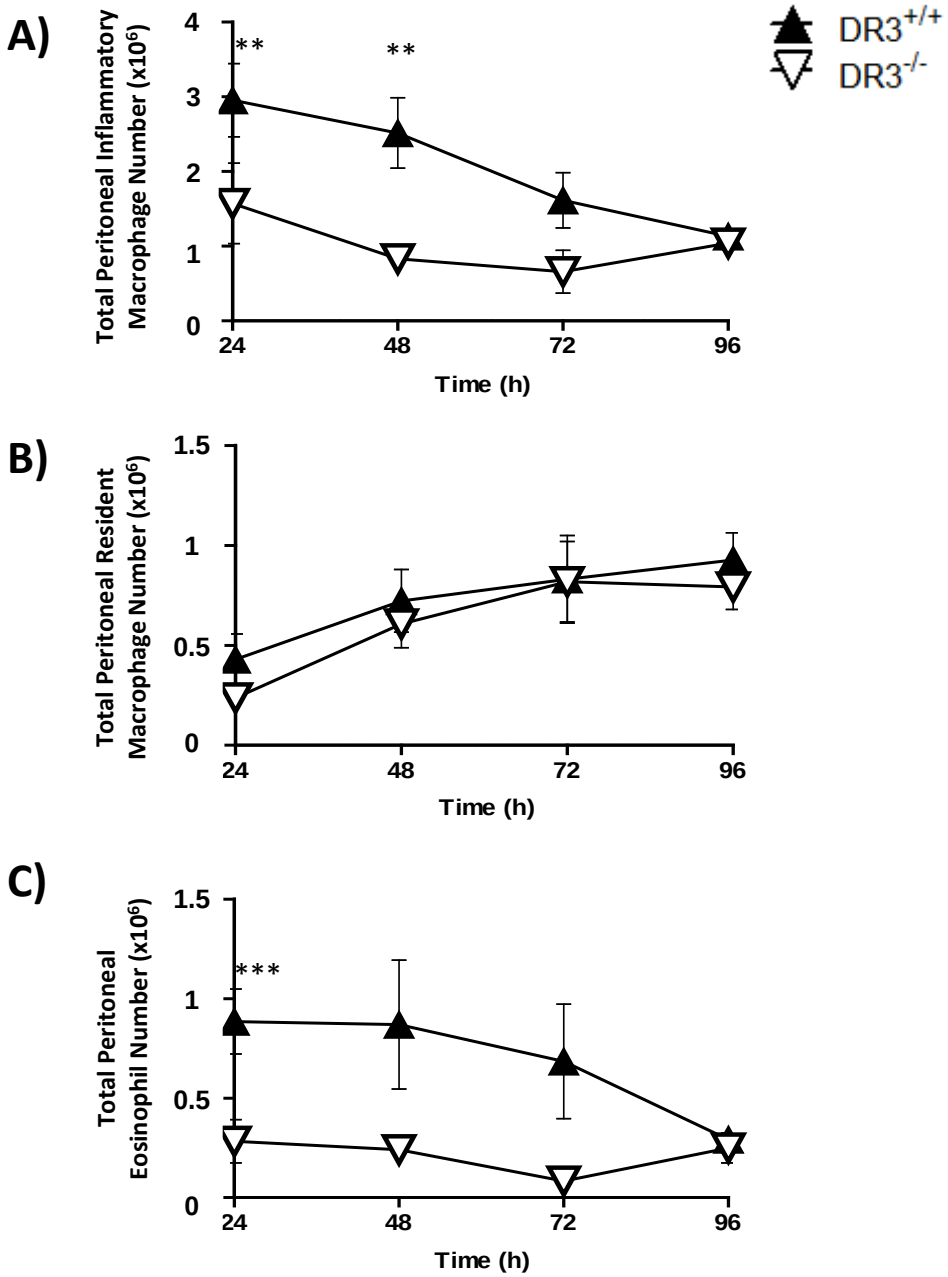

Figure 5.4 - Significantly higher numbers of inflammatory macrophages and eosinophils but not resident macrophages accumulated in the peritoneal cavity of DR3$^{+/+}$ mice compared to DR3$^{-/-}$ mice after SES induced inflammation. Inflammation in the cavity was induced via an i.p. injection of SES. Peritoneal leukocytes were isolated from the cavity by lavage. A) Inflammatory Macrophages, were identified by a CD11b^{int} F4/80^{int} phenotype (p<0.01 by ANOVA, Bonferroni post hoc test **p<0.01 after 24 and 48h) B) Resident Macrophages were identified by a CD11b^{+} F4/80^{+} phenotype and C) Eosinophils identified by F4/80^{int}, CD11b^{int} and their forward and side scatter properties (p<0.01 by ANOVA, Bonferroni post hoc test ***p<0.001 after 24h). Subset numbers calculated by percentage proportion of total leukocytes, determined using a Beckman Coulter counter Z2 (each symbol represents mean of n=6 DR3$^{+/+}$ mice (▲) and DR3$^{-/-}$ mice (▽) per time point, error bars correspond to mean ± SEM, analysed by ANOVA and Bonferroni post hoc test).

5.2.2.4 Accumulation of lymphocyte cell subsets in $DR3^{+/+}$ and $DR3^{-/-}$ peritoneal cavities during later stages of acute SES induced inflammation

Lymphocyte accumulation first observed during the early phase (Section 4.2.2.4) continued into the late phase of inflammation (Figure 5.5-5.7). During this period $DR3^{-/-}$ mice were found to have significantly decreased numbers of T cells ($DR3^{+/+}$ mice $8.5 \pm 3.3 \times 10^5$, $DR3^{-/-}$ mice $2.4 \pm 0.5 \times 10^5$ total T cells after 72 hours) ($p<0.01$), including both $CD4^+$ ($DR3^{+/+}$ mice $4.8 \pm 2.2 \times 10^5$, $DR3^{-/-}$ mice $1.5 \pm 0.3 \times 10^5$ total $CD4^+$ T cells after 72 hours) ($p<0.01$) and $CD8^+$ ($DR3^{+/+}$ mice $1.6 \pm 0.7 \times 10^5$, $DR3^{-/-}$ mice $4.8 \pm 1.2 \times 10^4$ total $CD8^+$ T cells after 72 hours) ($p<0.01$) (Figure 5.5) T cell subsets compared to $DR3^{+/+}$ mice, with T cell differences in the peritoneal cavities of the mice of each genotype at their greatest after 72 hours. Substantially fewer B cells were also observed in $DR3^{-/-}$ mice during the late phase ($DR3^{+/+}$ mice $2.3 \pm 0.8 \times 10^6$, $DR3^{-/-}$ mice $8.1 \pm 1.9 \times 10^5$ total B cells after 72 hours) ($p<0.01$), with lower numbers of both B1 ($DR3^{+/+}$ mice $1.2 \pm 0.3 \times 10^6$, $DR3^{-/-}$ mice $4.1 \pm 1.2 \times 10^5$ total B1 cells after 72 hours) ($p<0.01$) and B2 ($DR3^{+/+}$ mice $1.0 \pm 0.5 \times 10^6$, $DR3^{-/-}$ mice $3.1 \pm 0.8 \times 10^5$ total B2 cells after 72 hours) ($p<0.01$) (Figure 5.6) B cell subsets in the cavity compared to $DR3^{+/+}$ mice, with peak divergence between the 2 genotypes also found after 72 hours. $DR3^{-/-}$ mice ($7.9 \pm 1.5 \times 10^4$ total NKT cells after 48 hours) also had significantly fewer NKT cells compared to $DR3^{+/+}$ mice ($1.8 \pm 0.2 \times 10^5$ total NKT cells after 48 hours) ($p<0.01$) (Figure 5.7B), with maximum differences between the 2 genotypes after 48 hours of inflammation. However $DR3^{-/-}$ mice ($2.0 \pm 0.4 \times 10^5$ total NK cells after 48 hours) were found to have comparable numbers of NK cells in their cavity as $DR3^{+/+}$ mice ($3.0 \pm 0.5 \times 10^5$ total NK cells after 48 hours) (Figure 5.7A).

In summary, DR3$^{-/-}$ mice exhibit lower numbers of cells in their cavity during the late stage of inflammation, including a wide range of leukocyte subsets. These include inflammatory macrophages, eosinophils, T, B and NKT cells but exclude resident macrophages and NK cells.

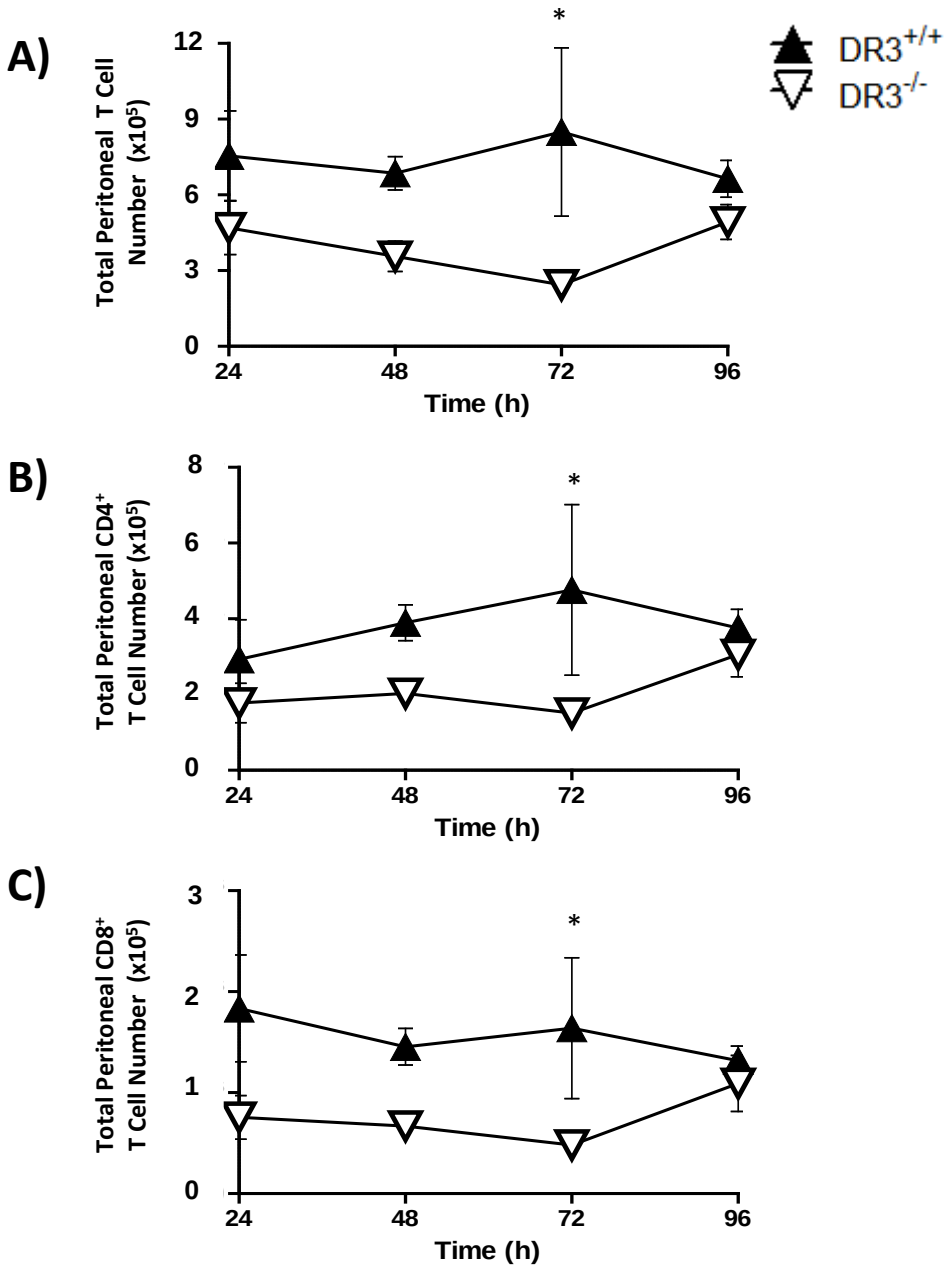

Figure 5.5 - Significantly higher numbers of T cell subsets accumulated in the peritoneal cavity of DR3$^{+/+}$ mice compared to DR3$^{-/-}$ mice after SES induced inflammation. Inflammation in the cavity was induced via an i.p. injection of SES. Peritoneal leukocytes were isolated from the cavity by lavage. A) T cells were identified by a CD3$^+$, TCRαβ$^+$ phenotype (p<0.01 by ANOVA, Bonferroni post hoc test *p<0.05 after 72h). B) T helper cells were identified by a CD3$^+$ CD4$^+$, TCRαβ$^+$ phenotype (p<0.01 by ANOVA, Bonferroni post hoc test *p<0.05 after 72h) and C) T cytotoxic cells identified by a CD3$^+$ CD8$^+$, TCRαβ$^+$ phenotype (p<0.01 by ANOVA, Bonferroni post hoc test *p<0.05 after 72h). Subset numbers calculated by percentage proportion of total leukocytes, determined using a Beckman Coulter counter Z2 (each symbol represents mean of n=6 DR3$^{+/+}$ mice (▲) and DR3$^{-/-}$ mice (▽) per time point, error bars correspond to mean ± SEM, analysed by ANOVA and Bonferroni post hoc test).

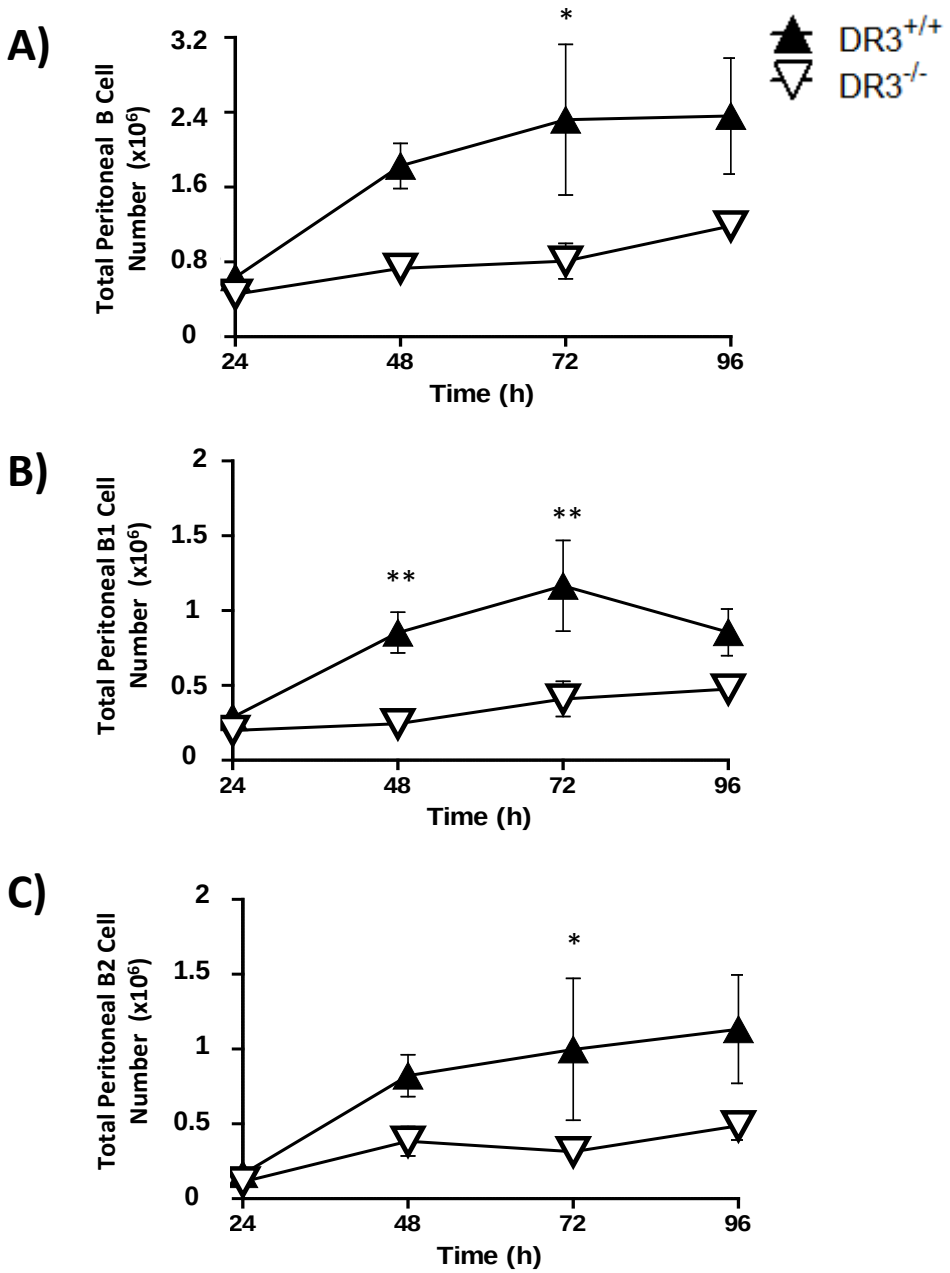

Figure 5.6 - Significantly higher numbers of B cell subsets accumulated in the peritoneal cavity of DR3$^{+/+}$ mice compared to DR3$^{-/-}$ mice after SES induced inflammation. Inflammation in the cavity was induced via an i.p. injection of SES. Peritoneal leukocytes were isolated from the cavity by lavage. A) B cells were identified by a CD19^{+}, B220^{+} phenotype (p<0.01 by ANOVA, Bonferroni post hoc test *p<0.05 after 72h). B) B1 cells were identified by a CD19^{+} B220^{int}, CD11b^{int} phenotype (p<0.01 by ANOVA, Bonferroni post hoc test **p<0.01 after 48 and 72h) and C) B2 cells identified by a CD19^{+} B220^{+}, CD11b^{-} phenotype (p<0.01 by ANOVA, Bonferroni post hoc test *p<0.05 after 72h). Subset numbers calculated by percentage proportion of total leukocytes, determined using a Beckman Coulter counter Z2 (each symbol represents mean of n=6 DR3$^{+/+}$ mice (▲) and DR3$^{-/-}$ mice (▽) per time point, error bars correspond to mean ± SEM, analysed by ANOVA and Bonferroni post hoc test).

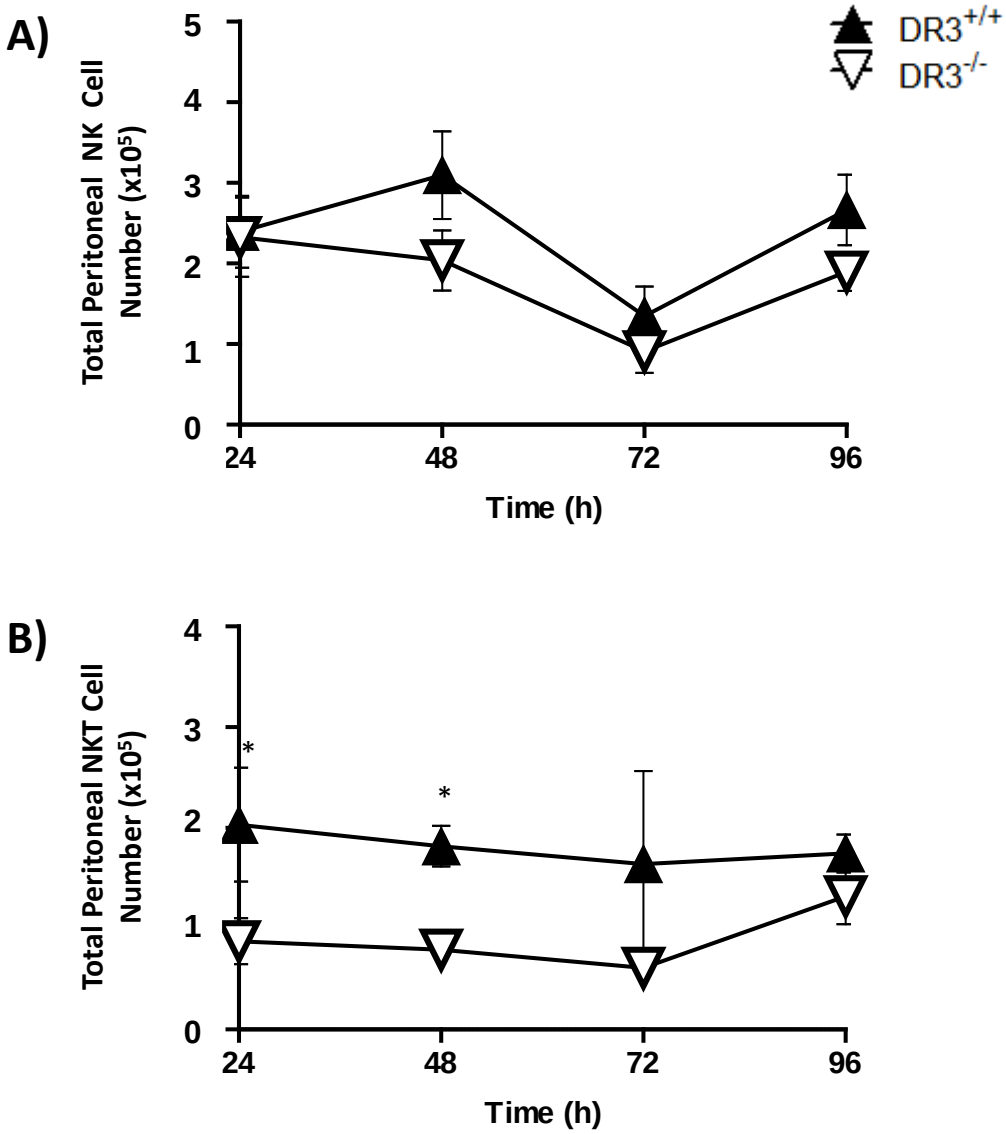

Figure 5.7 - Significantly higher numbers of NKT cells but not NK cells accumulated in the peritoneal cavity of DR3$^{+/+}$ mice compared to DR3$^{-/-}$ mice after SES induced inflammation. Inflammation in the cavity was induced via an i.p. injection of SES. Peritoneal leukocytes were isolated from the cavity by lavage. A) NK cells were identified by a NK1.1^{+}, TCRαβ^{-} phenotype. B) NKT cells were identified by a NK1.1^{+}, TCRαβ^{+} phenotype (p<0.01 by ANOVA, Bonferroni post hoc test *p<0.05 after 24 and 48h). Subset numbers calculated by percentage proportion of total leukocytes, determined using a Beckman Coulter counter Z2 (each symbol represents mean of n=6 DR3$^{+/+}$ mice (▲) and DR3$^{-/-}$ mice (▽) per time point, error bars correspond to mean ± SEM, analysed by ANOVA and Bonferroni post hoc test).

5.2.3.1 Levels of leukocyte proliferation in the peritoneal cavity of $DR3^{+/+}$ and $DR3^{-/-}$ mice 48 hours after the induction of SES inflammation

DR3 has previously been shown to affect cell proliferation (Taraban, Slebioda et al. 2011; Twohig, Marsden et al. 2012), therefore the proliferative levels of leukocyte subsets were investigated as a possible cause of reduced numbers of selected cell subsets in the peritoneal cavity of $DR3^{-/-}$ mice. Prior work has shown peak proliferation in the inflamed cavity occurs 48 hours after the induction of inflammation (Davies, Rosas et al. 2011). Proliferation at this time was studied using intracellular staining for Ki67 as described in Chapter 3. Significant increases in the percentage of proliferating cells were noted 48 hours after SES challenge in all subsets tested (Figure 5.8-5.11) compared to the naive cavity (Figure 3.7-3.10). However no disparity was observed in the proportion of any myeloid (resident macrophages: $DR3^{+/+}$ mice 42.4 ± 13.2%, $DR3^{-/-}$ mice 44.5 ± 8.2%, inflammatory macrophages: $DR3^{+/+}$ mice 43.7 ± 11.5%, $DR3^{-/-}$ mice 47.9 ± 7.7%) or lymphocyte (T cells: $DR3^{+/+}$ mice 49.3 ± 2.3%, $DR3^{-/-}$ mice 50.5 ± 7.5%, B cells: $DR3^{+/+}$ mice 36.9 ± 2.8%, $DR3^{-/-}$ mice 28.8 ± 8.2%, NK cells: $DR3^{+/+}$ mice 35.2 ± 10.4%, $DR3^{-/-}$ mice 38.2 ± 3.8%, NKT cells: $DR3^{+/+}$ mice 47.7 ± 3.8%, $DR3^{-/-}$ mice 51.8 ± 10.1%) cell subset expressing Ki67 in the challenged cavity of $DR3^{-/-}$ mice compared to $DR3^{+/+}$ mice (Figure 5.8-5.11).

Hence, in contrast to previous reports, DR3 is not essential in maintaining leukocyte proliferation in this particular model.

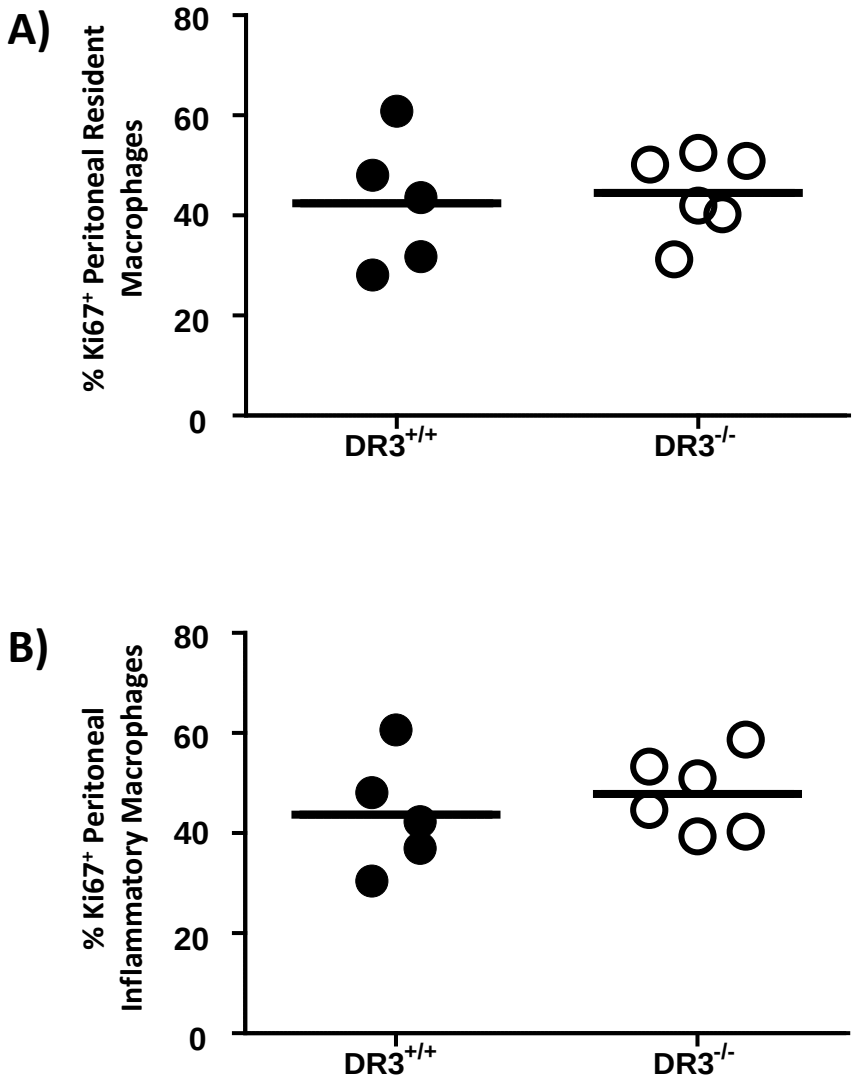

Figure 5.8 - No significant differences were seen in the percentages of proliferating macrophage subsets in the peritoneal cavity of DR3$^{+/+}$ mice and DR3$^{-/-}$ mice 48 hours after induction of SES inflammation. Inflammation in the cavity was induced via an i.p. injection of SES. Peritoneal leukocytes were isolated from the cavity by lavage. A) Resident Macrophages were identified by a CD11b^{+} F4/80^{+} phenotype B) and Inflammatory Macrophages, were identified by a CD11b^{int} F4/80^{int} phenotype. Percentages of proliferating macrophage subsets were calculated by the percentage of the subset positive for the marker Ki67 (each symbol represents a single mouse, bar corresponds to mean from n=5 or 6, N.S.D by Mann-Whitney test).

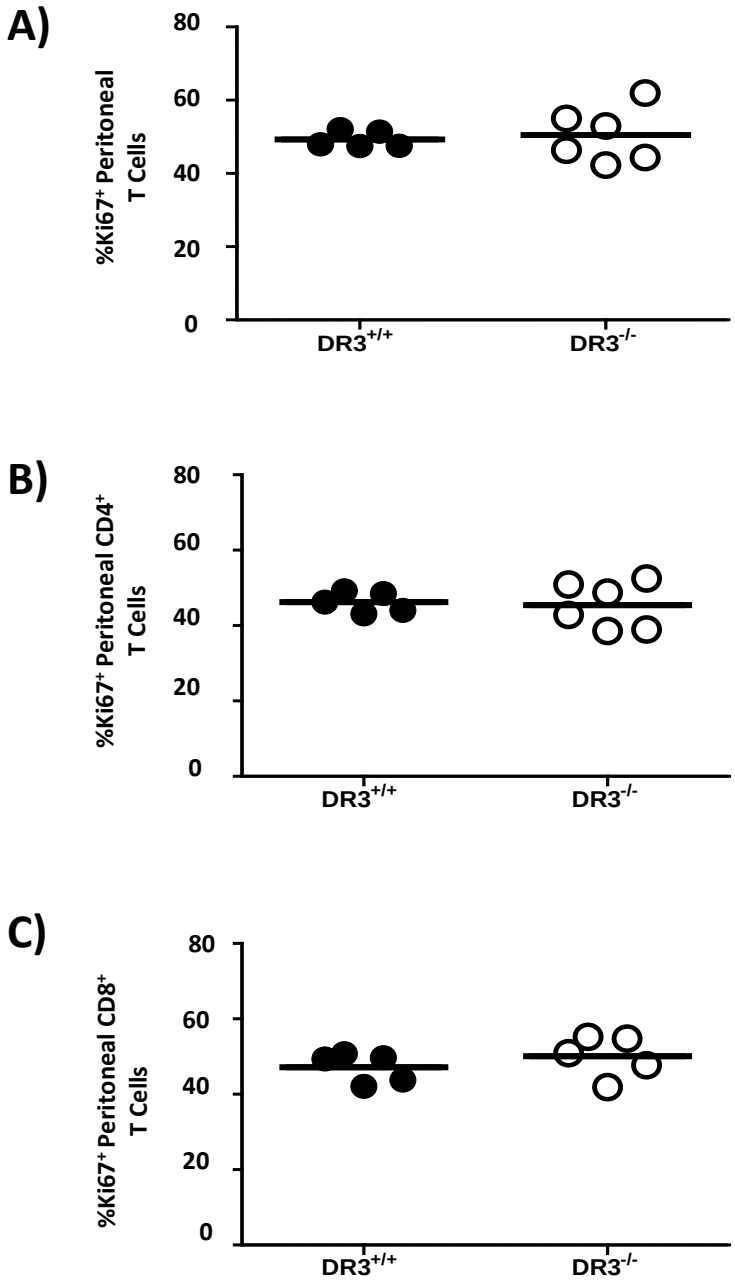

Figure 5.9 - No significant differences were seen in the percentages of proliferating T cell subsets in the peritoneal cavity of DR3$^{+/+}$ mice and DR3$^{-/-}$ mice 48 hours after induction of SES inflammation. Inflammation in the cavity was induced via an i.p. injection of SES. Peritoneal leukocytes were isolated from the cavity by lavage. A) T cells were identified by a CD3^{+}, TCRαβ^{+} phenotype, B) T helper cells were identified by a CD3^{+} CD4^{+}, TCRαβ^{+} phenotype and C) T cytotoxic cells identified by a CD3^{+} CD8^{+}, TCRαβ^{+} phenotype. Percentages of proliferating T cell subsets were calculated by the percentage of the subset positive for the marker Ki67 (each symbol represents a single mouse, bar corresponds to mean from n=5 or 6, N.S.D by Mann-Whitney test).

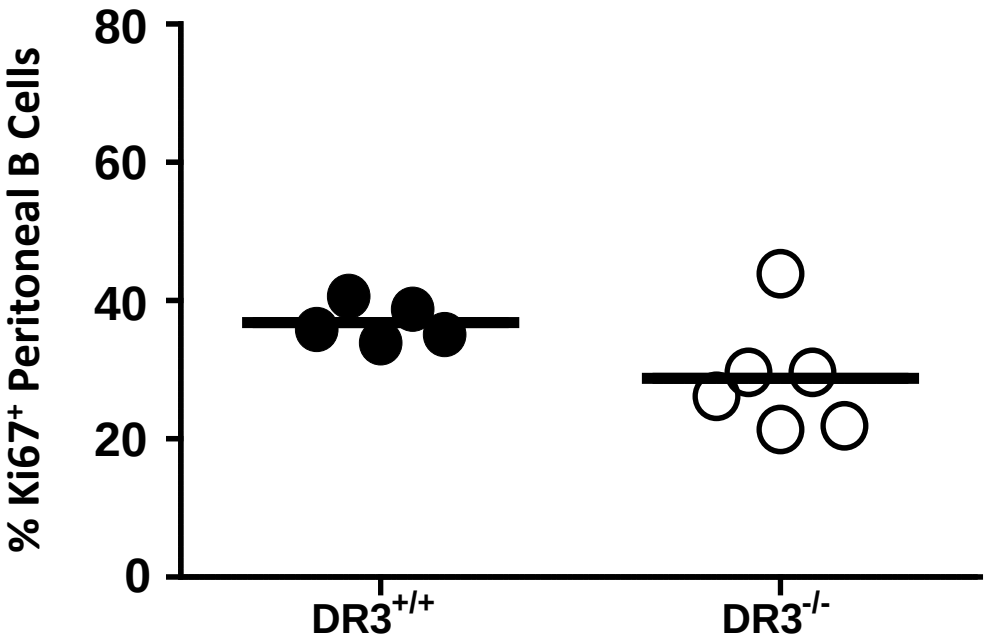

Figure 5.10 - No significant differences were seen in the percentages of proliferating B cells in the peritoneal cavity of DR3$^{+/+}$ mice and DR3$^{-/-}$ mice 48 hours after induction of SES inflammation. Inflammation in the cavity was induced via an i.p. injection of SES. Peritoneal leukocytes were isolated from the cavity by lavage. B cells were identified by a CD19^{+}, B220^{+} phenotype. Percentages of proliferating B cells were calculated by the percentage of the subset positive for the marker Ki67 (each symbol represents a single mouse, bar corresponds to mean from n=5 or 6, N.S.D by Mann-Whitney test).

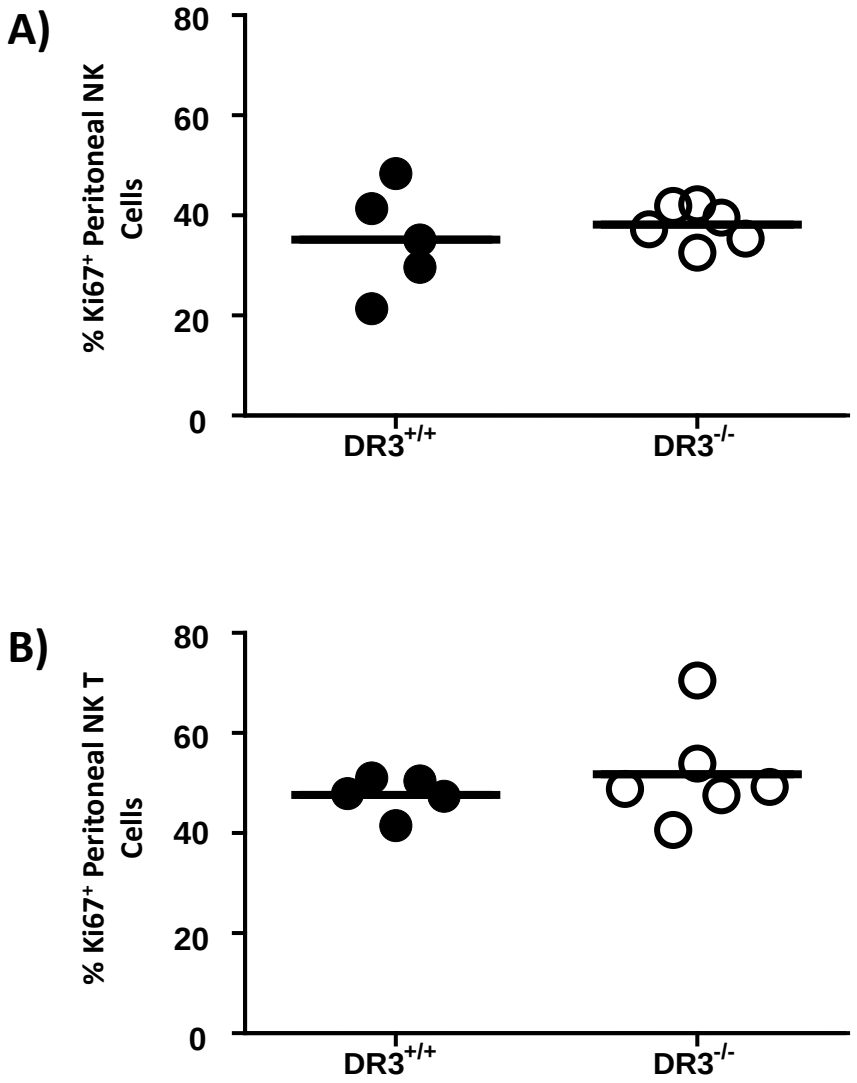

Figure 5.11 - No significant differences were seen in the percentages of proliferating NK and NKT cell subsets in the peritoneal cavity of DR3$^{+/+}$ mice and DR3$^{-/-}$ mice 48 hours after induction of SES inflammation. Inflammation in the cavity was induced via an i.p. injection of SES. Peritoneal leukocytes were isolated from the cavity by lavage. A) NK cells were identified by a NK1.1^{+}, TCRαβ^{-} phenotype B) and NKT cells were identified by a NK1.1^{+}, TCRαβ^{+} phenotype. Percentages of proliferating NK subsets were calculated by the percentage of the subset positive for the marker Ki67 (each symbol represents a single mouse, bar corresponds to mean from n=5 or 6, N.S.D by Mann-Whitney test).

5.2.3.2 Levels of chemoattractants in $DR3^{+/+}$ and $DR3^{-/-}$ peritoneal cavities in later stages of acute SES induced inflammation

Since the absence of DR3 had no effect on the proliferation of leukocyte subsets in the challenged cavity, a second hypothesis was tested to explain the leukocyte accumulation defect observed in $DR3^{-/-}$ mice. Chemoattractant release has previously been shown to play an important role in the movement of leukocytes in this model (Hurst, Wilkinson et al. 2001; McLoughlin, Hurst et al. 2004; McLoughlin, Jenkins et al. 2005) and $DR3^{-/-}$ mice were found to be associated with reduced levels of KC (Figure 4.14A) during the early phase of SES induced inflammation (Chapter 4).

Significantly lower levels of CCL2 ($DR3^{+/+}$ mice 1919 ± 164 pg/ml, $DR3^{-/-}$ mice 524 ± 149 pg/ml after 1 hour) (Figure 5.12A) ($p<0.01$), CCL7 ($DR3^{+/+}$ mice 1251 ± 345 pg/ml, $DR3^{-/-}$ mice 113 ± 57 pg/ml after 1 hour) (Figure 5.12B) ($p<0.05$), CCL3 ($DR3^{+/+}$ mice 162 ± 44 pg/ml, $DR3^{-/-}$ mice 56 ± 7 pg/ml after 6 hours) (Figure 5.13A) ($p<0.01$), CCL4 ($DR3^{+/+}$ mice 1279 ± 16 pg/ml, $DR3^{-/-}$ mice 204 ± 52 pg/ml after 6 hours) (Figure 5.13B) ($p<0.01$), CXCL10 ($DR3^{+/+}$ mice 391 ± 111 pg/ml, $DR3^{-/-}$ mice 158 ± 21 pg/ml after 3 hours) (Figure 5.14A) ($p<0.01$) and CXCL13 ($DR3^{+/+}$ mice 2801 ± 162 pg/ml, $DR3^{-/-}$ mice 1014 ± 295 pg/ml after 24 hours) (Figure 5.15) ($p<0.01$) were detected in $DR3^{-/-}$ supernatants compared to $DR3^{+/+}$ supernatants following SES challenge. However CCL5 was present at similar levels in the supernatants of both $DR3^{+/+}$ (79 ± 9 pg/ml after 3 hours) and $DR3^{-/-}$ (82 ± 8 pg/ml after 3 hours) mice (Figure 5.14B).

Thus SES challenge leads to the release of multiple chemoattractants in $DR3^{+/+}$ mice, with significantly lower levels of selected chemokines found in $DR3^{-/-}$ mice.

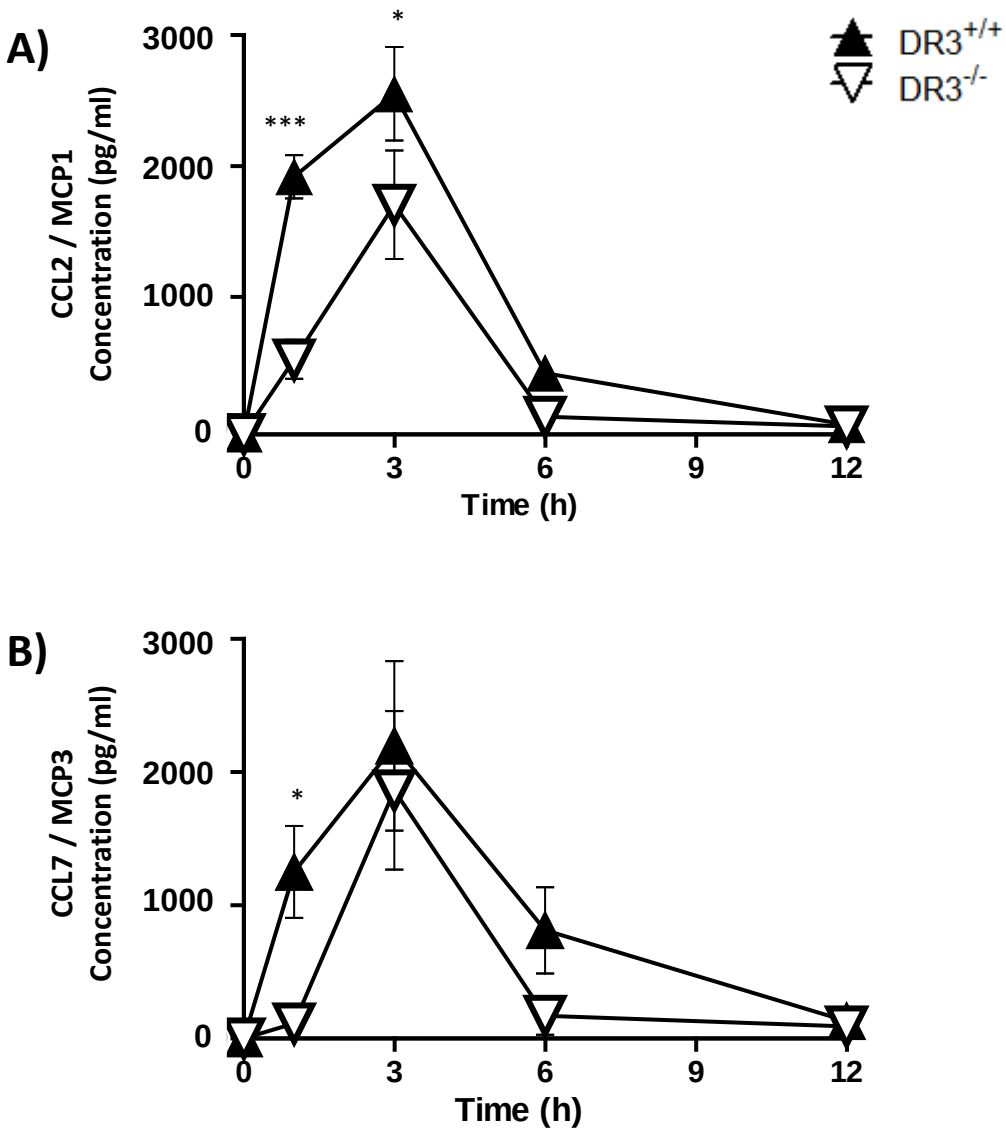

Figure 5.12 - Significantly higher levels of CCL2 and CCL7 were found in the peritoneal cavity of DR3$^{+/+}$ mice compared to DR3$^{-/-}$ mice after induction of SES inflammation. Inflammation in the cavity was induced via an i.p. injection of SES and cell free supernatants analysed for levels of A) CCL2 (***p<0.01) B) and CCL7 (*p<0.05) by ELISA (each symbol represents mean of n=5 DR3$^{+/+}$ mice (▲) and DR3$^{-/-}$ mice (▽) per time point, error bars correspond to mean ± SEM, analysed by ANOVA and p values calculated using Bonferonni's post hoc test).

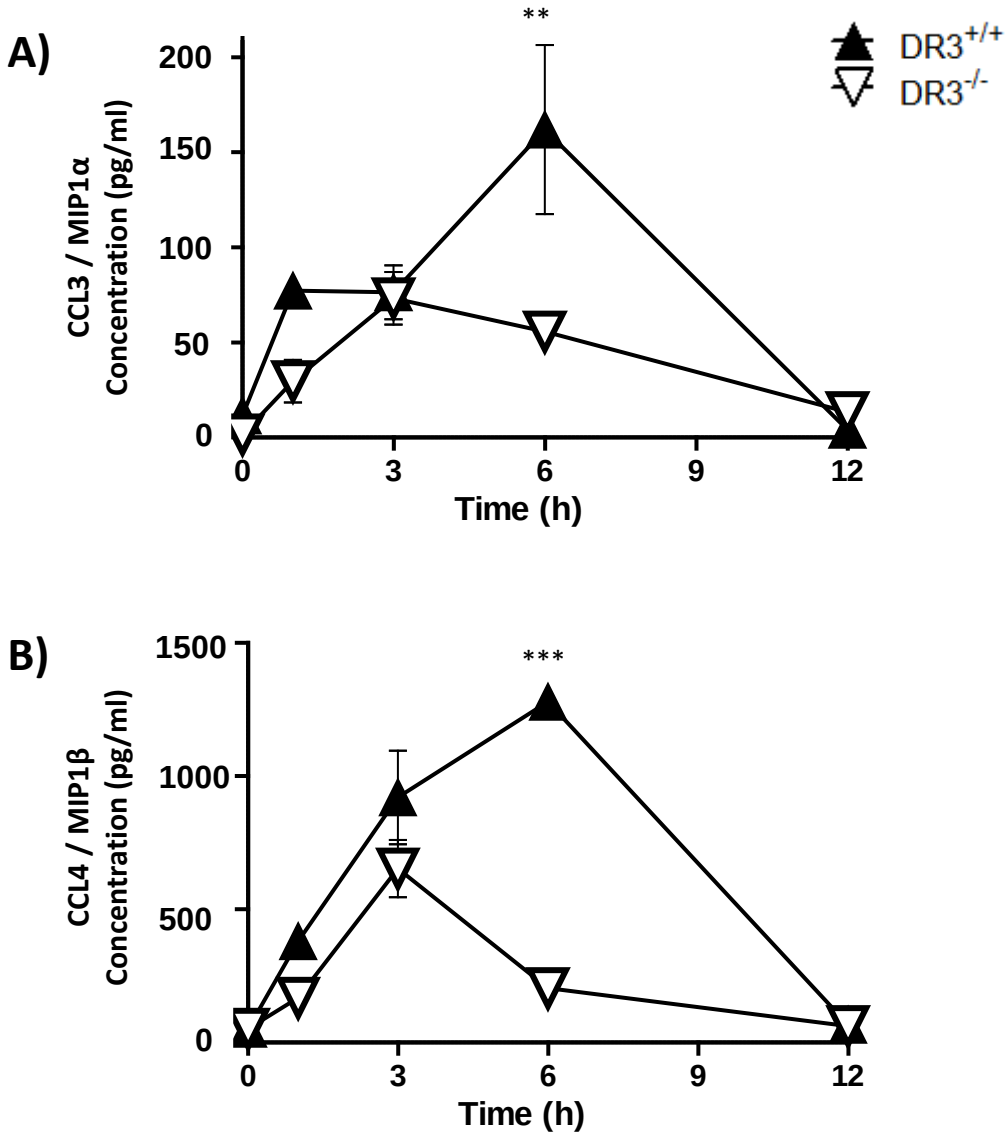

Figure 5.13 - Significantly higher levels of CCL3 and CCL4 were found in the peritoneal cavity of DR3$^{+/+}$ mice compared to DR3$^{-/-}$ mice after induction of SES inflammation. Inflammation in the cavity was induced via an i.p. injection of SES and cell free supernatants analysed for levels of A) CCL3 (**p<0.01) and B) CCL4 (***p<0.01) by ELISA (each symbol represents mean of n=5 DR3$^{+/+}$ mice (▲) and DR3$^{-/-}$ mice (▽) per time point, error bars correspond to mean ± SEM, analysed by ANOVA and p values calculated using Bonferonni's post hoc test).

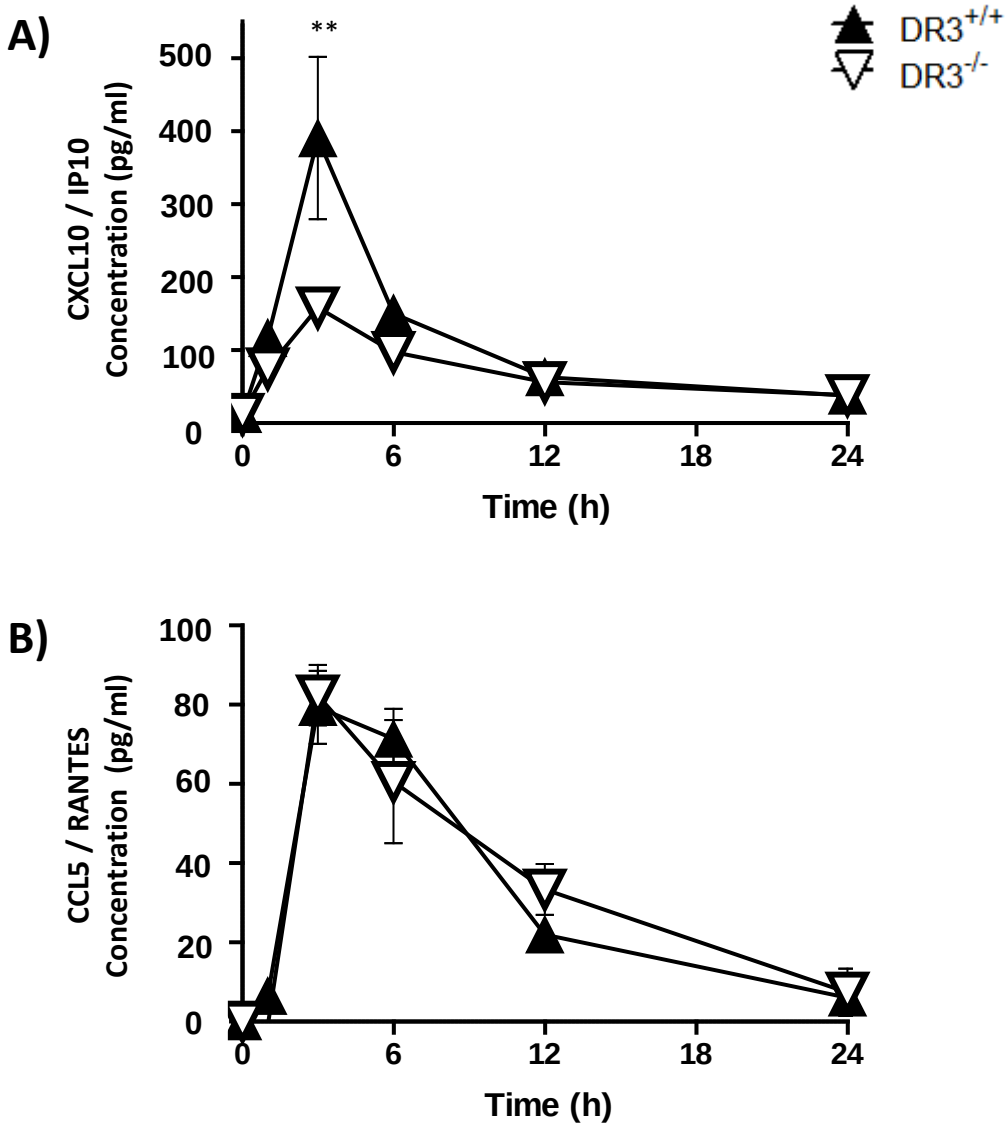

Figure 5.14 - Significantly higher levels of CXCL10 but not CCL5 were found in the peritoneal cavity of DR3$^{+/+}$ mice compared to DR3$^{-/-}$ mice after induction of SES inflammation. Inflammation in the cavity was induced via an i.p. injection of SES and cell free supernatants analysed for levels of A) CXCL10 (**p<0.01) and B) CCL5 by ELISA (each symbol represents mean of n=5 DR3$^{+/+}$ mice (▲) and DR3$^{-/-}$ mice (▽) per time point, error bars correspond to mean ± SEM, analysed by ANOVA and p values calculated using Bonferonni's post hoc test).

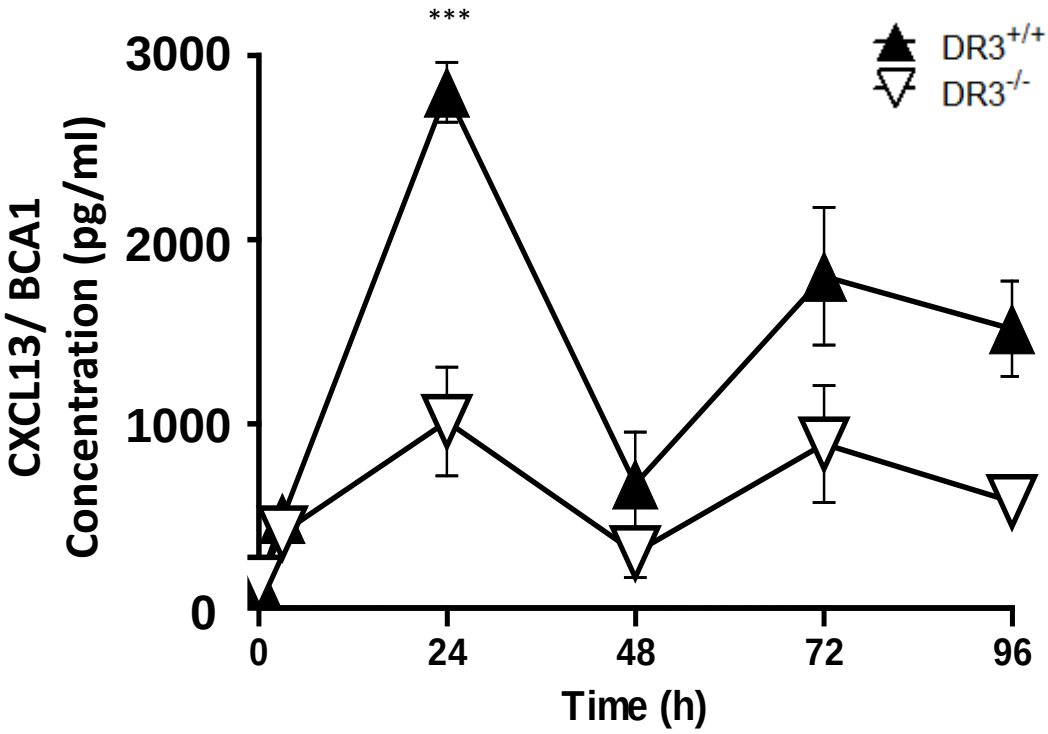

Figure 5.15 - Significantly higher levels of CXCL13 were found in the peritoneal cavity of DR3$^{+/+}$ mice compared to DR3$^{-/-}$ mice after induction of SES inflammation. Inflammation in the cavity was induced via an i.p. injection of SES and cell free supernatants analysed for levels of CXCL13 by ELISA (each symbol represents mean of n=5 DR3$^{+/+}$ mice (▲) and DR3$^{-/-}$ mice (▽) per time point, error bars correspond to mean ± SEM, analysed by ANOVA, ***p<0.01 using Bonferonni's post hoc test).

5.2.3.3 RQ of late phase chemoattractant mRNA in $DR3^{+/+}$ and $DR3^{-/-}$ peritoneal membranes after SES induced inflammation

Mesothelial cells found within the peritoneal membrane have previously been shown to express DR3 (Chapter 3) and be a source of chemoattractants (Li, Davenport et al. 1998; Hurst, Wilkinson et al. 2001; McLoughlin, Hurst et al. 2004); the membrane was also shown to be a likely source of both the ELR^+ chemoattractants KC and MIP2 in Chapter 4. Consequently the RQ of chemoattractants in the membrane during inflammation was investigated by qPCR (Section 2.5). Selected chemokines mRNA rapidly increased after the induction of SES inflammation (Figure 5.16-5.19). Comparable RQ of CCL3 ($DR3^{+/+}$ mice 0.8 ± 1.0, $DR3^{-/-}$ mice 2.2 ± 1.0 RQ after 3 hours) (Figure 5.17A), CCL4 ($DR3^{+/+}$ mice 7.0 ± 3.3, $DR3^{-/-}$ mice 7.7 ± 3.1 RQ after 3 hours) (Figure 5.17B), CCL5 ($DR3^{+/+}$ mice 0.9 ± 0.3, $DR3^{-/-}$ mice 3.3 ± 1.6 RQ after 3 hours) (Figure 5.18B) and CXCL10 ($DR3^{+/+}$ mice 22.8 ± 14, $DR3^{-/-}$ mice 11.3 ± 10.1 RQ after 3 hours) (Figure 5.18A) mRNA was found in the $DR3^{+/+}$ and $DR3^{-/-}$ membrane. However significantly reduced quantities of CCL2 ($DR3^{+/+}$ mice 20.7 ± 7.0, $DR3^{-/-}$ mice 2.5 ± 1.3 RQ after 1 hour) (Figure 5.16A) ($p<0.01$), CCL7 ($DR3^{+/+}$ mice 6.4 ± 1.8, $DR3^{-/-}$ mice 0.9 ± 0.4 RQ after 1 hour) (Figure 5.16B) ($p<0.01$) and CXCL13 ($DR3^{+/+}$ mice 3.2 ± 0.8, $DR3^{-/-}$ mice 0.6 ± 0.4 RQ after 1 hour) (Figure 5.19) ($p<0.05$) mRNA was measured in the $DR3^{-/-}$ membrane compared to $DR3^{+/+}$ after SES challenge and correlates with reduced levels of these chemoattractants in the $DR3^{-/-}$ cavity tested by ELISA (Figure 5.12 and Figure 5.15).

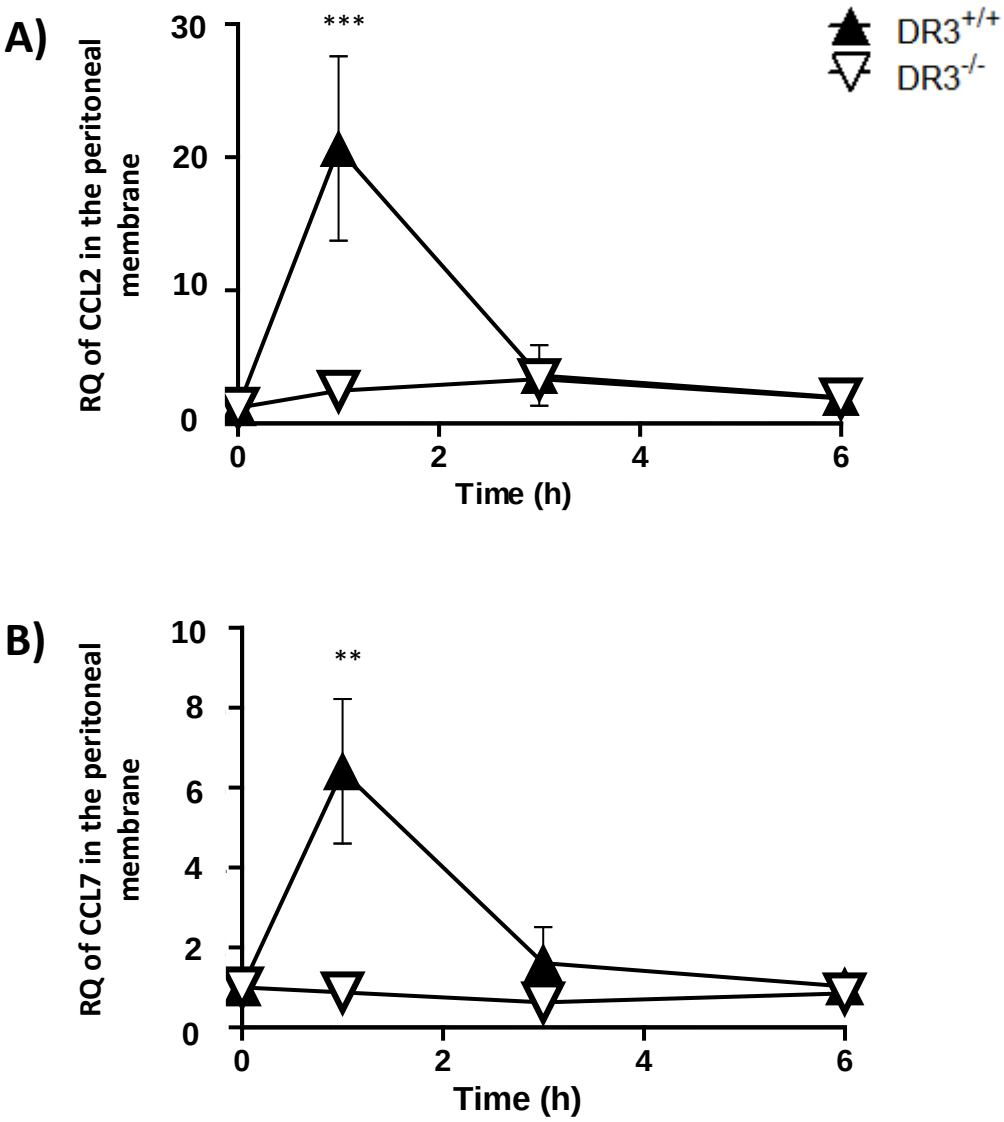

Figure 5.16 - Significantly higher relative quantity of CCL2 and CCL7 mRNA was found in the peritoneal membrane of DR3$^{+/+}$ mice compared to DR3$^{-/-}$ mice after induction of SES inflammation. Inflammation in the cavity was induced via an i.p. injection of SES and mRNA levels of A) CCL2 (***p<0.01) and B) CCL7 (**p<0.01) in the membrane measured by qPCR. Values correspond to mean ± SEM, n=5 mice per genotype per time point, analysed by ANOVA (each symbol represents mean of n=5 DR3$^{+/+}$ mice (▲) and DR3$^{-/-}$ mice (▽) per time point, error bars correspond to mean ± SEM, analysed by ANOVA and p values calculated using Bonferonni's post hoc test).

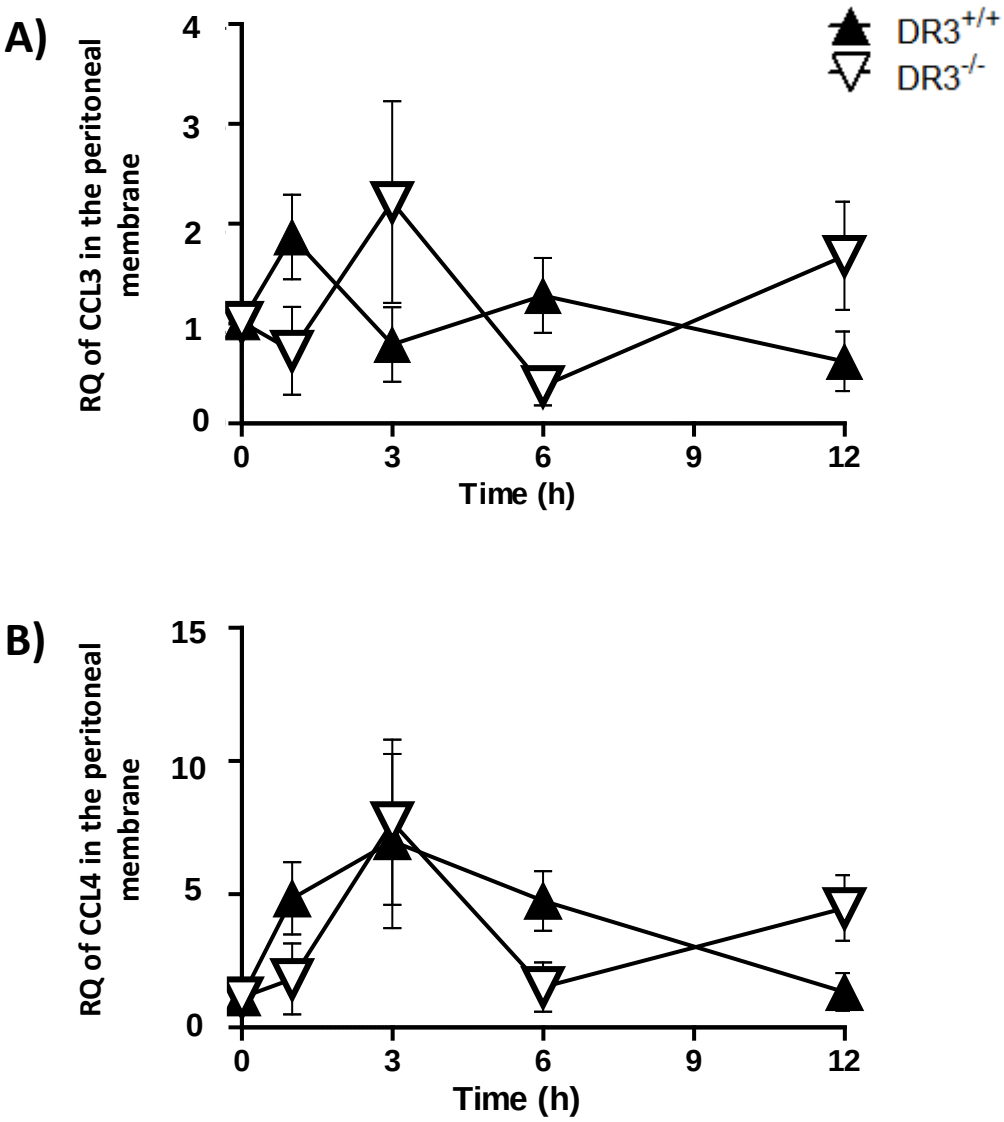

Figure 5.17 - No significant differences were seen in the relative quantity of CCL3 and CCL4 mRNA in the peritoneal membrane of DR3$^{+/+}$ mice and DR3$^{-/-}$ mice after induction of SES inflammation. Inflammation in the cavity was induced via an i.p. injection of SES and mRNA levels of A) CCL3 and B) CCL4 in the membrane measured by qPCR (each symbol represents mean of n=5 DR3$^{+/+}$ mice (▲) and DR3$^{-/-}$ mice (▽) per time point, error bars correspond to mean ± SEM, N.S.D by ANOVA).

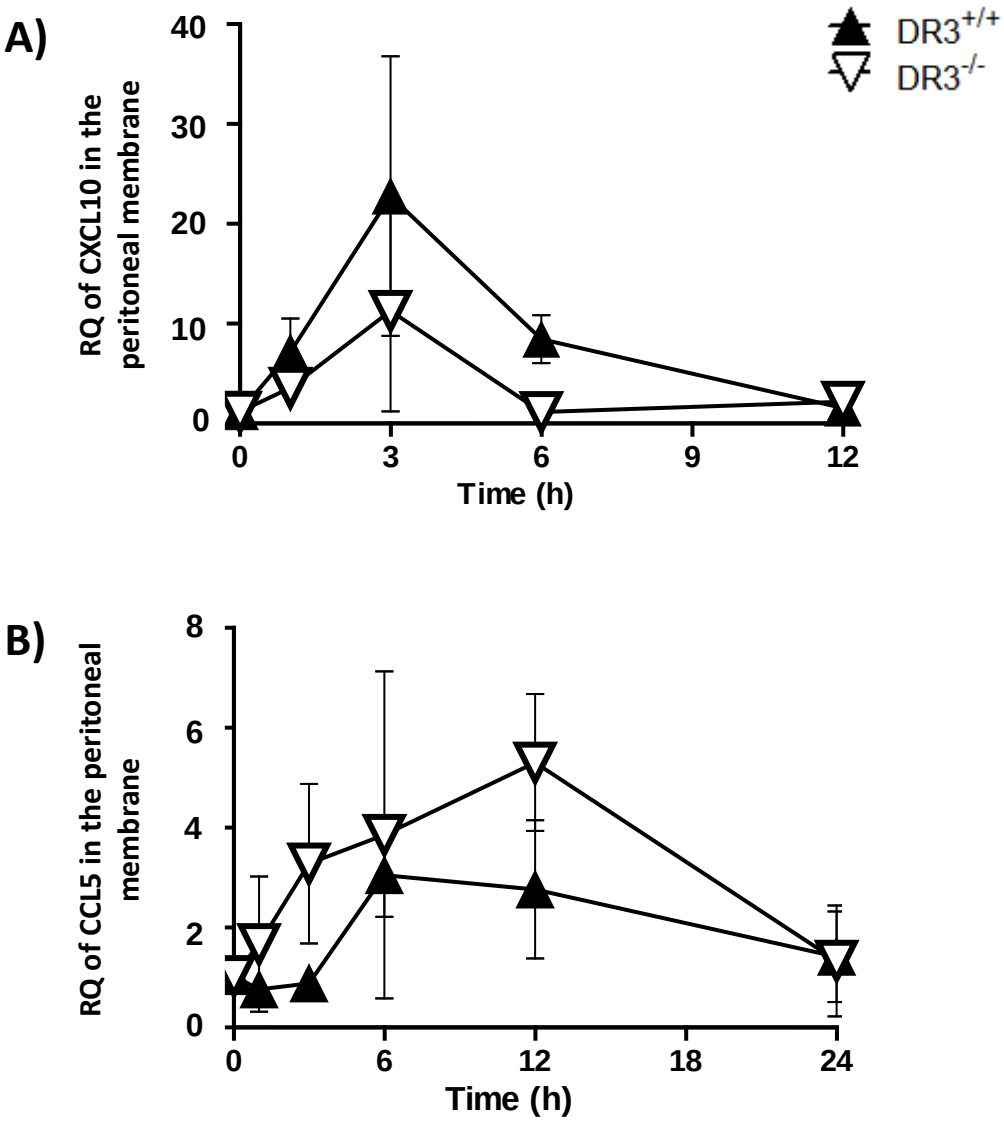

Figure 5.18 - No significant differences were seen in the relative quantity of CXCL10 and CCL5 mRNA in the peritoneal membrane of DR3$^{+/+}$ mice and DR3$^{-/-}$ mice after induction of SES inflammation. Inflammation in the cavity was induced via an i.p. injection of SES and mRNA levels of A) CXCL10 and B) CCL5 in the membrane measured by qPCR (each symbol represents mean of n=5 DR3$^{+/+}$ mice (▲) and DR3$^{-/-}$ mice (▽) per time point, error bars correspond to mean ± SEM, N.S.D by ANOVA).

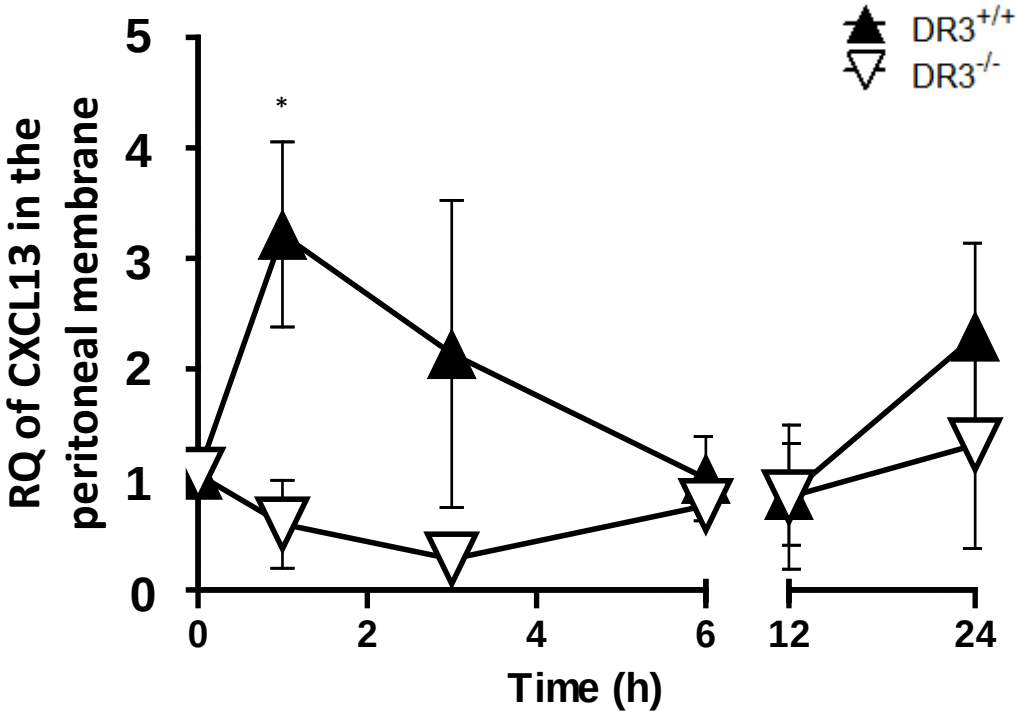

Figure 5.19 - Significantly higher relative quantity of CXCL13 mRNA was found in the peritoneal membrane of DR3$^{+/+}$ mice compared to DR3$^{-/-}$ mice after induction of SES inflammation. Inflammation in the cavity was induced via an i.p. injection of SES and mRNA levels of CXCL13 in the membrane measured by qPCR (each symbol represents mean of n=5 DR3$^{+/+}$ mice (▲) and DR3$^{-/-}$ mice (▽) per time point, error bars correspond to mean ± SEM, analysed by ANOVA, *p<0.05 calculated using Bonferonni's post hoc test.)

5.2.3.4 Correlation between peak chemokine level in peritoneal supernatants and peak chemoattractant mRNA level in the membrane after induction of SES inflammation.

To examine if higher chemokine RQ in the peritoneal membrane (Figure 5.16-5.19) correlated with increased levels in peritoneal supernatants (Figure 5.12-5.15) after SES challenge, peak RQ of chemoattractants in the membrane was plotted against peak levels in the supernatant. No substantial correlation was present between the maximum level of CCL3 (Figure 5.21B), CCL4 (Figure 5.21A), CCL5 (Figure 5.22B) and CXCL10 (Figure 5.22A) and the RQ of that chemoattractant in the membrane. However correlation was found between CCL2 (Figure 5.20A) (R=0.70, p=0.02), CCL7 (Figure 5.20B, R=0.69, p=0.02) and CXCL13 (Figure 5.23) (R=0.68, p=0.02), with the peak RQ of these chemoattractants in the membrane positively associated with higher levels of their levels in the peritoneal supernatant.

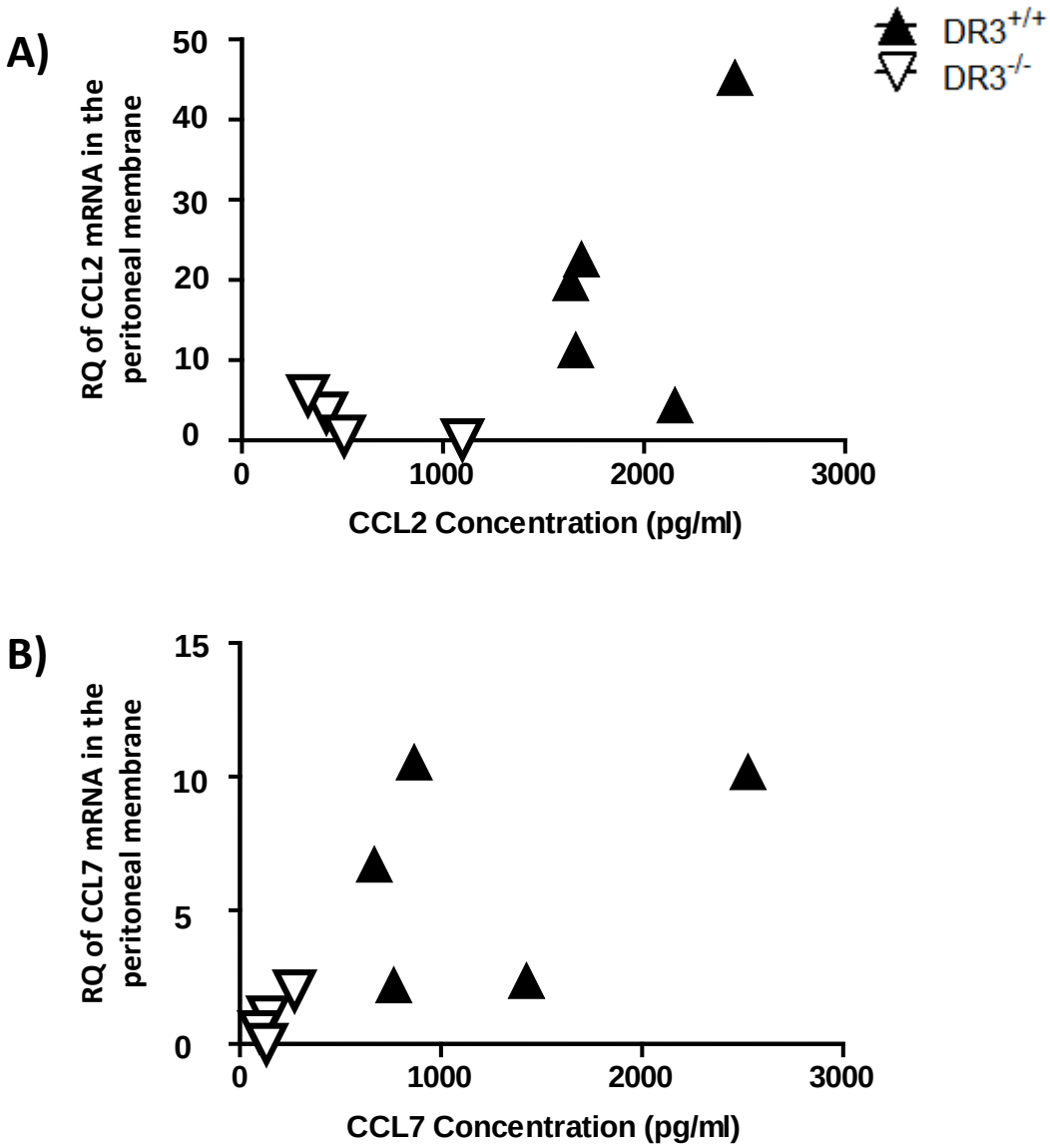

Figure 5.20 - Significant correlation was found between peak levels of CCL2 and CCL7 in the cavity and peak RQ of CCL2 and CCL7 mRNA in the peritoneal membrane of DR3$^{+/+}$ mice and DR3$^{-/-}$ mice after induction of SES inflammation. Inflammation in the cavity was induced via an i.p. injection of SES and cell free supernatants analysed for chemokine levels by ELISA. Peritoneal membranes were analysed for the RQ of chemoattractant mRNA in the membrane by qPCR. Correlation between the level of A) CCL2 (R=0.70, *p*=0.02) and B) CCL7 (R=0.69, *p*=0.02) in the supernatants was then plotted against the RQ of the chemoattractant mRNA found in the membrane (each symbol represents a single DR3$^{+/+}$ (▲) or DR3$^{-/-}$ mouse (▽), analysed by Pearson R correlation test).

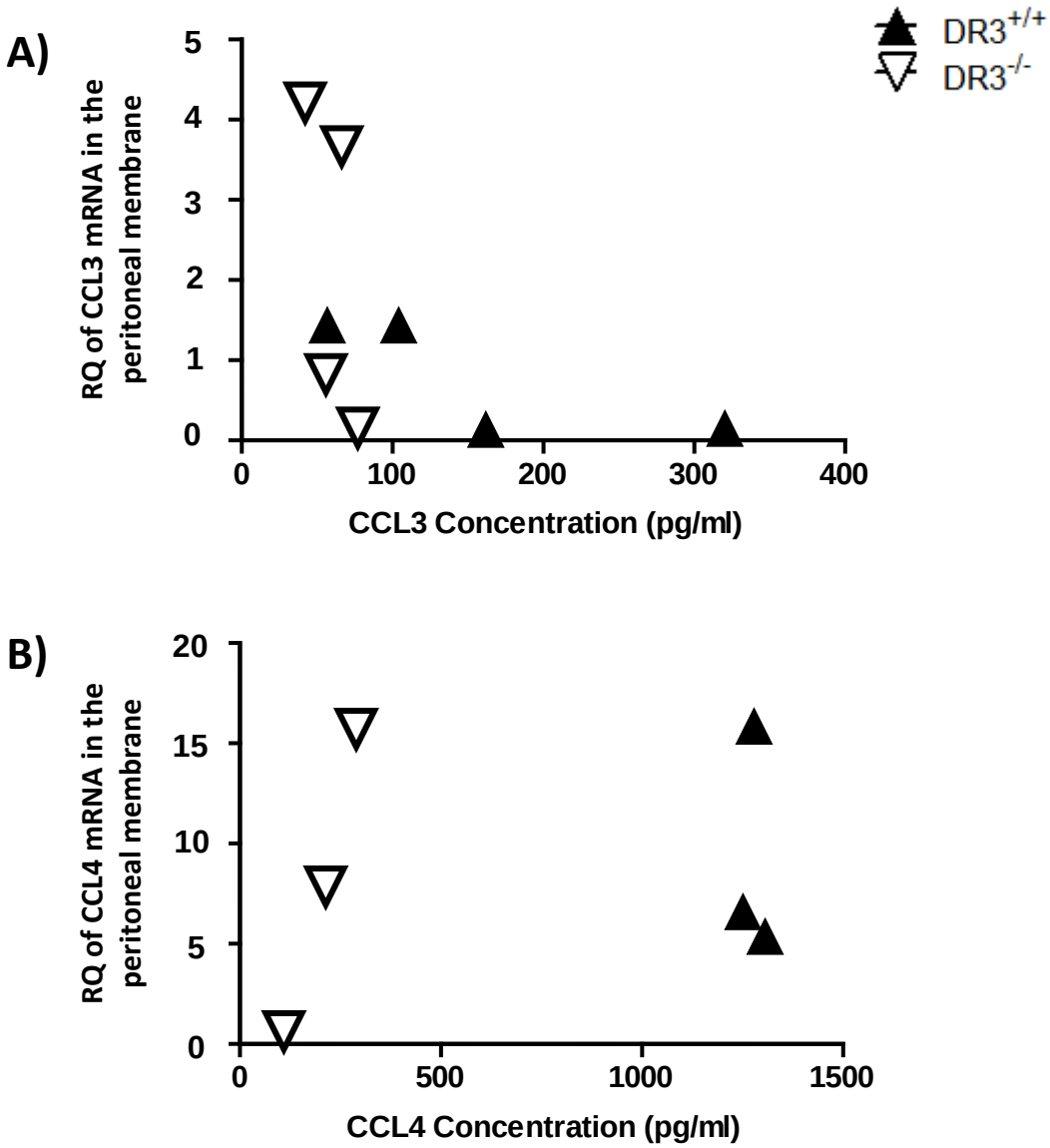

Figure 5.21 - No significant correlation was found between peak levels of CCL3 and CCL4 in the cavity and peak RQ of CCL3 and CCL4 mRNA in the peritoneal membrane of DR3$^{+/+}$ mice and DR3$^{-/-}$ mice after induction of SES inflammation. Inflammation in the cavity was induced via an i.p. injection of SES and cell free supernatants analysed for chemokine levels by ELISA. Peritoneal membranes were analysed for the RQ of chemoattractant mRNA in the membrane by qPCR. Correlation between the level of A) CCL3 and B) CCL4 in the supernatants was then plotted against the RQ of the chemoattractant mRNA found in the membrane (each symbol represents a single DR3$^{+/+}$ (▲) or DR3$^{-/-}$ mouse (▽), analysed by Pearson R correlation test).

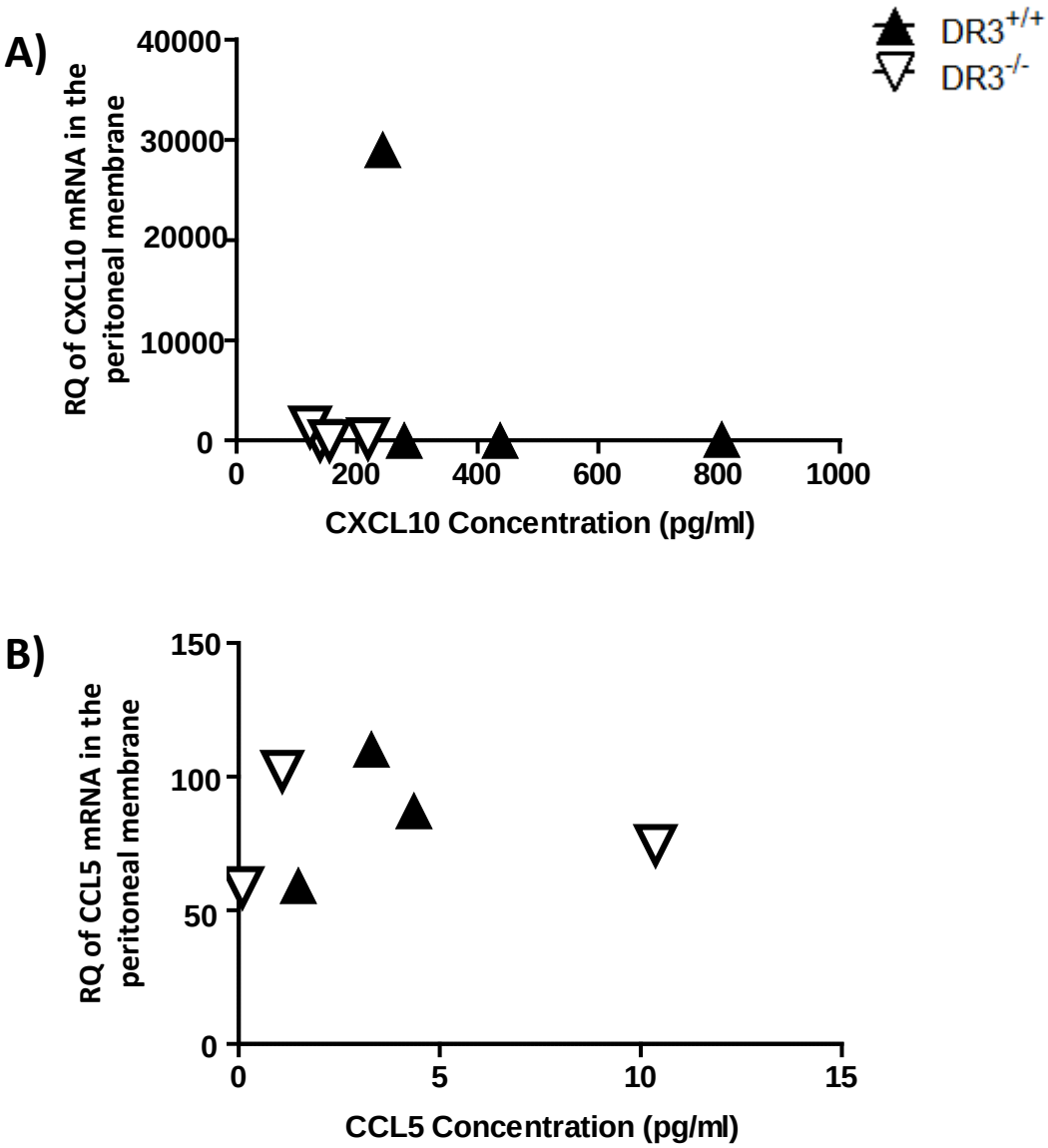

Figure 5.22 - No significant correlation was found between peak levels of CXCL10 and CCL5 in the cavity and peak RQ of CXCL10 and CCL5 mRNA in the peritoneal membrane of DR3$^{+/+}$ mice and DR3$^{-/-}$ mice after induction of SES inflammation. Inflammation in the cavity was induced via an i.p. injection of SES and cell free supernatants analysed for chemokine levels by ELISA. Peritoneal membranes were analysed for the RQ of chemoattractant mRNA in the membrane by qPCR. Correlation between the level of A) CXCL10 and B) CCL5 in the supernatants was then plotted against the RQ of the chemoattractant mRNA found in the membrane (each symbol represents a single DR3$^{+/+}$ (▲) or DR3$^{-/-}$ mouse (▽), analysed by Pearson R correlation test).

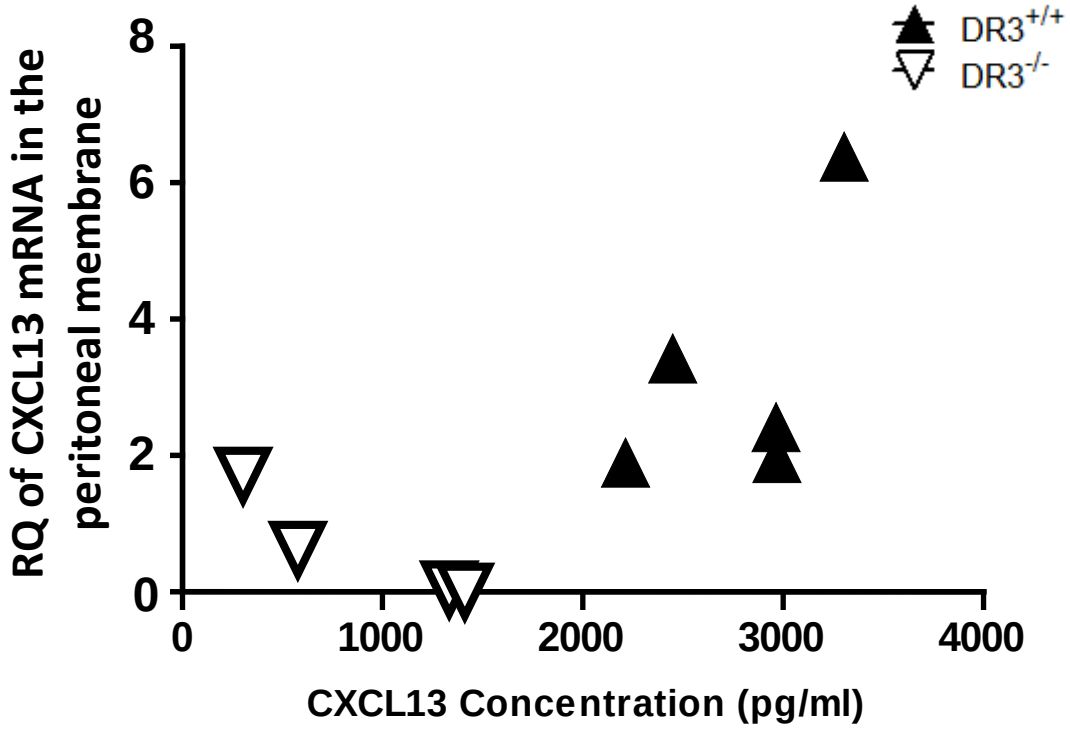

Figure 5.23 - Significant correlation was found between the peak level of CXCL13 in the cavity and peak RQ of CXCL13 mRNA in the peritoneal membrane of DR3$^{+/+}$ mice and DR3$^{-/-}$ mice after induction of SES inflammation. Inflammation in the cavity was induced via an i.p. injection of SES and cell free supernatants analysed for CXCL13 levels by ELISA. Peritoneal membranes were analysed for the RQ of CXCL13 mRNA in the membrane by qPCR. Correlation between the level of CXCL13 in the supernatants was then plotted against the RQ of CXCL13 mRNA found in the membrane (each symbol represents a single DR3$^{+/+}$ (▲) or DR3$^{-/-}$ mouse (▽), R=0.68, *p*=0.02 by Pearson R correlation test).

5.3 Summary

- DR3 is not expressed on the mesothelial layer of the peritoneal membrane during the late phase of SES induced inflammation.
- DR3 is essential in the regulation of leukocyte trafficking during the late phase of the innate immune response.
- $DR3^{-/-}$ mice had considerably reduced accumulation of selected myeloid and lymphoid subsets compared to $DR3^{+/+}$ mice.
- DR3 had no effect on the proliferation of infiltrating leukocytes in the inflamed cavity.
- Significantly lower levels of selected chemoattractants from the C-C and C-X-C families of chemokines were found in the $DR3^{-/-}$ compared to $DR3^{+/+}$ peritoneal supernatants.
- The peritoneal membrane appears to be a likely source of chemokines, which peak in the supernatants 3 hours after the induction of inflammation (except CXCL13).
- RQ of mRNA from chemokines which peak in the supernatants 3 hours after challenge are found at lower levels in the $DR3^{-/-}$ compared to $DR3^{+/+}$ membrane.
- Chemokines which peak later in the supernatants (6 hours after SES challenge) have comparable RQ of mRNA in the membrane of the 2 genotypes.
- Peak RQ of CCL2, CCL7 and CXCL13 mRNA in the peritoneal membrane was found to correlate with the maximum level of these chemoattractants found in the cavity.

Table 5.1- Summary of peritoneal cell numbers post 24 hours of SES challenge

Cell subset	Peritoneal cell numbers*			
	Time point (h)^	DR3$^{+/+}$	DR3$^{-/-}$	Significance$
Leukocytes	48	$9.1 \pm 0.9 \times 10^6$	$4.5 \pm 0.5 \times 10^6$	$p<0.01$
Neutrophils	48	$8.9 \pm 2.8 \times 10^4$	$3.7 \pm 0.9 \times 10^4$	$p<0.01$
Inflammatory Macrophages	48	$2.5 \pm 0.5 \times 10^6$	$8.3 \pm 0.9 \times 10^5$	$p<0.01$
Resident Macrophages	48	$7.2 \pm 1.6 \times 10^5$	$6.1 \pm 1.2 \times 10^5$	N.S.D
Eosinophils	48	$8.7 \pm 3.2 \times 10^5$	$2.4 \pm 0.6 \times 10^5$	$p<0.01$
T Cells	72	$8.5 \pm 3.3 \times 10^5$	$2.4 \pm 0.5 \times 10^5$	$p<0.01$
CD4$^+$ T Cells	72	$4.8 \pm 2.2 \times 10^5$	$1.5 \pm 0.3 \times 10^5$	$p<0.01$
CD8$^+$ T Cells	72	$1.6 \pm 0.7 \times 10^5$	$4.8 \pm 1.2 \times 10^4$	$p<0.01$
B Cells	72	$2.3 \pm 0.8 \times 10^6$	$8.1 \pm 1.9 \times 10^5$	$p<0.01$
Peritoneal B1 Cells	72	$1.2 \pm 0.3 \times 10^6$	$4.1 \pm 1.2 \times 10^5$	$p<0.01$
Peritoneal B2 Cells	72	$1.0 \pm 0.5 \times 10^6$	$3.1 \pm 0.8 \times 10^5$	$p<0.01$
NK Cells	48	$3.0 \pm 0.5 \times 10^5$	$2.0 \pm 0.4 \times 10^5$	N.S.D
NKT Cells	48	$1.8 \pm 0.2 \times 10^5$	$7.9 \pm 1.5 \times 10^4$	$p<0.01$

^ Peak/ noteworthy time point in the cavity during late inflammation,
* Values correspond to number of peritoneal leukocytes ± SEM (n=6),
$ Significance between two genotypes using ANOVA and Bonferonni's post hoc test, N.S.D = no significant difference.

Table 5.2- Summary of cell proliferation 48 hours after SES challenge

	Ki67^{+} Proliferation ^		
Cell subset	**DR3$^{+/+}$**	**DR3$^{-/-}$**	**Significance***
Resident macrophages	42.4 ± 13.2	44.5 ± 8.2	N.S.D
Inflammatory macrophages	43.7 ± 11.5	47.9 ± 7.7	N.S.D
T Cells	49.3 ± 2.3	50.5 ± 7.5	N.S.D
B Cells	36.9 ± 2.8	28.8 ± 8.2	N.S.D
NK Cells	35.2 ± 10.4	38.2 ± 3.8	N.S.D
NK T Cells	47.7 ± 3.8	51.8 ± 10.1	N.S.D

^ Values correspond to % proliferating cells of subsets in the peritoneal cavity 48 hours after SES challenge ± SEM (n= 5 or 6),
* Significance between two genotypes using Mann Whitney test, N.S.D = no significant difference.

Table 5.3- Summary of chemokine levels and mRNA

		Chemokine levels^				RQ of Chemokine mRNA*			Correlation~
Chemokine	Time (h)$	DR3$^{+/+}$	DR3$^{-/-}$	Significance#	Time (h)$	DR3$^{+/+}$	DR3$^{-/-}$	Significance#	
CCL2	1	1919 ± 164	524 ± 149	$p<0.01$	1	20.7 ± 6.9	2.47 ± 1.3	$p<0.01$	R=0.7, $p<0.05$
CCL3	6	162 ± 44	56 ± 7	$p<0.01$	3	0.8 ± 1.0	2.2 ± 1.0	N.S.D	N.S.D
CCL4	6	1279 ± 16	204 ± 52	$p<0.01$	3	7.0 ± 3.3	7.7 ± 3.1	N.S.D	N.S.D
CCL5	3	79 ± 9	82 ± 8	N.S.D	3	0.9 ± 0.3	3.3 ± 1.6	N.S.D	N.S.D
CCL7	1	1251 ± 345	113 ± 57	$p<0.05$	1	6.4 ± 1.8	0.9 ± 0.4	$p<0.01$	R=0.7, $p<0.05$
CXCL10	3	391 ± 111	158 ± 21	$p<0.01$	3	22.8 ± 14	11.3 ± 10.1	N.S.D	N.S.D
CXCL13	24	2801 ± 162	1014 ± 295	$p<0.01$	1	3.2 ± 0.8	0.6 ± 0.4	$p<0.05$	R=0.7, $p<0.05$

^ Values correspond to pg/ml of chemoattractants in the inflamed cavity ± SEM (n=5),
* Values correspond to relative quantity of chemokine mRNA in the peritoneal membrane ± SEM (n=5),
$ Peak/ noteworthy time point,
# Significance between two genotypes using ANOVA and Bonferonni's post hoc test, N.S.D = no significant difference,
~ Corresponds to correlation by Pearson R correlation test between pg/ml of chemoattractants and the relative quantity of chemokine mRNA in the membrane

Chapter 6 – The role of DR3 after the induction of repeated acute peritoneal inflammatory episodes

6.1 Introduction

DR3 plays an important role in the innate immune response by regulating the accumulation of specific leukocyte subsets in the peritoneal cavity after the induction of an acute inflammatory event via SES challenge, by promoting the release of certain chemoattractants (Chapter 4 and 5). This early pro-inflammatory role during the innate anti-bacterial immune response and inferior control of bacteria and viruses in $DR3^{-/-}$ mice (Buchan, Taraban et al. 2012; Twohig, Marsden et al. 2012) indicate that the DR3/TL1A pathway is important for immunity to pathogens, but contrasts with its reported damaging role in the acquired immune response during chronic inflammation.

Chronic inflammatory models have found DR3 to play a significant role in promoting the number of inflammatory leukocytes at localised sites of inflammation (Bamias, Martin et al. 2003; Meylan, Davidson et al. 2008) as well as supporting differentiation (Bull, Williams et al. 2008), proliferation (Pappu, Borodovsky et al. 2008) and/or maintenance (Jones, Stumhofer et al. 2011) of many of these infiltrating leukocytes. Currently, the influence of DR3 expression during recurrent inflammatory episodes in the peritoneal cavity has not been studied.

Recurrent peritoneal inflammation can be induced by 4 i.p. injections of SES, once per week for 4 weeks. Multiple peritoneal inflammatory events have previously been shown to induce aberrant inflammation causing damage to the morphology membrane resulting in tissue fibrosis (Davies, Bryan et al. 1996; Selgas, Bajo et al. 2006) which is a typical feature of disease (Wynn 2007).

This chapter aims to investigate the role of DR3 in driving fibrosis as a consequence of repeated episodes of acute SES-driven peritoneal inflammation.

6.2 Results

6.2.1 The effect of repeated inflammatory episodes of SES on total mouse leukocyte numbers in $DR3^{+/+}$ and $DR3^{-/-}$ peritoneal cavities

After the induction of recurrent peritoneal inflammation (4xSES) mice were maintained until the endpoint of the experiment, 49 days after the first injection (Section 2.2.6.2). Leukocyte accumulation in $DR3^{+/+}$ and $DR3^{-/-}$ peritoneal cavities during recurrent inflammation was also compared to the number of leukocytes in the unchallenged (Naive) cavity (unchallenged mice maintained for 49 days) and after induction of acute inflammation (1xSES) (single i.p. injection of SES and mice maintained until endpoint, 49 days after injection). No differences were observed in the total number of leukocytes after multiple SES injections (4xSES) in the $DR3^{-/-}$ cavity ($3.6 \pm 0.3 \times 10^6$ total cells) compared to $DR3^{+/+}$ mice ($3.6 \pm 0.4 \times 10^6$ total cells). Comparable leukocyte numbers after repeated inflammatory episodes (4xSES) were also found at the endpoint (49 days) after the induction of either no (Naive) ($DR3^{+/+}$ mice $3.2 \pm 0.4 \times 10^6$, $DR3^{-/-}$ mice $3.3 \pm 0.8 \times 10^6$ total cells) or acute SES inflammation (1xSES) ($DR3^{+/+}$ mice $3.5 \pm 0.3 \times 10^6$, $DR3^{-/-}$ mice $3.0 \pm 0.3 \times 10^6$ total cells) (Figure 6.1).

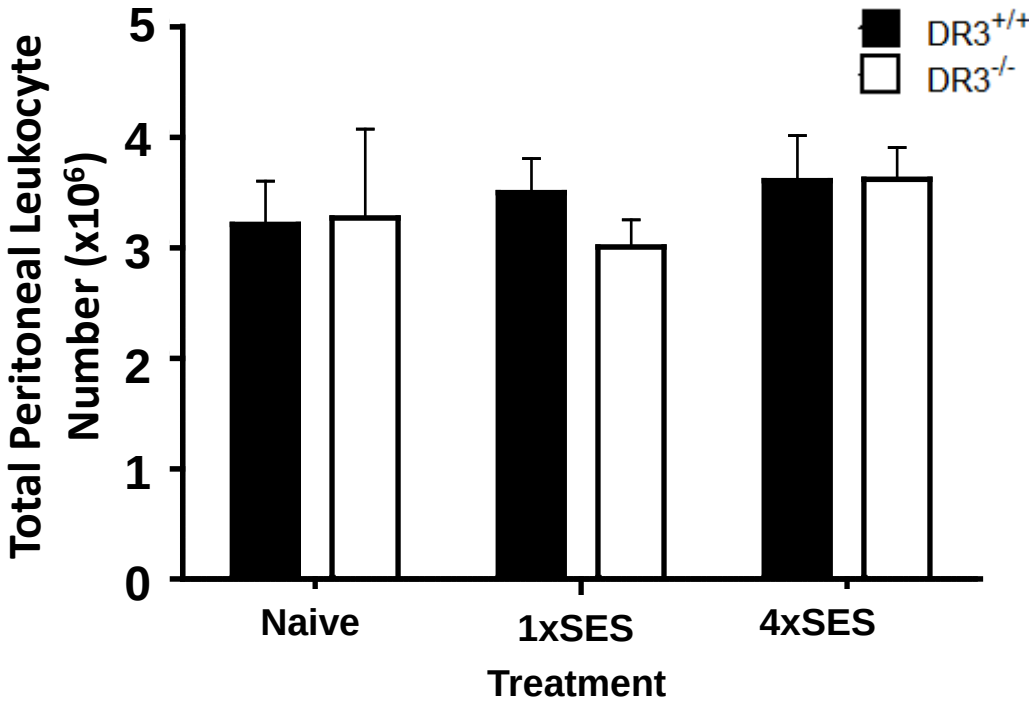

Figure 6.1 - No significant differences were seen in total peritoneal leukocyte numbers in DR3$^{+/+}$ mice and DR3$^{-/-}$ mice after repeated induction of SES inflammation. Mice received either no challenge (Naive), a single injection of SES (1xSES) or repeated episodes of SES induced inflammation (4xSES) and were aged for 49 days from the start of the experiment. Peritoneal leukocytes were isolated from the cavity by lavage, total cell number was calculated using a Beckman Coulter counter Z2 (each bar represents mean of n=5 DR3$^{+/+}$ (■) and DR3$^{-/-}$ mice (□) per treatment group, error bars correspond to mean ± SEM, N.S.D by t-test).

6.2.2 The effect of repeated inflammatory episodes of SES on myeloid cell subset numbers in DR3$^{+/+}$ and DR3$^{-/-}$ peritoneal cavities

Although absence of DR3 did not affect the total number of cells in the cavity after the induction of recurrent peritoneal inflammation (acute inflammation or without challenge), numbers of different leukocyte subsets were examined to determine if there were alterations in the composition of infiltrating leukocytes after 49 days. At the endpoint DR3$^{-/-}$ and DR3$^{+/+}$ mice were found to have equivalent numbers of macrophages (Figure 6.2A) and eosinophils (Figure 6.2B) after induction of recurrent inflammation and in all other treatment groups (Table 6.1). Increased macrophage numbers were seen in the cavities of both DR3$^{+/+}$ and DR3$^{-/-}$ after the induction of recurrent inflammation (4xSES) but this was not significantly different compared to the numbers found in the naive cavity (Figure 6.2A).

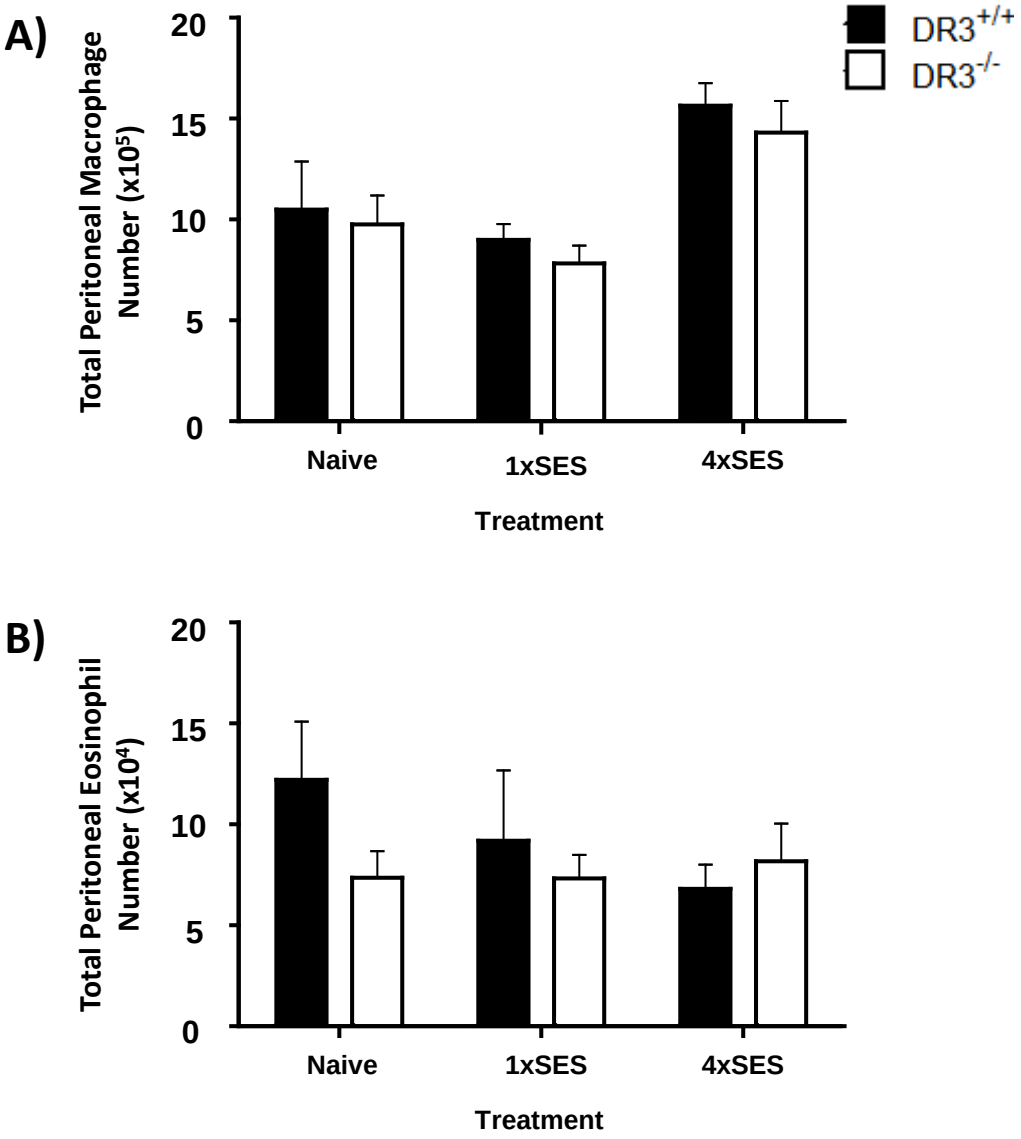

Figure 6.2 - No significant differences were seen in the numbers of myeloid subsets in the peritoneal cavity of DR3$^{+/+}$ mice compared to DR3$^{-/-}$ mice after repeated induction of SES inflammation. Mice received either no challenge (Naive), a single injection of SES (1xSES) or repeated episodes of SES induced inflammation (4xSES) and were aged for 49 days from the start of the experiment. Peritoneal leukocytes were isolated from the cavity by lavage. A) Macrophages, were identified by a CD11b^{+} F4/80^{+}, MHC II^{int} phenotype and B) Eosinophils identified by F4/80^{int}, CD11b^{int} and their forward and side scatter properties. Subset numbers calculated by percentage proportion of total leukocytes, determined using a Beckman Coulter counter Z2 (each bar represents mean of n=5 DR3$^{+/+}$ mice (■) and DR3$^{-/-}$ mice (□) per treatment group, error bars correspond to mean ± SEM, N.S.D by t-test).

6.2.3 The effect of repeated inflammatory episodes of SES on lymphocyte cell subset numbers in $DR3^{+/+}$ and $DR3^{-/-}$ peritoneal cavities

After 49 days, $DR3^{-/-}$ and $DR3^{+/+}$ mice had similar numbers of T cells (Figure 6.3A) including $CD4^{+}$ (Figure 6.3B) and $CD8^{+}$ (Figure 6.3C) subsets, after repeated injections of SES and in all other treatment groups. Comparable numbers of B cells (Figure 6.4A) including B1 (Figure 6.4B) and B2 (Figure 6.4C) subsets, were also found between the two genotypes in all experimental groups, as well as analogous numbers of NK (Figure 6.5A) and NKT cells (Figure 6.5B) (Table 6.1).

Therefore at the endpoint of the experiment, no significant differences were observed between the number or composition of peritoneal leukocytes in $DR3^{-/-}$ mice compared to $DR3^{+/+}$ mice.

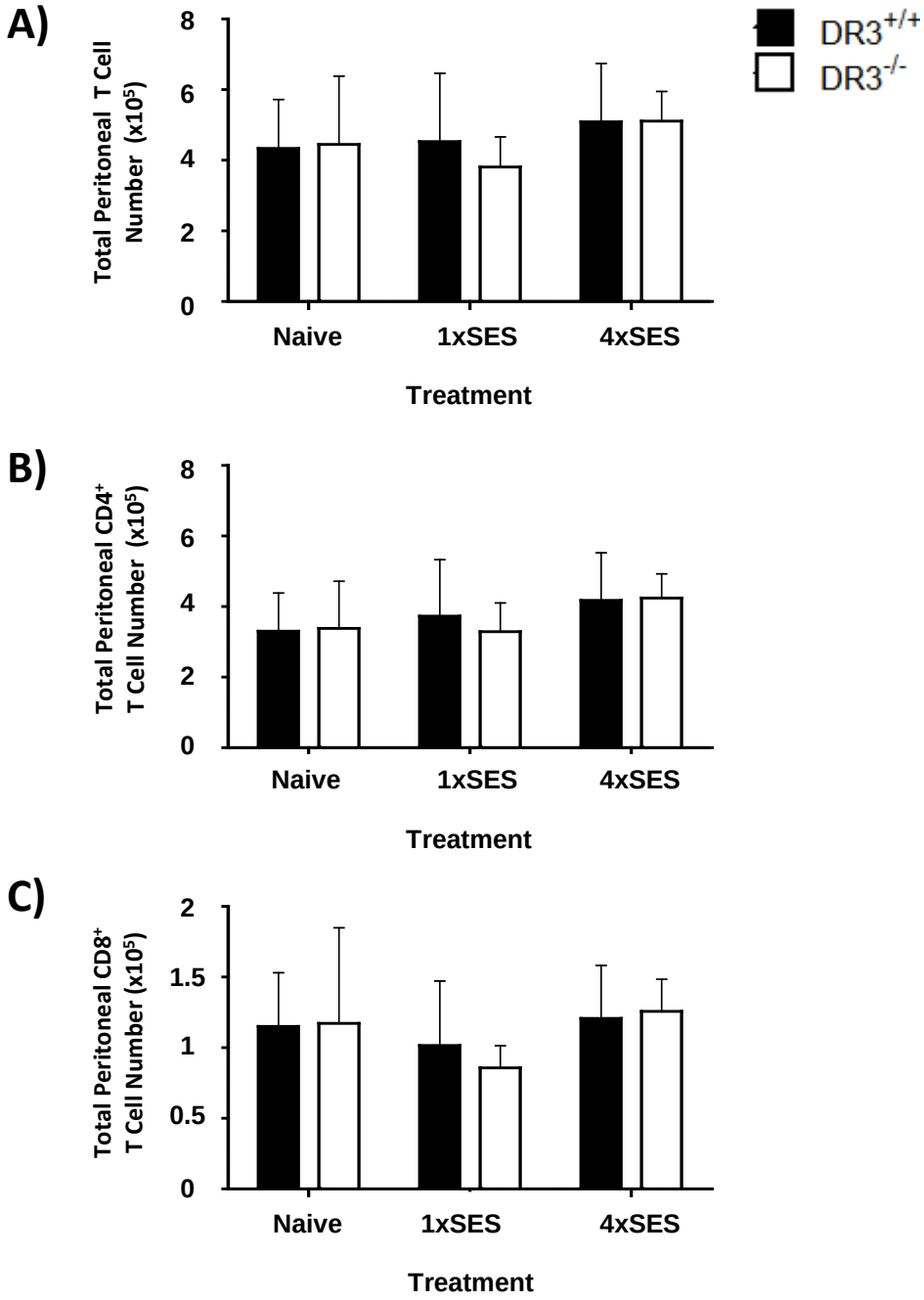

Figure 6.3 - No significant differences were seen in the numbers of T cell subsets in the peritoneal cavity of DR3$^{+/+}$ mice compared to DR3$^{-/-}$ mice after repeated induction of SES inflammation. Mice received either no challenge (Naive), a single injection of SES (1xSES) or repeated episodes of SES induced inflammation (4xSES) and were aged for 49 days from the start of the experiment. Peritoneal leukocytes were isolated from the cavity by lavage. A) T cells were identified by a CD3$^+$, TCRαβ$^+$ phenotype, B) T helper cells were identified by a CD3$^+$ CD4$^+$, TCRαβ$^+$ phenotype and C) T cytotoxic cells identified by a CD3$^+$ CD8$^+$, TCRαβ$^+$ phenotype. Subset numbers calculated by percentage proportion of total leukocytes, determined using a Beckman Coulter counter Z2 (each bar represents mean of n=5 DR3$^{+/+}$ mice (■) and DR3$^{-/-}$ mice (□) per treatment group, error bars correspond to mean ± SEM, N.S.D by t-test).

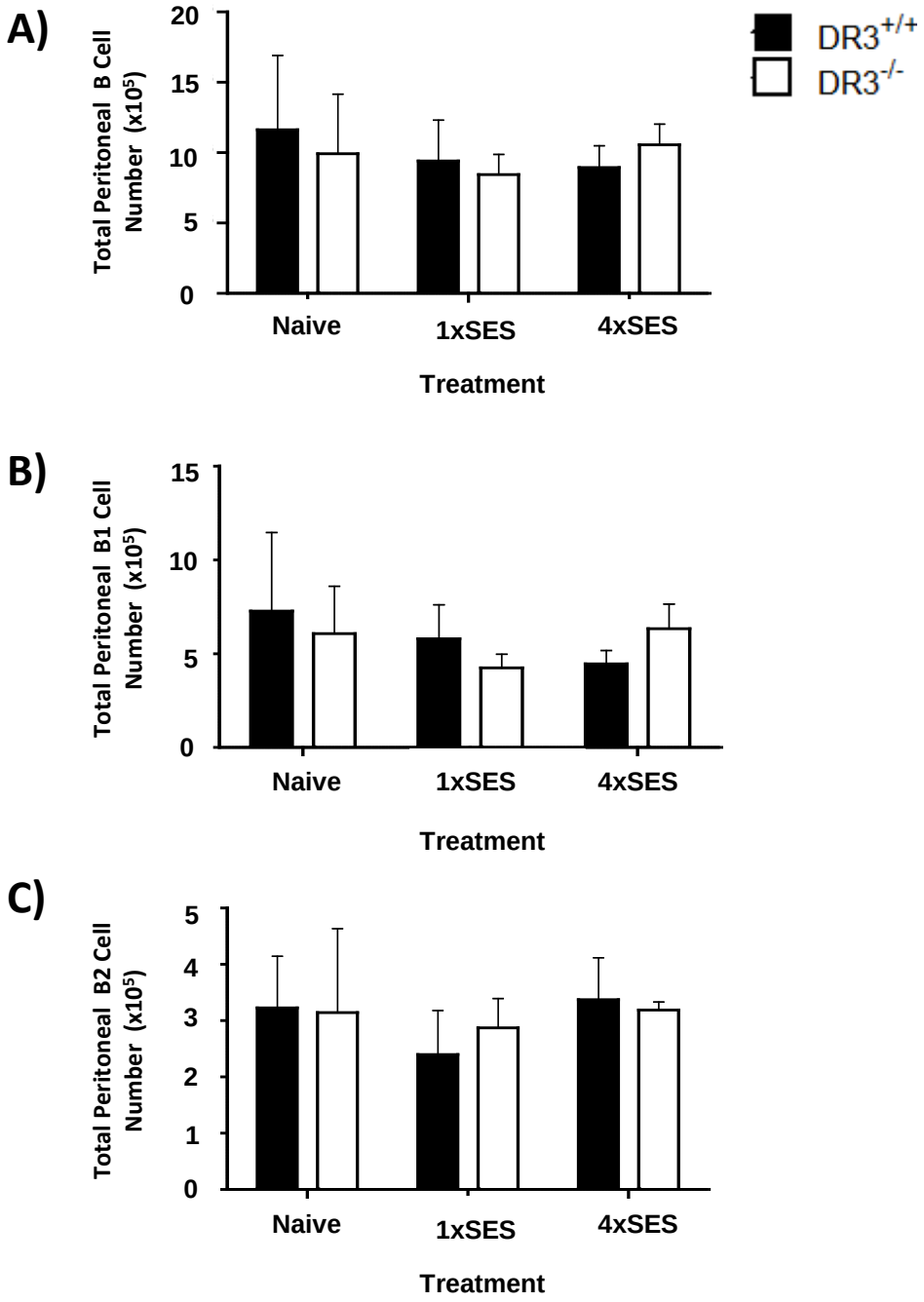

Figure 6.4 - No significant differences were seen in the numbers of B cell subsets in the peritoneal cavity of DR3$^{+/+}$ mice compared to DR3$^{-/-}$ mice after repeated induction of SES inflammation. Mice received either no challenge (Naive), a single injection of SES (1xSES) or repeated episodes of SES induced inflammation (4xSES) and were aged for 49 days from the start of the experiment. A) B cells were identified by a CD19^{+}, B220^{+} phenotype, B) Resident B1 cells were identified by a CD19^{+} B220^{int}, CD11b^{int} phenotype and C) Infiltrating B2 cells identified by a CD19^{+} B220^{+}, CD11b^{-} phenotype. Subset numbers calculated by percentage proportion of total leukocytes, determined using a Beckman Coulter counter Z2 (each bar represents mean of n=5 DR3$^{+/+}$ mice (■) and DR3$^{-/-}$ mice (□) per treatment group, error bars correspond to mean ± SEM, N.S.D by t-test).

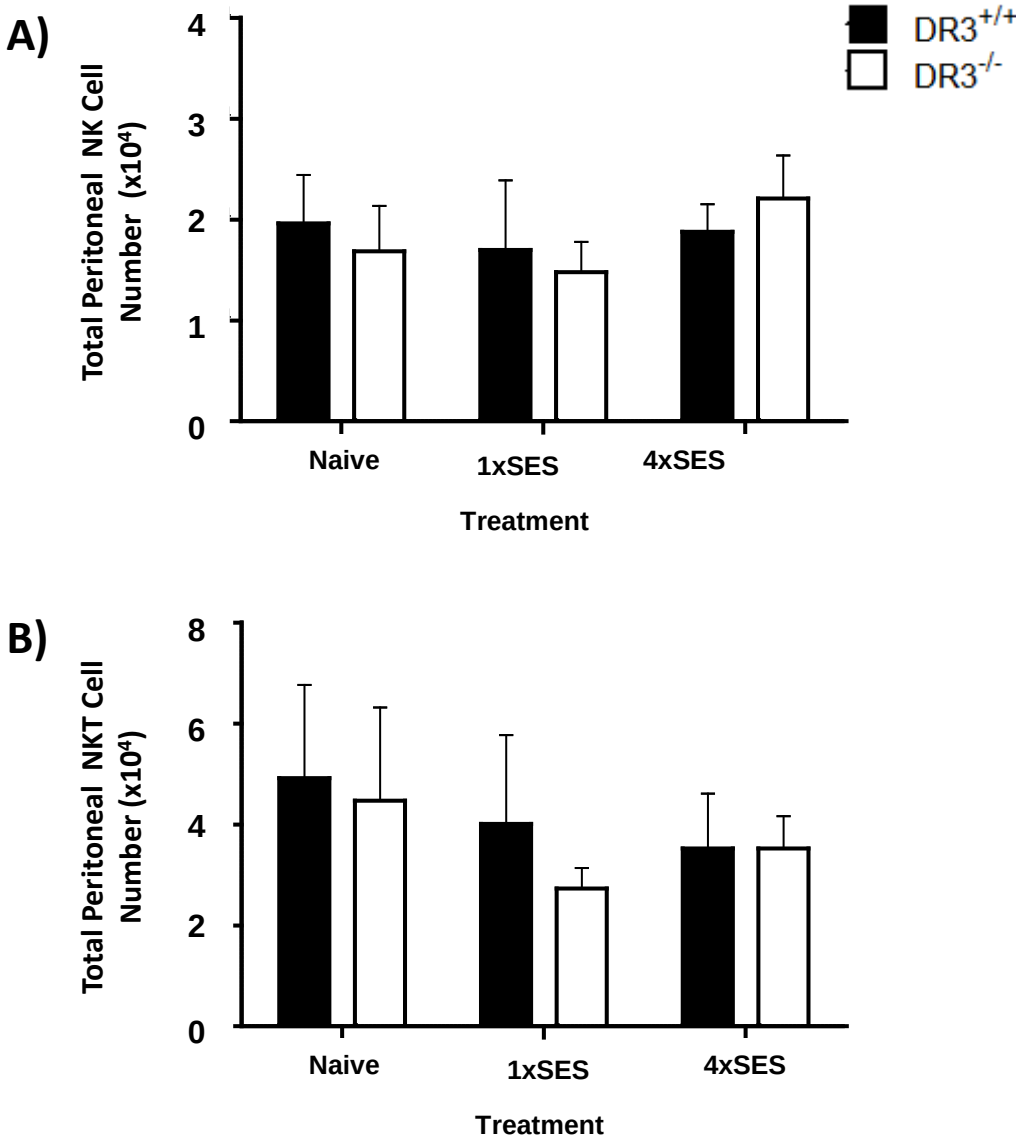

Figure 6.5 No significant differences were seen in the numbers of NK and NKT cells in the peritoneal cavity of DR3$^{+/+}$ mice compared to DR3$^{-/-}$ mice after repeated induction of SES inflammation. Mice received either no challenge (Naive), a single injection of SES (1xSES) or repeated episodes of SES induced inflammation (4xSES) and were aged for 49 days from the start of the experiment. A) NK cells were identified by a NK1.1^{+}, TCRαβ^{-} phenotype. B) NKT cells were identified by a NK1.1^{+}, TCRαβ^{+} phenotype. Subset numbers calculated by percentage proportion of total leukocytes, determined using a Beckman Coulter counter Z2 (each bar represents mean of n=5 DR3$^{+/+}$ mice (■) and DR3$^{-/-}$ mice (□) per treatment group, error bars correspond to mean ± SEM, N.S.D by t-test).

6.2.4 Histological changes to the peritoneal membrane after repeated inflammatory episodes of SES in DR3$^{+/+}$ and DR3$^{-/-}$ peritoneal cavities

Despite the fact that an absence of DR3 did not affect the quantity or constitution of cells residing in the cavity after the induction of recurrent inflammation, the mesothelial layer of the peritoneal membrane was examined to investigate if a deficiency in DR3 affected its morphology. The mesothelial layer is a thin layer of cells found on top of a layer of muscle tissue within the peritoneal membrane. The thickness of this layer in DR3$^{+/+}$ and DR3 $^{-/-}$ mice was measured at multiple points along the membrane at the endpoint of the experiment. Comparable mesothelial layer thickness was recorded between DR3$^{+/+}$ and DR3 $^{-/-}$ mice in the naive (DR3$^{+/+}$ mice 18.6 ± 1.3 μm, DR3$^{-/-}$ mice 21.1 ± 1.3 μm) and acute inflammatory groups (1xSES) (DR3$^{+/+}$ mice 19.1 ± 1.5 μm, DR3$^{-/-}$ mice 20.7 ± 1.5 μm) (Figure 6.6 and 6.7). The mesothelial layer of DR3$^{+/+}$ mice (30.2 ± 2.9 μm) was found to have undergone significant thickening after the induction of repeated inflammation (4xSES) (p<0.01), while the DR3$^{-/-}$ mesothelial layer was protected from this type of fibrosis (18.2 ± 0.7 μm), closely resembling the morphology of the naive membrane (Figure 6.6 and 6.7).

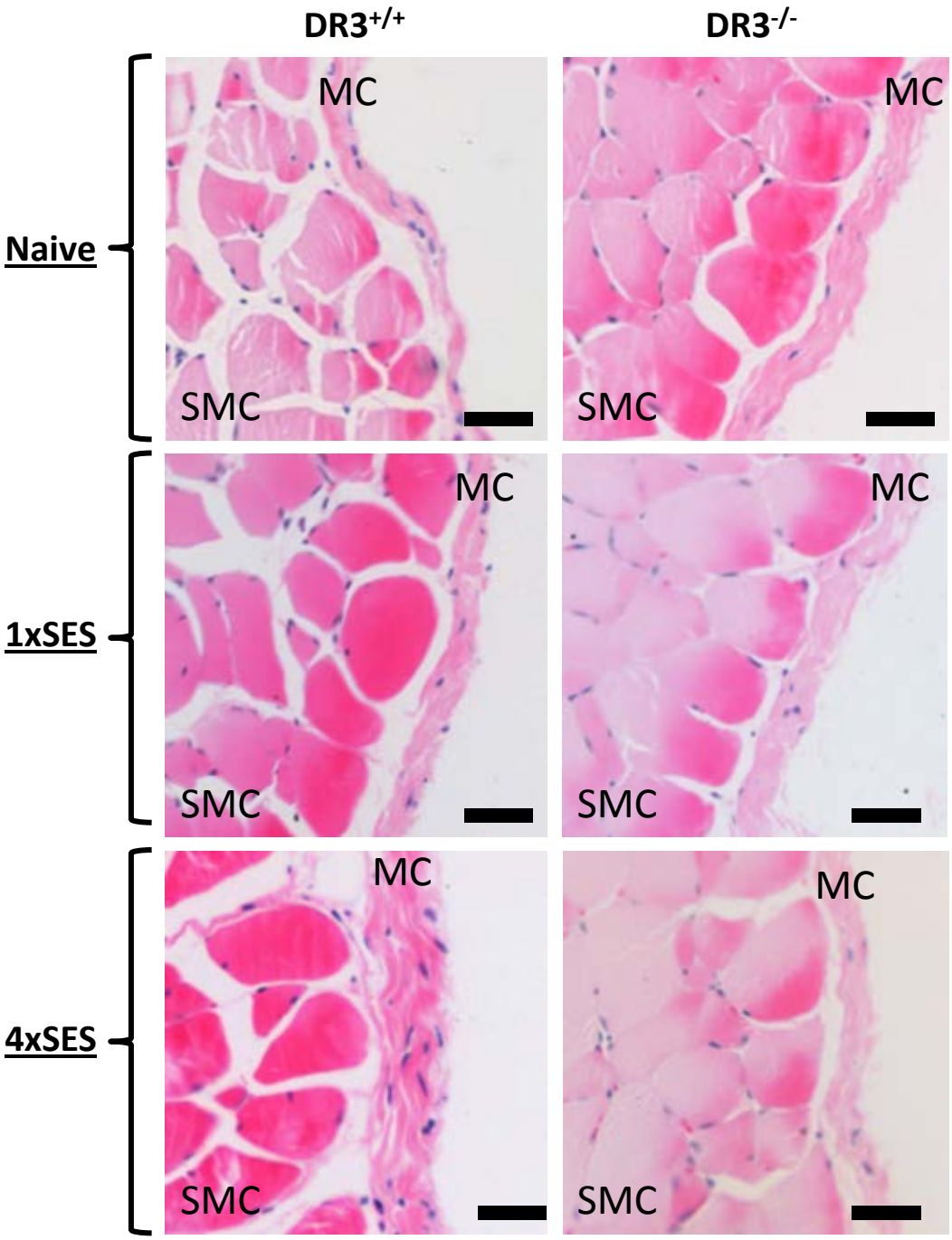

Figure 6.6 - Significant thickening of the mesothelial layer was found in the peritoneal membrane of DR3$^{+/+}$ mice after repeated induction of SES inflammation. Mice received either no challenge (Naive), a single injection of SES (1xSES) or repeated episodes of SES induced inflammation (4xSES) and were aged for 49 days from the start of the experiment. Haematoxylin and eosin stained membrane slides were viewed using Qwin V3 software on a Leica microscope. Pictures were also taken using the Leica microscope (Bar corresponds to 25μm, MC- mesothelial cell layer, SMC- sub mesothelial compact zone).

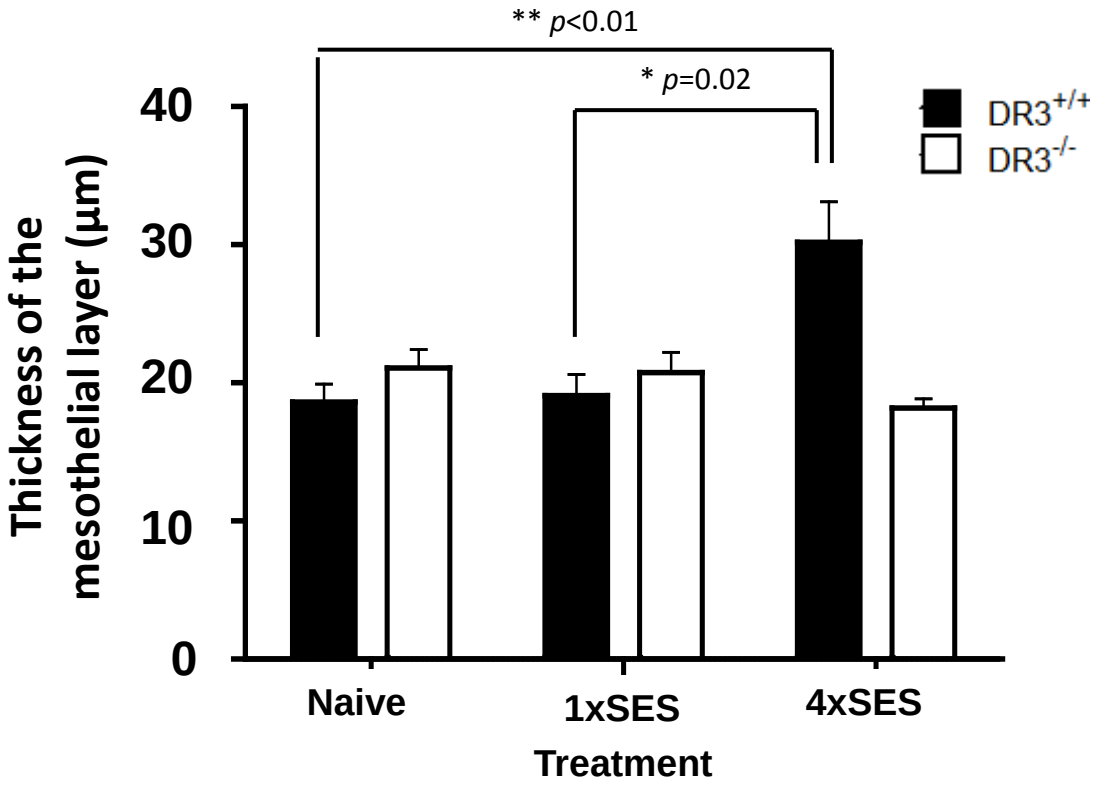

Figure 6.7 - Significant thickening of the mesothelial layer was found in the peritoneal membrane of DR3$^{+/+}$ mice compared to DR3$^{-/-}$ mice after repeated induction of SES inflammation. Mice received either no challenge (Naive), a single injection of SES (1xSES) or repeated episodes of SES induced inflammation (4xSES) and were aged for 49 days from the start of the experiment. Stained membrane slides were analysed by measuring the width of the membrane at multiple points using Qwin V3 software on a Leica microscope. Pictures were also taken using the Leica microscope (each bar represents mean of n=5 DR3$^{+/+}$ mice (■) and DR3$^{-/-}$ mice (□) per treatment group, error bars correspond to mean ± SEM, analysed by t-test).

6.3 Summary

- No significant differences were observed in either the number of leukocytes in the cavity of the 2 genotypes or between the 3 experimental groups (Naive, 1xSES and 4xSES).
- Significant fibrosis of the $DR3^{+/+}$ peritoneal membrane was observed 49 days after repeated induction of inflammation. Fibrosis of the membrane was confirmed to be associated with the induction of multiple inflammatory events as opposed to an acute SES inflammatory episode.
- The mesothelial layer of the $DR3^{-/-}$ membrane was not susceptible to any fibrotic thickening even after the induction of multiple inflammatory events.

Table 6.1- Summary of peritoneal cell numbers

Cell subset*	Naive^		1xSES$		4xSES#	
	DR3$^{+/+}$	DR3$^{-/-}$	DR3$^{+/+}$	DR3$^{-/-}$	DR3$^{+/+}$	DR3$^{-/-}$
Leukocytes	$3.2 \pm 0.4 \times 10^6$	$3.3 \pm 0.8 \times 10^6$	$3.5 \pm 0.3 \times 10^6$	$3.0 \pm 0.3 \times 10^6$	$3.6 \pm 0.4 \times 10^6$	$3.6 \pm 0.3 \times 10^6$
Macrophages	$1.0 \pm 0.2 \times 10^6$	$9.8 \pm 1.4 \times 10^5$	$9.0 \pm 0.8 \times 10^5$	$7.8 \pm 0.9 \times 10^5$	$1.6 \pm 0.1 \times 10^6$	$1.4 \pm 0.2 \times 10^6$
Eosinophils	$1.2 \pm 0.3 \times 10^5$	$7.4 \pm 1.3 \times 10^4$	$9.2 \pm 3.5 \times 10^4$	$7.3 \pm 1.2 \times 10^4$	$6.8 \pm 1.2 \times 10^4$	$8.2 \pm 1.9 \times 10^4$
T Cells	$4.3 \pm 1.4 \times 10^5$	$4.4 \pm 1.9 \times 10^5$	$4.5 \pm 1.9 \times 10^5$	$3.8 \pm 0.9 \times 10^5$	$5.1 \pm 1.7 \times 10^5$	$5.1 \pm 0.8 \times 10^5$
CD4$^+$ T Cells	$3.3 \pm 1.1 \times 10^5$	$3.4 \pm 1.3 \times 10^5$	$3.7 \pm 1.6 \times 10^5$	$3.3 \pm 0.8 \times 10^5$	$4.2 \pm 1.3 \times 10^5$	$4.2 \pm 0.7 \times 10^5$
CD8$^+$ T Cells	$1.2 \pm 0.4 \times 10^5$	$1.2 \pm 0.7 \times 10^5$	$1.0 \pm 0.5 \times 10^5$	$8.6 \pm 1.6 \times 10^4$	$1.2 \pm 0.4 \times 10^5$	$1.3 \pm 0.2 \times 10^5$
B Cells	$1.2 \pm 0.5 \times 10^6$	$9.9 \pm 4.2 \times 10^5$	$9.4 \pm 2.9 \times 10^5$	$8.4 \pm 1.4 \times 10^5$	$8.9 \pm 1.5 \times 10^5$	$1.1 \pm 0.2 \times 10^6$
Peritoneal B1 Cells	$7.3 \pm 4.2 \times 10^5$	$6.1 \pm 2.5 \times 10^5$	$5.8 \pm 1.8 \times 10^5$	$4.2 \pm 0.7 \times 10^5$	$4.5 \pm 0.7 \times 10^5$	$6.3 \pm 1.3 \times 10^5$
Peritoneal B2 Cells	$3.2 \pm 0.9 \times 10^5$	$3.1 \pm 1.5 \times 10^5$	$2.4 \pm 0.8 \times 10^5$	$2.9 \pm 0.5 \times 10^5$	$3.4 \pm 0.8 \times 10^5$	$3.2 \pm 0.1 \times 10^5$
NK Cells	$2.0 \pm 0.5 \times 10^4$	$1.7 \pm 0.5 \times 10^4$	$1.7 \pm 0.7 \times 10^4$	$1.5 \pm 0.3 \times 10^4$	$1.9 \pm 0.3 \times 10^4$	$2.2 \pm 0.4 \times 10^4$
NKT Cells	$4.9 \pm 1.8 \times 10^4$	$4.5 \pm 1.7 \times 10^4$	$4.0 \pm 1.8 \times 10^4$	$2.7 \pm 0.4 \times 10^4$	$3.5 \pm 1.1 \times 10^4$	$3.5 \pm 0.6 \times 10^4$

* Values correspond to number of peritoneal leukocytes ± SEM, no significant difference was found either between genotypes or experimental groups in any cell subset tested by t-test,

^ Peritoneal leukocytes in the unchallenged cavity collected after 49 days (n=5),

$ Peritoneal leukocytes in the cavity 49 days after a single SES injection (n=5),

Peritoneal leukocytes in the cavity following 1 SES injection per week for 4 weeks, leukocytes collected 49 days after first injection (n=5).

Chapter 7 – General Discussion

7.1 Discussion

Findings presented in this thesis highlight a non-redundant role for TL1A interaction with stromal DR3 in promoting a pro-inflammatory phenotype, via the downstream release of chemoattractants after the induction of acute inflammation which effect; (i) the accumulation of neutrophils (Figure 7.1), inflammatory myeloid cells (Figure 7.2) and B cells and (ii) the indirect influx of selected lymphocyte subsets (Figure 7.3). Results in this thesis also identify a non-redundant role of DR3 in supporting peritoneal membrane fibrosis after repeated inflammatory events.

Findings are summarised in bullet points for each section before being more fully discussed thereafter:

7.1.1 DR3 expression patterns

- DR3 was found on the mesothelial layer of the naive peritoneal membrane; its expression fluctuated after SES induced inflammation.
- DR3 was found on naive T cells; higher levels of expression were detected on $CD4^+$ T cells compared to $CD8^+$ T cells.
- Expression on these different T cell subsets altered following SES challenge with $CD4^+$ T cells maintaining levels throughout the inflammatory time course, but $CD8^+$ T cells losing expression.
- Both naive and challenged NKT cells expressed DR3.
- No specific DR3 expression was detected on NK cells before or after SES challenge.

- No shift in signal could be detected in $DR3^{+/+}$ myeloid or B cells compared to those from $DR3^{-/-}$ mice.

Although DR3 expression was originally reported to be restricted to lymphocytes (Marsters, Sheridan et al. 1998), more recent papers have described DR3 expression on stromal surfaces, including vascular endothelial (VECs) and tubular epithelial cells (TECs) in human renal samples (Al-Lamki, Wang et al. 2003) and healthy and psoriatic skin (Bamias, Evangelou et al. 2011). However, DR3 expression patterns in each tissue seem distinct.

In this thesis, DR3 expression was found on the naive peritoneal membrane and varied after SES challenge (no longer detected at 6 hours; returning to even higher levels at 12 hours before disappearing again by 24, Figure 4.4), whereas no DR3 was found on VECs and TECs in human renal tissue until after induction of acute cellular rejection or ischaemic injury. Arguably the most similar pattern of stromal DR3 expression to the peritoneal membrane is found in human skin where DR3 is constitutively expressed in healthy subjects, but increases in psoriasis patients (Bamias, Evangelou et al. 2011).

The variation in DR3 expression on tissue surfaces may be due to different tissue-specific functions of DR3, however, the immunofluorescence and IHC imaging techniques used in all these studies cannot differentiate between DR3 splice variants (which will be discussed later in this section).

Membrane-bound DR3 expression was observed on mouse peritoneal T cells by flow cytometry, which is in agreement with previous reports from the mouse spleen (Fang, Adkins et al. 2008; Twohig, Marsden et al. 2012) and in the human system

e.g. IBD patient intestinal lamina propria (Bamias, Martin et al. 2003). Interestingly, mDR3 expression was found at lower levels on $CD8^+$ T cells compared to $CD4^+$ T cells, which is also in agreement with previous studies (Fang, Adkins et al. 2008; Twohig, Marsden et al. 2012) suggesting DR3 expression on these subsets may be differentially regulated.

Detection of DR3 was found on mouse peritoneal NKT cells (Figure 4.6B) and is in agreement with reports from the spleen (Twohig, Marsden et al. 2012) and lymph nodes (Fang, Adkins et al. 2008). Expression has also been reported on NKT cells isolated from human peripheral blood monocytes (PBMCs) (Papadakis, Prehn et al. 2004). However a non-specific signal was found on $DR3^{-/-}$ NKT cells (Figure 3.19), which was not observed in other investigations using this polyclonal reagent (Twohig, Marsden et al. 2012) or reports from other laboratories using their own monoclonal antibody (mAb) (Fang, Adkins et al. 2008). Potential explanations for this could be partial failure of the blocking step when staining cells for flow cytometry or alternatively, variation between different batches of the polyclonal reagent.

No specific signal for membrane-bound DR3 was observed on naive mouse NK cells or at any point after challenge with SES (Figure 4.6A), which is in agreement with work by Twohig et al. (2012), but is in contrast to Fang et al. (2008), who detected DR3 expression on a subpopulation of NK cells in the spleen and lymph node using their in-house mAb. However, similar to NKT cells, a non-specific signal was detected on $DR3^{-/-}$ NK cells as well as with the isotype control. This signal is most likely due to failure in the blocking procedure, resulting in non-specific binding to Fc receptors on NK cells.

No DR3-specific shifts were observed in $DR3^{+/+}$ myeloid and B cells compared to the $DR3^{-/-}$ and isotype control (Figure 3.20), suggesting that either; (i) DR3 is not present on these cell subsets, (ii) the DR3 specific positive signal is being masked by the autofluorescent properties of these cell subsets (Lohmeyer, Friedrich et al. 1994; Weyde, Wassermann et al. 1997) or (iii) non-specific binding of the polyclonal antibody. To date little work has been carried out on mouse DR3 expression on myeloid or B cells, however recent human studies have shown DR3 expression on B cells, stimulated with anti-IgM for 24 hours (Cavallini, Lovato et al. 2013) and myeloid cells including; THP1 cells (a human peripheral blood monocyte cell line), which constitutively express DR3 (Kang, Kim et al. 2005; McLaren, Calder et al. 2010) and PBMCs stimulated with LPS (Kang, Kim et al. 2005). Thus although no DR3 expression was detected on mouse myeloid and B cells in this study, findings in humans suggest DR3 is expressed on these cell subsets. It would be interesting to extend qPCR/RT-PCR techniques currently being used to profile different DR3 isoforms on T cells to other cell types that may have the potential to express DR3, overcoming possible limitations of flow cytometry using the polyclonal antibody discussed above.

Ideally a range of DR3 monoclonal antibodies of known specificity would be beneficial to standardise detection of DR3, removing; (i) potential inconsistencies between batches of the commercially available polyclonal antibody and (ii) differentiate between the expression patterns of separate DR3 isoforms, providing a better measure than current techniques (qPCR or RT-PCR) by avoiding post-translational artefacts of DR3 gene expression. In mouse, splice variants include variant 1 (full-length membrane-bound), variant 2 (soluble form) and variant 3 (truncated membrane-bound) (Wang, Kitson et al. 2001). Recent work examining

DR3 mRNA has shown activation-induced differential regulation for different isoforms on T cell subsets. DR3 expression has also been found on activated and differentiated $CD4^+$ T cells which have differentiated into Th1 (Bamias, Martin et al. 2003), Th2 (Fang, Adkins et al. 2008), Th17 (Pappu, Borodovsky et al. 2008) and Treg (Schreiber, Wolf et al. 2010) subsets. Naive T cells were found to have low levels of variants 1 and 3, which were replaced by much higher levels of variants 1 and 2 after stimulating with peptide (Bamias, Mishina et al. 2006; Twohig, Marsden et al. 2012). High levels of variant 3 have been found on Tregs contrasting with predominantly variant 1 on Th17 cells (Pappu, Borodovsky et al. 2008). Addition of an agonistic DR3 antibody (Schreiber, Wolf et al. 2010) or a soluble TL1A fusion protein (Khan, Tsai et al. 2013) has been shown to induce Treg expansion, which can then be maintained by daily injections of the TL1A fusion protein (Khan, Tsai et al. 2013). Further, mice that constitutively express TL1A were found to promote *in vivo* Treg activation and *in vitro* expansion, however greater TL1A driven Th17 and Th2 phenotypes overcame Treg suppressive effects resulting in disruption of normal function in the intestine (Shih, Barrett et al. 2011; Taraban, Slebioda et al. 2011). Thus differential regulation of DR3 isoforms may alter the functional response of these subsets and underlines the importance of further understanding the expression profile of these isoforms, which may place current conflicting DR3 findings into context.

It is tempting to draw comparisons between human and mouse systems, however up to 13 DR3 isoforms (10 membrane-bound, 3 soluble) have been reported in man (Kitson, Raven et al. 1996; Screaton, Xu et al. 1997; Warzocha, Ribeiro et al. 1998). DR3's function in humans is further complicated by a decoy receptor (DcR3), which has no mouse homologue and binds 2 other TNFSF members in addition to TL1A;

FasL (Pitti, Marsters et al. 1998) and LIGHT (Yu, Kwon et al. 1999). Some studies have speculated sDR3 in mice may fulfil a similar role to DcR3 (Bamias, Mishina et al. 2006; Pappu, Borodovsky et al. 2008) however actual function has not been investigated and does not explain the continued presence of sDR3 isoforms in humans in addition to DcR3 (Screaton, Xu et al. 1997).

The first identified role of DcR3 was as an inhibitory molecule that is upregulated in tumours and inflammatory diseases (Yu, Kwon et al. 1999; Connolly, Cho et al. 2001; Zhang, Salcedo et al. 2001; Yang, Wang et al. 2004; Han and Wu 2009), the levels of which have been shown to correlate with disease progression (Chen, Yang et al. 2009), including peritonitis (Chang, Lin et al. 2012). Other non-decoy effector functions such as, promotion of cell differentiation (Hsu, Lin et al. 2004; Chang, Chen et al. 2008) and invasion (Lin and Hsieh 2011), have more recently been reported. Further transgenic mice expressing human DcR3 were found to reduce Th1 responses and presented a predisposition towards a Th2 polarized phenotype (Hsu, Wu et al. 2005; Han, Bojalil et al. 2008). DcR3 may also be able to differentially bind its 3 TNFSF ligands and in so doing preferentially act on one pathway in preference to another (Wroblewski, Witcher et al. 2003; Bossen, Ingold et al. 2006; Han, Moore et al. 2007). Despite stronger structural binding kinetics for TL1A (Migone, Zhang et al. 2002), DcR3 has been most commonly implicated in FasL-dependent effects, such as preventing FasL-dependent chemotaxis (Roth, Isenmann et al. 2001; Shi, Wu et al. 2003) and Fas/LIGHT induced apoptosis (Pitti, Marsters et al. 1998; Yu, Kwon et al. 1999). Therefore whilst comparisons between mouse and human systems should not be ignored, careful consideration of the greater number of isoforms and the role of DcR3 in humans should be borne in mind when comparing findings between the 2 species.

7.1.2 The role of DR3 in maintaining the number of peritoneal or blood leukocytes in the unchallenged mouse

- Similar numbers of resident leukocytes were found in the naive peritoneal cavity of $DR3^{-/-}$ and $DR3^{+/+}$ mice, reflected in analogous numbers of individual myeloid and lymphoid cell subsets.
- No significant differences were found in proliferation or cell death of leukocyte subsets in the $DR3^{-/-}$ and $DR3^{+/+}$ cavity.
- Equivalent levels of chemoattractant were observed in the naive $DR3^{-/-}$ and $DR3^{+/+}$ cavity.
- Parallel numbers of leukocytes subsets were found in the naive peripheral blood of $DR3^{-/-}$ and $DR3^{+/+}$ mice.

Findings outlined in Chapter 3 show DR3 to be non-essential in the maintenance of leukocytes during resting conditions in the peritoneal cavity. This is in keeping with other work in the Wang laboratory showing comparable leukocyte subset numbers in the unchallenged lung and spleen (Singh and Twohig respectively, personal communication). Initial analysis of the $DR3^{-/-}$ mouse demonstrated a non-redundant role for DR3 in negative selection in the thymus, though no autoimmunity was observed and $DR3^{-/-}$ mice had normal immune cell phenotype in the naive state (Wang, Thern et al. 2001). Observations in Chapter 3 are consistent with the literature that suggests DR3 primarily exerts its effects after immune challenge.

7.1.3 Regulation of neutrophil influx into the peritoneal cavity by the DR3/TL1A pathway

- The levels of TL1A mRNA increased in resident macrophages, but not the peritoneal membrane, following SES induced inflammation.
- Significantly reduced levels of the ELR^{+} neutrophilic chemoattractant KC were found in $DR3^{-/-}$ compared to $DR3^{+/+}$ supernatants after SES challenge.
- This mirrored levels of KC mRNA in $DR3^{-/-}$ and $DR3^{+/+}$ membranes following the induction of inflammation.
- Reduced numbers of neutrophils accumulated in the $DR3^{-/-}$ cavity compared to $DR3^{+/+}$ mice after challenge and this correlated with the level of KC.

Acute inflammation was provoked using SES and the innate immune response engaged by SES interaction with TLR2 on resident macrophages (Hurst, Wilkinson et al. 2001; McLoughlin, Witowski et al. 2003). Detection of SES or zymosan by these resident macrophages has previously been shown to lead to the release of pro-inflammatory cytokines such as IFNγ (McLoughlin, Witowski et al. 2003), IL6 (Hurst, Wilkinson et al. 2001; McLoughlin, Witowski et al. 2003) and TNFα (Vonasmuth, Maessen et al. 1990), which then co-ordinate the production of chemoattractants and adhesion molecules that promote leukocyte accumulation (Jones 2005).

Based on observations in Chapter 4, TL1A can also be considered as one of these pro-inflammatory cytokines present prior to the release of the first chemoattractants, with increased levels triggered after SES detection by the TLR pathway (Figure 7.1). Whilst this time point is the earliest report of an increase in TL1A mRNA expression

from macrophages (Figure 4.2), numerous studies have found increased TL1A mRNA production in myeloid cells following various stimulation protocols. These include Ova/anti-Ova immune complexes (after 3 hours) (Cassatella, da Silva et al. 2007) or LPS stimulation of: (i) monocytes and DCs isolated from PBMC after 6 hours (Prehn, Thomas et al. 2007); (ii) bone marrow derived DCs (~100 fold increase after 3 hours) (Meylan, Davidson et al. 2008); (iii) U937 cells (a human monocytic cell line) after 24 hours (Endo, Kinouchi et al. 2009) and; (iv) mouse $CD11c^{+}$ DCs (after 4 hours). In the latter case, TL1A was also triggered by polyinosinic-polycytidylic acid (pIC) stimulation after 6 hours (Taraban, Slebioda et al. 2011), while a 12 fold increase in TL1A mRNA was also described from splenic macrophages 4 hours after *Salmonella enterica* infection (Buchan, Taraban et al. 2012).

TL1A may then directly bind DR3 present on the naive mesothelium (Figure 3.16) leading to the downstream release of chemoattractants from mesothelial cells in the membrane (Robson, Witowski et al. 1997; Jones 2005), suggesting a novel role for DR3/TL1A signalling on a stromal surface (Figure 7.1). However this model assumes DR3 is membrane-bound and not in a soluble form (as postulated in Section 7.1.1) and requires further investigation. Following DR3/TL1A interaction ELR^{+} chemoattractants are the first chemokines to be released and have been reported to come from the membrane (Hurst, Wilkinson et al. 2001; McLoughlin, Witowski et al. 2003; McLoughlin, Hurst et al. 2004). Consistent with this, significantly reduced levels of KC mRNA were detected in the membranes of $DR3^{-/-}$ compared to $DR3^{+/+}$ mice after challenge (Figure 4.15A) and correlated with reduced protein levels in peritoneal supernatants (Figure 4.14A).

Lower levels of KC in DR3$^{-/-}$ supernatants correlated with a significant reduction in the accumulation of neutrophils into the cavity (Figure 4.8B), which is in agreement with findings of Wang, Newton et al. (appendix), who found reduced levels of KC and neutrophil numbers in the DR3$^{-/-}$ knee joint 3 days after inducing AIA. Therefore DR3 acts to promote rather than curtail the initial stages of the innate inflammatory response.

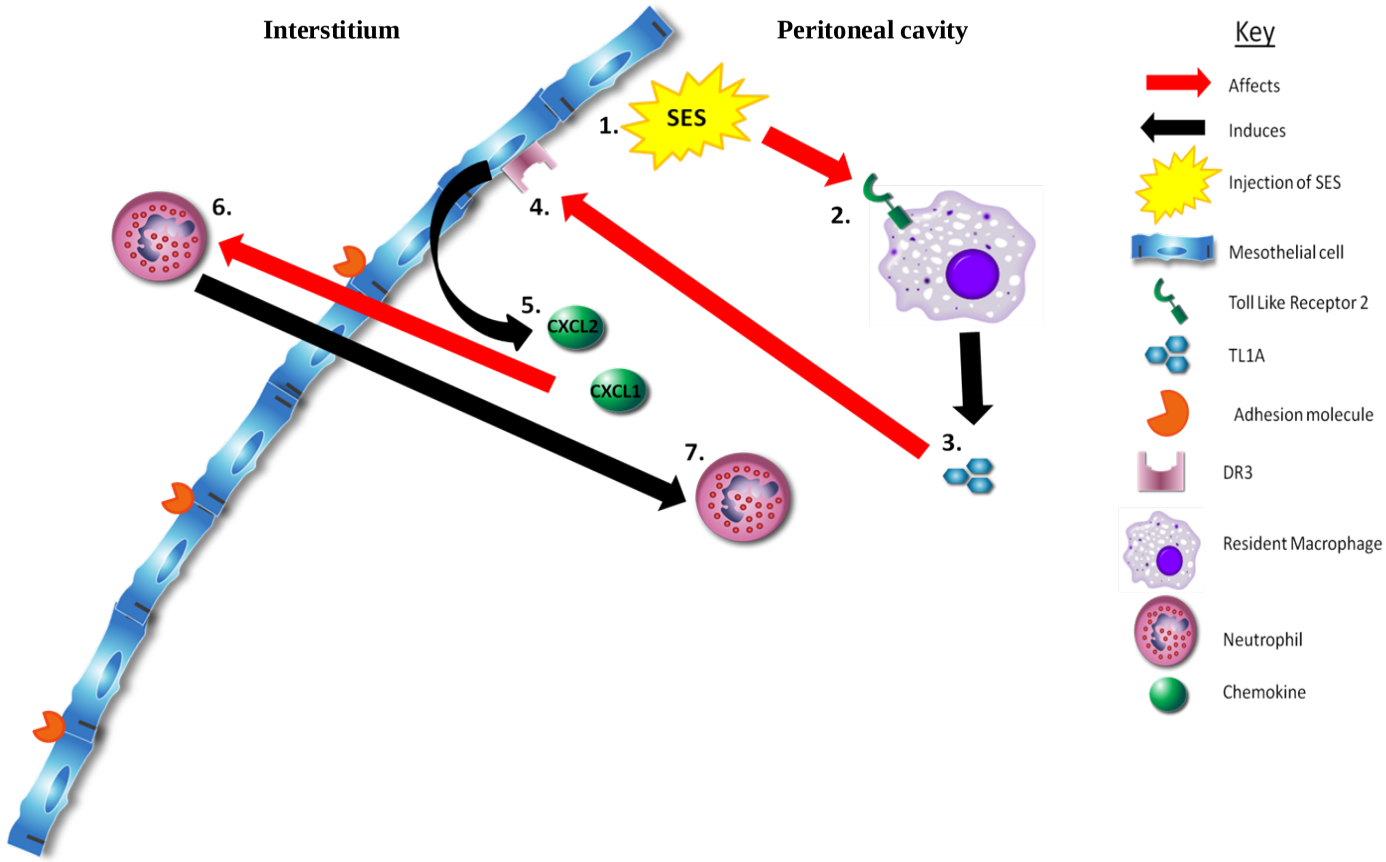

Figure 7.1 - Proposed role for DR3 in co-ordinating neutrophil accumulation during the early phase of acute peritoneal inflammation. Following the injection of SES, TLR2 activation on resident macrophages leads to TL1A production. TL1A binds DR3 on mesothelial cells in the peritoneal membrane which results in the production of neutrophilic chemoattractants. These chemoattractants then promote the entry of neutrophils into the peritoneal cavity down the chemoattractant gradient.

7.1.4 Regulation of accumulation of other myeloid and lymphocytic subsets by the DR3/TL1A pathway

- Reduced numbers of inflammatory macrophages and eosinophils, but not resident macrophages, accumulated in the peritoneal cavity of $DR3^{-/-}$ compared to $DR3^{+/+}$ mice after SES challenge.
- Lower numbers of several lymphocyte subsets including T, B and NKT, but not NK, cells were found in the $DR3^{-/-}$ compared to $DR3^{+/+}$ cavity after challenge.
- No significant differences in proliferation were observed in any of these subsets.
- Significantly reduced levels of multiple chemokines associated with the recruitment of myeloid and lymphoid cell subsets were noted in $DR3^{-/-}$ compared to $DR3^{+/+}$ supernatants.
- The mRNA levels of several chemoattractants that promote the accumulation of myeloid cells were found to be considerably reduced in the $DR3^{-/-}$ compared to the $DR3^{+/+}$ membrane following the induction of inflammation.
- No significant differences were seen in mRNA levels of most chemoattractants linked to the recruitment of lymphocytes, with the exception of CXCL13 that was significantly reduced in the $DR3^{-/-}$ membrane after SES challenge.

The rapid influx of neutrophils into the cavity is followed by a more prolonged accumulation of other myeloid cell subsets and a later influx of lymphocytes from the peripheral blood. These subsets are recruited by other chemoattractants, which may be released by both leukocytes and mesothelial cells (Hurst, McLoughlin et al. 2002; McLoughlin, Hurst et al. 2004; Jones 2005; McLoughlin, Jenkins et al. 2005; Hams, Colmont et al. 2008).

DR3$^{-/-}$ mice were found to have significantly reduced numbers of both (i) selected myeloid subsets including; inflammatory macrophages (Figure 5.4A) and eosinophils (Figure 5.4C) and (ii) all lymphocyte subsets studied, with the exception of NK cells including; T cells, B cells, and NKT cells (Figure 5.5-5.7) following SES challenge. Initial studies implicated DR3 signalling with the NFκB pathway suggesting DR3 is capable of influencing cellular expansion and has since been shown in CD4^{+} and CD8^{+} T cells (Marsters, Sheridan et al. 1996; Meylan, Davidson et al. 2008). However DR3$^{-/-}$ mice showed no defect in the percentage of proliferating cells of any myeloid or lymphocyte cell subset investigated in the peritonitis model (Figure 5.8-5.11). Eosinophil expansion was also investigated at this point (data not shown) but no proliferation was observed. Thus DR3 is not interacting with the proliferative pathway to promote expansion of leukocytes in this model.

Findings presented in this thesis found DR3$^{-/-}$ supernatants to have significant reductions in the level of multiple chemoattractants including; CCL2, CCL3, CCL4, CCL7, CXCL10 and CXCL13 (Figure 5.12-5.15). The membrane was shown to be a source of selected chemokines including; CCL2, CCL7 (Figure 5.16) and CXCL13 (Figure 5.19), that were all present at reduced levels in the DR3$^{-/-}$ membrane. Differences observed in the other chemoattractants do not appear to originate from the membrane (Figure 5.17-5.18) and may be released by leukocytes recruited earlier in the innate immune response, such as neutrophils, which have previously been shown to release CCL3 (Kasama, Strieter et al. 1993), CCL4 (Kasama, Strieter et al. 1994) and CXCL10 (Cassatella, Gasperini et al. 1997; Molesworth-Kenyon, Popham et al. 2012).

Consistent with the impairment in certain leukocyte subsets (discussed earlier) CCL2 and CCL7 have formerly been associated with promoting the accumulation of myeloid cells and CXCL13 is exclusively involved in B cell recruitment (Ansel, Harris et al. 2002). However, attributing specific chemoattractants to the recruitment of individual subsets can be difficult due to the promiscuity of some chemokines and previous studies have shown many of them to be capable of recruiting different cell subsets based on the context of inflammation (Murphy, Baggiolini et al. 2000; Zlotnik and Yoshie 2000; Moser, Wolf et al. 2004).

Nonetheless, these findings allow a model to be proposed whereby TL1A interaction with DR3 on mesothelial cells can lead (i) directly to the downstream production of monocytic chemoattractants, which promote the influx of selected myeloid cell subsets (Figure 7.2) and (ii) indirectly effect lymphocyte accumulation, as initial defects in selected myeloid subset influx earlier in the innate response may cause lower overall levels of lymphocytic chemoattractants (Figure 7.3).

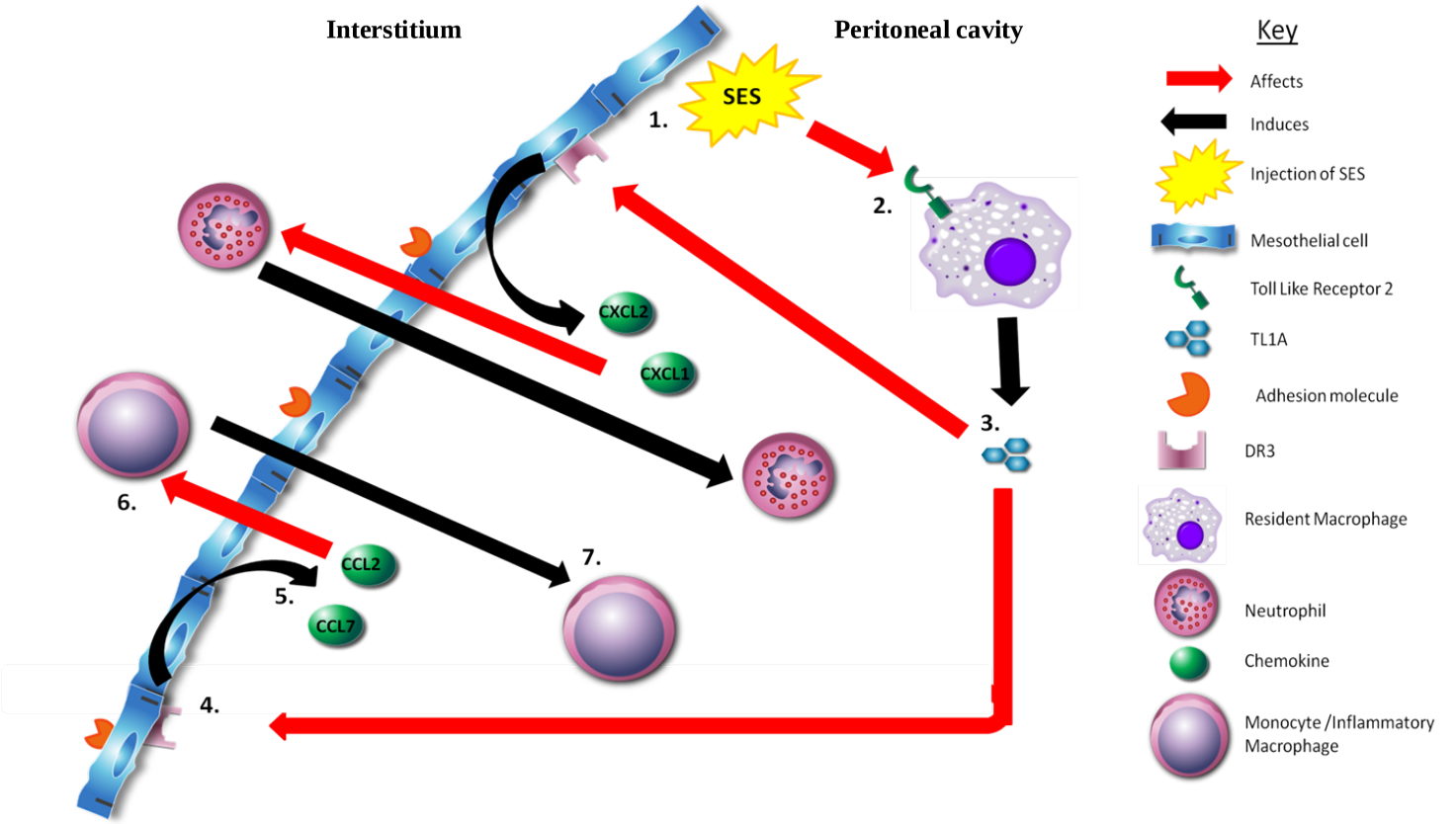

Figure 7.2 - Proposed role for DR3 in co-ordinating the accumulation of myeloid cell subsets during acute peritoneal inflammation. Following the injection of SES, TLR2 activation on resident macrophages leads to TL1A production. TL1A then binds DR3 on mesothelial cells in the peritoneal membrane which result in the production of chemoattractants. These chemoattractants then promote the entry of myeloid subsets, such as monocytes from the circulation into the peritoneal cavity down the chemoattractant gradient.

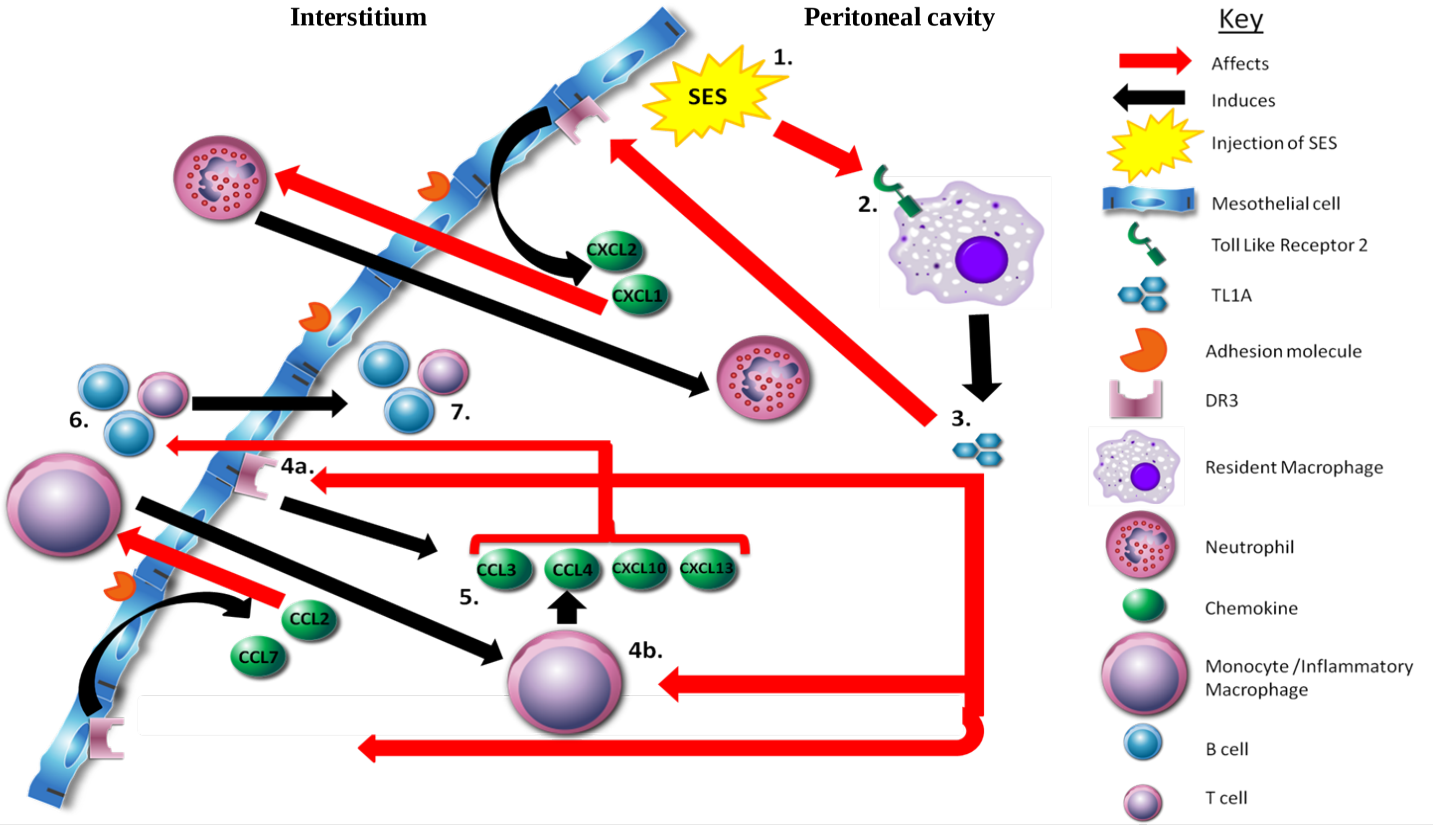

Figure 7.3 - Proposed role for DR3 in co-ordinating the accumulation of lymphocytic cell subsets during the late phase of acute peritoneal inflammation. Following the injection of SES, TLR2 activation on resident macrophages leads to TL1A production. TL1A binds DR3 on mesothelial cells in the peritoneal membrane which results in the production of chemoattractants promoting the entry of myeloid subsets. Lymphocyte entry is then supported by chemoattractant release, either directly from DR3/TL1A binding on mesothelial cells or from inflammatory myeloid subsets which have accumulated in the cavity earlier during inflammation due to myeloid chemoattractant release by mesothelial cells.

7.1.5 Contribution of the DR3/TL1A pathway to tissue damage in the peritoneal cavity after repeated peritoneal inflammatory episodes

- Equivalent numbers of leukocytes and all subsets investigated were found in both genotypes in each experimental group.
- Repeated SES induced inflammation resulted in significant fibrosis of the $DR3^{+/+}$ peritoneal membrane.
- The mesothelial layer of the $DR3^{-/-}$ membrane was not susceptible to fibrotic thickening after the induction of a single or multiple inflammatory events.

Following the accumulation of lymphocytes after the induction of acute inflammation, the inflammatory leukocyte profile is resolved and naive conditions restored by the replenishment of resident cell subsets in the cavity. However, if repeated inflammatory events occur preventing the resolution of inflammation, aberrant inflammatory conditions can develop, which lead to dysregulation of the immune response and ultimately tissue damage (Davies, Bryan et al. 1996; Williams, Craig et al. 2002; Jones 2005; Wynn 2007).

After repeated inflammatory events the peritoneal membranes of $DR3^{+/+}$ mice were found to have undergone significant fibrosis (Figure 6.7A), which has been observed in previous studies using the SES model (Fielding et al. appendix) and other experimental models of peritoneal inflammation (Takahashi, Taniguchi et al. 2009; Jiang, Zhang et al. 2011; Washida, Wakino et al. 2011; Nishino, Ashida et al. 2012). Conversely, $DR3^{-/-}$ mice were found to be protected from any thickening of their mesothelial layer (Figure 6.7B). This fibrosis in $DR3^{+/+}$ mice suggests that the

pro-inflammatory role of DR3/TL1A during the innate immune response may exert detrimental effects after repeated inflammatory episodes.

However no significant differences were observed in the number of any peritoneal leukocyte subset investigated between the 2 genotypes after the induction of repeated inflammatory events. Comparable leukocyte numbers may be explained by the nature of the challenge and as the cavity was not sampled until day 49 (28 days since the last inflammatory event was induced) the inflammatory leukocyte profile may have been resolved. Indeed similar leukocyte subset numbers are observed in both the repeat hit group and the naive group (Figure 6.2-6.5), and lack of neutrophils and inflammatory macrophages in the repeat hit group (data not shown) are consistent with resolution of inflammation.

Without further investigation into the mechanism DR3 utilises to cause tissue damage, only a hypothesis can be proposed by considering other studies using the SES model in the context of previous DR3 findings. During repeated peritoneal inflammation TL1A produced by resident macrophages (Figure 4.2) (Endo, Kinouchi et al. ; Cassatella, da Silva et al. 2007; Prehn, Thomas et al. 2007; Meylan, Davidson et al. 2008; Buchan, Taraban et al. 2012) may bind DR3 expressed on T cells (Figure 4.5) (Fang, Adkins et al. 2008; Jones, Stumhofer et al. 2011; Twohig, Marsden et al. 2012), which are maintained in the cavity (by repeated SES challenge). DR3 then effects T cell responses which co-ordinate the immune reaction, such as the release of IFNγ (Fielding et al. appendix).

IFNγ may promote an increased inflammatory profile by; (i) increased STAT1 (which is not present during acute inflammation) (Boehm, Klamp et al. 1997) and enhanced STAT3 signalling by mesothelial cells (that promotes stronger

chemoattractant release) (Platanias 2005; Fielding et al. appendix). (ii) Upregulation of adhesion molecules, such as, ICAM-1, VCAM-1 and CD62L that further promote cellular influx (Jonjic, Peri et al. 1992; Betjes, Tuk et al. 1993; Liberek, Topley et al. 1996; Li, Davenport et al. 1998) and (iii) IL15 production by mesothelial cells, which is a potent activator of leukocytes (Hausmann, Rogachev et al. 2000).

Myeloid subsets sustained in the cavity by recurrent inflammation may then release degrading enzymes (such as MMPs) and reactive oxygen species (NO, H_2O_2), which promote tissue damage (Duffield, Erwig et al. 2000; Duffield, Ware et al. 2001; Kipari and Hughes 2002; Serbina, Salazar-Mather et al. 2003; Gueders, Foidart et al. 2006; Stary, Bangert et al. 2007). TGFβ release to repair the tissue can then result in fibrosis by driving epithelial to mesenchymal transition (EMT) of mesothelial cells leading to the production of increased extracellular matrix (fibrosis) (Bissell, Wang et al. 1995; Selgas, Bajo et al. 2006).

7.2 Future Work

The findings of this thesis have shown a role for DR3 in controlling the release of selected chemoattractants and the downstream accumulation of multiple leukocyte subsets in the innate immune response, though DR3/TL1A interaction can also lead to tissue damage after repeated SES inflammation. However further experiments are necessary to understand these findings and the transition from DR3's effects during the innate immune response to the tissue damage caused during recurrent inflammation.

- **Examining the differential regulation and potential roles of DR3 splice variants.** To date a lack of reagents to identify DR3 and TL1A have hindered profiling their expression and how this alters during inflammation, throughout the experiments described in this thesis and in the wider literature. However, development of specific monoclonal antibodies against each DR3 isoform should allow the expression patterns of each DR3 variant to be scrutinised and any differential effects exerted by them to be further elucidated, both in the context of this model and others. In addition new TL1A reagents, including; development of specific TL1A primers and a soon to be released mouse TL1A ELISA (eBioscience) will further improve the range of reagents available to investigate DR3/TL1A biology.

- **Determining the role of DR3 in the transition between innate and adaptive immunity and how the mechanism of DR3 signalling may alter during adaptive immunity.** Preliminary findings in this thesis have identified a DR3-dependent effect (fibrosis) after repeated inflammatory events. Analysis of intracellular mechanisms which act during acute inflammation and how these may alter after the induction of recurrent inflammation, such as the ratio of STAT1/STAT3 signalling is crucial to understand if DR3's effect during acute inflammation may influence the shift towards adaptive immunity. It would also be interesting to examine levels of other important factors associated with recurrent inflammation, which promote autoimmunity, such as up-regulation of adhesion molecules, IFNγ, IL15, TNFα, IL1β, TGFβ and MMPs after repeated induction of inflammation and if these levels vary between the 2 genotypes.

Additionally, investigation of leukocyte subsets over a time course after the induction of the fourth inflammatory event (Day 21) is important to determine how the leukocyte accumulation profile changes compared to the profile during an acute inflammatory event, and what differences are observed between the 2 genotypes which encourage fibrosis in $DR3^{+/+}$ mice. However it may be more appropriate to use a more severe experimental model, such as infection with live *S. epidermidis* or *E. coli* which more closely replicates continuous episodes of chronic peritonitis (Gallimore, Gagnon et al. 1987; Wang, Nie et al. 2010) and allows investigation into potential DR3-dependent effects on peritoneal bacterial clearance which has been shown in *S. enterica* infection (Buchan, Taraban et al. 2012) in addition to increased viral titres in MCMV (Twohig, Marsden et al. 2012). Investigation with other TLR agonists is also important to examine TLR cross talk with DR3 signalling.

- **Investigating DR3 findings outlined in this thesis in the human system and the potential of anti-TL1A as a potential therapeutic target.** Initial study of TL1A and DR3 expression levels in human samples, particularly from end stage renal failure patients undergoing peritoneal dialysis treatment (compared to healthy controls) is required to investigate if DR3/TL1A interaction is also induced in human disease. However any DR3/TL1A dependent role in the human immune response may diverge from findings in the mouse system due to the presence of other DR3 splice variants (at least 13) and a decoy receptor (DcR3), which binds TL1A as well as other TNFSF members. Injections of anti-TL1A in $DR3^{+/+}$ mice would also be interesting to test if it resulted in ameliorated fibrosis and aligned with $DR3^{-/-}$ mice, potentially identifying

anti-TL1A as a possible therapeutic target for treating fibrosis of the peritoneal membrane.

- **Further examining the source of chemoattractants after DR3/TL1A interaction.** Data presented within this thesis suggest certain chemokines (namely KC, CCL2, CCL7 and CXCL13) are produced by the membrane. However additional experiments i.e. bone marrow chimeras are required to definitively identify the cellular source (be it the stroma, leukocytes or both) of each chemoattractant that promotes the accumulation of leukocytes during inflammation.

- **Investigating DR3's effect on other leukocyte subsets during inflammation.** Although Chapter 3 measured the number of DCs in the naive cavity, investigation of DCs by flow cytometry during inflammation was not possible due to the influx of inflammatory macrophages. Recent findings allow the use of CD226 along with antibodies already utilised (CD11c, CD11b and F4/80) to separate DCs from other leukocyte subsets, including inflammatory macrophages (Liao, personal communication). Mast cells were also not investigated in this thesis, though investigation into their role may be important as they are significant producers of cytokines such as; IL3, IL4, IL6, TNFα and IFNγ (Metcalfe, Baram et al. 1997) and are present in the resident population of the naive cavity. The use of CD117 and FcεR1 will allow these to be investigated by flow cytometry.

7.3 Final Conclusion

This work has shown for the first time an important role for stromal DR3 signalling in the innate inflammatory response after the induction of acute peritoneal inflammation and that repeated induction of inflammation leads to changes in the immune response, which result in fibrosis of the peritoneal membrane. Removal of DR3 via a gene knockout impairs the innate immune response but conveys protection to any damage of the peritoneal membrane during recurrent inflammation. Further work is necessary to determine how the apparently protective innate DR3-dependent response, outlined in this thesis, interlinks with adverse DR3-dependent effects during the acquired immune response and at which point during the immune response DR3 exerts its most important effects.

Chapter 8 – References

Aggarwal, B. B. (2003). "Signalling pathways of the TNF superfamily: A double-edged sword." Nature Reviews Immunology **3**(9): 745-756.

Adams, D. H. and A. R. Lloyd (1997). "Chemokines: Leucocyte recruitment and activation cytokines." Lancet **349**(9050): 490-495.

Aggarwal, B. B. (2003). "Signalling pathways of the TNF superfamily: A double-edged sword." Nature Reviews Immunology **3**(9): 745-756.

Akgul, C., D. A. Moulding, et al. (2001). "Molecular control of neutrophil apoptosis." Febs Letters **487**(3): 318-322.

Al-Lamki, R. S., J. Wang, et al. (2008). "TL1A both promotes and protects from renal inflammation and injury." Journal of the American Society of Nephrology **19**(5): 953-960.

Al-Lamki, R. S., J. Wang, et al. (2003). "Expression of silencer of death domains and death-receptor-3 in normal human kidney and in rejecting renal transplants." American Journal of Pathology **163**(2): 401-411.

Ansel, K. M., R. B. S. Harris, et al. (2002). "CXCL13 is required for B1 cell homing, natural antibody production, and body cavity immunity." Immunity **16**(1): 67-76.

Ashkenazi, A. (2002). "Targeting death and decoy receptors of the tumour-necrosis factor superfamily." Nature Reviews Cancer **2**(6): 420-430.

Ashkenazi, A. and V. M. Dixit (1998). "Death receptors: Signaling and modulation." Science **281**(5381): 1305-1308.

Auffray, C., D. Fogg, et al. (2007). "Monitoring of blood vessels and tissues by a population of monocytes with patrolling behavior." Science **317**(5838): 666-670.
Baggiolini, M. (1998). "Chemokines and leukocyte traffic." Nature **392**(6676): 565-568.

Baggiolini, M., B. Dewald, et al. (1997). "Human chemokines: An update." Annual Review of Immunology **15**: 675-705.

Baggiolini, M. and P. Loetscher (2000). "Chemokines in inflammation and immunity." Immunology Today **21**(9): 418-420.

Bai, C., B. Connolly, et al. (2000). "Overexpression of M68/DcR3 in human gastrointestinal tract tumors independent of gene amplification and its location in a four-gene cluster." Proceedings of the National Academy of Sciences of the United States of America **97**(3): 1230-1235.

Bamias, G., K. Evangelou, et al. (2011). "Upregulation and nuclear localization of TNF-like Cytokine 1A (TL1A) and its receptors DR3 and DcR3 in psoriatic skin lesions." Experimental Dermatology **20**(9): 725-731.

Bamias, G., C. Martin, et al. (2003). "Expression, localization, and functional activity of TL1A, a novel Th1-polarizing cytokine in inflammatory bowel disease." Journal of Immunology **171**(9): 4868-4874.

Bamias, G., M. Mishina, et al. (2006). "Role of TL1A and its receptor DR3 in two models of chronic murine ileitis." Proceedings of the National Academy of Sciences of the United States of America **103**(22): 8441-8446.

Bamias, G., S. I. Siakavellas, et al. (2008). "Circulating levels of TNF-like cytokine 1A (TL1A) and its decoy receptor 3 (DcR3) in rheumatoid arthritis." Clinical Immunology **129**(2): 249-255.

Bamias, G., K. Stamatelopoulos, et al. (2013). "Circulating levels of TNF-like Cytokine 1A correlate with the progression of atheromatous lesions in patients with Rheumatoid Arthritis." Clinical Immunology(0).

Banner, D. W., A. Darcy, et al. (1993). "CRYSTAL-STRUCTURE OF THE SOLUBLE HUMAN 55 KD TNF RECEPTOR-HUMAN TNF-BETA COMPLEX - IMPLICATIONS FOR TNF RECEPTOR ACTIVATION." Cell **73**(3): 431-445.

Bazan, J. F., K. B. Bacon, et al. (1997). "A new class of membrane-bound chemokine with a CX(3)C motif." Nature **385**(6617): 640-644.

Bellingan, G. J., H. Caldwell, et al. (1996). "In vivo fate of the inflammatory macrophage during the resolution of inflammation - Inflammatory macrophages do not die locally, but emigrate to the draining lymph nodes." Journal of Immunology **157**(6): 2577-2585.

Betjes, M. G. H., C. W. Tuk, et al. (1993). "INTERLEUKIN-8 PRODUCTION BY HUMAN PERITONEAL MESOTHELIAL CELLS IN RESPONSE TO TUMOR-NECROSIS-FACTOR-ALPHA, INTERLEUKIN-1, AND MEDIUM CONDITIONED BY MACROPHAGES COCULTURED WITH STAPHYLOCOCCUS-EPIDERMIDIS." Journal of Infectious Diseases **168**(5): 1202-1210.

Bishop, G. A., C. R. Moore, et al. (2007). "TRAF proteins in CD40 signaling." Tnf Receptor Associated Factors (Trafs) **597**: 131-151.

Bissell, D. M., S. S. Wang, et al. (1995). "CELL-SPECIFIC EXPRESSION OF TRANSFORMING GROWTH-FACTOR-BETA IN RAT-LIVER - EVIDENCE FOR AUTOCRINE REGULATION OF HEPATOCYTE PROLIFERATION." Journal of Clinical Investigation **96**(1): 447-455.

Bodmer, J. L., K. Burns, et al. (1997). "TRAMP, a novel apoptosis-mediating receptor with sequence homology to tumor necrosis factor receptor 1 and Fas(Apo-1/CD95)." Immunity **6**(1): 79-88.

Bodmer, J. L., N. Holler, et al. (2000). "TRAIL receptor-2 signals apoptosis through FADD and caspase-8." Nature Cell Biology **2**(4): 241-243.

Bodmer, J. L., P. Schneider, et al. (2002). "The molecular architecture of the TNF superfamily." Trends in Biochemical Sciences **27**(1): 19-26.

Boehm, U., T. Klamp, et al. (1997). "Cellular responses to interferon-gamma." Annual Review of Immunology **15**: 749-795.

Borisov, A. V. (1964). "LYMPHATIC CAPILLARIES + BLOOD VESSELS OF MILKY SPOTS IN HUMAN GREATER OMENTUM." Federation Proceedings **23**(1P2): T150-&.

Borregaard, N. and J. B. Cowland (1997). "Granules of the human neutrophilic polymorphonuclear leukocyte." Blood **89**(10): 3503-3521.

Borysenko, C. W., V. Garcia-Palacios, et al. (2006). "Death receptor-3 mediates apoptosis in human osteoblasts under narrowly regulated conditions." Journal of Cellular Physiology **209**(3): 1021-1028.

Bossen, C., K. Ingold, et al. (2006). "Interactions of tumor necrosis factor (TNF) and TNF receptor family members in the mouse and human." Journal of Biological Chemistry **281**(20): 13964-13971.

Brinkmann, V., U. Reichard, et al. (2004). "Neutrophil extracellular traps kill bacteria." Science **303**(5663): 1532-1535.

Brown, S. A. N., C. M. Richards, et al. (2003). "The Fn14 cytoplasmic tall binds tumour-necrosis-factor-receptor-associated factors 1, 2, 3 and 5 and mediates nuclear factor-kappa B activation." Biochemical Journal **371**: 395-403.

Buchan, S. L., V. Y. Taraban, et al. (2012). "Death receptor 3 is essential for generating optimal protective CD41 T-cell immunity against Salmonella." European Journal of Immunology **42**(3): 580-588.

Bull, M. J., A. S. Williams, et al. (2008). "The Death Receptor 3-TNF-like protein 1A pathway drives adverse bone pathology in inflammatory arthritis." Journal of Experimental Medicine **205**(11): 2457-2464.

Cannistra, S. A., C. Ottensmeier, et al. (1994). "VASCULAR CELL-ADHESION MOLECULE-1 EXPRESSED BY PERITONEAL MESOTHELIUM PARTLY MEDIATES THE BINDING OF ACTIVATED HUMAN T-LYMPHOCYTES." Experimental Hematology **22**(10): 996-1002.

Carswell, E. A., L. J. Old, et al. (1975). "ENDOTOXIN-INDUCED SERUM FACTOR THAT CAUSES NECROSIS OF TUMORS." Proceedings of the National Academy of Sciences of the United States of America **72**(9): 3666-3670.

Cassatella, M. A., G. P. da Silva, et al. (2007). "Soluble TNF-like cytokine (TL1A) production by immune complexes stimulated monocytes in rheumatoid arthritis." Journal of Immunology **178**(11): 7325-7333.

Cassatella, M. A., S. Gasperini, et al. (1997). "Regulated production of the interferon-gamma-inducible protein-10 (IP-10) chemokine by human neutrophils." European Journal of Immunology **27**(1): 111-115.

Cassatella, M. A., S. Gasperini, et al. (1997). Cytokine expression and release by neutrophils. Phagocytes: Biology, Physiology, Pathology, and Pharmacotherapeutics. R. Paoletti, A. Notario and G. Ricevuti. **832:** 233-242.

Cavallini, C., O. Lovato, et al. (2013). "The TNF-Family Cytokine TL1A Inhibits Proliferation of Human Activated B Cells." Plos One **8**(4): e60136-e60136.

Chang, E.-P., Y.-S. Lin, et al. (2012). "High serum DcR3 levels are associated with the occurrence of peritonitis in patients receiving chronic peritoneal dialysis." Journal of the Chinese Medical Association **75**(12): 644-648.

Chang, Y.-C., T.-C. Chen, et al. (2008). "Epigenetic control of MHC class II expression in tumor-associated macrophages by decoy receptor 3." Blood **111**(10): 5054-5063.

Chen, C.-Y., K.-Y. Yang, et al. (2009). "Decoy Receptor 3 Levels in Peripheral Blood Predict Outcomes of Acute Respiratory Distress Syndrome." American Journal of Respiratory and Critical Care Medicine **180**(8): 751-760.

Chinnaiyan, A. M., K. Orourke, et al. (1996). "Signal transduction by DR3, a death domain-containing receptor related to TNFR-1 and CD95." Science **274**(5289): 990-992.

Clark, S. R., A. C. Ma, et al. (2007). "Platelet TLR4 activates neutrophil extracellular traps to ensnare bacteria in septic blood." Nature Medicine **13**(4): 463-469.

Claudio, E., K. Brown, et al. (2002). "BAFF-induced NEMO-independent processing of NF-kappa B2 in maturing B cells." Nature Immunology **3**(10): 958-965.

Coene, M. C., C. Vanhove, et al. (1982). "ARACHIDONIC-ACID METABOLISM BY CULTURED MESOTHELIAL CELLS - DIFFERENT TRANSFORMATIONS OF EXOGENOUSLY ADDED AND ENDOGENOUSLY RELEASED SUBSTRATE." Biochimica Et Biophysica Acta **710**(3): 437-445.

Connolly, K., Y. H. Cho, et al. (2001). "In vivo inhibition of Fas ligand-mediated killing by TR6, a Fas ligand decoy receptor." Journal of Pharmacology and Experimental Therapeutics **298**(1): 25-33.

Coope, H. J., P. G. P. Atkinson, et al. (2002). "CD40 regulates the processing of NF-kappa B2 p100 to p52." Embo Journal **21**(20): 5375-5385.

Dale, D. C., L. Boxer, et al. (2008). "The phagocytes: neutrophils and monocytes." Blood **112**(4): 935-945.

Davies, L. C., M. Rosas, et al. (2011). "A quantifiable proliferative burst of tissue macrophages restores homeostatic macrophage populations after acute inflammation." European Journal of Immunology **41**(8): 2155-2164.

Davies, S. J., J. Bryan, et al. (1996). "Longitudinal changes in peritoneal kinetics: The effects of peritoneal dialysis and peritonitis." Nephrology Dialysis Transplantation **11**(3): 498-506.

Dejardin, E., N. M. Droin, et al. (2002). "The lymphotoxin-beta receptor induces different patterns of gene expression via two NF-kappa B pathways." Immunity **17**(4): 525-535.

Derudder, E., E. Dejardin, et al. (2003). "RelB/p50 dimers are differentially regulated by tumor necrosis factor-alpha and lymphotoxin-beta receptor activation - Critical roles for p100." Journal of Biological Chemistry **278**(26): 23278-23284.

Desouza, G. E. P. and S. H. Ferreira (1985). "BLOCKADE BY ANTIMACROPHAGE SERUM OF THE MIGRATION OF PMN NEUTROPHILS INTO THE INFLAMED PERITONEAL-CAVITY." Agents and Actions **17**(1): 97-103.

Digenis, G. E. (1984). "ANATOMY OF THE PERITONEAL MEMBRANE." Peritoneal Dialysis Bulletin **4**(2): 63-69.

Dipaolo, N., G. Sacchi, et al. (1986). "MORPHOLOGY OF THE PERITONEAL MEMBRANE DURING CONTINUOUS AMBULATORY PERITONEAL-DIALYSIS." Nephron **44**(3): 204-211.

Dobbie, J. W. and J. D. Anderson (1996). "Ultrastructure, distribution, and density of lamellar bodies in human peritoneum." Peritoneal Dialysis International **16**(5): 482-487.

Duchrow, M., J. Gerdes, et al. (1994). "THE PROLIFERATION-ASSOCIATED KI-67 PROTEIN - DEFINITION IN MOLECULAR TERMS." Cell Proliferation **27**(5): 235-242.

Duffield, J. S., L. P. Erwig, et al. (2000). "Activated macrophages direct apoptosis and suppress mitosis of mesangial cells." Journal of Immunology **164**(4): 2110-2119.

Duffield, J. S., C. F. Ware, et al. (2001). "Suppression by apoptotic cells defines tumor necrosis factor-mediated induction of glomerular mesangial cell apoptosis by activated macrophages." American Journal of Pathology **159**(4): 1397-1404.

Dunn, D. L., R. A. Barke, et al. (1985). "ROLE OF RESIDENT MACROPHAGES, PERIPHERAL NEUTROPHILS, AND TRANSLYMPHATIC ABSORPTION IN BACTERIAL CLEARANCE FROM THE PERITONEAL-CAVITY." Infection and Immunity **49**(2): 257-264.

Dynek, J. N., T. Goncharov, et al. (2010). "c-IAP1 and UbcH5 promote K11-linked polyubiquitination of RIP1 in TNF signalling." Embo Journal **29**(24): 4198-4209.

Endo, K., Y. Kinouchi, et al. (2009). "Involvement of NF-kappa B pathway in TL1A gene expression induced by lipopolysaccharide." Cytokine **49**(2): 215-220.

Fadok, V. A., P. P. McDonald, et al. (1998). "Regulation of macrophage cytokine production by phagocytosis of apoptotic and post-apoptotic cells." Biochemical Society Transactions **26**(4): 653-656.

Fang, L., B. Adkins, et al. (2008). "Essential role of TNF receptor superfamily 25 (TNFRSF25) in the development of allergic lung inflammation." Journal of Experimental Medicine **205**(5): 1037-1048.

Faurschou, M. and N. Borregaard (2003). "Neutrophil granules and secretory vesicles in inflammation." Microbes and Infection **5**(14): 1317-1327.

Fieren, M. (1996). "Mechanisms regulating cytokine release from peritoneal macrophages during continuous ambulatory peritoneal dialysis." Blood Purification **14**(2): 179-187.

Flessner, M. F. (1997). The peritoneal dialysis system: Importance of each component, Vicenza, Italy.

Fong, A. and S. C. Sun (2002). "Genetic evidence for the essential role of beta-transducin repeat-containing protein in the inducible processing of NF-kappa B2/p100." Journal of Biological Chemistry **277**(25): 22111-22114.

Fuss, I. J., M. Neurath, et al. (1996). "Disparate CD4(+) lamina propria (LP) lymphokine secretion profiles in inflammatory bowel disease - Crohn's disease LP cells manifest increased secretion of IFN-gamma, whereas ulcerative colitis LP cells manifest increased secretion of IL-5." Journal of Immunology **157**(3): 1261-1270.

Gabay, C. (2006). "Interleukin-6 and chronic inflammation." Arthritis Research & Therapy **8**.

Gallimore, B., R. F. Gagnon, et al. (1987). "RESPONSE TO INTRAPERITONEAL STAPHYLOCOCCUS-EPIDERMIDIS CHALLENGE IN RENAL-FAILURE MICE." Kidney International **32**(5): 678-683.

Gavett, S. H., X. L. Chen, et al. (1994). "DEPLETION OF MURINE CD4+ T-LYMPHOCYTES PREVENTS ANTIGEN-INDUCED AIRWAY HYPERREACTIVITY AND PULMONARY EOSINOPHILIA." American Journal of Respiratory Cell and Molecular Biology **10**(6): 587-593.

Geissmann, F., S. Jung, et al. (2003). "Blood monocytes consist of two principal subsets with distinct migratory properties." Immunity **19**(1): 71-82.

Gerlach, B., S. M. Cordier, et al. (2011). "Linear ubiquitination prevents inflammation and regulates immune signalling." Nature **471**(7340): 591-+.

Gjersten, M. K., I. Saeterdal, et al. (1996). "Antigen-presenting function of human peritoneum mesothelial cells isolated from a pancreatic carcinoma patient after mutant Ras peptide vaccination." Cancer Immunology Immunotherapy **43**(5): 262-268.

Gordon, S. (2007). "The macrophage: Past, present and future." European Journal of Immunology **37**: S9-S17.

Gordon, S. and P. R. Taylor (2005). "Monocyte and macrophage heterogeneity." Nature Reviews Immunology **5**(12): 953-964.

Gout, S., C. Morin, et al. (2006). "Death receptor-3, a new E-selectin counter-receptor that confers migration and survival advantages to colon carcinoma cells by triggering p38 and ERK MAPK activation." Cancer Research **66**(18): 9117-9124.

Graham, G. J. (2009). "D6 and the atypical chemokine receptor family: Novel regulators of immune and inflammatory processes." European Journal of Immunology **39**(2): 342-351.

Griffin, F. M. (1981). "ROLES OF MACROPHAGE FC AND C3B RECEPTORS IN PHAGOCYTOSIS OF IMMUNOLOGICALLY COATED CRYPTOCOCCUS-NEOFORMANS." Proceedings of the National Academy of Sciences of the United States of America-Biological Sciences **78**(6): 3853-3857.

Gueders, M. M., J. M. Foidart, et al. (2006). "Matrix metalloproteinases (MMPs) and tissue inhibitors of MMPs in the respiratory tract: Potential implications in asthma and other lung diseases." European Journal of Pharmacology **533**(1-3): 133-144.

Haas, T. L., C. H. Emmerich, et al. (2009). "Recruitment of the Linear Ubiquitin Chain Assembly Complex Stabilizes the TNF-R1 Signaling Complex and Is Required for TNF-Mediated Gene Induction." Molecular Cell **36**(5): 831-844.

Hams, E., C. S. Colmont, et al. (2008). "Oncostatin M receptor-beta signaling limits monocytic cell recruitment in acute inflammation." Journal of Immunology **181**(3): 2174-2180.

Han, B., R. Bojalil, et al. (2008). "DcR3 as a diagnostic parameter and risk factor for systemic lupus erythematosus." International Immunology **20**(8): 1067-1075.

Han, B., P. A. Moore, et al. (2007). "Overexpression of human decoy receptor 3 in mice results in a systemic lupus erythematosus-like syndrome." Arthritis and Rheumatism **56**(11): 3748-3758.

Han, B. and J. Wu (2009). "DcR3 Protects Islet beta Cells from Apoptosis through Modulating Adcyap1 and Bank1 Expression." Journal of Immunology **183**(12): 8157-8166.

Hartmann, J., V. Maassen, et al. (1995). "T-LYMPHOCYTES FROM NORMAL HUMAN PERITONEUM ARE PHENOTYPICALLY DIFFERENT FROM THEIR COUNTERPARTS IN PERIPHERAL-BLOOD AND CD3(-) LYMPHOCYTE SUBSETS CONTAIN MESSENGER-RNA FOR THE RECOMBINATION ACTIVATING GENE RAG-1." European Journal of Immunology **25**(9): 2626-2631.

Hartmann, L. C., L. K. Tschettier, et al. (1997). "Granulocyte colony-stimulating factor in severe chemotherapy-induced afebrile neutropenia." New England Journal of Medicine **336**(25): 1776-1780.

Hastings, W. D., J. R. Tumang, et al. (2006). "Peritoneal B-2 cells comprise a distinct B-2 cell population with B-1b-like characteristics." European Journal of Immunology **36**(5): 1114-1123.

Hausmann, M. J., B. Rogachev, et al. (2000). "Accessory role of human peritoneal mesothelial cells in antigen presentation and T-cell growth." Kidney International **57**(2): 476-486.

Heidemann, S. C., V. Chavez, et al. (2010). "TL1A Selectively Enhances IL-12/IL-18-Induced NK Cell Cytotoxicity against NK-Resistant Tumor Targets." Journal of Clinical Immunology **30**(4): 531-538.

Heusch, M., L. Lin, et al. (1999). "The generation of nfkb2 p52: mechanism and efficiency." Oncogene **18**(46): 6201-6208.

Hjelle, J. T., M. A. Millerhjelle, et al. (1995). “The biology of the mesothelium during peritoneal-dialysis.” Peritoneal Dialysis International **15**(7): S13-22.

Holmes, C. J. (1994). “Peritoneal host-defence mechanisms in peritoneal-dialysis.” Kidney International **48** (Supplement): 58-70.

Houck, J. C. and C. M. Chang (1977). "The purification and characterization of a lymphokine chemotactic for lymphocytes--lymphotactin." Inflammation **2**(2): 105-13.

Hsu, M. J., W. W. Lin, et al. (2004). "Enhanced adhesion of monocytes via reverse signaling triggered by decoy receptor 3." Experimental Cell Research **292**(2): 241-251.

Hsu, T. L., Y. Y. Wu, et al. (2005). "Attenuation of Th1 response in decoy receptor 3 transgenic mice." Journal of Immunology **175**(8): 5135-5145.

Hurst, S. M., R. M. McLoughlin, et al. (2002). "Secretion of oncostatin M by infiltrating neutrophils: Regulation of IL-6 and chemokine expression in human mesothelial cells." Journal of Immunology **169**(9): 5244-5251.

Hurst, S. M., T. S. Wilkinson, et al. (2001). "IL-6 and its soluble receptor orchestrate a temporal switch in the pattern of leukocyte recruitment seen during acute inflammation." Immunity **14**(6): 705-714.

Hymowitz, S. G., H. W. Christinger, et al. (1999). "Triggering cell death: The crystal structure of Apo2L/TRAIL in a complex with death receptor 5." Molecular Cell **4**(4): 563-571.

Hymowitz, S. G., D. R. Patel, et al. (2005). "Structures of APRIL-receptor complexes - Like BCMA, TACI employs only a single cysteine-rich domain for high affinity ligand binding." Journal of Biological Chemistry **280**(8): 7218-7227.

Idriss, H. T. and J. H. Naismith (2000). "TNF alpha and the TNF receptor superfamily: Structure-function relationship(s)." Microscopy Research and Technique **50**(3): 184-195.

Ikeda, F., N. Crosetto, et al. (2010). "What Determines the Specificity and Outcomes of Ubiquitin Signaling?" Cell **143**(5): 677-681.

Jiang, C., M. Zhang, et al. (2011). "Tanshinone IIA Attenuates Peritoneal Fibrosis through Inhibition of Fibrogenic Growth Factors Expression in Peritoneum in a Peritoneal Dialysis Rat Model." Renal Failure **33**(3): 355-362.

Jones, G. W., J. S. Stumhofer, et al. (2011). "Naive and activated T cells display differential responsiveness to TL1A that affects Th17 generation, maintenance, and proliferation." Faseb Journal **25**(1): 409-419.

Jones, S. A. (2005). "Directing transition from innate to acquired immunity defining a role for IL-6." Journal of Immunology **175**(6): 3463-3468.

Jones, S. A., B. Dewald, et al. (1997). "Chemokine antagonists that discriminate between interleukin-8 receptors - Selective blockers of CXCR2." Journal of Biological Chemistry **272**(26): 16166-16169.

Jones, S. A., M. Wolf, et al. (1996). "Different functions for the interleukin 8 receptors (IL-8R) of human neutrophil leukocytes: NADPH oxidase and phospholipase D are activated through IL-8R1 but not IL-8R2." Proceedings of the National Academy of Sciences of the United States of America **93**(13): 6682-6686.

Jonjic, N., G. Peri, et al. (1992). "EXPRESSION OF ADHESION MOLECULES AND CHEMOTACTIC CYTOKINES IN CULTURED HUMAN MESOTHELIAL CELLS." Journal of Experimental Medicine **176**(4): 1165-1174.

Kamada, N., T. Hisamatsu, et al. (2010). "TL1A Produced by Lamina Propria Macrophages Induces Th1 and Th17 Immune Responses in Cooperation with IL-23 in Patients with Crohn's Disease." Inflammatory Bowel Diseases **16**(4): 568-575.

Kang, Y. J., W. J. Kim, et al. (2005). "Involvement of TL1A and DR3 in induction of pro-inflammatory cytokines and matrix metalloproteinase-9 in atherogenesis." Cytokine **29**(5): 229-235.

Kaptein, A., M. Jansen, et al. (2000). "Studies on the interaction between TWEAK and the death receptor WSL-1/TRAMP (DR3)." Febs Letters **485**(2-3): 135-141.

Karin, M. and Y. Ben-Neriah (2000). "Phosphorylation meets ubiquitination: The control of NF-kappa B activity." Annual Review of Immunology **18**: 621-+.

Kasama, T., R. M. Strieter, et al. (1994). "REGULATION OF NEUTROPHIL-DERIVED CHEMOKINE EXPRESSION BY IL-10." Journal of Immunology **152**(7): 3559-3569.

Kasama, T., R. M. Strieter, et al. (1993). "EXPRESSION AND REGULATION OF HUMAN NEUTROPHIL-DERIVED MACROPHAGE INFLAMMATORY PROTEIN-1-ALPHA." Journal of Experimental Medicine **178**(1): 63-72.

Kayagaki, N., M. H. Yan, et al. (2002). "BAFF/BLyS receptor 3 binds the B cell survival factor BAFF ligand through a discrete surface loop and promotes processing of NF-kappa B2." Immunity **17**(4): 515-524.

Khan, S. Q., M. S. Tsai, et al. (2013). "Cloning, Expression, and Functional Characterization of TL1A-Ig." Journal of Immunology **190**(4): 1540-1550.

Kim, C. H., L. M. Pelus, et al. (1998). "Differential chemotactic behavior of developing T cells in response to thymic chemokines." Blood **91**(12): 4434-4443.

Kim, S. H., W. H. Lee, et al. (2001). "Tumor necrosis factor receptor superfamily 12 may destabilize atherosclerotic plaques by inducing matrix metalloproteinases." Japanese Circulation Journal-English Edition **65**(2): 136-138.

Kim, W. J., Y. J. Kang, et al. (2008). "Comparative analysis of the expression patterns of various TNFSF/TNFRSF in atherosclerotic plaques." Immunological Investigations **37**(4): 359-373.

Kinnaert, P., J. P. DeWilde, et al. (1996). "Direct activation of human peritoneal mesothelial cells by heat-killed microorganisms." Annals of Surgery **224**(6): 749-755.

Kipari, T. and J. Hughes (2002). "Macrophage-mediated renal cell death." Kidney International **61**(2): 760-761.

Kitson, J., T. Raven, et al. (1996). "A death-domain-containing receptor that mediates apoptosis." Nature **384**(6607): 372-375.

Kolaczkowska, E. (2010). "METALLOPROTEINASE 9 (MMP-9) AS A UNIQUE MEMBER OF THE MATRIX METALLOPROTEINASE FAMILY: ROLE IN INFLUX OF NEUTROPHILS AND THEIR APOPTOSIS DURING INFLAMMATION." Postepy Biologii Komorki **37**(2): 471-499.

Kolaczkowska, E., A. Koziol, et al. (2010). "Inflammatory macrophages, and not only neutrophils, die by apoptosis during acute peritonitis." Immunobiology **215**(6): 492-504.

Kolaczkowska, E., A. Koziol, et al. (2009). "Altered apoptosis of inflammatory neutrophils in MMP-9-deficient mice is due to lower expression and activity of caspase-3." Immunology Letters **126**(1-2): 73-82.

Krediet, R. T., B. Lindholm, et al. (2000). "Pathophysiology of peritoneal membrane failure." Peritoneal Dialysis International **20**: S22-S42.

Kuang, Y. N., Y. P. Wu, et al. (1996). "Selective G protein coupling by C-C chemokine receptors." Journal of Biological Chemistry **271**(8): 3975-3978.

Lanfrancone, L., D. Boraschi, et al. (1992). "HUMAN PERITONEAL MESOTHELIAL CELLS PRODUCE MANY CYTOKINES (GRANULOCYTE COLONY-STIMULATING FACTOR [CSF], GRANULOCYTE-MONOCYTE-CSF, MACROPHAGE-CSF, INTERLEUKIN-1 [IL-1], AND IL-6) AND ARE ACTIVATED AND STIMULATED TO GROW BY IL-1." Blood **80**(11): 2835-2842.

Lapidot, T., A. Dar, et al. (2005). "How do stem cells find their way home?" Blood **106**(6): 1901-1910.

Li, F. K., A. Davenport, et al. (1998). Leukocyte migration across human peritoneal mesothelial cells is dependent on directed chemokine secretion and ICAM-1 expression, Edinburgh, Scotland.

Liang, C. Y., M. Y. Zhang, et al. (2006). "beta-TrCP binding and processing of NF-kappa B2/p100 involve its phosphorylation at serines 866 and 870." Cellular Signalling **18**(8): 1309-1317.

Liberek, T., N. Topley, et al. (1996). "Adherence of neutrophils to human peritoneal mesothelial cells: Role of intercellular adhesion molecule-1." Journal of the American Society of Nephrology **7**(2): 208-217.

Lin, W.-W. and S.-L. Hsieh (2011). "Decoy receptor 3: A pleiotropic immunomodulator and biomarker for inflammatory diseases, autoimmune diseases and cancer." Biochemical Pharmacology **81**(7): 838-847.

Lo, Y.-C., S.-C. Lin, et al. (2009). "Structural Basis for Recognition of Diubiquitins by NEMO." Molecular Cell **33**(5): 602-615.

Locksley, R. M., N. Killeen, et al. (2001). "The TNF and TNF receptor superfamilies: Integrating mammalian biology." Cell **104**(4): 487-501.

Lohmeyer, J., J. Friedrich, et al. (1994). "MULTIPARAMETER FLOW CYTOMETRIC ANALYSIS OF INFLAMMATORY CELLS CONTAINED IN BRONCHOALVEOLAR LAVAGE FLUID." Journal of Immunological Methods **172**(1): 59-70.

Lynch, C. N., Y. C. Wang, et al. (1999). "TWEAK induces angiogenesis and proliferation of endothelial cells." Journal of Biological Chemistry **274**(13): 8455-8459.

MacEwan, D. J. (2002). "TNF ligands and receptors - a matter of life and death." British Journal of Pharmacology **135**(4): 855-875.

Macher-Goeppinger, S., S. Aulmann, et al. (2008). "Decoy receptor 3 is a prognostic factor in renal cell cancer." Neoplasia **10**(10): 1049-U52.

Mantovani, A., M. Locati, et al. (2001). "Decoy receptors: a strategy to regulate inflammatory cytokines and chemokines." Trends in Immunology **22**(6): 328-336.

Marsters, S. A., J. P. Sheridan, et al. (1996). "Apo-3, a new member of the tumor necrosis factor receptor family, contains a death domain and activates apoptosis and NF-kappa B." Current Biology **6**(12): 1669-1676.

Marsters, S. A., J. P. Sheridan, et al. (1998). "Identification of a ligand for the death-domain-containing receptor Apo3." Current Biology **8**(9): 525-528.

Matsuoka, K., N. Inoue, et al. (2004). "T-bet upregulation and subsequent interleukin 12 stimulation are essential for induction of Th1 mediated immunopathology in Crohn's disease." Gut **53**(9): 1303-1308.

McLaren, J. E., C. J. Calder, et al. (2010). "In vitro promotion of macrophage foam cell formation by Death Receptor 3 and its ligand TL1A." Immunology **131**: 103-103.

McLoughlin, R. M., S. M. Hurst, et al. (2004). "Differential regulation of neutrophil-activating chemokines by IL-6 and its soluble receptor isoforms." Journal of Immunology **172**(9): 5676-5683.

McLoughlin, R. M., J. Witowski, et al. (2003). "Interplay between IFN-gamma and IL-6 signaling governs neutrophil trafficking and apoptosis during acute inflammation." Journal of Clinical Investigation **112**(4): 598-607.

McLoughlin, R. M., B. J. Jenkins, et al. (2005). "IL-6 trans-signaling via STAT3 directs T cell infiltration in acute inflammation." Proceedings of the National Academy of Sciences of the United States of America **102**(27): 9589-9594.

Mei, C.-l., Z.-j. Chen, et al. (2007). "Interleukin-10 inhibits the down-regulation of ATP binding cassette transporter A1 by tumour necrosis factor-alpha in THP-1 macrophage-derived foam cells." Cell Biology International **31**(12): 1456-1461.

Messmer, U. K. and J. Pfeilschifter (2000). "New insights into the mechanism for clearance of apoptotic cells." Bioessays **22**(10): 878-881.

Metcalfe, D. D., D. Baram, et al. (1997). "Mast cells." Physiological Reviews **77**(4): 1033-1079.

Meylan, F., T. S. Davidson, et al. (2008). "The TNF-family receptor DR3 is essential for diverse T cell-mediated inflammatory diseases." Immunity **29**(1): 79-89.

Migone, T. S., J. Zhang, et al. (2002). "TL1A is a TNF-like ligand and functions as a T cell for DR3 and TR6/DcR3 costimulator." Immunity **16**(3): 479-492.

Molesworth-Kenyon, S. J., N. Popham, et al. (2012). "Resident Corneal Cells Communicate with Neutrophils Leading to the Production of IP-10 during the Primary Inflammatory Response to HSV-1 Infection." International journal of inflammation **2012**: 810359-810359.

Moser, B., M. Wolf, et al. (2004). "Chemokines: multiple levels of leukocyte migration control." Trends in Immunology **25**(2): 75-84.

Munroe, M. E. and G. A. Bishop (2004). "Role of tumor necrosis factor (TNF) receptor-associated factor 2 (TRAF2) in distinct and overlapping CD40 and TNF receptor 2/CD120b-mediated B lymphocyte activation." Journal of Biological Chemistry **279**(51): 53222-53231.

Murdoch, C. and A. Finn (2000). "Chemokine receptors and their role in inflammation and infectious diseases." Blood **95**(10): 3032-3043.

Murphy, P. M., M. Baggiolini, et al. (2000). "International union of pharmacology. XXII. Nomenclature for chemokine receptors." Pharmacological Reviews **52**(1): 145-176.

Mutsaers, S. E. (2004). "The mesothelial cell." International Journal of Biochemistry & Cell Biology **36**(1): 9-16.

Nagy, J. A. and R. W. Jackman (1998). "Anatomy and physiology of the peritoneal membrane." Seminars in Dialysis **11**(1): 49-56.

Nathan, C. F. and J. B. Hibbs (1991). "ROLE OF NITRIC-OXIDE SYNTHESIS IN MACROPHAGE ANTIMICROBIAL ACTIVITY." Current Opinion in Immunology **3**(1): 65-70.

Nathan, C. F. and R. K. Root (1977). "HYDROGEN-PEROXIDE RELEASE FROM MOUSE PERITONEAL MACROPHAGES - DEPENDENCE ON SEQUENTIAL ACTIVATION AND TRIGGERING." Journal of Experimental Medicine **146**(6): 1648-1662.

Nathan, C. F., S. C. Silverstein, et al. (1979). "EXTRACELLULAR CYTOLYSIS BY ACTIVATED MACROPHAGES AND GRANULOCYTES .2. HYDROGEN-PEROXIDE AS A MEDIATOR OF CYTOTOXICITY." Journal of Experimental Medicine **149**(1): 100-113.

Nishikori, M., H. Ohno, et al. (2005). "Stimulation of CD30 in anaplastic large cell lymphoma leads to production of nuclear factor-kappa B p52, which is associated with hyperphosphorylated Bcl-3." Cancer Science **96**(8): 487-497.

Nishino, T., R. Ashida, et al. (2012). "Involvement of Lymphocyte Infiltration in the Progression of Mouse Peritoneal Fibrosis Model." Renal Failure **34**(6): 760-766.

Nonaka, M., R. Horie, et al. (2005). "Aberrant NF-kappa B2/p52 expression in Hodgkin/Reed-Sternberg cells and CD30-transformed rat fibroblasts." Oncogene **24**(24): 3976-3986.

Norris, P. S. and C. F. Ware (2007). "The LT beta R signaling pathway." Tnf Receptor Associated Factors (Trafs) **597**: 160-172.

Novack, D. V., L. Yin, et al. (2003). "The I kappa B function of NF-kappa B2 p100 controls stimulated osteoclastogenesis." Journal of Experimental Medicine **198**(5): 771-781.

Orlinick, J. R. and M. V. Chao (1998). "TNF-related ligands and their receptors." Cellular Signalling **10**(8): 543-551.

Osawa, K., N. Takami, et al. (2004). "Death receptor 3 (DR3) gene duplication in a chromosome region 1p36.3: gene duplication is more prevalent in rheumatoid arthritis." Genes and Immunity **5**(6): 439-443.

Papadakis, K. A., J. Prehn, et al. (2004). "TL1A synergizes with IL-12/IL-18 to enhance IFN-gamma production in human T and NK cells." Faseb Journal **18**(4): A465-A465.

Papadakis, K. A., J. L. Prehn, et al. (2004). "TL1A synergizes with IL-12 and IL-18 to enhance IFN-gamma production in human T cells and NK cells." Journal of Immunology **172**(11): 7002-7007.

Papadakis, K. A., D. C. Zhu, et al. (2005). "Dominant role for TL1A/DR3 pathway in IL-12 plus IL-18-induced IFN-gamma production by peripheral blood and mucosal CCR9(+) T lymphocytes'." Journal of Immunology **174**(8): 4985-4990.

Pappu, B. P., A. Borodovsky, et al. (2008). "TL1A-DR3 interaction regulates Th17 cell function and Th17-mediated autoimmune disease." Journal of Experimental Medicine **205**(5): 1049-1062.

Persson, J., J. Nilsson, et al. (2008). "Interleukin-1 beta and tumour necrosis factor-alpha impede neutral lipid turnover in macrophage-derived foam cells." Bmc Immunology **9**.

Philpott, N. J., A. J. C. Turner, et al. (1996). "The use of 7-amino actinomycin D in identifying apoptosis: Simplicity of use and broad spectrum of application compared with other techniques." Blood **87**(6): 2244-2251.

Pickering, M. C., M. Botto, et al. (2000). "Systemic lupus erythematosus, complement deficiency, and apoptosis." Advances in immunology **76**: 227-324.

Pitti, R. M., S. A. Marsters, et al. (1998). "Genomic amplification of a decoy receptor for Fas ligand in lung and colon cancer." Nature **396**(6712): 699-703.

Platanias, L. C. (2005). "Mechanisms of type-I- and type-II-interferon-mediated signalling." Nature Reviews Immunology **5**(5): 375-386.

Porquet, N., A. Poirier, et al. (2011). "Survival advantages conferred to colon cancer cells by E-selectin-induced activation of the PI3K-NF kappa B survival axis downstream of Death receptor-3." Bmc Cancer **11**.

Prehn, J. L., L. S. Thomas, et al. (2007). "The T cell costimulator TL1A is induced by Fc gamma R signaling in human monocytes and dendritic cells." Journal of Immunology **178**(7): 4033-4038.

Rahighi, S., F. Ikeda, et al. (2009). "Specific Recognition of Linear Ubiquitin Chains by NEMO Is Important for NF-kappa B Activation." Cell **136**(6): 1098-1109.

Ramakrishnan, P., W. X. Wang, et al. (2004). "Receptor-specific signaling for both the alternative and the canonical NF-kappa B activation pathways by NF-kappa B-inducing kinase." Immunity **21**(4): 477-489.

Rauert, H., A. Wicovsky, et al. (2010). "Membrane Tumor Necrosis Factor (TNF) Induces p100 Processing via TNF Receptor-2 (TNFR2)." Journal of Biological Chemistry **285**(10): 7394-7404.

Rennard, S. I., M. C. Jaurand, et al. (1984). "ROLE OF PLEURAL MESOTHELIAL CELLS IN THE PRODUCTION OF THE SUBMESOTHELIAL CONNECTIVE-TISSUE MATRIX OF LUNG." American Review of Respiratory Disease **130**(2): 267-274.

Robson, R. L., R. M. McLoughlin, et al. (2001). "Differential regulation of chemokine production in human peritoneal mesothelial cells: IFN-gamma controls neutrophil migration across the mesothelium in vitro and in vivo." Journal of Immunology **167**(2): 1028-1038.

Robson, R. L., J. Witowski, et al. (1997). "Interferon-gamma (IFN-gamma) differentially regulates C-C and C-X-C chemokine synthesis by and leukocyte migration across human peritoneal mesothelial cells (HPMC)." Journal of the American Society of Nephrology **8**: A1246-A1246.

Rollins, B. J. (1997). "Chemokines." Blood **90**(3): 909-928.

Rossi, D. and A. Zlotnik (2000). "The biology of chemokines and their receptors." Annual Review of Immunology **18**: 217-243.

Roth, W., S. Isenmann, et al. (2001). "Soluble decoy receptor 3 is expressed by malignant gliomas and suppresses CD95 ligand-induced apoptosis and chemotaxis." Cancer Research **61**(6): 2759-2765.

Rubin, J., M. Clawson, et al. (1988). "MEASUREMENTS OF PERITONEAL SURFACE-AREA IN MAN AND RAT." American Journal of the Medical Sciences **295**(5): 453-458.

Rus, H. G., F. Niculescu, et al. (1991). "TUMOR-NECROSIS-FACTOR-ALPHA IN HUMAN ARTERIAL-WALL WITH ATHEROSCLEROSIS." Atherosclerosis **89**(2-3): 247-254.

Saitoh, T., M. Nakayama, et al. (2003). "TWEAK induces NF-kappa B2 p100 processing and long lasting NF-kappa B activation." Journal of Biological Chemistry **278**(38): 36005-36012.

Sanui, H., S. Yoshida, et al. (1982). "PERITONEAL-MACROPHAGES WHICH PHAGOCYTOSE AUTOLOGOUS POLYMORPHONUCLEAR LEUKOCYTES IN GUINEA-PIGS .1. INDUCTION BY IRRITANTS AND MICROORGANISMS AND INHIBITION BY COLCHICINE." British Journal of Experimental Pathology **63**(3): 278-284.

Saruta, M., K. S. Michelsen, et al. (2009). "TLR8-mediated activation of human monocytes inhibits TL1A expression." European Journal of Immunology **39**(8): 2195-2202.

Sasada, M. and R. B. Johnston (1980). "MACROPHAGE MICROBICIDAL ACTIVITY - CORRELATION BETWEEN PHAGOCYTOSIS-ASSOCIATED OXIDATIVE-METABOLISM AND THE KILLING OF CANDIDA BY MACROPHAGES." Journal of Experimental Medicine **152**(1): 85-98.

Savill, J. S., A. H. Wyllie, et al. (1989). "MACROPHAGE PHAGOCYTOSIS OF AGING NEUTROPHILS IN INFLAMMATION - PROGRAMMED CELL-DEATH IN THE NEUTROPHIL LEADS TO ITS RECOGNITION BY MACROPHAGES." Journal of Clinical Investigation **83**(3): 865-875.

Scapini, P., J. A. Lapinet-Vera, et al. (2000). "The neutrophil as a cellular source of chemokines." Immunological Reviews **177**: 195-203.

Schreiber, T. H., D. Wolf, et al. (2010). "Therapeutic Treg expansion in mice by TNFRSF25 prevents allergic lung inflammation." Journal of Clinical Investigation **120**(10): 3629-3640.

Screaton, G. R., X. N. Xu, et al. (1997). "LARD: A new lymphoid-specific death domain containing receptor regulated by alternative pre-mRNA splicing." Proceedings of the National Academy of Sciences of the United States of America **94**(9): 4615-4619.

Segerer, S., P. J. Nelson, et al. (2000). "Chemokines, chemokine receptors, and renal disease: From basic science to pathophysiologic and therapeutic studies." Journal of the American Society of Nephrology **11**(1): 152-176.

Selgas, R., A. Bajo, et al. (2006). "Epithelial-to-mesenchymal transition of the mesothelial cell - its role in the response of the peritoneum to dialysis." Nephrology Dialysis Transplantation **21**.

Senftleben, U., Y. X. Cao, et al. (2001). "Activation by IKK alpha of a second, evolutionary conserved, NF-kappa B signaling pathway." Science **293**(5534): 1495-1499.

Serbina, N. V., T. P. Salazar-Mather, et al. (2003). "TN/iNOS-producing dendritic cells mediate innate immune defense against bacterial infection." Immunity **19**(1): 59-70.

Shen, H. M. and S. Pervaiz (2006). "TNF receptor superfamily-induced cell death: redox-dependent execution." Faseb Journal **20**(10): 1589-1598.

Shi, G. X., Y. L. Wu, et al. (2003). "Death decoy receptor TR6/DcR3 inhibits T cell chemotaxis in vitro and in vivo." Journal of Immunology **171**(7): 3407-3414.

Shih, D. Q., R. Barrett, et al. (2011). "Constitutive TL1A (TNFSF15) Expression on Lymphoid or Myeloid Cells Leads to Mild Intestinal Inflammation and Fibrosis." Plos One **6**(1).

Shih, D. Q., L. Y. Kwan, et al. (2009). "Microbial induction of inflammatory bowel disease associated gene TL1A (TNFSF15) in antigen presenting cells." European Journal of Immunology **39**(11): 3239-3250.

Simionescu, M. and N. Simionescu (1977). "ORGANIZATION OF CELL JUNCTIONS IN PERITONEAL MESOTHELIUM." Journal of Cell Biology **74**(1): 98-110.

Skaug, B., X. M. Jiang, et al. (2009). The Role of Ubiquitin in NF-kappa B Regulatory Pathways. Annual Review of Biochemistry. **78:** 769-796.

Solan, N. J., H. Miyoshi, et al. (2002). "RelB cellular regulation and transcriptional activity are regulated by p100." Journal of Biological Chemistry **277**(2): 1405-1418.

Springer, T. A. (1990). "ADHESION RECEPTORS OF THE IMMUNE-SYSTEM." Nature **346**(6283): 425-434.

Stamenkovic, I., E. A. Clark, et al. (1989). "A B-LYMPHOCYTE ACTIVATION MOLECULE RELATED TO THE NERVE GROWTH-FACTOR RECEPTOR AND INDUCED BY CYTOKINES IN CARCINOMAS." Embo Journal **8**(5): 1403-1410.

Stary, G., C. Bangert, et al. (2007). "Tumoricidal activity of TLR7/8-activated inflammatory dendritic cells." Journal of Experimental Medicine **204**(6): 1441-1451.

Steinhauer, H. B. and P. Schollmeyer (1986). "PROSTAGLANDIN-MEDIATED LOSS OF PROTEINS DURING PERITONITIS IN CONTINUOUS AMBULATORY PERITONEAL-DIALYSIS." Kidney International **29**(2): 584-590.

Strieter, R. M., M. D. Burdick, et al. (2005). "CXC chemokines in angiogenesis." Cytokine & Growth Factor Reviews **16**(6): 593-609.

Strieter, R. M., T. J. Standiford, et al. (1996). ""The good, the bad, and the ugly": The role of chemokines in models of human disease - Commentary." Journal of Immunology **156**(10): 3583-3586.

Suassuna, J. H. R., F. C. Dasneves, et al. (1994). "IMMUNOHISTOCHEMICAL STUDIES OF THE PERITONEAL MEMBRANE AND INFILTRATING CELLS IN NORMAL SUBJECTS AND IN PATIENTS ON CAPD." Kidney International **46**(2): 443-454.

Sun, S. C. (2010). "Controlling the Fate of NIK: A Central Stage in Noncanonical NF-kappa B Signaling." Science Signaling **3**(123).

Sun, S. C. (2011). "Non-canonical NF-kappa B signaling pathway." Cell Research **21**(1): 71-85.

Sunderkotter, C., T. Nikolic, et al. (2004). "Subpopulations of mouse blood monocytes differ in maturation stage and inflammatory response." Journal of Immunology **172**(7): 4410-4417.

Takahashi, S., Y. Taniguchi, et al. (2009). "Mizoribine Suppresses the Progression of Experimental Peritoneal Fibrosis in a Rat Model." Nephron Experimental Nephrology **112**(2): E59-E69.

Takedatsu, H., K. S. Michelsen, et al. (2008). "TL1A (TNFSF15) regulates the development of chronic colitis by modulating both T-helper 1 and T-helper 17 activation." Gastroenterology **135**(2): 552-567.

Tan, K. B., J. Harrop, et al. (1997). "Characterization of a novel TNF-like ligand and recently described TNF ligand and TNF receptor superfamily genes and their constitutive and inducible expression in hematopoietic and non-hematopoietic cells." Gene **204**(1-2): 35-46.

Taraban, V. Y., T. J. Slebioda, et al. (2011). "Sustained TL1A expression modulates effector and regulatory T-cell responses and drives intestinal goblet cell hyperplasia." Mucosal Immunology **4**(2): 186-196.

Taylor, P. R. and S. Gordon (2003). "Monocyte heterogeneity and innate immunity." Immunity **19**(1): 2-4.

Taylor, P. R., L. Martinez-Pomares, et al. (2005). Macrophage receptors and immune recognition. Annual Review of Immunology. **23:** 901-944.

Thompson, J. S., S. A. Bixler, et al. (2001). "BAFF-R, a newly identified TNF receptor that specifically interacts with BAFF." Science **293**(5537): 2108-2111.

Tokunaga, F., S.-i. Sakata, et al. (2009). "Involvement of linear polyubiquitylation of NEMO in NF-kappa B activation." Nature Cell Biology **11**(2): 123-U40.

Topley, N., Z. Brown, et al. (1993). "HUMAN PERITONEAL MESOTHELIAL CELLS SYNTHESIZE INTERLEUKIN-8 - SYNERGISTIC INDUCTION BY INTERLEUKIN-1-BETA AND TUMOR-NECROSIS-FACTOR-ALPHA." American Journal of Pathology **142**(6): 1876-1886.

Topley, N., T. Liberek, et al. (1996). "Activation of inflammation and leukocyte recruitment into the peritoneal cavity." Kidney Int Suppl **56**: S17-21.

Topley, N., M. M. Petersen, et al. (1994). "HUMAN PERITONEAL MESOTHELIAL CELL PROSTAGLANDIN SYNTHESIS - INDUCTION OF CYCLOOXYGENASE MESSENGER-RNA BY PERITONEAL MACROPHAGE-DERIVED CYTOKINES." Kidney International **46**(3): 900-909.

Tremelling, M., D. C. Massey, et al. (2008). "Association of non-coding il12b variants with inflammatory bowel disease confirms importance of il23-il17 signalling pathway in disease pathogenesis." Gut **57**: A150-A150.

Turchyn, L. R., T. J. Baginski, et al. (2007). "Phenotypic and functional analysis of murine resident and induced peritoneal macrophages." Comparative Medicine **57**(6): 574-580.

Twohig, J. P., M. Marsden, et al. (2012). "The death receptor 3/TL1A pathway is essential for efficient development of antiviral CD4(+) and CD8(+) T-cell immunity." Faseb Journal **26**(8): 3575-3586.

Twohig, J. P., M. I. Roberts, et al. (2010). "Age-Dependent Maintenance of Motor Control and Corticostriatal Innervation by Death Receptor 3." Journal of Neuroscience **30**(10): 3782-3792.

Ulvmar, M. H., E. Hub, et al. (2011). "Atypical chemokine receptors." Experimental Cell Research **317**(5): 556-568.

Vaira, S., T. Johnson, et al. (2008). "RelB is the NF-kappa B subunit downstream of NIK responsible for osteoclast differentiation." Proceedings of the National Academy of Sciences of the United States of America **105**(10): 3897-3902.

Valle, M. T., M. L. Deglinnocenti, et al. (1995). "ANTIGEN-PRESENTING FUNCTION OF HUMAN PERITONEUM MESOTHELIAL CELLS." Clinical and Experimental Immunology **101**(1): 172-176.

Vanoers, M. H. J., C. P. M. Reutelingsperger, et al. (1994). "ANNEXIN-V FOR FLOW CYTOMETRIC DETECTION OF PHOSPHATIDYLSERINE EXPRESSION ON B-CELLS UNDERGOING APOPTOSIS." Blood **84**(10): A291-A291.

Verhelst, K., I. Carpentier, et al. (2011). "Regulation of TNF-induced NF-kappa B activation by different cytoplasmic ubiquitination events." Cytokine & Growth Factor Reviews **22**(5-6): 277-286.

Visser, C. E., J. Tekstra, et al. (1998). "Chemokines produced by mesothelial cells: huGRO-alpha, IP-10, MCP-1 and RANTES." Clinical and Experimental Immunology **112**(2): 270-275.

Vonasmuth, E. J. U., J. G. Maessen, et al. (1990). "TUMOR NECROSIS FACTOR-ALPHA (TNF-ALPHA) AND INTERLEUKIN-6 IN A ZYMOSAN-INDUCED SHOCK MODEL." Scandinavian Journal of Immunology **32**(4): 313-319.

Walczak, H., K. Iwai, et al. (2012). "Generation and physiological roles of linear ubiquitin chains." Bmc Biology **10**.

Wang, E. C. Y., J. Kitson, et al. (2001). "Genomic structure, expression, and chromosome mapping of the mouse homologue for the WSL-1 (DR3, Apo3, TRAMP, LARD, TR3, TNFRSF12) gene." Immunogenetics **53**(1): 59-63.

Wang, E. C. Y., A. Thern, et al. (2001). "DR3 regulates negative selection during thymocyte development." Molecular and Cellular Biology **21**(10): 3451-3461.

Wang, J., H. J. Chun, et al. (2001). "Caspase-10 is an initiator caspase in death receptor signaling." Proceedings of the National Academy of Sciences of the United States of America **98**(24): 13884-13888.

Wang, X., J. Nie, et al. (2010). "Impaired TGF-beta signalling enhances peritoneal inflammation induced by E-Coli in rats." Nephrology Dialysis Transplantation **25**(2): 399-412.

Ware, C. F. (2008). "The TNF Superfamily-2008." Cytokine & Growth Factor Reviews **19**(3-4): 183-186.

Warzocha, K., P. Ribeiro, et al. (1998). "A new death receptor 3 isoform: Expression in human lymphoid cell lines and non-Hodgkin's lymphomas." Biochemical and Biophysical Research Communications **242**(2): 376-379.

Washida, N., S. Wakino, et al. (2011). "Rho-kinase inhibition ameliorates peritoneal fibrosis and angiogenesis in a rat model of peritoneal sclerosis." Nephrology Dialysis Transplantation **26**(9): 2770-2779.

Weissman, B. S. K. a. S. M. (1989). "cDNA sequences of two inducible T-cell genes." PNAS **86**(6): 1963-1967

Wen, L., L. Zhuang, et al. (2003). "TL1A-induced NF-kappa B activation and c-IAP2 production prevent DR3-mediated apoptosis in TF-1 cells." Journal of Biological Chemistry **278**(40): 39251-39258.

Weyde, J., K. Wassermann, et al. (1997). "Analysis of single and double-stained alveolar macrophages by flow cytometry." Journal of Immunological Methods **207**(2): 115-123.

Wiley, S. R., L. Cassiano, et al. (2001). "A novel TNF receptor family member binds TWEAK and is implicated in angiogenesis." Immunity **15**(5): 837-846.

Williams, J. D., K. J. Craig, et al. (2002). "Morphologic changes in the peritoneal membrane of patients with renal disease." Journal of the American Society of Nephrology **13**(2): 470-479.

Witz, C. A., I. A. Montoya-Rodriguez, et al. (2001). "Composition of the extracellular matrix of the peritoneum." Journal of the Society for Gynecologic Investigation **8**(5): 299-304.

Wroblewski, V. J., D. R. Witcher, et al. (2003). "Decoy receptor 3 (DcR3) is proteolytically processed to a metabolic fragment having differential activities against Fas ligand and LIGHT." Biochemical Pharmacology **65**(4): 657-667.

Wu, D. Q., G. J. Larosa, et al. (1993). "G-PROTEIN-COUPLED SIGNAL-TRANSDUCTION PATHWAYS FOR INTERLEUKIN-8." Science **261**(5117): 101-103.

Wynn, T. A. (2007). "Common and unique mechanisms regulate fibrosis in various fibroproliferative diseases." Journal of Clinical Investigation **117**(3): 524-529.

Xiao, G. T., E. W. Harhaj, et al. (2001). "NF-kappa B-inducing kinase regulates the processing of NF-kappa B2 p100." Molecular Cell **7**(2): 401-409.

Yamazaki, K., D. McGovern, et al. (2005). "Single nucleotide polymorphisms in TNFSF15 confer susceptibility to Crohn's disease." Human Molecular Genetics **14**(22): 3499-3506.

Yang, C. R., J. H. Wang, et al. (2004). "Decoy receptor 3 (DcR3) induces osteoclast formation from monocyte/macrophage lineage precursor cells." Cell Death and Differentiation **11**: S97-S107.

Yu, K. Y., B. Kwon, et al. (1999). "A newly identified member of tumor necrosis factor receptor superfamily (TR6) suppresses LIGHT-mediated apoptosis." Journal of Biological Chemistry **274**(20): 13733-13736.

Yue, T. L., J. Ni, et al. (1999). "TL1, a novel tumor necrosis factor-like cytokine, induces apoptosis in endothelial cells - Involvement of activation of stress protein kinases (stress-activated protein kinase and p38 mitogen-activated protein kinase) and caspase-3-like protease." Journal of Biological Chemistry **274**(3): 1479-1486.

Yung, S. and T. M. Chan (2009). "INTRINSIC CELLS: MESOTHELIAL CELLS - CENTRAL PLAYERS IN REGULATING INFLAMMATION AND RESOLUTION." Peritoneal Dialysis International **29**: S21-S27.

Zabel, B. A., L. Zuniga, et al. (2006). "Chemoattractants, extracellular proteases, and the integrated host defense response." Experimental Hematology **34**(8): 1021-1032.

Zhai, Y. F., J. Ni, et al. (1999). "VEGI, a novel cytokine of the tumor necrosis factor family, is an angiogenesis inhibitor that suppresses the growth of colon carcinomas in vivo." Faseb Journal **13**(1): 181-189.

Zhai, Y. F., J. Y. Yu, et al. (1999). "Inhibition of angiogenesis and breast cancer xenograft tumor growth by VEGI, a novel cytokine of the TNF superfamily." International Journal of Cancer **82**(1): 131-136.

Zhang, J., T. W. Salcedo, et al. (2001). "Modulation of T-cell responses to alloantigens by TR6/DcR3." Journal of Clinical Investigation **107**(11): 1459-1468.

Zhang, J., X. H. Wang, et al. (2009). "Role of TL1A in the Pathogenesis of Rheumatoid Arthritis." Journal of Immunology **183**(8): 5350-5357.

Zlotnik, A. and O. Yoshie (2000). "Chemokines: A new classification system and their role in immunity." Immunity **12**(2): 121-127.

Zucchelli, M., M. Camilleri, et al. (2011). "Association of TNFSF15 polymorphism with irritable bowel syndrome." Gut **60**(12): 1671-1677.

Appendix

Paper removed by author for copyright reasons